THE DRYING OF FIBROUS AND POROUS-GRANULAR MATERIALS IN A HOT AIRSTREAM

A thesis presented by

Kenneth Clark Kirkwood, B.Sc.

in fulfilment of the requirements of
the degree of Doctor of Philosophy
of the University of Glasgow.

Department of Chemical Technology,
Royal College of Science and Technology,
Glasgow, C.1.

February, 1962.

A C K N O W L E D G M E N T S

The author wishes to thank Professor P. D. Ritchie, F.R.S.E. for providing facilities for this research. The author is also indebted to Dr. T. J. Mitchell, F.R.I.C., who supervised the research, and to Mr D. Smith, A.R.C.S.T., for his advice on the statistical aspects of the work.

Thanks are also due to the staff of the departmental workshop for their assistance in the construction of the apparatus.

To the Department of Scientific and Industrial Research goes the author's gratitude for the Research Studentship which made this investigation possible.

THE DRYING OF FIBROUS AND POROUS-GRANULAR MATERIALS IN A HOT AIRSTREAM

SUMMARY

Before a hot-air drier can be designed to dry a given material, the effects of loading of material per unit area of the drier, airflow, air temperature and humidity on the drying time of the material must be estimated accurately. Since such estimates cannot be made from theoretical considerations alone, the effects of the various factors on the drying time of a material are usually estimated from the results of a series of drying tests in which each factor in turn is varied while the rest are kept constant.

This "classical" method of experimentation of studying each factor in turn assumes that the effect of each factor acts independently of the other factors. There is, however, no reason why this should be so, and the magnitude of the effect of a factor estimated by this method may be a function of the arbitrary constant values chosen for the other factors. If such interactions between the effects of the various factors are present, the classical experiment cannot detect them and will give estimates of the drying time of a material which will be in error to a degree depending on the values of the factors chosen and on the magnitude of the interactions.

Such interactions could be detected by using a programme of drying tests based on the factorial method of experimentation in which the effect of each factor is evaluated over the range of values studied of each of the other factors. As far as is known, this method of experimentation has not been previously applied to drying problems. It is

employed in the present work to examine the possibility of there being interactions between the effects of loading of material, airflow, air temperature and humidity on the drying times of porous-granular, and fibrous materials in cross-circulation and through-circulation driers.

The porous-granular materials studied were $\frac{1}{4}$ inch long, $\frac{1}{4}$ inch diameter porous-ceramic granules, and $\frac{1}{8}$ to $\frac{3}{8}$ inch mesh coke; the fibrous material was brewers' spent-grain. The approximate ranges of the various factors studied were:

Air Temperature	120 to 210°F
Air Humidity	0.01 to 0.08 lb water/lb dry air
Airflow	4 to 13 lb dry air/(sq.ft. drier area)(min)
Loading of Material	single layer to $\frac{3}{4}$ inch layer (cross-circulation drier tests)
	single layer to 4 inch layer (through-circulation drier tests)

A preliminary two-level factorial experiment, involving sixteen drying tests covering all combinations of the extreme values of the ranges of the various factors, was done on each material; the drying behaviour of the material in each drying test was characterized by the constant drying rate $\frac{dW}{d\theta}$ lb water/(lb dry solid)(hr), the critical moisture content W_c lb water/lb dry solid, and a falling-rate Constant C (the slope of a plot of moisture content W against the logarithm of the drying time in minutes θ' described by the equation:
$W = C \log_{10} \theta' + \text{constant}$). A fractional three-level factorial experiment involving twenty-eight to thirty-six additional tests was designed to elucidate any effects or interactions of loading, airflow, air temperature and humidity on $\frac{dW}{d\theta}$, W_c and C which appeared, from an

analysis of the values of $\frac{dW}{d\Theta}$, W_c and C obtained in the preliminary sixteen tests, to be significant. The third level of each factor studied in this experiment was the median of the factor range.

The results of the fractional three-level factorial experiments on the three materials dried in the cross-circulation and through-circulation driers - involving a total of three hundred drying tests - are summarized in graphs showing the variations in $\log_{10} \frac{dW}{d\Theta}$, W_c and C with changes in loading, airflow, air temperature and humidity. From these graphs, the drying times of the various materials in the cross-circulation drier could be estimated within ± 16% of the experimental values, and the drying times in the through-circulation drier within ± 10%. Interactions between the effects of the various factors on $\frac{dW}{d\Theta}$, W_c and C were found to be small, except the interaction between the effects of air temperature and humidity on $\frac{dW}{d\Theta}$; the magnitude of this interaction corresponded with that predicted by the existing theory of the constant drying-rate period.

From experience gained in the present investigation, a tentative design is presented for a small fractional three-level factorial experiment suitable for obtaining data from which predictions accurate to within ± 30% may be made of the drying times of porous-granular and fibrous materials in cross-circulation and through-circulation driers. The experiment involves eleven drying tests which may be performed using an airstream of atmospheric humidity.

CONTENTS

GENERAL INTRODUCTION

Drying generally means the removal of a liquid (usually water) from a solid by thermal means, as distinct from mechanical methods such as draining, filtration or centrifuging. It is distinguished from evaporation by the equipment used, and by the fact that evaporation processes in general remove much larger quantities of water per unit weight of dry solids than do drying processes.

Drying of a material may be necessary or desirable for many reasons. It may be necessary to facilitate handling in further processing, and to permit satisfactory use of the final product; thus some products, especially foodstuffs, must be dried to prevent their decomposition in storage, and sometimes a by-product is dried to increase its commercial value. Drying of a material increases the capacity of other equipment in a process by reducing the weight, and often the volume, of material to be handled; this reduction in weight and volume may also allow considerable economy in storage and freight costs.

There are many types of industrial driers, all of which dry the material by supplying heat to evaporate the water in it, and by removing the water vapour from the surface of the material. Driers may be classified according to whether they supply heat directly by hot gases, or indirectly by conduction through a metal wall; both classes may be subdivided into batch, and continuous-process driers.

The selection of a drier for a given application depends mainly on the kind of material to be dried. For each type of material only a few types of driers are suitable; thus slurries are usually dried in drum, or spray driers; granules in through-circulation, rotary or tray driers; and materials in continuous sheets on heated rollers. The choice of drier is influenced by the handling properties (e.g. stickiness and particle size) of the material, and by its liability to contamination by contact with furnace gases. The operating conditions chosen are restricted by the temperature the material can stand without decomposing, and by its tendency to shrink, crack, or form dust during drying.

Usually a few types of driers appear capable of producing the desired dry product. The final choice is generally based on a consideration of the optimum size and consequent capital and operating costs of each, estimated from experimental data obtained on small-scale driers simulating each type. Laboratory drying tests on the wet material are almost invariably used, since they provide, at present, the simplest and most accurate method of finding the optimum operating conditions and corresponding drying time on which the above estimatesof the size and cost of each type of drier are based.

This thesis describes the limitations of theoretical methods of predicting the drying times of a material under various operating conditions in driers using through-circulation and cross-circulation airflows. The limitations of available empirical methods of predicting drying times are also discussed, and a new empirical method, based on an alternative programme of drying tests, is proposed. This method is illustrated by applying it to the drying of fibrous, and porous-granular materials in both types of drier.

CROSS-CIRCULATION DRYING

1. INTRODUCTION

In the cross-circulation or tray drier, the wet material is spread on trays and dried by passing a hot airstream over its surface.

This type of drier is commonly used to dry small batches of materials; it is simple in construction, versatile in operation, and can dry a great variety of materials including pastes, granular materials, and large manufactured articles such as pottery. For large-scale operation, drying may be made continuous by loading the trays on racks mounted on trolleys and moving them slowly along a tunnel through which hot air is circulated; the dry product is removed at the other end of the tunnel.

The great disadvantage of cross-circulation drying is that the hot airstream contacts only the surface layer of the wet material on the trays. Drying efficiency (lbs. water removed per lb. dry air) is thus low, and materials dry slowly. In addition, only shallow beds (up to about $1\frac{1}{2}$ inches deep) can be dried economically since drying times increase enormously as bed depth is increased. Drying by this method is expensive because of the poor drying efficiency, low output, and high cost of labour required to load and unload the trays.

The main operating variables affecting the drying time of a material in a cross-circulation drier are the loading of material per unit tray-area, and the temperature, humidity, and velocity of the airstream. The designer must estimate the effect of each of these variables on the drying time, and hence on the operating costs, so that the most economical drier can be built.

Section 2., which follows, outlines the present drying theory concerning the effects of the above variables, and of the physical structure of a material, on its drying time. Section 3. discusses the limitations of drying theory when used to predict the drying time of a material under a specified set of operating conditions. Subsequent Sections 4. to 6. review available empirical methods of predicting drying times, and illustrate a new empirical method which gives accurate predictions of drying times over a wider range of operating conditions than previous methods have done.

2. THEORY OF DRYING

When a saturated material, with free surface moisture, is exposed to an airstream of constant temperature, humidity and velocity, drying generally proceeds for a time at a constant rate, after which the drying rate falls off continuously until drying is complete.

2.1. Constant Drying Rate Period

During the constant drying rate period, the surface of the material is kept saturated with water from the interior, and behaves essentially as a free water surface. The drying rate of the material is thus the same as the rate of evaporation from a free water surface exposed to similar air conditions, and is dependent only on the air conditions used; different materials, however, dry at slightly different rates owing to differences in the surface area which each presents to the airstream.

2.2. Factors Affecting The Constant Drying Rate

Evaporation from a water surface has been explained (1) as the diffusion of water vapour through a stagnant air-film adjacent to the water surface, followed by its rapid removal by mixing with the turbulent airstream beyond. The rate of evaporation is controlled by the rate of vapour diffusion through the air-film.

According to the law of diffusion, the rate of vapour diffusion is directly proportional to the area of water surface available for evaporation and to the difference between the vapour pressures at the water surface and in the airstream, and is inversely proportional to the air-film thickness. This relationship can be expressed by the equation.

$$\frac{dw}{d\theta} = KA(p_s - p_a) \quad \ldots \quad \text{Equation 1.}$$

where $\frac{dw}{d\theta}$ = diffusion or drying rate lb/hr.

K = coefficient of mass transfer lb/(hr) (sq. ft) (atm. partial pressure difference)

A = drying surface available sq. ft.

p_s = vapour pressure of water at water/air interface atm.

p_a = partial pressure of water vapour in the airstream atm.

The mass transfer coefficient K allows for the effect of variations in the thickness of the air-film on the drying rate. Although the thickness of the air-film cannot be readily measured, it is known that an increase in airflow decreases its thickness with a consequent increase in the drying rate. Equation 1 may be modified to include the effect of airflow on the drying rate.

$$\frac{dw}{d\theta} = K'AG^n(p_s - p_a) \quad \ldots \quad \text{Equation 2.}$$

where K', n = empirical constants

G = airflow lb. dry air/(sq. ft drier cross-section)(hr)

The value of n varies with the type of airflow (turbulent or laminar), and with its angle of incidence on the wet surface. For example, n is about 0·8 for turbulent flow parallel to the surface (2, 3), and for flow perpendicular to the surface a value of 0·37 has been reported (4).

The value of K' for any material depends mainly on its physical structure (which affects the surface area available for evaporation) and to a lesser extent on the drying conditions used (which affect the thickness of the air-film). Owing to the complexity of the factors involved, K' cannot be accurately estimated from theoretical considerations, and is usually determined experimentally.

Effect Of Wet Surface Area On The Constant Drying Rate

When a material is drying on a tray, the constant drying rate per unit area of tray surface increases with the wet surface area of the material exposed to the airstream. The drying rate of a bed of material thus depends on the factors influencing its surface area: namely, the shape, size and surface porosity of its particles, and their manner of packing in the bed.

The drying rates of wet surfaces of various shapes and sizes have been studied by Powell and Griffiths (5), and Powell (6); Powell (6) found that a sphere gave the highest drying rate for a solid of specified area.

Because of the increased area exposed to the airstream, a bed of large particles (greater than about $\frac{1}{8}$ inch mesh) dries faster that a free water surface covering the same area (7) - the drying rate increasing as the particle size decreases. This increase in drying rate is not maintained with particles smaller than about $\frac{1}{8}$ inch mesh, and the drying rate falls off with decreasing particle size. Shepherd, Hadlock and Brewer (3), and Sherwood and Comings (8), found that the drying rates of fine materials such as clays and sands, which form fairly level beds, were virtually independent of the particle size of the material and were approximately the same as that of a free water surface. Ceaglske and Hougen (2), however, disagreed with these workers, and claimed that the drying rate of sand was lower than that of a free water surface and increased with particle size.

Corben and Newitt (9) found that porous granules dried faster than solid granules of the same size.

Effect Of Airflow On The Constant Drying Rate

As mentioned previously, an increase in airflow increases the drying rate - an effect accounted for by the airflow term G^n in Equation 2.

Maisel and Sherwood (10), however, found that a further increase in drying rate could be obtained by increasing the turbulence of the airstream. Localized increases in drying rate may occur in a drier due to turbulence produced by chance obstructions such as the edges of trays (6), or by the surface of the material being dried (2). An enhanced drying rate can often be obtained by increasing the turbulence of the airstream by designing the drier with obstructions or "turbulence promoters" in the airstream (6, 7, 11).

Effect Of Air Temperature And Humidity On The Constant Drying Rate

The effect of air temperature and humidity on the constant drying rate is allowed for by the vapour pressure difference $(p_s - p_a)$

in Equation 2 — p_a increases with humidity; p_s depends on the temperature of the wet surface during drying, this temperature being a function of the temperature and humidity of the airstream.

The temperature of the wet surface, and hence the effect of air temperature and humidity on the constant drying rate, may be evaluated in terms of heat transfer as follows.

Evaporation from a wet surface depends on the supply of heat which, in the absence of any other source, must come from the airstream. If the wet surface is colder than the airstream, heat flows to it by convection from the airstream as given by the equation.

$$q = h_c A(t_a - t_s) \quad \ldots \text{ Equation 3.}$$

where q = rate of heat transfer B.T.U./hr.

h_c = convection coefficient of heat transfer B.T.U./(hr.) (sq. ft.) (°F)

t_a = air temperature °F

t_s = temperature of wet surface °F

The temperature of the wet surface rises and the rate of evaporation increases until the wet surface attains an equilibrium temperature at which the rate of heat supplied by the airstream balances the rate of evaporation. The equilibrium temperature, known as the wet-bulb temperature, is a well-established function (12, 13) of the velocity, temperature and humidity of the airstream. The rate of evaporation at equilibrium is

$$\frac{dw}{d\theta} = KA(p_w - p_a) = h_c A(t_a - t_w) \quad \ldots \text{ Equation 4.}$$

where t_w = wet-bulb temperature (W.B.T.), °F

p_W = vapour pressure of water at the W.B.T., atm.

λ = latent heat of water at the W.B.T. B.T.U./lb

Shepherd, Hadlock and Brewer (3) used the results of their experimental drying tests, and those of previous workers (2, 5, 14, 15, 16, 17) to test the use of Equation 4 to estimate the drying rate of a bed of saturated material in a cross-circulation drier. They found that the calculated values of the mass transfer coefficient K were erratic, and that the heat transfer coefficient h_c gave a much more reliable estimate of the drying rate. The value of h_c varied with airflow according to the equation.

$$h_c = 0{\cdot}0128G^{0{\cdot}8} \qquad \ldots \text{ Equation 5.}$$

They recommended the following equation for the constant drying rate from a plane wet surface exposed to a cross-circulation airflow.

$$\frac{dw}{d\theta} = \frac{0{\cdot}0128G^{0{\cdot}8}A(t_a - t_W)}{\lambda} \qquad \ldots \text{ Equation 6.}$$

Effects Of Heat Conduction And Radiation On The Constant Drying Rate

Equation 6 applies when heat from the airstream is supplied by convection alone, and the surface of the wet material is at the wet-bulb temperature. In an industrial drier, however, heat radiated from the walls of the drier or from the bottoms of trays, and heat conducted through the trays, frequently raises the surface temperature and increases the drying rate.

To calculate the increased drying rate which may be expected due to heat radiation or conduction, it is necessary to know the surface temperature of the material. Since its measurement is usually impracticable, this temperature must be estimated by means of heat balances - described in detail by Perry (13). Perry also gives methods of calculating an overall heat transfer coefficient h_t to include heat transferred to the material by convection and conduction, by convection and radiation, and by all three together. The drying rate is then calculated by the equation.

$$\frac{dw}{d\theta} = \frac{h_t A(t_a - t_s)}{\lambda} \qquad \ldots \text{ Equation 7.}$$

where h_t = overall heat transfer coefficient B.T.U./(hr) (sq. ft) (°F)

2.3. Falling-Rate Drying Period

A wet material dries at a constant rate until a critical moisture content is reached when the flow of water from the underlying layers becomes insufficient to keep the surface of the material saturated; the drying rate then decreases continuously until drying is complete.

A knowledge of the drying characteristics of a material during this falling-rate period is essential to the designer of drying plant, since this period usually constitutes the major part of the total drying period, and since it is in this period that differences in the drying characteristics of different materials become most marked.

2.4. Factors Affecting The Drying Rate In The Falling-Rate Period

When a bed of material dries, water must travel to the surface of the bed either as liquid or vapour before it can be removed by the airstream. During the constant drying-rate period water can reach the surface as fast as it is removed in the airstream, and the drying rate depends only on the air conditions used, as described in Section 2.2.

During the falling-rate period, however, the drying rate is controlled by the rate at which water moves to the surface, and the drying rate depends not only on the air conditions but also on the mechanism by which the water is drawn to the surface.

The mechanism of water movement in a material during drying is not yet fully understood, but it is known to depend primarily on the moisture content and physical structure of the material. Several possible mechanisms have been suggested, including liquid and vapour diffusion (18, 19, 20), gravity (13), capillarity (2, 21, 22), convection (22), shrinkage and pressure gradients (23), and vaporization/condensation sequences caused by temperature gradients in the material (13).

Of the above mechanisms only the movement of water by diffusion and by capillarity have received adequate theoretical treatment to allow the prediction of the water distribution in a bed of material during drying.

2.5. Movement Of Water In A Material By Diffusion

Several workers (18, 19, 20, 24), assuming that during drying moisture moved through a wet material by diffusion (i.e. by random movement of the water molecules), developed theoretical equations, for materials of various shapes, relating the moisture content of the material with its drying time. These equations were based on the assumption that the rate of moisture diffusion was proportional to the moisture content gradient in the material - this may be represented by the equation.

$$\frac{\partial W}{\partial \theta} = D \frac{\partial^2 W}{\partial x^2} \qquad \ldots \text{ Equation 8.}$$

where $\frac{\partial W}{\partial \theta}$ = rate of moisture diffusion lbs water/(lb dry solid) (hr)

D = diffusivity of water ft^2/hr.

W = moisture content of material at time θ lbs water/lb dry solid.

x = distance from midplane of material in direction of diffusion. ft.

Equation 8 was integrated for various initial moisture distributions assuming that the diffusivity remained constant throughout the drying period. The integrated equations, which give the variation in the average moisture content of the material with time, are complex and tedious to calculate - for example, Sherwood (18) obtained the equation for an infinite slab drying from one surface only, and with an initially uniform moisture distribution.

$$\frac{W - W_e}{W_1 - W_e} = \frac{8}{\pi^2}\left[e^{-D\theta\left(\frac{\pi}{2a}\right)^2} + \frac{1}{9} e^{-9D\theta\left(\frac{\pi}{2a}\right)^2} + \frac{1}{25} e^{-25D\theta\left(\frac{\pi}{2a}\right)^2} + \ldots \right] \qquad \ldots \text{ Equation 9.}$$

where θ = drying time hrs.

W_1 = initial moisture content lbs water/lb dry solid

W_e = final (equilibrium moisture content) "

a = slab thickness ft.

Later workers (25, 26, 27) found that equations assuming a constant moisture diffusivity did not explain the experimentally observed drying behaviour of a number of materials; they suggested that an allowance had to be made for a decrease in moisture diffusivity with the moisture content of the material. The complexity of the mathematics involved prevented any useful analytical integration of the diffusion equation taking into account varying diffusivity. Van Arsdel (28), however, described an approximate numerical method of integrating the diffusion equation allowing for variable moisture diffusivities; and Peck, Griffith and Rao (27) suggested an empirical graphical method of representing the variation of diffusivity with moisture content which could be used to work out the moisture distribution in a wood slab at various times during drying.

Hougen, McCauley and Marshall (26) summarized the limitations of diffusion equations by stating that they could only be used to predict the drying behaviour of slow drying materials such as soap and pastes, and for the last stages of drying clays, textiles, paper and wood.

They also pointed out that diffusion equations did not give satisfactory predictions of the moisture content gradients occurring in these materials during drying; they therefore concluded that the frequent agreement between the predicted and experimentally observed drying behaviour was largely fortuitous. Sherwood, one of the early advocates of the diffusion theory (18), later reached a similar conclusion (29), and also pointed out that the basic assumption of the diffusion theory - that the rate of moisture diffusion was proportional to the moisture content gradient in the material - had apparently never been demonstrated experimentally.

Ceaglske and Hougen (2) showed conclusively that water movement in a bed of granular material was controlled by capillarity and gravity, and not by diffusion; they demonstrated this experimentally by showing that the water distribution in a bed of sand during drying could be explained by capillarity and gravity but not by diffusion, and by showing that capillarity could make water flow from a region of low moisture content to one of high moisture content - behaviour entirely inconsistent with the principles of diffusion.

FIGURE I

FORMS IN WHICH WATER IS PRESENT DURING DRYING OF A BED OF UNIFORM NON-POROUS SPHERES (ACCORDING TO HAINES (30))

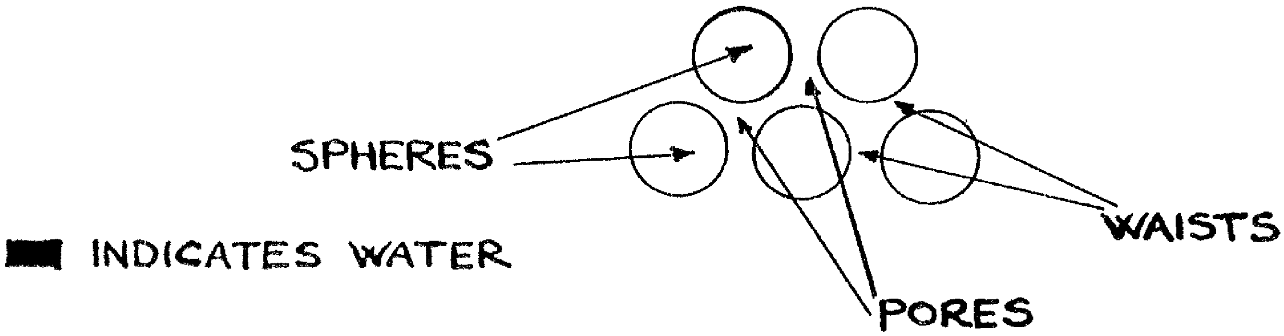

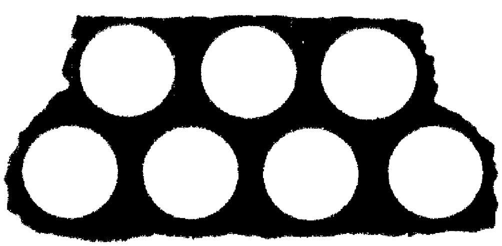

STATE 1

THE CAPILLARY STATE

(PORES COMPLETELY FULL OF WATER)

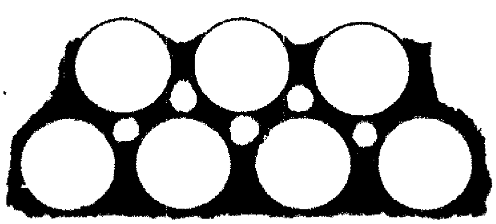

STATE 2

THE FUNICULAR STATE

(PORES PARTLY EMPTY, BUT SPHERES STILL COVERED BY A CONTINUOUS WATER-FILM)

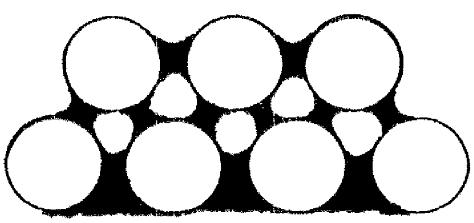

STATE 3

THE PENDULAR STATE

(CONTINUOUS WATER-FILM IS BROKEN AND WATER IS RETAINED AS LENS-SHAPED RINGS AT THE POINTS OF CONTACT OF THE SPHERES)

2.6. Movement Of Water In A Material By Capillarity

Several experimenters (2, 21, 22, 30) developed the capillary theory of drying which explains the movement of water in a bed of granular material during drying in terms of capillary forces acting on the water in the network of pores and narrow connecting-passages, called waists, enclosed by the solid particles.

The initial development of the capillary theory of drying was due to Haines (30) who made an extensive study of water movement and distribution in beds of uniform non-porous spheres. He distinguished three forms in which water may be present in a bed during drying (shown diagrammatically in Figure 1), and found that water movement could be described in terms of capillarity.

Capillarity is a well-known phenomenon, in which surface tension forces acting on a liquid enclosed in a capillary produce a suction, known as a suction potential, which is able to support the liquid in the capillary above the general liquid level. If the liquid is water, the suction potential P_s will cause the level in a uniform capillary to rise to a height h_s given by the equation.

$$P_s = h_s = \frac{2\sigma}{r' \rho g} \qquad \text{... Equation 10.}$$

where σ = surface tension of water g/sec^2

ρ = density of water g/cm^3

g = acceleration due to gravity cm/sec^2

r' = radius of capillary cm

P_s = suction potential just below the meniscus in the capillary cm water

The suction potential P_h at any other level in the capillary a distance h cms. below the meniscus is given by the equation.

$$P_s = P_h + h \qquad \ldots \text{ Equation 11.}$$

Haines (30) found that water movement in a bed of uniform non-porous spherical particles was due to similar suction potentials developing in the non-uniform interstitial capillaries - water being sucked from regions of low suction potential to those of high suction potential.

As can be seen from Equation 10, the suction potential exerted by a pore or waist is inversely proportional to its radius. An important result of this is that the removal of water from a pore is controlled by the higher suction potentials exerted by the narrower waists surrounding it. The suction potential required to suck water from a pore past the narrow waists protecting it is known as the entry suction potential of the pore.

The theoretical suction potential P of a pore formed by regularly packed, uniform, non-porous spherical particles can be calculated from a knowledge of the geometry of the pores and waists enclosed by the particles by the equation.

$$P = \frac{b\sigma}{r\rho g} \qquad \ldots \text{ Equation 12.}$$

where b = a factor depending on the type of packing of spheres.

r = radius of spherical particles cm.

If there is more than one type of packing present in a bed, the ability of a pore at the surface to suck water from another pore at a depth h' cm below it may be calculated using Equation 12 and the equation.

$$P_1 = P_2 + h' \qquad \text{... Equation 13.}$$

where P_1 = entry suction potential of surface pore cm.

P_2 = entry suction potential of a pore h' cm. below the surface cm.

When a bed is composed of granular material with irregularly shaped particles, the suction potentials of the pores cannot be calculated but must be measured experimentally by methods such as those described by Haines (30), and Oliver and Newitt (31).

The Capillary Theory Of Drying

Several workers (2, 22) have given the following explanation of the internal movement of water during the drying of a bed of granular material, initially saturated to the capillary state.

When drying commences, the water surface recedes into the waists between the surface particles, forming menisci which exert a suction potential on the water below. As evaporation proceeds, the menisci recede further into the narrower sections of the surface waists, and the suction potential increases. When it exceeds the entry suction potential of the largest surface pores, water is sucked from them and air enters the bed.

As drying continues, the suction potential at the surface of the bed continues to increase, and the largest pores at progressively greater depths are emptied and their contents drawn to the surface by the menisci in the finer surface waists.

During this period the drying rate is virtually constant, and the water in the bed is partly in the capillary state and partly in the funicular state.

On further drying, the entry suction potentials of progressively smaller surface pores are reached, and these, and similar pores within the bed, begin to empty with the result that the drying rate begins to fall off owing to the decreasing wet surface area available for evaporation. This process of emptying surface and internal pores continues until the funicular state breaks down at the surface, and water can no longer be drawn to the surface by capillary action.

Further drying of the pendular water in the bed must take place from a zone of vaporisation which recedes into the bed - the water vapour diffusing to the surface through the dry capillaries above them.

Limitations Of The Capillary Theory Of Drying

Pearse, Oliver and Newitt (22) considered that water flowing to the surface of a bed through interstitial capillaries would encounter a frictional or viscous drag proportional to its rate of flow. They thus proposed a modified form of Equation 13, containing a frictional term h_f, which gave the surface suction potential required to maintain a flow of water from a depth h' cm. below the surface.

$$P_1 = P_2 + h' + h_f \qquad \text{... Equation 14.}$$

where h_f = frictional resistance to flow through h' cm of bed cm water

They estimated the value of h_f to be expected in beds of spherical granules of various particle sizes. They found that for coarse particles of 10^{-1} to 10^{-2} cm. radius, frictional forces were negligible and capillary and gravitational forces were in equilibrium throughout the bed; for particles of 10^{-3} to 10^{-4} cm. radius, gravitational and frictional forces were unimportant; for very fine particles of 10^{-5} cm. radius and smaller, gravitational forces were negligible and both capillary and frictional forces were important.

Later work by Newitt and his co-workers (31, 32) showed that even the above modified capillary theory did not explain the drying behaviour of very fine materials.

Thus Oliver and Newitt (31) obtained results for silica flour of particle size $2 \cdot 5 \times 10^{-4}$ cm. radius which indicated that the water in the bed was less mobile than predicted by capillary theory. They suggested that the reason for this lack of mobility was that the high suction potentials produced in a bed of fine material could cause dissolved air to come out of solution forming bubbles which disrupted the capillary threads of water leading to the surface. Water could not therefore be drawn to the surface and drying proceeded by diffusion of water vapour to the surface, part of it inside the air bubbles.

In addition, Newitt and Coleman (32) found that water became immobile in the later stages of drying china clay, although all the pores were full of water. They postulated that water was adsorbed, or held by osmotic forces on the capillary walls, and thus had to vaporize inside the bed and diffuse as vapour to the surface.

Corben and Newitt (9), however, recently found that the drying behaviour of porous granules could be satisfactorily explained in terms of the capillary theory. Their postulated drying mechanism was similar to that described above for non-porous granules, but took into account the fact that the capillary movement of water could take place in the pores within the granules as well as in the voids between them.

3. LIMITATIONS OF DRYING THEORY WHEN USED TO PREDICT DRYING TIMES

The time taken to dry a material in a cross-circulation drier depends on the tray-loading used, and on the temperature, humidity and velocity of the airstream. To predict the drying time of a material under any specified drying conditions, it is therefore necessary to know accurately the combined effect of the above four factors on the drying time.

The problem of predicting drying times may be conveniently considered in two parts - the estimation of the duration of (a) the constant drying-rate period and (b) the falling-rate period.

3.1. Limitations Of Drying Theory When Used To Predict The Duration Of The Constant-Rate Period

Drying theory states that the drying rate of a material during the constant-rate period depends only on the air conditions used. The effect of air conditions on the constant drying rate has been described in Section 2.2. and may be represented by the various drying rate equations presented in that Section.

These equations are similar in that they all contain a driving force term which describes the effect of air temperature and humidity; an area term which describes the effect of surface area available for drying; and a proportionality constant which describes the effect of airflow and the physical structure of the material on the drying rate. Equation 7 may be taken as an example,

$$\frac{dw}{d\theta} = \frac{h_t A}{\lambda} (t_a - t_s)$$

where $(t_a - t_s)$ is the driving force term, A is the area term and h_t/λ is the proportionality constant.

The difficulty of applying equations of this type to a drying problem is the evaluation of the h_t term. While h_t can be calculated for a bed of small particles, such as sand, which has a plane bed-surface (3), it cannot be readily calculated for a bed of larger particles (greater than about $\frac{1}{8}$ inch mesh) for which the bed-surface is not plane, and the surface area exposed to the airstream is greater than the tray-area. For such material h_t must be found experimentally taking the area A in Equation 7 as the tray-area.

Even when the constant drying rate can be estimated, the duration of the constant drying-rate period cannot be calculated unless it is known how much water can be removed from the bed before the critical moisture content is reached, at which the constant drying-rate period ends. The critical moisture content of a bed of material, however, is a complex function of the physical structure of the material, the tray-loading and the air conditions. Since this has not yet been evaluated theoretically, the critical moisture content of a material under any specified drying conditions must be found experimentally.

3.2. Limitations Of Drying Theory Of The Falling-Rate Period

The greatest difficulty in predicting the drying time of a material is to estimate the duration of the falling-rate period. During this period the drying rate depends mainly on the rate at which water can reach the surface of the bed. The drying time increases rapidly with tray-loading because of the greater distances water must travel to the surface, and because of the difficulty, once the zone of vaporisation recedes below the surface, of supplying heat to the lower layers of the bed. Drying conditions have less effect on the drying rate than they have in the constant-rate period and the main factor influencing the drying rate is the resistance of the physical structure of the material to the movement of water.

The difficulty in predicting the drying rate during this period lies in the variety and complexity of the physical structures of different materials, in which water may be held in many forms. Thus water may be present as free water in the spaces between granules or fibres; it may be loosely held in some way inside pores or capillaries; strongly held inside cell-walls or adsorbed on pore walls; or very strongly held as chemically-bound water of hydration. Considering the variety of possible resistances to water movement in even a single material, it is not surprising that no general method of predicting the duration of the falling-rate period has yet been produced.

Drying theory of the falling-rate period has been mainly concerned with explaining the mechanism of moisture movement, and the resulting moisture distribution in a bed during drying. Of the several mechanisms of moisture movement mentioned in Section 2.4, only two - diffusion and capillarity - have been studied sufficiently to allow reasonably accurate estimates of the moisture movement to be made.

Each of these mechanisms applies to only a limited number of materials: the diffusion mechanism (Section 2.5) to slow drying materials like soap and pastes and to the last stages of drying wood, clays, textiles and paper; the capillary mechanism (Section 2.6) to small particles in the approximate size range 10^{-1} to 10^{-4} cm. radius. Although these mechanisms probably occur in other materials, fairly large deviations from the moisture movement predicted by the theory of either mechanism frequently occur - possibly owing to more than one mechanism occurring simultaneously, or to the mechanism changing in the course of drying.

The only theoretical method of predicting the duration of the falling-rate period which has appeared in the drying literature has been the use of integrated diffusion equations. The limitations of these equations (discussed in Section 2.5), however, indicate that predictions obtained by this method may be greatly inaccurate. In addition, these equations cannot be applied unless the diffusivity of water through the material is known; this usually has to be found from an experimental drying test.

Owing to the doubtful accuracy of the above theoretical equations, and since drying tests are required whether theoretical equations are used or not, the duration of the falling-rate period under various operating conditions is usually found directly from drying tests on the material in question.

4. EMPIRICAL METHODS OF PREDICTING DRYING TIMES

An experimental drying test is usually made by drying a tray of material under constant conditions of air temperature, humidity and velocity, and weighing the tray at intervals to determine the moisture loss; a drying curve of moisture content of the material against drying time can then be plotted, from which the drying time between any moisture contents can be obtained.

The individual effects of tray-loading, air temperature, humidity and velocity on the drying time are found by conducting a series of drying tests in which each factor in turn is given a number of different values in successive tests while the other factors are kept constant.

Three main methods of presenting the experimentally determined effects of the above four factors have been used, the purpose of each method being to facilitate the prediction of the drying time of the test material under any combination of operating conditions within the experimentally tested ranges of each factor.

The first method is to incorporate the effects of the various factors in empirical equations. This method has been used by several workers (24, 33, 34, 35, 36, 37) to describe the falling-rate period of a variety of materials. The equations usually relate the drying rate of the material with its free moisture content $(W - W_e)$. An example of this type of equation is that given by Simons, Koffolt and Withrow (33) for the drying rate of rayon yarn.

$$\frac{dW}{d\theta} = 0{\cdot}0031\ G^{1{\cdot}47}(H_s - H_a)\ (W - W_e) \qquad \ldots \text{ Equation 15.}$$

where $\frac{dW}{d\theta}$ = drying rate lbs water/(lb dry solid) (hr.)

H_s = saturation humidity of air corresponding to wet-bulb temp. of airstream lb water/lb dry air

H_a = humidity of airstream "

This method of predicting drying times is limited in application since it is not always possible to express the experimental results in an empirical equation.

The second method of presenting the effects of the various factors was used by Ede and Hales (7) to predict the drying times of various chopped vegetables. The method was based on the theoretical relationship (stated in Equation 4) that the drying rate of a surface-wet material is proportional to the wet-bulb depression ($t_a - t_w$) of the airstream used.

In this method a standard drying test was made with the tray-loading of material, air temperature, humidity and velocity at standard values, and the resulting drying curve of W against θ was re-plotted with the time co-ordinates multiplied by the value of the wet-bulb depression of the airstream used. This graph was taken to represent the drying curve which would have been obtained using an airstream of unit wet-bulb depression and standard conditions of airflow and tray-loading. To predict the drying time under any proposed operating conditions, the drying time shown on this curve was divided by the proposed wet-bulb depression of the airstream, and by separate correction factors to allow for differences in the proposed air velocity and tray-loading from the standard values.

The disadvantage of this method is that it can only be applied to very wet materials drying in the constant-rate period or in the first stages of the falling-rate period if moisture can be easily removed. It does not apply at lower moisture contents when the drying rate is not proportional to the wet-bulb depression.

The third method of presenting the effects of the various factors is in the form of nomographs. This method was used extensively by American workers to predict the drying times of various vegetables (38, 39). The nomographs predicted the drying times for each material at a standard tray-loading and air velocity, and for various wet-bulb temperatures and wet-bulb depressions. To allow for the different drying behaviour of the vegetables at high and low moisture contents, two nomographs were given for each material - one for moisture contents down to 0·1 lb water/lb bone dry solid, the other for moisture contents below this. Correction factors to allow for variations in air velocity and tray-loading from their standard values were given for each nomograph.

This method of predicting drying times may be applied to almost any material.

4.1. The Classical Method Of Experimentation

All these empirical methods of predicting drying times appear to have been based on experimental programmes planned by the method Brownlee (40) calls the "classical method of experimentation". By this method, the individual effects of several factors on a process are determined in a series of tests in which each factor in turn is varied while the rest are kept constant. There are two serious objections to this method of experimentation.

The first objection is that it assumes that each factor exerts its effect independently of the others. There is no fundamental reason why this should be so, and quite often the effect of a factor depends on the values of the other factors - the factors are said to interact.

As an illustration, assuming that a process yield depends on two factors A and B, then the effect of changing factor A from its normal value A_1 to a new value A_2 may produce a given change in the process yield when factor B is at a value B_1, but a different change in yield when factor B is at a value B_2.

The classical method of experimentation obviously cannot detect such interactions between factors since the effect of each factor is determined at only one value of the other factors. To get a fair assessment of the effect of a particular factor, the other factors must also be varied over their full range.

The second objection to the classical method of experimentation is that in determining the effect of each factor, the other factors must be kept constant at arbitrary values. If any of the factors interact, the estimated effect of each depends on the constant values chosen for the others. An estimate of the combined effect of all the factors affecting a process will therefore be accurate only if the interaction is small, or if the proposed design values of the various factors are close to the constant values for each used in the experimental tests. A grossly inaccurate estimate may be obtained if the interaction is large and the design values of the various factors are appreciably different from the constant values used in the tests.

There is fortunately an alternative method of experimentation - the factorial method - which can provide a solution to the above difficulties in estimating the combined effect of a number of factors.

4.2. The Factorial Method Of Experimentation

The factorial method of experimentation, which was originally developed to analyse the results of agricultural experiments by Fisher (41), and Yates (42), requires the effect of each factor on a process to be evaluated over the range of values chosen for each of the other factors.

In a preliminary study of a process it is usually sufficient to test two values (levels) of each factor; therefore in a factorial experiment to determine the effects of three factors, A, B and C on a process, eight tests covering all combinations of factor levels would be required. Denoting the lower and higher levels of each factor by the subscripts 1 and 2 these tests would be

$A_1\ B_1\ C_1$ $\quad$ $A_1\ B_2\ C_1$ $\quad$ $A_2\ B_1\ C_1$ $\quad$ $A_2\ B_2\ C_1$

$A_1\ B_1\ C_2$ $\quad$ $A_1\ B_2\ C_2$ $\quad$ $A_2\ B_1\ C_2$ $\quad$ $A_2\ B_2\ C_2$

The factorial method has three main advantages over the classical method of experimentation.

a) More precise estimates of the effects of the various factors may be obtained from a given number of tests, since the symmetrical programme of tests required by this method allows the result of every test to be used many times to determine the effect of each factor.

b) Since the tests required by this method cover a range of values of each factor, interactions between the factors can be detected, and the conclusions drawn from the tests are valid over a much wider range of operating conditions than those obtained by the classical method.

c) The tests required by this method provide an estimate of the experimental error (necessary to test whether the effect of a factor is real or due to experimental error) without the need for duplicate tests.

The above advantages of the factorial over the classical method of experimentation may be illustrated by considering both methods as applied to an experiment to determine the effect on a process yield y of changing three process variables A, B and C from their normal levels A_1 B_1 C_1 to some new values A_2 B_2 C_2.

In the classical experiment a test is made with the factors at their normal levels A_1 B_1 C_1 to find the yield $(A_1\ B_1\ C_1)y$ obtained under normal conditions. To estimate the effect of factor A, a second test is made with A at the new level A_2 and the other two factors still at their normal levels B_1 and C_1 - this test may be denoted by A_2 B_1 C_1 and the yield obtained under these conditions by $(A_2\ B_1\ C_1)y$. The difference in the two yields is the estimated effect of A. Thus

$$\text{Effect of A} = (A_1\ B_1\ C_1)y - (A_2\ B_1\ C_1)y$$

Similarly the effects of factors B and C can be found from tests A_1 B_2 C_1 and A_1 B_1 C_2 respectively.

$$\text{Effect of B} = (A_1\ B_1\ C_1)y - (A_1\ B_2\ C_1)y$$

$$\text{Effect of C} = (A_1\ B_1\ C_1)y - (A_1\ B_1\ C_2)y$$

Without an estimate of the experimental error it is, however, impossible to say whether any of these effects is real, or is due to experimental error. Since the experimental error cannot be estimated from less than two observations, each of the tests must be repeated at least once, so that a total of eight tests must be made.

Each effect is thus estimated as the difference between two means, each of which is the mean result of two tests.

This experiment cannot detect interactions between the factors – thus the effect of A with B at B_1 may be quite different from its effect with B at B_2 but the experiment can only estimate the effect of A with B at B_1.

In the factorial experiment the eight tests shown on page 33 are made. To make the following discussion of the experiment easier to understand, the tests may be visualized as the co-ordinates of the eight corners of a cube whose axes are A, B and C.

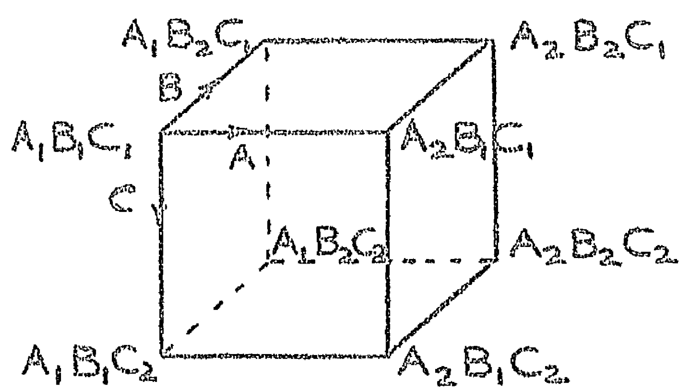

The effect of A is estimated as the difference between the average yield of the tests in the A_1 plane (i.e. the average of $(A_1\ B_1\ C_1)y$, $(A_1\ B_1\ C_2)y$, $(A_1\ B_2\ C_1)y$ and $(A_1\ B_2\ C_2)y$) and the average yield of the tests in the A_2 plane (i.e. the average of $(A_2\ B_1\ C_1)y$, $(A_2\ B_1\ C_2)y$, $(A_2\ B_2\ C_1)y$ and $(A_2\ B_2\ C_2)y$). The reasoning behind this estimate of the effect of A is that, as a first approximation, the effect of changing from A_1 to A_2 is independent of the values of B and C used. The differences in yields obtained in tests at the corresponding corners of the cube in the A_1 and A_2 planes are therefore all considered as independent estimates of the effect of A.

The effects of B and C are estimated similarly.

The advantage of the factorial experiment in giving more precise estimates of the effects of a number of factors for a given number of tests is illustrated by the fact that in the present experiment the effects of A, B and C are each estimated as the difference between the mean yields obtained in two sets of four tests, while in the classical experiment they were estimated as the difference between the mean yields obtained in two sets of two tests. Each experiment required eight tests. The superiority of the factorial experiment lies in the fact that the result of each test is used many times over, while in the classical experiment only the result of the standard test is used more than once.

In addition to estimating the main effects A, B and C the factorial experiment can detect interactions between the various factors.

To estimate the interaction between the A and B factors, the four yields in the C_1 plane at the top of the cube are averaged with the corresponding four yields in the C_2 plane at the bottom of the cube. e.g.

$$\frac{(A_1\ B_1\ C_1)y + (A_1\ B_1\ C_2)y}{2} = (A_1\ B_1)y\ \bar{C}$$

$\bar{C}$ indicating that the yields are averaged over C. The four averages over C obtained are.

$(A_1\ B_1)y\ \bar{C}$, $(A_2\ B_1)y\ \bar{C}$ from the front face of cube

$(A_1\ B_2)y\ \bar{C}$ $(A_2\ B_2)y\ \bar{C}$ from the back face of cube

the difference between the two front face averages estimate the effect of A at B_1, and the difference between the back face averages estimate the effect of A at B_2. Since each of the above averages was the mean yield of two tests, the experimental error can be estimated and can be used to test whether the effect of A at B_1 is significantly different from the effect of A at B_2 (the method of making this statistical significance test is described under the Analysis of Variance). If these two effects differ significantly there is said to be an interaction between A and B.

The interactions between the other factors can be estimated similarly.

The Analysis Of Variance

Owing to the great expense involved in constructing a full-scale chemical plant or in experimenting on an existing full-scale plant, considerable sums of money frequently depend on the conclusions drawn from a limited number of experimental tests.

The experimenter may make two serious types of error in interpreting his experimental results: he may pronounce an effect or interaction to be real when in fact it is not, with the result that further expensive testing is undertaken; or he may overlook an effect or interaction which is real, with the possible result that a superior process may be overlooked. The chance of making a wrong conclusion is greatly increased, and mental judgement of experimental results becomes almost impossible, when the effects or interactions to be considered are approximately of the same magnitude as the experimental error.

Fortunately there are statistical tests of significance which, when used to analyse experimental data, can identify the significant effects and interactions, and also indicate the probability of an incorrect conclusion.

The programme of tests used in a factorial experiment is designed so that the effects and interactions estimated from the test results can be analysed efficiently by a statistical test of significance known as the "Analysis of Variance". The theoretical basis of the analysis of variance can be found in any standard statistical textbook (43, 44, 45, 46) but the principles of the analysis may be outlined in the following manner:

The various combinations of experimental conditions used in the series of tests making up a factorial experiment generally produce a range of values in the dependent variable measured in the tests. The scatter of the values obtained may be measured by the statistical quantity known as the "variance". In addition to the total variance of the values obtained, smaller variances can be attributed to the effects of the various factors and to interactions between them. Variance, however, is an additive quantity and the total variance is equal to the sum of the component variances, plus the residual variance which cannot be attributed to any definite cause; this residual variance is used as a measure of the experimental error.

The method used to test whether the effect of a certain factor can be considered significant, is to postulate that the effect does not exist, and to see whether on this hypothesis the observed difference between the variance attributed to this effect and the experimental error variance can be reasonably expected to occur by chance. Interactions between the factors are tested similarly. The difference between the two variances is calculated by the ratio

$$\frac{\text{Variance due to effect or interaction}}{\text{Variance due to experimental error}} = F$$

and from tables of F (47) the probability of an equally large value of F occurring by chance (i.e. when there is no real effect or interaction) can be found. Before an effect or interaction is considered significant this probability must usually be below an arbitrary level of 5%. By choosing this probability level (or significance level as it is sometimes called) there is a smaller than 5% chance of being wrong in asserting that an effect or interaction is significant. Other significance levels e.g. 10%, 1%, 0·1% may, however, be used, depending on the degree of certainty required in the conclusions drawn from the experiment.

The method of conducting the analysis of variance for the four-factor, two-level factorial experiments used in this thesis, is described in Appendix 2.

Disadvantages Of The Factorial Method Of Experimentation

The main disadvantage of the factorial method of experimentation is that the number of tests required rapidly becomes excessive if there are more than a few factors to be tested: even if each factor is tested at only two levels a factorial experiment for n factors requires 2^n tests; a six factor experiment therefore requires 2^6 = 64 tests.

A disadvantage of the simple two-level factorial experiment is that although it identifies the significant effects and interactions between the factors affecting a process, it gives little information on the relationship between the value of the dependent variable and the values of the significant factors involved. To define this relationship a more elaborate factorial experiment encompassing at least three levels of each factor is required. Such an experiment requires many more tests than the two-level experiment - 3^n instead of 2^n, which for a four factor experiment would be an increase from 16 to 81 tests.

Two methods of experimentation have been developed to reduce the number of tests required in a multi-factor factorial experiment to manageable proportions.

Fractional Factorial Experiments

The first method was based on the observation that a considerable proportion of the tests required in a large factorial experiment are wasted in estimating the experimental error to an unnecessary degree of precision, and in estimating high order interactions (i.e. interactions involving a large number of factors) which are almost certain to be insignificant. By sacrificing these high order interactions and some of the precision in estimating the experimental error it was found (48) that only a selected fraction of the complete factorial experiment need be done to obtain satisfactory estimates of the main effects and low order interactions.

Such fractional experiments have been found useful in the preliminary exploration of a large number of factors to pick out the factors worthy of further study (49).

The Sequential Method Of Experimentation

The second method of reducing the number of tests required in a multi-factor factorial experiment is to conduct the experiment in a series of small groups of tests - the tests in each group being planned from the results of the previous group. In addition to reducing the number of tests required, this sequential method of experimentation often gives more information than the rigid programme of tests required by the complete factorial: this is possible because the scope of the investigation can be narrowed after each stage to study only the significant factors in greater and greater detail; moreover, the tests can be stopped at any stage when sufficient data on the significant factors have been obtained.

In practice, an experiment based on this method of experimentation would probably start with a small, two-level factorial experiment testing some of the factors, or with a fractional factorial experiment testing all the factors. In subsequent stages of the experiment, insignificant factors would be kept constant, further factors might be examined, and significant factors would be tested at more levels.

4.3. The Scope Of The Present Investigation

A two-level factorial experiment is used to examine the effects of loading of material, air temperature, humidity and velocity on the drying times of fibrous, and porous-granular materials in

a) a cross-circulation drier.

b) a through-circulation drier.

From the information gained in this experiment concerning the effects of the above factors, a more elaborate fractional three-level factorial experiment is designed to provide the data necessary to allow the drying times of these materials to be predicted under any set of operating conditions within the experimentally tested ranges of the above factors.

The accuracy of the predictions based on this experiment is compared with the probable accuracy of predictions based on a corresponding classical experiment.

5. EXPERIMENTAL APPARATUS AND PROCEDURE

5.1. Description Of The Experimental Cross-Circulation Drier.

An experimental cross-circulation drier was built for the drying tests. A sketch of the drier is shown in Figure 2 and a photograph in Figure 3.

A fan produced a steady airstream which was heated and humidified to the desired temperature and humidity, and passed across the surface of a tray of the wet material; the progress of drying was followed by recording weight-loss of the material.

The airflow across the tray could be varied by altering the fan-speed by means of a nine-position starter (rough control), and a rheostat (fine control) fitted to the D.C. fan-motor. Airflows from 3 to 15 lbs dry air/(sq. ft. drier cross-section) (min) could be maintained across the tray. The airflow was measured by a $1\frac{1}{2}$ inch diameter orifice plate in the 5 inch diameter inlet pipe, connected to an inclined "U" tube water manometer.

A 1/16 inch mesh copper-gauze partition across the duct at the fan outlet distributed the airstream evenly over the heaters.

Eight independently controlled 1 kW. electric bar heaters, one of which was controlled by a "Sunvic" thermostat, could heat the airstream to any temperature up to 250°F and maintain it within $\pm$ 0·5F°.

The heated airstream passed up a rising duct, designed to prevent radiation from the heaters reaching the inlet thermometers and wet material in the test section. Four aluminium baffles which mixed the airstream to give it an even temperature distribution across

FIGURE 2

CROSS-CIRCULATION DRIER

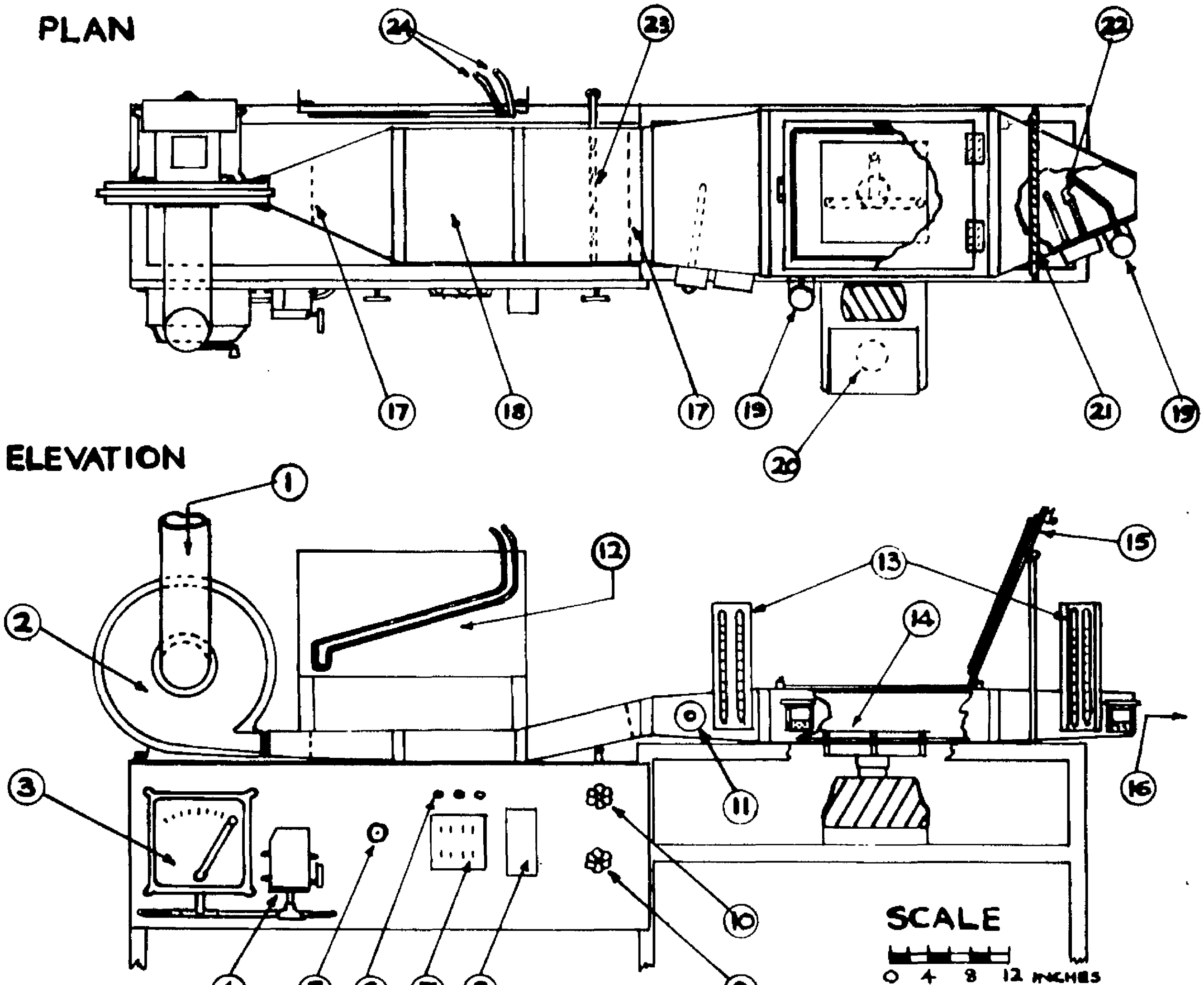

1 AIR INLET	9 MAINS STEAM VALVE	17 COPPER GAUZE
2 FAN	10 STEAM CONTROL-VALVE	18 HEATER BOX
3 FAN STARTER	11 THERMOSTAT CONTROL	19 WATER RESERVOIR
4 FAN FUSEBOX	12 WATER MANOMETER	20 BALANCE
5 FAN FINE CONTROL	13 THERMOMETERS	21 DOOR SUPPORT
6 INDICATOR LIGHTS	14 WEIGHING PAN	22 WET-BULB WICK
7 HEATER SWITCHES	15 DOOR	23 STEAM INJECTOR
8 THERMOSTAT	16 AIR OUTLET	24 CONNECTING TUBES FROM ORIFICE PLATE

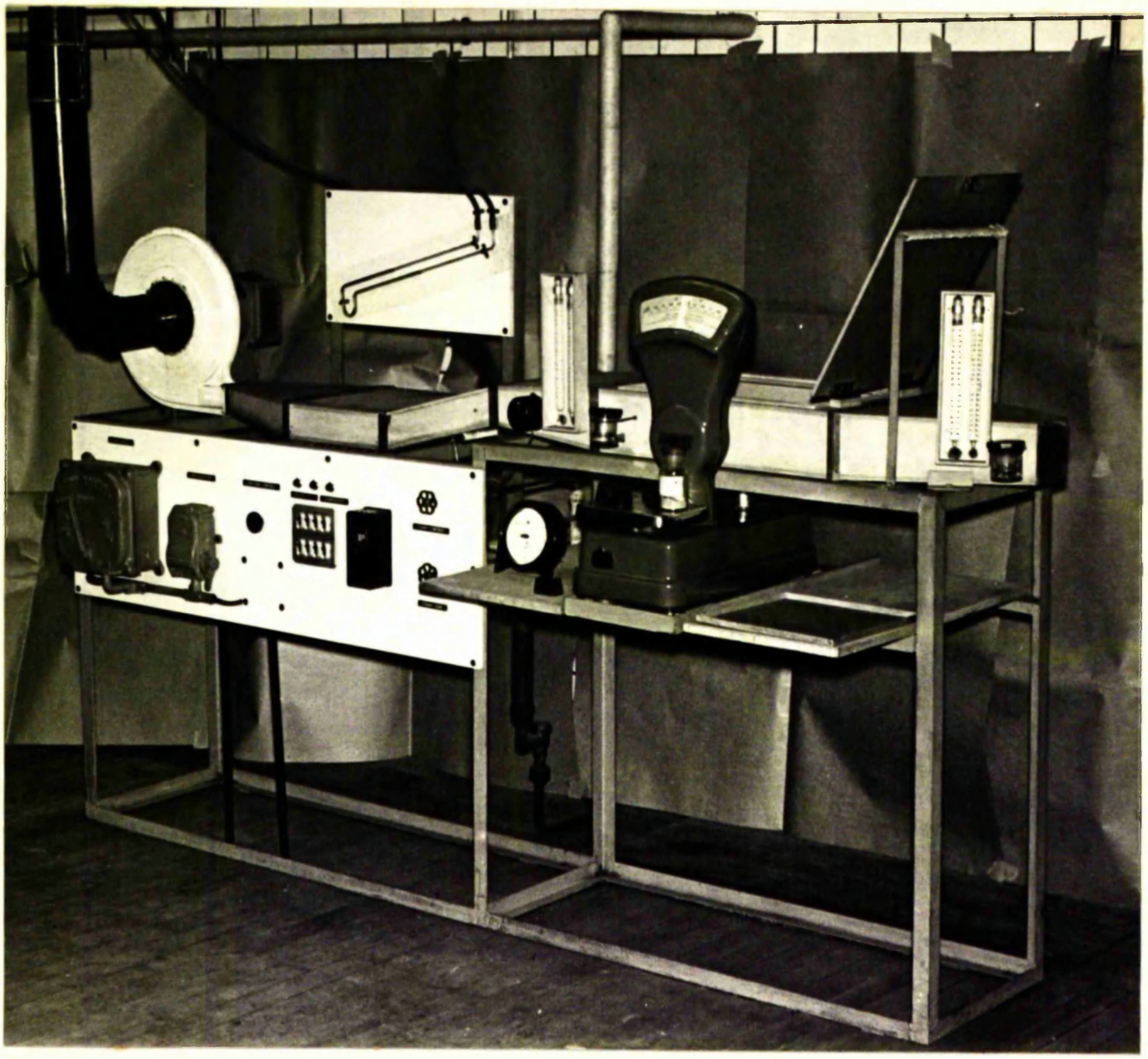

FIGURE 3.

EXPERIMENTAL CROSS-CIRCULATION DRIER.

the duct, also helped to prevent radiation reaching the test section.

The airstream could be humidified by injecting low pressure steam (at 15 lb/sq. in. gauge) through four jets drilled in the floor of the duct. A steam separator and steam trap removed condensate from the steam supplied to the jets; a ¼ inch high steel weir and a drain were placed at the lower end of the duct to prevent damage to the heaters by condensate seeping down the duct if the steam separator failed. Manual operation of the steam control-valve kept the airstream humidity constant during a drying test.

A 1/16 inch mesh copper-gauze partition at the top of the duct distributed the airflow evenly across the test tray.

The temperature and humidity of the airstream were measured by dry-bulb and wet-bulb thermometers at the inlet and outlet of the test section; the wet-bulb wicks were supplied with distilled water from reservoirs fitted externally on the side of the drier.

During a drying test, the wet material, spread on a 12 inch square aluminium tray with ½ inch sides, was weighed continuously on an "Avery" automatic balance, the weighing pan of which was mounted inside the drier on three ½ inch diameter brass pins passing through close-clearance holes in the floor of the drier. The weighing accuracy was ± 0·001 lb.

The drier ducting was constructed entirely of ⅜ inch thick "Sindanyo" asbestos-cement insulating board. The ducting was in sections, held together by 1 inch broad steel straps, the joints between the section ends being made airtight with heat-resisting cement. Any section could be easily opened to allow maintenance

FIGURE 4

CROSS-CIRCULATION DRIER

HEATER BOX WITH COVER REMOVED

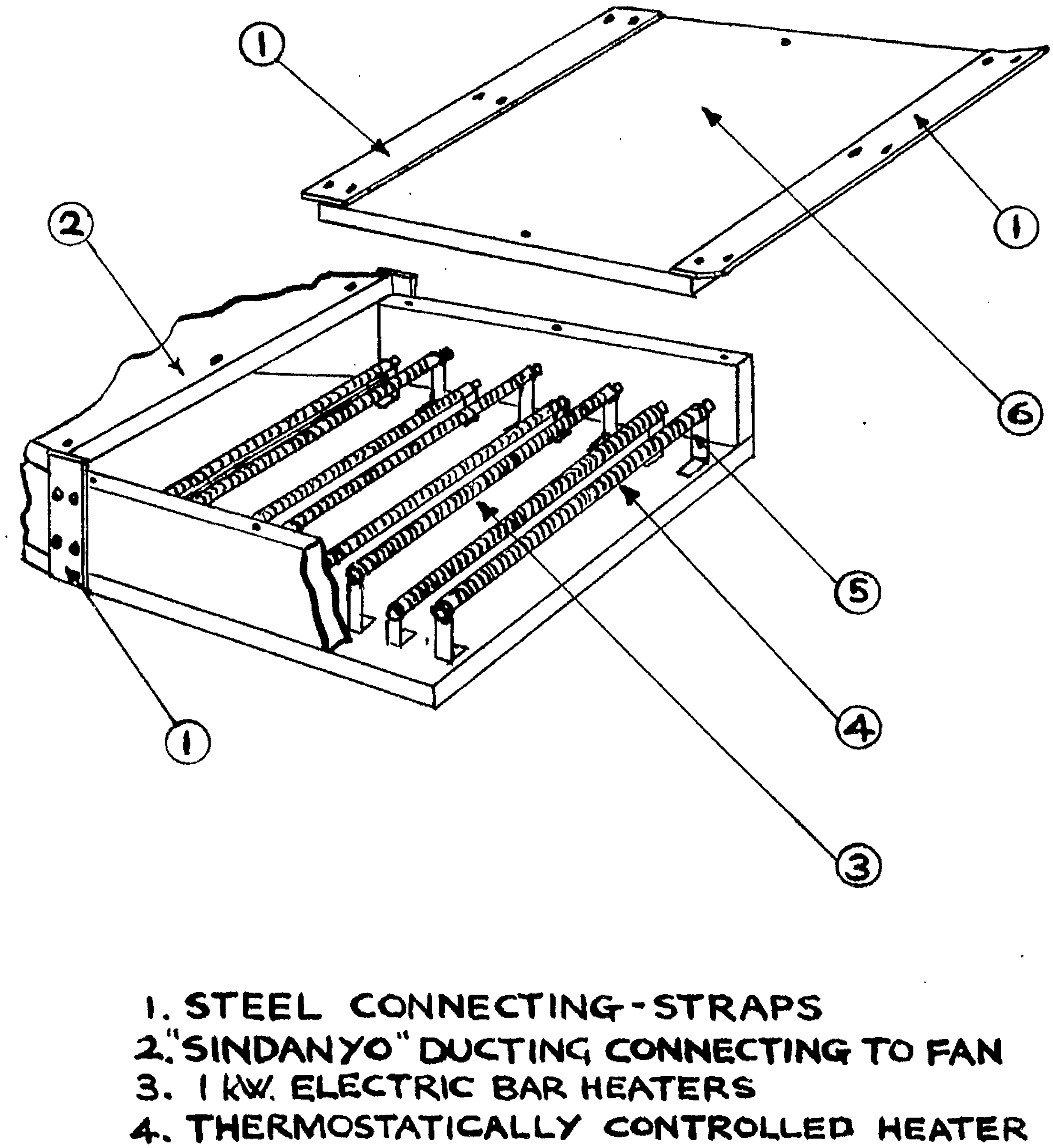

1. STEEL CONNECTING-STRAPS
2. "SINDANYO" DUCTING CONNECTING TO FAN
3. 1 KW. ELECTRIC BAR HEATERS
4. THERMOSTATICALLY CONTROLLED HEATER
5. BRASS SUPPORT FOR HEATER
6. HEATER BOX COVER

of the heaters, steam jets etc., by removing the top straps holding it at the ends and unscrewing the top board from the sides of the duct.

The fan controls, steam valves and heater switches were mounted on a control panel, and the control element of the "Sunvic" thermostat was mounted in the airstream at the inlet to the test section of the drier. Separate red lights on the control panel indicated when the A.C. electricity for the heaters, the D.C. electricity for the fan, and the thermostatically controlled heater were in use.

5.2. Calibration Of Control Instruments

The readings on the inclined "U" tube water manometer indicating the airflow across the test tray were calibrated in lbs dry air passing/(sq. ft. cross sectional area of the test section) (min) by measuring various airflows through the drier by means of a vane anemometer held in the outlet duct of the drier.

The thermometers were checked against a standard thermometer.

The wet-bulb thermometer readings were checked at various temperatures and airflows by finding the atmospheric humidity at room temperature by means of a sling psychrometer, and calculating from a psychrometric chart (13), the wet-bulb temperature of this air when heated in the drier to a given temperature. The wet-bulb thermometers were found to read up to 2F° high at high temperatures and low airflows; corrections to the observed wet-bulb temperatures were calculated for the various airflows and temperatures used in the drying tests.

5.3. Experimental Procedure

The fan was started and the fan-speed was adjusted to give the desired airflow; this airflow was maintained steady during the drying test by manual operation of the rheostat.

Sufficient heaters were switchedontoheat the airstream to just below the required temperature, and the thermostatically controlled heater was set to make the final temperature adjustment.

If necessary, the humidity of the airstream was raised by steam injection. Before operating the steam injector, the steam line to the drier was purged of condensate by opening the steam mains-valve with the steam control-valve closed (see Figure 6); when the line was clear, steam was admitted to the drier by opening the steam control-valve, and the humidity of the airstream was maintained at the desired value by manual operation of the steam control-valve.

While the drier heated up, the test tray was counterpoised on the balance with the drier closed. The tray was then removed and the required loading of wet material was spread evenly on it. When the air conditions in the drier had stabilised at the required temperature, humidity and airflow, the tray was replaced on the balance pan, the drier was closed, and the timer was started.

The progress of drying was followed by noting the weight of the material at regular intervals - usually five minutes for the first hour, ten minutes for the next four hours, and twenty minutes for the remainder of the test. The test was stopped after eight to ten hours or sooner if the weight loss became less than 0·001 lb in ten minutes; the residual moisture in the material was determined by oven drying duplicate samples (approximately 30g. for coke; 60g. for porous-ceramic granules; 9g. for brewers' spent-grain) for twenty-four hours at 110°C.

FIGURE 5

CROSS-CIRCULATION DRIER

SIDE ELEVATION OF RISING DUCT

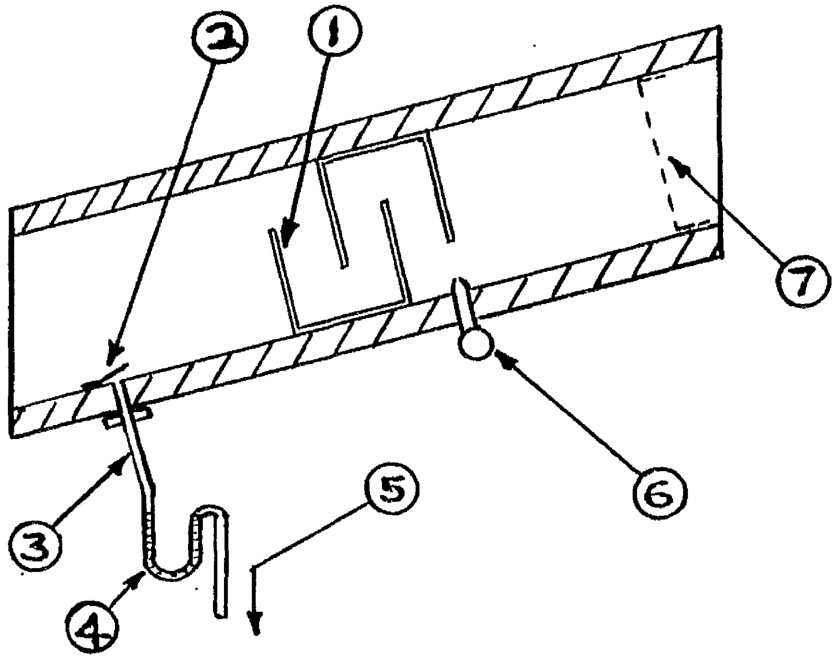

1 BAFFLES
2 WEIR
3 DRAIN
4 WATER SEAL TO PREVENT AIR LEAKAGE
5 CONDENSATE TO DRAIN
6 STEAM INJECTOR
7 COPPER GAUZE

FIGURE 6

REAR VIEW OF RISING DUCT SHOWING DETAIL OF STEAM INJECTION SYSTEM

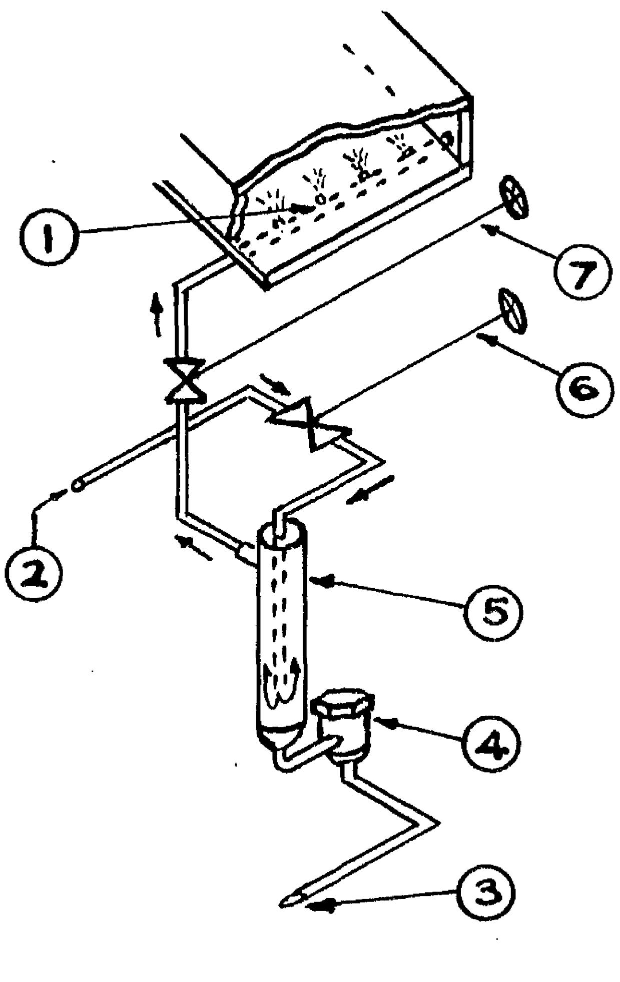

THE ARROWS INDICATE THE PATH OF THE STEAM THROUGH THE SYSTEM.

1 STEAM JETS
2 STEAM INLET
3 CONDENSATE OUTLET
4 STEAM TRAP
5 STEAM SEPARATOR
6 STEAM MAINS-VALVE
7 STEAM CONTROL-VALVE

5.4. Presentation Of The Results Of A Drying Test

A specimen of the data obtained in a drying test is given in Appendix 1.

The weight of bone-dry solid (B.D.S.) in the material used in the test was calculated from its final weight and residual moisture content. By subtracting the weight of B.D.S. from the total weight of material, the weight of water in the material and hence its average moisture content W(lbs water/lb B.D.S.) was calculated at the various times during the test. The drying curve of moisture content W against drying time θ' in mins. was then plotted.

The constant drying rate was found by measuring the slope of the linear portion of the drying curve.

The form of the relationship between the moisture content and the drying time in the falling rate period was found by plotting various transformations of the test data such as log W against log θ'; W against log θ'; log W against θ'; until a linear relationship was found between the transformed variables. The slope of the graph was used to characterize the exact relationship between the transformed variables so that by stating the transformation used and the slope obtained, the drying time between any moisture contents in the falling rate period could be calculated.

The critical moisture content was found from the drying curve of W against θ'.

6. CROSS-CIRCULATION DRYING RESULTS

6.1. Drying of Porous-Ceramic Granules

The first porous-granular material tested was porous-ceramic granules of the porcelain grade F10 manufactured by Doulton Industrial Porcelains Ltd., Tamworth, Staffs. This material was chosen as representative of a porous-granular material of homogeneous physical structure, with particles of uniform shape and size which did not shrink or break down on drying, and which could also be conveniently dried in a through-circulation drier. The granules were cylindrical, ¼ inch long, and although of ¼ inch nominal diameter, they tapered slightly along their axis. Their average dimensions were ¼ inch long by ¼ inch diameter at one end tapering to 15/64 inch diameter at the other end. The maximum pore size of the material was 7-10 microns. The bulk density of the dry material was 46 lbs/cub.ft.

Preparation of the Granules for a Drying Test

The granules were soaked in distilled water for a standard period of twenty-four hours, then allowed to drain for ten minutes, and most of the excess surface moisture was removed by rolling the granules in a dry cloth before they were spread on the test-tray. This procedure left the granules with an approximately constant initial moisture content of 0.296 lb. water/lb. B.D.S. (the maximum moisture content obtained was 0.310, the minimum 0.272 lb. water/lb. B.D.S.).

Distilled water was used in preference to tap-water to soak the granules since these were re-used several times and there was a possibility of the dissolved salts in tap-water depositing in the pores of the granules, thus progressively changing the drying behaviour of the material during a series of drying tests.

Drying Conditions Used In The Drying Tests

Suitable experimental ranges were chosen for the four factors - loading, airflow, air temperature and humidity - whose effects on the drying times of the porous-ceramic granules, coke and brewers' spent-grain used in this investigation were to be studied. These ranges were determined from a series of preliminary drying tests on all three materials in the cross-circulation and through-circulation driers. The ranges chosen gave measurable differences in drying times but avoided excessively long or excessively short drying times. In addition, the ranges chosen for each material and drier were approximately the same, to facilitate comparison between the drying behaviour of the various materials and the drying performance of the two driers.

In this Section, and in subsequent Sections, the following nomenclature is used to denote the drying conditions used in a drying test.

D_1, D_2, D_3 = dry-bulb temperature of airstream ^oF

W_1, W_2, W_3 = wet-bulb " " " "

H_1, H_2, H_3 = humidity of airstream lb water/lb dry air

L_1, L_2, L_3 = dry loading of material lbs/sq.ft tray or basket area

G_1, G_2, G_3 = airflow lbs dry air/sq.ft drier cross-section)(min)

Subscript 1 refers to the minimum value; 2 to the middle value; and 3 to the maximum value of the respective factors.

The ranges of the various factors used in the cross-circulation drying tests on the porous-ceramic granules are shown in Table 1.

TABLE 1.

$D_1 = 130$	$W_1 = 95$	$L_1 = 1.40$(single layer)	$G_1 = 5$
$D_2 = 170$	$W_2 = 106$	$L_2 = 2.62$($\frac{5}{8}$ inch ")	$G_2 = 9$
$D_3 = 210$	$W_3 = 117$	$L_3 = 3.85$(1 inch ")	$G_3 = 13$

Note: From Table 1, it may be noted that the effect of the airstream humidity on the drying time of the granules was determined by testing a range of wet-bulb temperatures and not by testing a range of absolute air humidities. The advantage of studying W, rather than H, as a factor affecting the drying time of the granules, is that by studying W the experimental air humidities to be tested can be stated simply as values of D and W; if H is studied, a psychrometric chart has to be consulted to find the values of W to be used in the drier to correspond with the required air humidities at each value of D. Since the method of predicting drying times described in this Section is empirical, it is immaterial whether the effect of W, or of H, on the drying time is determined. To illustrate this, the effect of W on the drying time of porous-ceramic granules and coke, and the effect of H on the drying time of brewers' spent grain, have been studied in both experimental driers.

6. 2. Preliminary Two-Level Factorial Experiment On Porous-Ceramic Granules

The extreme values of the four factors given in Table 1 (i.e. levels 1 and 3) were used in a preliminary two-level factorial experiment involving sixteen drying tests. To minimise the chance of bias in the test results due to possible progressive changes in the granules with use, the drying tests were made in random order. The drying curves obtained in this experiment are shown in Figures 7,8,9 and 10 and the derived results are shown in Table 2.

TABLE 2: Results Of Preliminary Two-Level Factorial Experiment On Porous-Ceramic Granules

Test Conditions	$\frac{dW}{d\theta}$	$\log_{10}\frac{100dW}{d\theta}$	W_c	C
$D_1W_1L_1G_1$	0.0473	0.6749	0.142	-0.429
$D_1W_1L_1G_3$	0.1140	1.0569	0.136	-0.410
$D_1W_3L_1G_1$	0.0163	0.2122	-	-
$D_1W_3L_1G_3$	0.0464	0.6665	0.151	-0.405
$D_3W_1L_1G_1$	0.1600	1.2041	0.131	-0.361
$D_3W_1L_1G_3$	0.3660	1.5635	0.122	-0.388
$D_3W_3L_1G_1$	0.1371	1.1370	0.134	-0.377
$D_3W_3L_1G_3$	0.3085	1.4893	0.125	-0.382
$D_1W_1L_3G_1$	0.0145	0.1614	0.181	-0.258
$D_1W_1L_3G_3$	0.0441	0.6444	0.190	-0.250
$D_1W_3L_3G_1$	0.0053	-0.2757	-	-
$D_1W_3L_3G_3$	0.0154	0.1875	0.137	-0.271
$D_3W_1L_3G_1$	0.0586	0.7679	0.180	-0.273
$D_3W_1L_3G_3$	0.1320	1.1206	0.190	-0.302
$D_3W_3L_3G_1$	0.0440	0.6435	0.175	-0.299
$D_3W_3L_3G_3$	0.1090	1.0374	0.179	-0.305

The various quantities shown in Table 2 were derived as follows: The constant drying rate $\frac{dW}{d\theta}$ was calculated from the slope of the linear portion of the drying curve of W against θ' and the critical moisture content W_c was taken as the moisture content at which the drying curve departed from linearity. The rate constant C is the slope of the linear portion of the curve of W against $\log_{10}\theta'$ (see Figure 11). This transformation of the test data was used to describe the relationship between W and θ' in the falling-rate period since, when plotted, it

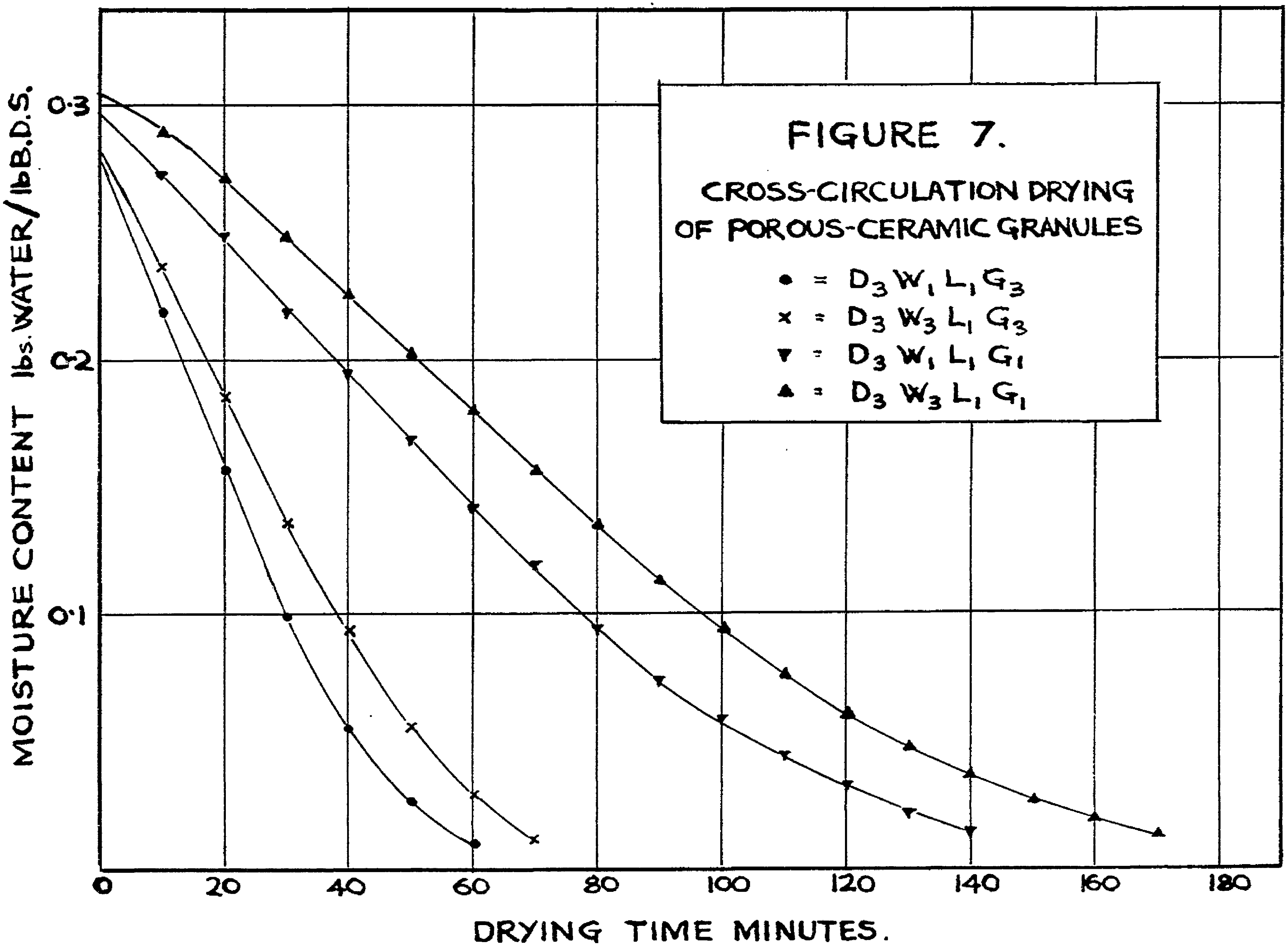
FIGURE 7.
CROSS-CIRCULATION DRYING
OF POROUS-CERAMIC GRANULES
● = D3 W1 L1 G3
× = D3 W3 L1 G3
▼ = D3 W1 L1 G1
▲ = D3 W3 L1 G1
MOISTURE CONTENT lbs. WATER/lb B.D.S.
0·3
0·2
0·1
0
20
40
60
80
100
120
140
160
180
DRYING TIME MINUTES.

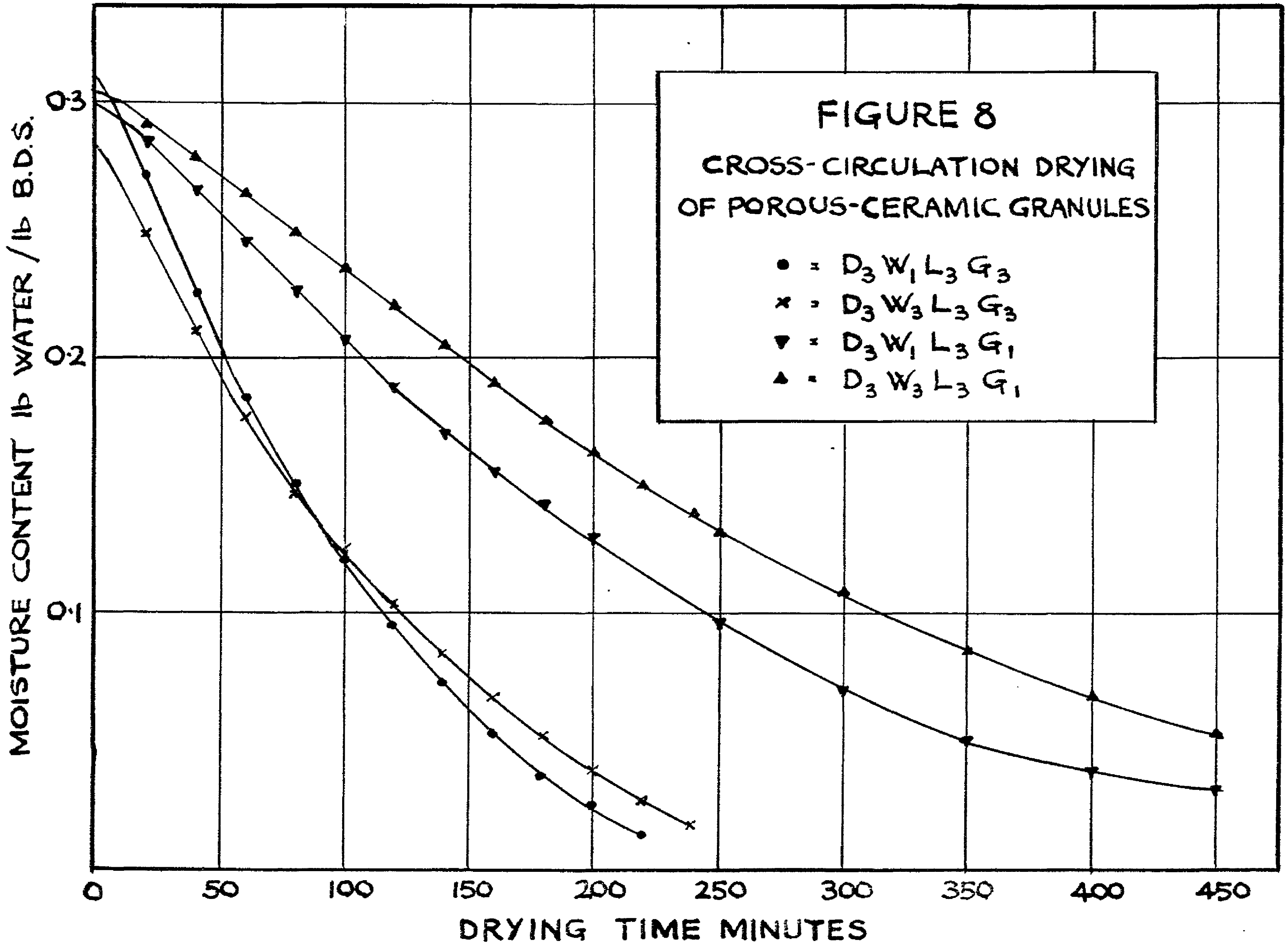
FIGURE 8
CROSS-CIRCULATION DRYING
OF POROUS-CERAMIC GRANULES
● = D3 W1 L3 G3
× = D3 W3 L3 G3
▼ = D3 W1 L3 G1
▲ = D3 W3 L3 G1
MOISTURE CONTENT lb WATER / lb B.D.S.
0·3
0·2
0·1
0
50
100
150
200
250
300
350
400
450
DRYING TIME MINUTES

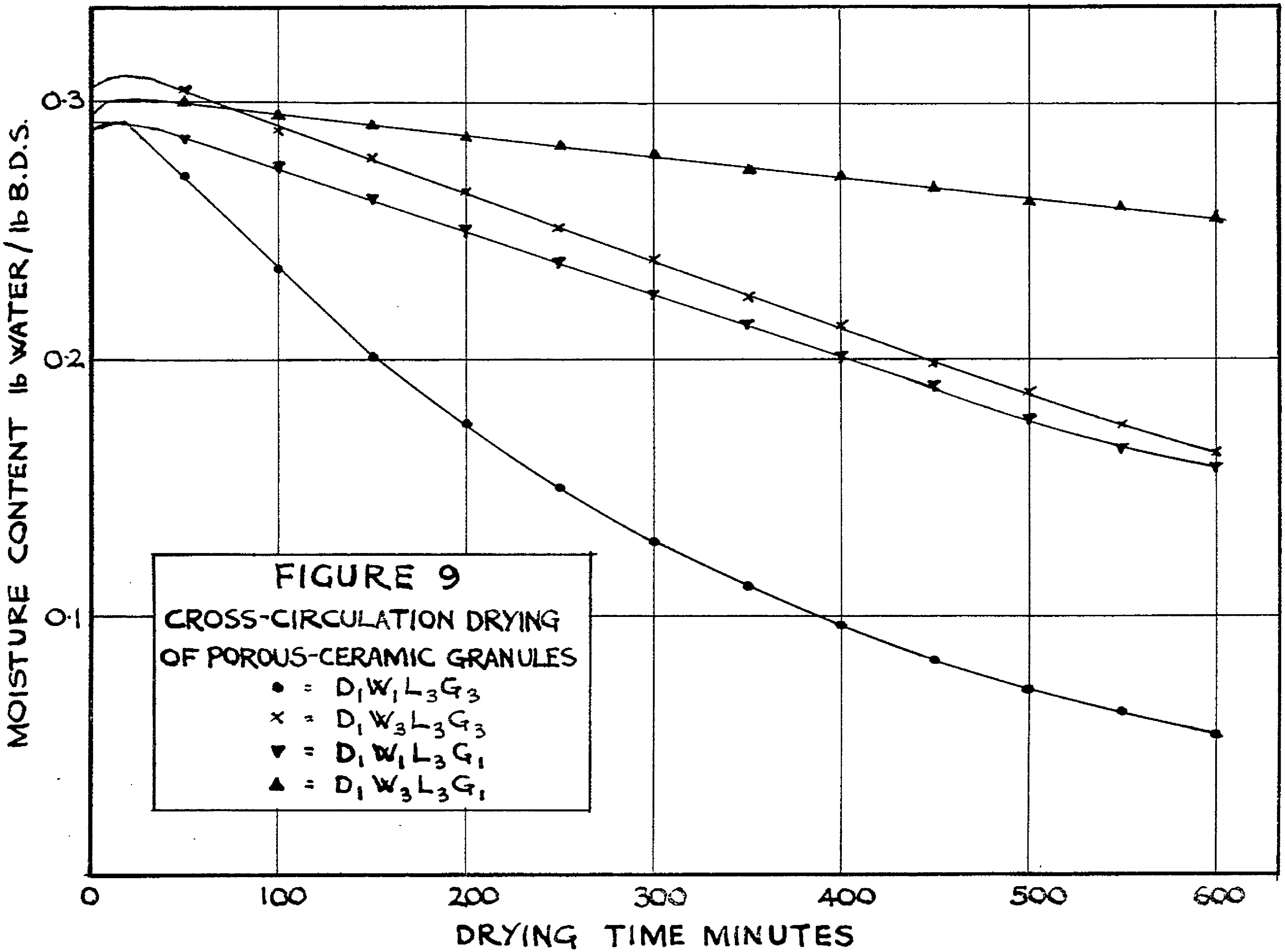

FIGURE 9

CROSS-CIRCULATION DRYING OF POROUS-CERAMIC GRANULES

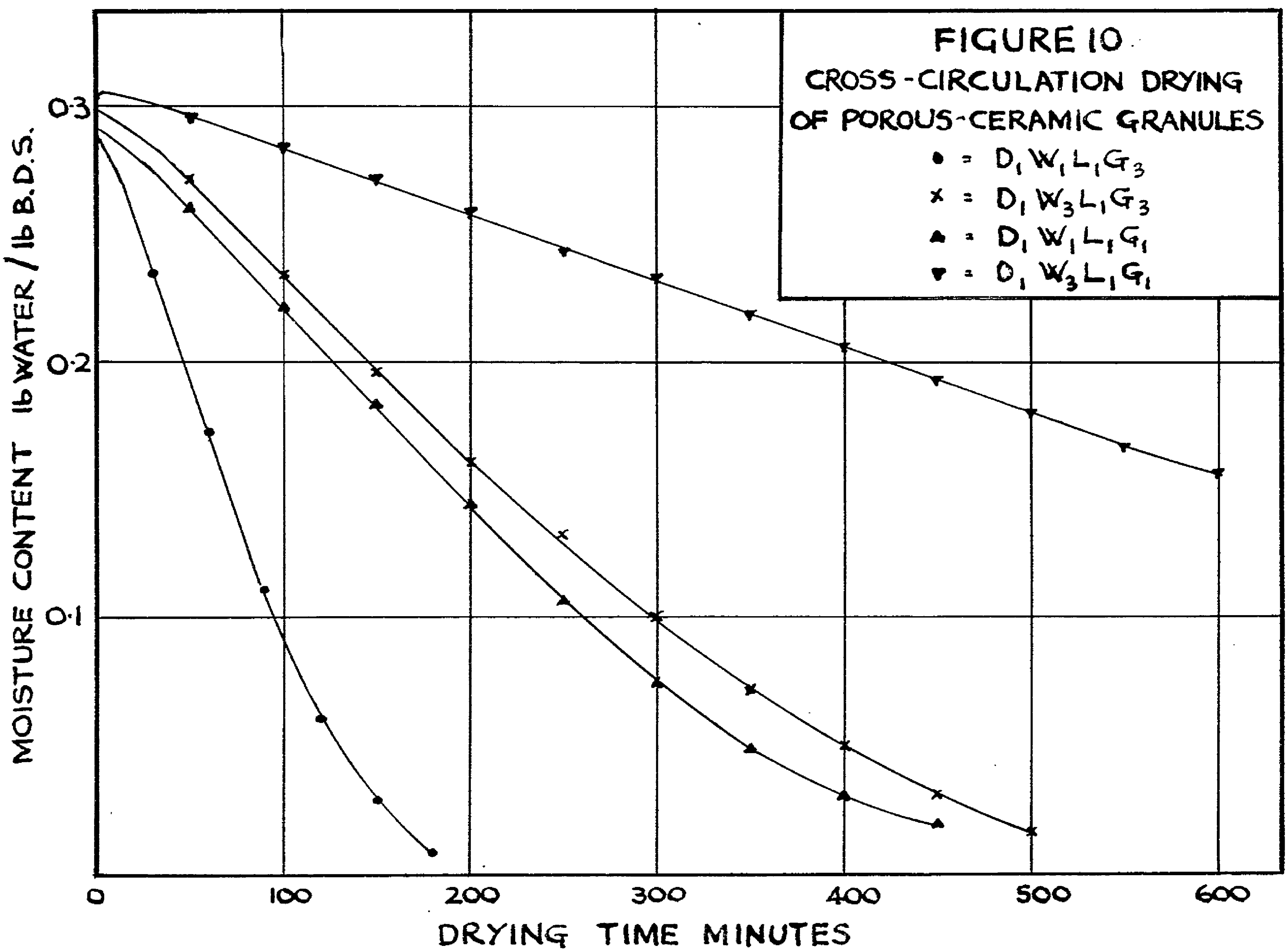
FIGURE 10
CROSS-CIRCULATION DRYING
OF POROUS-CERAMIC GRANULES
● = $D_1 W_1 L_1 G_3$
× = $D_1 W_3 L_1 G_3$
▲ = $D_1 W_1 L_1 G_1$
▼ = $D_1 W_3 L_1 G_1$
MOISTURE CONTENT lb WATER / lb B.D.S.
0·3
0·2
0·1
0
100
200
300
400
500
600
DRYING TIME MINUTES

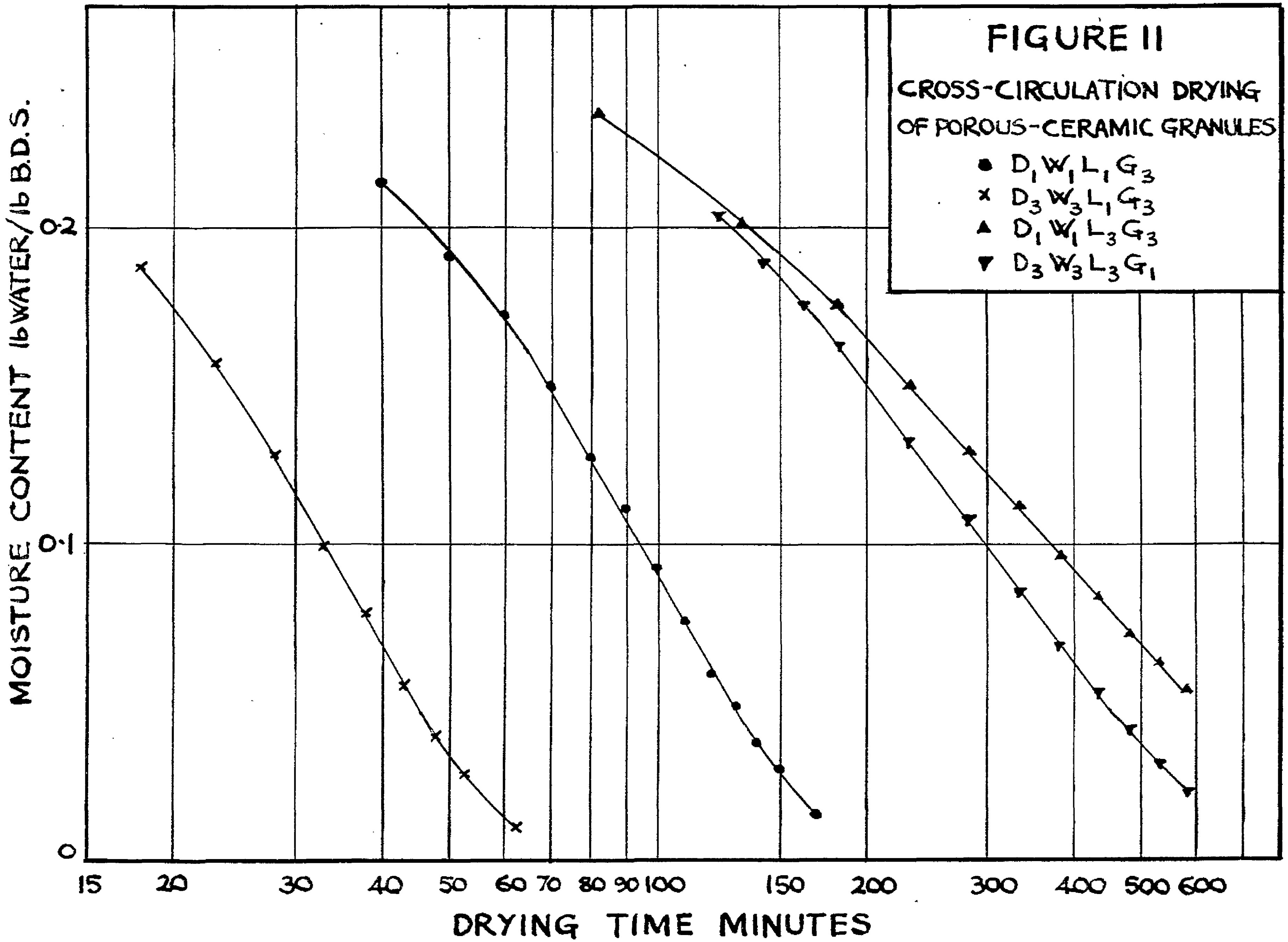

FIGURE II
CROSS-CIRCULATION DRYING
OF POROUS-CERAMIC GRANULES
● $D_1 W_1 L_1 G_3$
× $D_3 W_3 L_1 G_3$
▲ $D_1 W_1 L_3 G_3$
▼ $D_3 W_3 L_3 G_1$
MOISTURE CONTENT lb WATER/lb B.D.S.
0·2
0·1
0
15
20
30
40
50
60
70
80
90
100
150
200
300
400
500
600
DRYING TIME MINUTES

gave the best approximation to a straight line of the various transformations tried (see, for example Section 5.4). The linear relationship between W and $\log_{10}\theta'$ holds down to a moisture content of approximately 0.04 lb water/lb B.D.S. No attempt was made to find a suitable linear transformation of W and θ' at values of W less than 0.04, since W_e for the granules at room temperature was found to be approximately 0.05; it is therefore pointless to dry the granules below this moisture content since on standing they take up moisture from the atmosphere to reach $W_e = 0.05$.

Note: To allow for variations in the initial moisture content of the granules, θ' in the curves of W against $\log_{10}\theta'$ (Figure 11) was measured from a standard initial moisture content W = 0.296; this measurement of θ' was taken as the intercept of the linear portion of the drying curves of W against θ' (Figures 7 to 10) with a line parallel to the θ' axis through W = 0.296. This method of measuring θ' neglects the short curved section of the drying curve at the beginning of a drying test while the granules heat up to the wet-bulb temperature of the airstream. It also neglects the fact that during this heat-up period, condensation caused an initial increase in weight of the granules in the D_1W_3 tests (see Figure 9).

It will be noted that in Table 2, no values are given for W_e or C in the $D_1W_3L_1G_1$ and $D_1W_3L_3G_1$ tests. The reason for this is that the constant drying rates were so slow in these tests that the falling-rate period was not reached during the tests. Since an Analysis of Variance of the results of a factorial experiment can only be made if a complete set of results is available, only the constant drying-rate results could be analysed by this method.

This Analysis was done, not on the values of $\frac{dW}{d\theta}$, but on values of $\log_{10}\frac{dW}{d\theta}$. The reason for using logarithms was that from theoretical considerations the effects of the various factors on the constant drying rate were expected to be of the form of a product of several functions thus:

$$\frac{dW}{d\theta} = f(DW)\ f(G)\ f(L)$$

By taking logarithms, the correction factors for the various factors would be separated into additive functions thus:

$$\log \frac{dW}{d\theta} = \log f(DW) + \log f(G) + \log f(L)$$

In practice, however, the functions may be of various complexities, and various other interactions may be present, depending on the material being dried.

TABLE 3: Analysis Of Variance Of $Log_{10} \frac{100dW}{d\theta}$ For Porous-Ceramic Granules

Source of Variance	Sum of Squares
D	1.9847174
W	0.2745760
L	0.8636914 x
G	0.6564241
DW	0.1221853 x
DL	0.0002925
DG	0.0065691 x
WL	0.0007183
WG	0.0004687
LG	0.0013104
DWL	0.0000401
DWG	0.0000211
DLG	0.0003515
WLG	0.0001199
Residual	0.0012322
Total	3.9127180

To simplify the arithmetic of the Analysis by avoiding the use of negative logarithms, the Analysis was done on values of $\log_{10} \frac{100dW}{d\theta}$ (column two Table 2). Such a transformation of the original logarithms does not alter the results of the Analysis since differences within a group of numbers are not altered by adding a constant quantity to each. The method of conducting the Analysis of Variance is described in Appendix 2. The results of the Analysis are shown in Table 3, effects and interactions significant at the 5% probability level being identified thus x.

The Analysis indicated that the DW and DG interactions, and the

L main effect were significant; in other words the constant drying rate can be defined by the relationship:

$$\log_{10}\frac{dW}{d\theta} = f(DW) + f(DG) + f(L)$$

While Analyses of Variance of the values of W_c and C were not possible because no values for these variables were obtained in the $D_1W_3G_1$ tests, inspection of the values of W_c and C in Table 2 indicated the following points:

(a) The critical moisture content W_c appears to be unaffected by D, W and G but increases with loading.

(b) The rate constant C appears to be unaffected by G and W but it decreases (becomes less negative) with increase in loading. It also decreases with increase in D at L_1, but increases with increase in D at L_3; this indicates a DL interaction.

6.3 Fractional Three-Level Factorial Experiment On Porous-Ceramic Granules

A fractional three-level factorial experiment was used to study in more detail the factors shown by the preliminary two-level experiment to have significant effects on $\frac{dW}{d\theta}$, W_c and C. In the enlarged experiment, D, W, L and G were each tested at an additional level (level 2), which was midway between levels 1 and 3 (see Table 1). The purpose of this experiment was to confirm or discredit the results of the preliminary two-level experiment, and to provide enough experimental data to allow reasonably accurate estimates to be made of the probable values of $\frac{dW}{d\theta}$, W_c and C for any values of D, W, L and G within the experimentally tested ranges of these factors.

The fractional three-level factorial experiment involved 41 tests, including the 16 tests done for the preliminary two-level experiment. These 41 tests (shown in Table 4) represent approximately half of a complete three-level four-factor experiment (81 tests); they were selected to give information specifically on the significant effects and interactions of the various factors on $\frac{dW}{d\theta}$, W_c and C; tests giving information on insignificant effects and interactions were omitted.

Since of the three dependent variables — $\frac{dW}{d\theta}$, W_c and C — $\frac{dW}{d\theta}$ was the most affected by the values of D, W, L and G used, the enlarged experiment was designed primarily to evaluate f(DW), f(DG) and f(L) in the relationship for $\frac{dW}{d\theta}$ obtained from the Analysis of Variance of the two-level factorial experiment results:

$$\log_{10}\frac{dW}{d\theta} = f(DW) + f(DG) + f(L) \qquad \ldots \qquad \text{Equation A.}$$

The experiment was designed, however, in such a way that the tests involved also gave information on the effects of D and L on C, and on the effect of L on W_c.

To facilitate the prediction of $\frac{dW}{d\theta}$ under any drying conditions within the experimental ranges of D, W, L and G, the various functions in Equation A were evaluated as correction factors to be applied to the value of $\log_{10}\frac{dW}{d\theta}$ obtained in the $D_2W_2L_2G_2$ test. This standard test was replicated three times to ensure an accurate value of $\log_{10}\frac{dW}{d\theta}$; the average value obtained was -1.1433. $\frac{dW}{d\theta}$ may therefore be predicted from the relationship:

$$\log_{10}\frac{dW}{d\theta} = -1.1433 + f(DW) + f(DG) + f(L)$$

The values of the correction factor f(DW) for various levels of D and W were obtained from the values of $\log_{10}\frac{100dW}{d\theta}$ in Table 5 as the

TABLE 4: Values of $\frac{dW}{d\Theta}$ for porous-ceramic granules dried in the cross-circulation drier

	L_1G_1	L_1G_2	L_1G_3	L_2G_1	L_2G_2	L_2G_3	L_3G_1	L_3G_2	L_3G_3
D_1W_1	0.0473		0.1140				0.0145		0.0441
D_1W_2		0.0502		0.0145	0.0277	0.0439			
D_1W_3	0.0163		0.0464				0.0053		0.0154
D_2W_1		0.1661		0.0496	0.0909	0.1305			
D_2W_2	0.0789	0.1422	0.2100	0.0395	0.0719	0.1100	0.0268	0.0485	0.0725
D_2W_3		0.1158		0.0334	0.0631	0.0899			
D_3W_1	0.1600		0.3660				0.0586		0.1320
D_3W_2		0.2800		0.0766	0.1288	0.1855			
D_3W_3	0.1371		0.3085				0.0440		0.1090

TABLE 5: Values of $\log_{10} \frac{100dW}{d\Theta}$ for porous-ceramic granules dried in the cross-circulation drier

	L_1G_1	L_1G_2	L_1G_3	L_2G_1	L_2G_2	L_2G_3	L_3G_1	L_3G_2	L_3G_3
D_1W_1	0.6749		1.0569				0.1614		0.6444
D_1W_2		0.7007		0.1614	0.4425	0.6425			
D_1W_3	0.2122		0.6665				-0.2757		0.1875
D_2W_1		1.2203		0.6955	0.9586	1.1156			
D_2W_2	0.8971	1.1529	1.3222	0.5966	0.8567	1.0414	0.4281	0.6857	0.8603
D_2W_3		1.0639		0.5237	0.8000	0.9538			
D_3W_1	1.2041		1.5635				0.7679		1.1206
D_3W_2		1.4472		0.8842	1.1099	1.2684			
D_3W_3	1.1370		1.4893				0.6435		1.0374

TABLE 6: Values of W_c for porous-ceramic granules, dried in the cross-circulation drier

	L_1G_1	L_1G_2	L_1G_3	L_2G_1	L_2G_2	L_2G_3	L_3G_1	L_3G_2	L_3G_3
D_1W_1	0.142		0.136				0.181		0.190
D_1W_2		0.149		—	—	0.175			
D_1W_3	—		0.151				—		0.187
D_2W_1		0.135		0.175	0.182	0.172			
D_2W_2	0.133	0.150	0.124	0.163	0.160	0.166	0.191	0.172	0.185
D_2W_3		0.145		0.165	0.165	0.178			
D_3W_1	0.131		0.122				0.180		0.190
D_3W_2		0.140		0.165	0.172	0.160			
D_3W_3	0.134		0.125				0.175		0.179

TABLE 7: Values of Rate Constant C for porous-ceramic granules dried in the cross-circulation drier

	L_1G_1	L_1G_2	L_1G_3	L_2G_1	L_2G_2	L_2G_3	L_3G_1	L_3G_2	L_3G_3
D_1W_1	-0.429		-0.410				-0.258		-0.250
D_1W_2		-0.380		—	—	-0.281			
D_1W_3	—		-0.405				—		-0.271
D_2W_1		-0.370		-0.324	-0.306	-0.324			
D_2W_2	-0.385	-0.366	-0.391	-0.288	-0.310	-0.331	-0.256	-0.287	-0.289
D_2W_3		-0.376		-0.309	-0.340	-0.309			
D_3W_1	-0.361		-0.388				-0.273		-0.302
D_3W_2		-0.349		-0.345	-0.360	-0.325			
D_3W_3	-0.377		-0.382				-0.299		-0.305

average differences between the values in the various DW rows and the values in the corresponding LG columns in the D_2W_2 row. As an example, the correction factor for D_1W_1 was calculated as:

$$0.6749 - 0.8971 = -0.2222$$
$$1.0569 - 1.3222 = -0.2653$$
$$0.1614 - 0.4281 = -0.2667$$
$$0.6444 - 0.8603 = \underline{-0.2159}$$
$$\text{Average} = -0.2425$$

The experiment was designed in such a way that the values of f(DW) for the various levels of D and W were each determined as the average of four independent measurements. The values of f(DW) obtained were:

$D_1W_1 = -0.2425$	$D_2W_1 = 0.0856$	$D_3W_1 = 0.2871$
$D_1W_2 = -0.4251$	$D_2W_2 = 0.0000$	$D_3W_2 = 0.2655$
$D_1W_3 = -0.6793$	$D_2W_3 = -0.0765$	$D_3W_3 = 0.1999$

These values are shown graphically in Figure 12A.

The values of the correction factor f(DG), which estimates the changes in $\log_{10} \frac{dW}{d\theta}$ due to deviations in airflow from G_2, were obtained from the values in Table 5 by measuring, for each level of D, the average difference between values in the G_1 and G_3 tests at corresponding values of L and W; the difference thus obtained was then subdivided in the ratio: difference between G_1 and G_2 tests to difference between G_2 and G_3 tests.

For example, the D_1G_1 and D_1G_3 values of f(DG) were obtained by taking the G_1 to G_3 differences at D_1 i.e.

$$1.0569 - 0.6749 = 0.3820$$
$$0.6665 - 0.2122 = 0.4543$$
$$0.6425 - 0.1614 = 0.4811$$
$$0.6444 - 0.1614 = 0.4830$$
$$0.1875 - (-0.2757) = \underline{0.4632}$$
$$\text{Average} = 0.4527$$

0.4527 was then split up in the ratio: difference between the G_1 and G_2 tests = −0.2811 to difference between the G_2 and G_3 tests = 0.2000. The values of f(DG) for D_1G_1 and D_1G_3 were therefore −0.2644 and 0.1883 respectively. The other values of f(DG), which were obtained similarly, were:

D_1G_1 =	−0.2644	D_2G_1	−0.2663	D_3G_1	−0.2162
D_1G_2 =	0	D_2G_2	0	D_3G_2	0
D_1G_3 =	0.1883	D_2G_3	0.1622	D_3G_3	0.1523

These values are shown graphically in Figure 12B.

The values of the correction factor f(L), which estimates the effect on $\log_{10}\frac{dW}{d\theta}$ of deviations in loading from L_2, were obtained from the values in Table 5 by measuring the average difference between the L_1 and L_3 tests at corresponding values of D, W and G i.e. 0.6749 − 0.1614 = 0.5135, 1.0569 − 0.6444 = 0.4125 etc.; this average difference (0.4504) was divided in the ratio: difference between the L_1 and L_2 tests to the difference between the L_2 and L_3 tests. The values of f(L) obtained in this way were:

L_1 = −0.2769 L_2 = 0 L_3 = −0.1735

These values are given graphically in Figure 12C.

From an examination of the values of W_e in Table 6 it is apparent that, as indicated previously by the preliminary two-level experiment, the values of W_e show no definite trend with changes in D, W or G but increase appreciably with increase in loading. The values of W_e in Table 6, averaged over L_1, L_2 and L_3 were: L_1 = 0.157 L_2 = 0.167 L_3 = 0.183; these values are shown graphically in Figure 13B.

Examination of the values in Table 7 confirmed the findings of the preliminary two-level experiment — that the rate constant C was affected

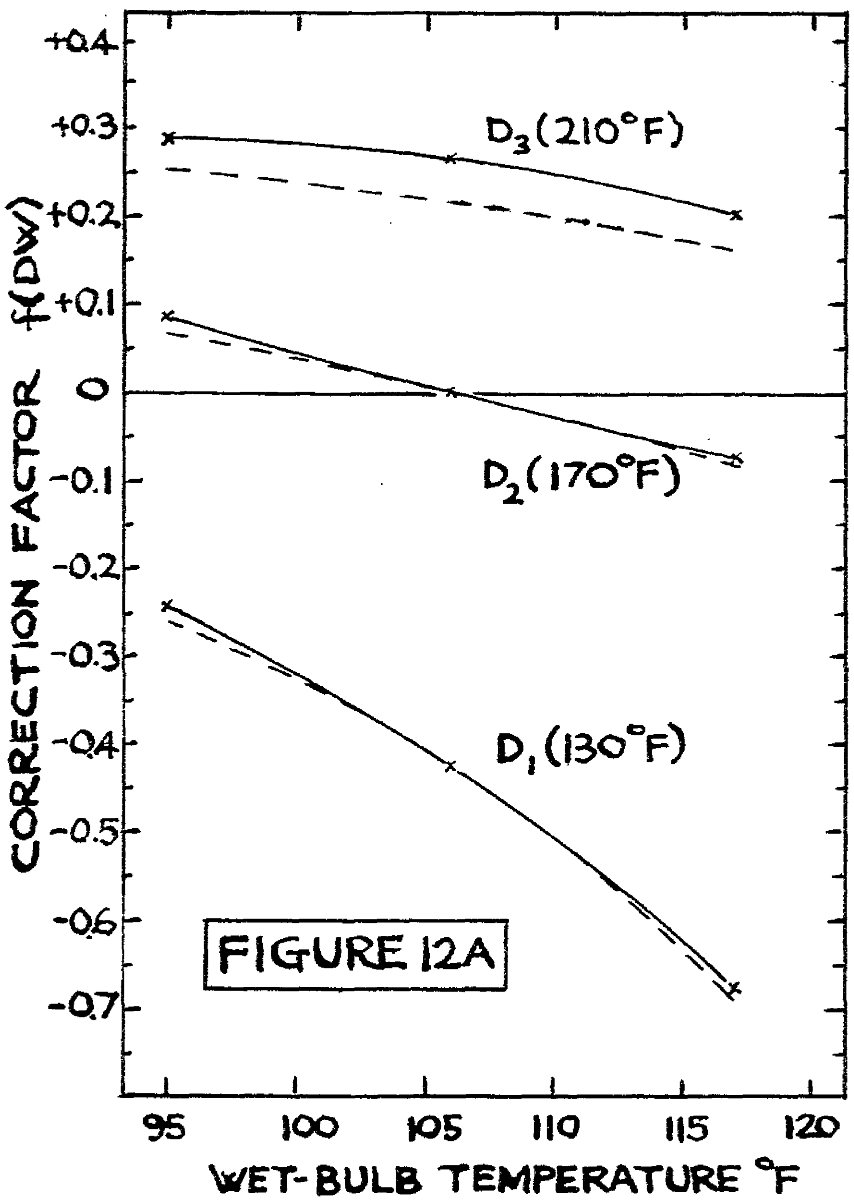

NOTE: THE DOTTED LINES ON THESE FIGURES DENOTE THE DRYING BEHAVIOUR PREDICTED BY DRYING THEORY.

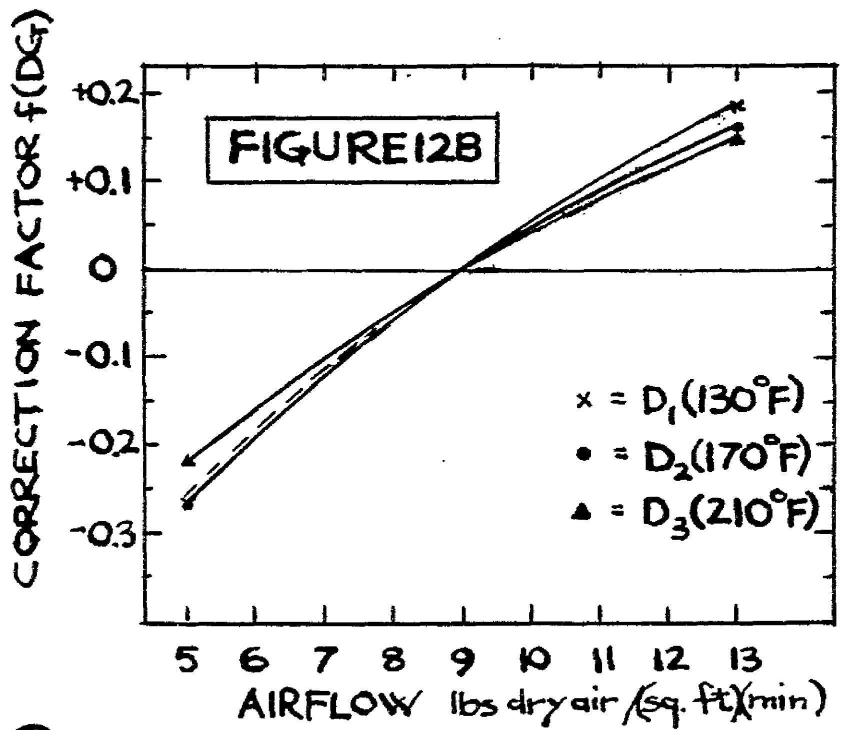

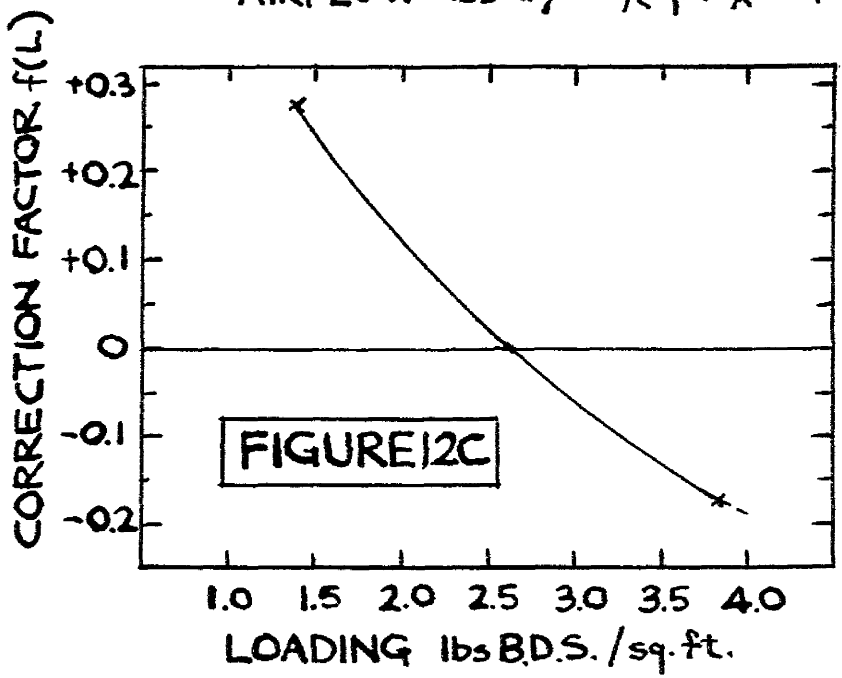

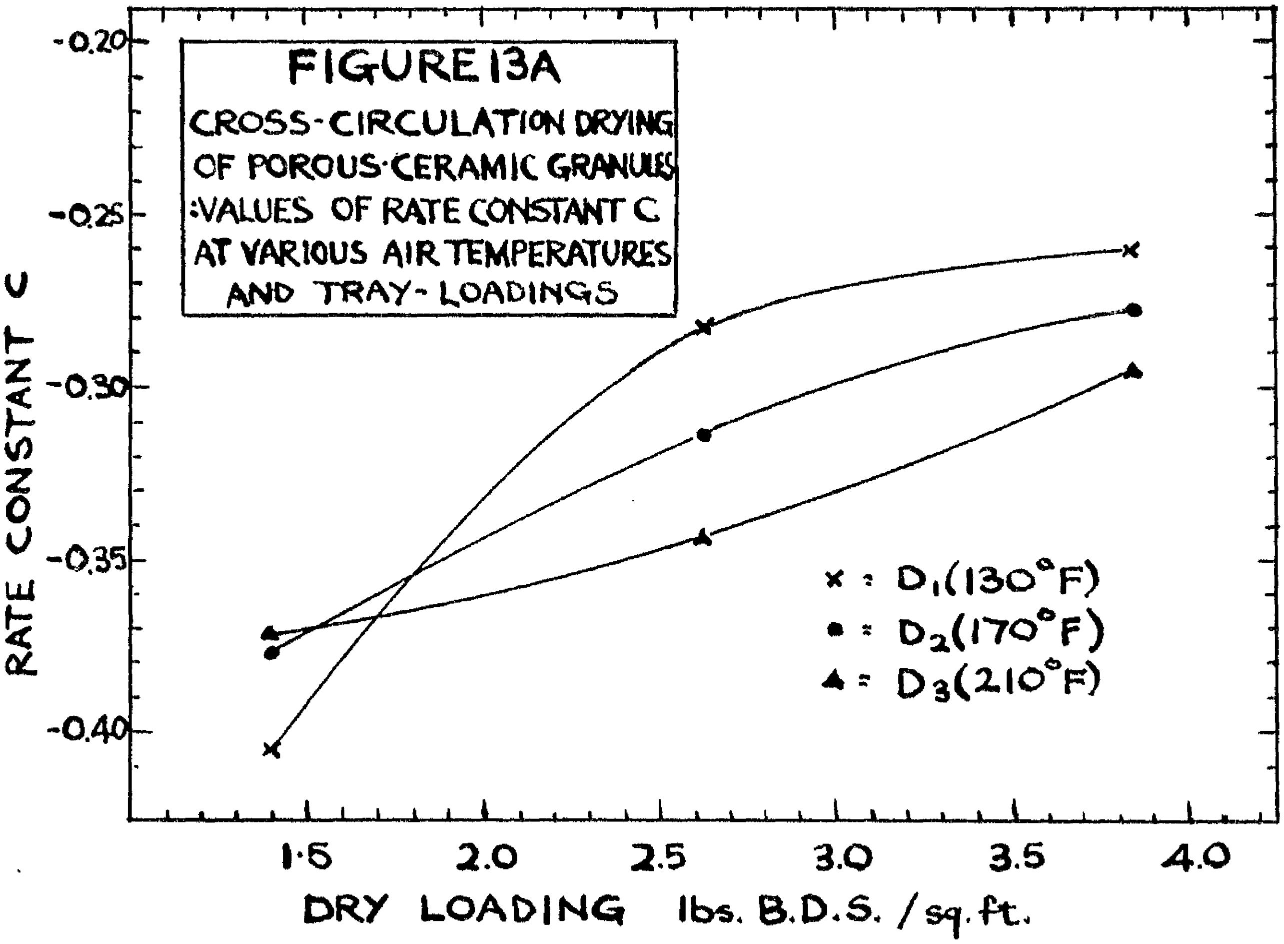
FIGURE 13A
CROSS-CIRCULATION DRYING OF POROUS-CERAMIC GRANULES :VALUES OF RATE CONSTANT C AT VARIOUS AIR TEMPERATURES AND TRAY-LOADINGS
RATE CONSTANT C
-0.20
-0.25
-0.30
-0.35
-0.40
× : D1(130°F)
• : D2(170°F)
▲ : D3(210°F)
1·5
2.0
2.5
3.0
3.5
4.0
DRY LOADING lbs. B.D.S. /sq. ft.

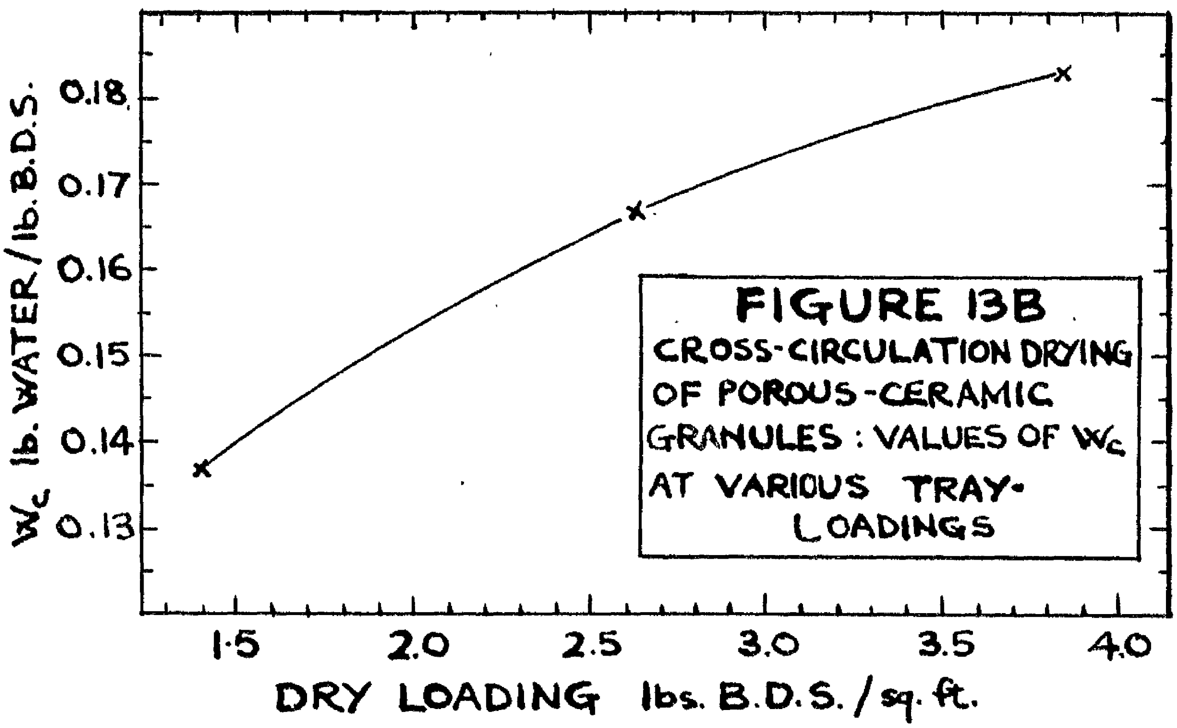
FIGURE 13B
CROSS-CIRCULATION DRYING OF POROUS-CERAMIC GRANULES : VALUES OF Wc AT VARIOUS TRAY-LOADINGS
Wc lb. WATER/lb. B.D.S.
0.18
0.17
0.16
0.15
0.14
0.13
1·5
2.0
2.5
3.0
3.5
4.0
DRY LOADING lbs. B.D.S. /sq. ft.

by the values of D and L but unaffected by the values of G and W. The values of C in Table 7 were therefore averaged over G and W for the various levels of D and L; these values of C were as follows:

$$D_1L_1 = -0.406 \quad D_1L_2 = -0.281 \quad D_1L_3 = -0.260$$
$$D_2L_1 = -0.377 \quad D_2L_2 = -0.314 \quad D_2L_3 = -0.277$$
$$D_3L_1 = -0.371 \quad D_3L_2 = -0.343 \quad D_3L_3 = -0.295$$

These values are shown graphically in Figure 13A.

6.4 Method Of Predicting The Drying Time Of Porous-Ceramic Granules In The Cross-Circulation Drier

The experimental results given in Section 6.3 may be used in the following manner to predict the drying time of the porous-ceramic granules from an initial moisture content W_1 to a final moisture content W_2 when dried under specified conditions of D, W, L and G.

(a) The constant drying rate $\frac{dW}{d\theta}$ is calculated from the expression:

$$\log_{10} \frac{dW}{d\theta} = -1.1433 + f(DW) + f(DG) + f(L)$$

the appropriate values of f(DW), f(DG) and f(L) being found from Figures 12A, 12B and 12C respectively.

(b) The critical moisture content W_c under the specified drying conditions is found from Figure 13B.

(c) The duration of the constant drying rate period θ_c' in minutes (measured from a standard moisture content $W_{st} = 0.296$) is found from the expression:

$$\theta_c' = \frac{60(0.296 - W_c)}{\frac{dW}{d\theta}}$$

(d) The value of the rate constant C appropriate to the specified drying conditions is found from Figure 13A.

(e) The drying time Θ_T' in minutes between W_{st} and W_2 is given by the expression:

$$\log_{10} \Theta_T' = \log_{10}\Theta_c' + \frac{W_2 - W_c}{C}$$

(f) The drying time Θ_1' between W_1 and W_{st} is given by the relationship:

$$\Theta_1' = \frac{60(W_1 - 0.296)}{\frac{dW}{d\Theta}}$$

The total drying time in minutes between W_1 and W_2 is therefore $\Theta' = \Theta_T' + \Theta_1'$

<u>Note</u>: The method described in steps (a) to (f) may be used to predict the drying time of the granules from an initial moisture content W_1 in the constant rate period to a final moisture content W_2 in the falling rate period.

Two other prediction problems may arise; these may be dealt with as follows:

(a) Drying may be all in the constant drying rate period i.e. W_1 and W_2 are greater than W_c. In this case, the drying time can be found simply from the relationship

$$\Theta' = \frac{60(W_1 - W_2)}{\frac{dW}{d\Theta}}$$

(b) Drying may be all in the falling-rate period. In this case the drying times from W_{st} to W_1 (Θ'_{TW_1}) and from W_{st} to W_2 (Θ'_{TW_2}) can be found from steps (a) to (e), and the drying time from W_1 to W_2 from the equation $\Theta' = \Theta'_{TW_2} - \Theta'_{TW_1}$

Example Of The Application Of The Prediction Method

Predict the drying time of the porous-ceramic granules used in this investigation, from an initial moisture content of $W_1 = 0.250$ to a final moisture content $W_2 = 0.080$, when dried in the cross-circulation drier at a tray-loading of $L = 3.85$ with air conditions $D = 210$, $W = 117$ and $G = 5$.

Solution

(a) $\log_{10} \frac{dW}{d\theta} = -1.1433 + f(DW) + f(DG) + f(L)$

$= -1.1433 + 0.200 - 0.216 - 0.174$

$= -1.3333$

therefore $\frac{dW}{d\theta} = 0.046$

(b) $W_c = 0.183$

(c) $\theta_c' = 60(0.296 - 0.183)/0.046 = 148$ minutes

(d) $C = -0.295$

(e) $\log_{10} \theta_T' = \log_{10} 148 + (0.080 - 0.183)/(-0.295)$

$= 2.519$

therefore $\theta_T' = 330$ minutes

(f) $\theta_1' = 60(0.250 - 0.296)/0.046 = - 60$ minutes

The drying time from $W_1 = 0.250$ to $W_2 = 0.080$ is therefore:

$= 330 - 60 = 270$ minutes

This value agrees well with the experimentally determined drying time of 285 minutes (see graph $D_3W_3L_3G_1$ on Figure 8).

6.5 Drying Of Coke

The second porous-granular material tested was a domestic grade of coke obtained from the Bakery Department of the College. The coke, which was approximately 1 inch mesh when received, was crushed in a jaw-crusher, and the fraction passing $\frac{3}{8}$ inch mesh and retained on $\frac{1}{4}$ inch mesh was used in the drying tests. Coke of this particle size was chosen as representative of a porous-granular material of irregular physical structure but of approximately the same particle size as the porous-ceramic granules tested previously; moreover, like the porous-ceramic granules, the coke did not shrink or break down appreciably on drying, and it was also in a form suitable for drying in a through-circulation drier. The dry coke had a bulk density of 23 lbs/cub.ft.

Method Of Preparing The Coke For A Drying Test

Method Of Preparing The Coke For A Drying Test

For each test, the appropriate weight of dry coke was soaked in distilled water for twenty-four hours, then allowed to drain for twenty minutes on a $\frac{1}{4}$ inch mesh sieve, and its excess surface moisture was removed by rolling it in a dry cloth before it was spread on the test tray. This standard procedure left the coke with an average initial moisture content of 0.271 lb water/lb B.D.S. which, however, varied somewhat from test to test - a minimum of 0.233 and a maximum of 0.314 lb water/lb B.D.S. being obtained. Since a small proportion of the coke broke down on handling, the dry coke obtained at the end of each test was sieved to remove particles smaller than $\frac{1}{4}$ inch mesh before re-use.

<u>The Drying Conditions Used In the Tests</u>

The ranges of D, W and G used in the drying tests on coke were the same as those used in the drying tests on porous-ceramic granules. In addition, the ranges of bed depths studied were approximately the same for both materials, but the range of L for each material was different since the two materials had different bulk densities. The ranges of the various factors used in the tests were as follows:

TABLE 8

$D_1 = 130$	$D_2 = 170$	$D_3 = 210$
$W_1 = 95$	$W_2 = 106$	$W_3 = 117$
$G_1 = 5$	$G_2 = 9$	$G_3 = 13$
$L_1 = 0.77$	$L_2 = 1.47$	$L_3 = 2.17$
(single layer)	($\frac{5}{8}$ inch layer)	(1 inch layer)

6.6. Preliminary Two-Level Factorial Experiment On Coke

Levels 1 and 3 of the four factors D, W, G and L shown in Table 8 were tested in a two-level factorial experiment involving the sixteen drying tests shown in Table 9. The drying curves obtained in these tests are shown in Figures 14, 15, 16 and 17. The values of $\frac{dW}{d\theta}$ and W_c given in Table 9 were measured graphically from these curves in the same way as were the corresponding quantities in the porous-ceramic granules tests (see Section 6.2). Of the various transformations of the test data tried, the plot of W against log θ' (see Figure 18) gave the best approximation to a straight line from W_c to W = 0.04 (W_c for coke at room temperature and humidity was approximately 0.06). The drying behaviour of the coke in the falling-rate period was therefore characterized by the rate constant C used previously in Section 6.2 to describe the falling-rate drying behaviour of the porous-ceramic

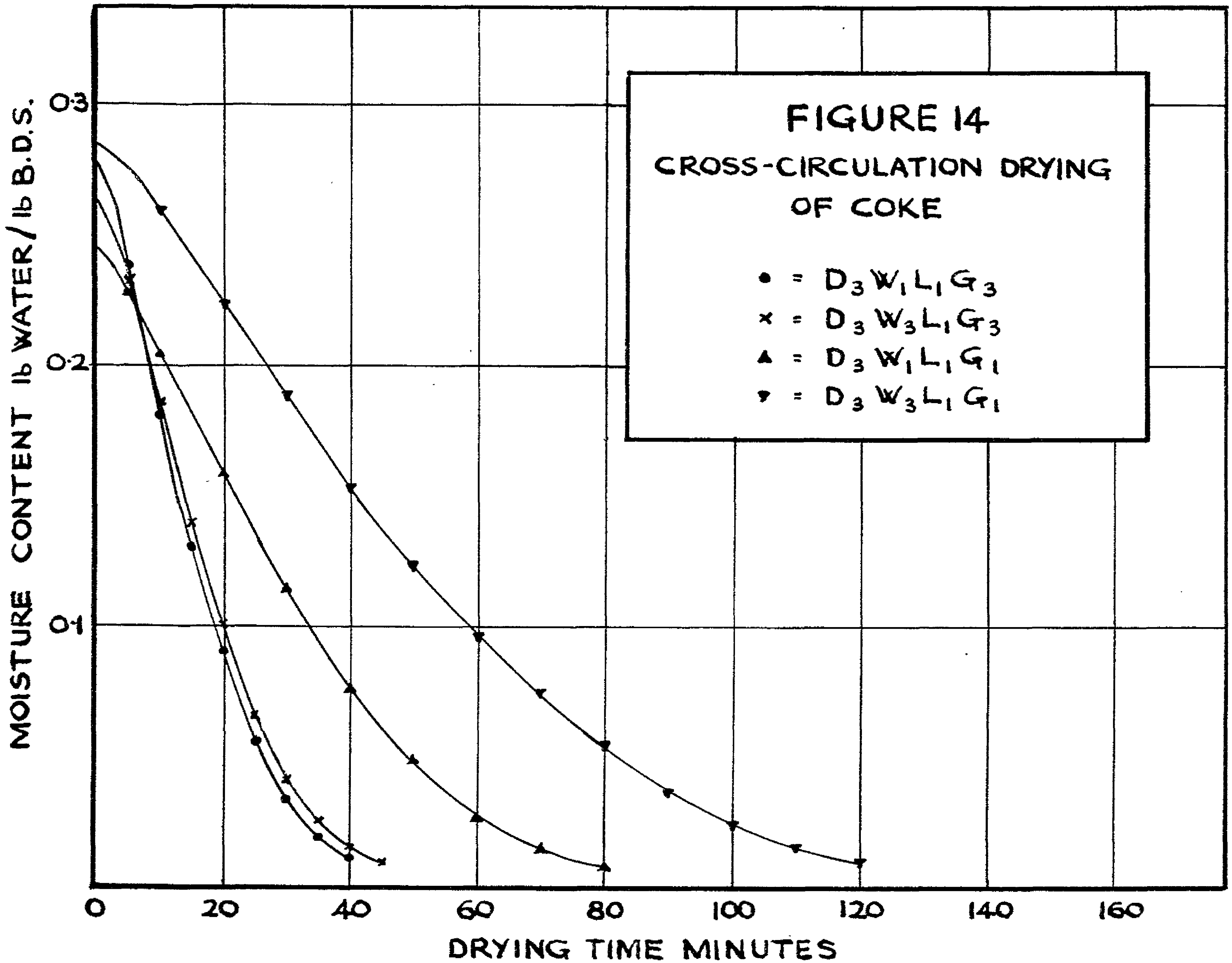
FIGURE 14
CROSS-CIRCULATION DRYING OF COKE
● = D3 W1 L1 G3
× = D3 W3 L1 G3
▲ = D3 W1 L1 G1
▼ = D3 W3 L1 G1
MOISTURE CONTENT lb WATER / lb B.D.S.
0·3
0·2
0·1
0
20
40
60
80
100
120
140
160
DRYING TIME MINUTES

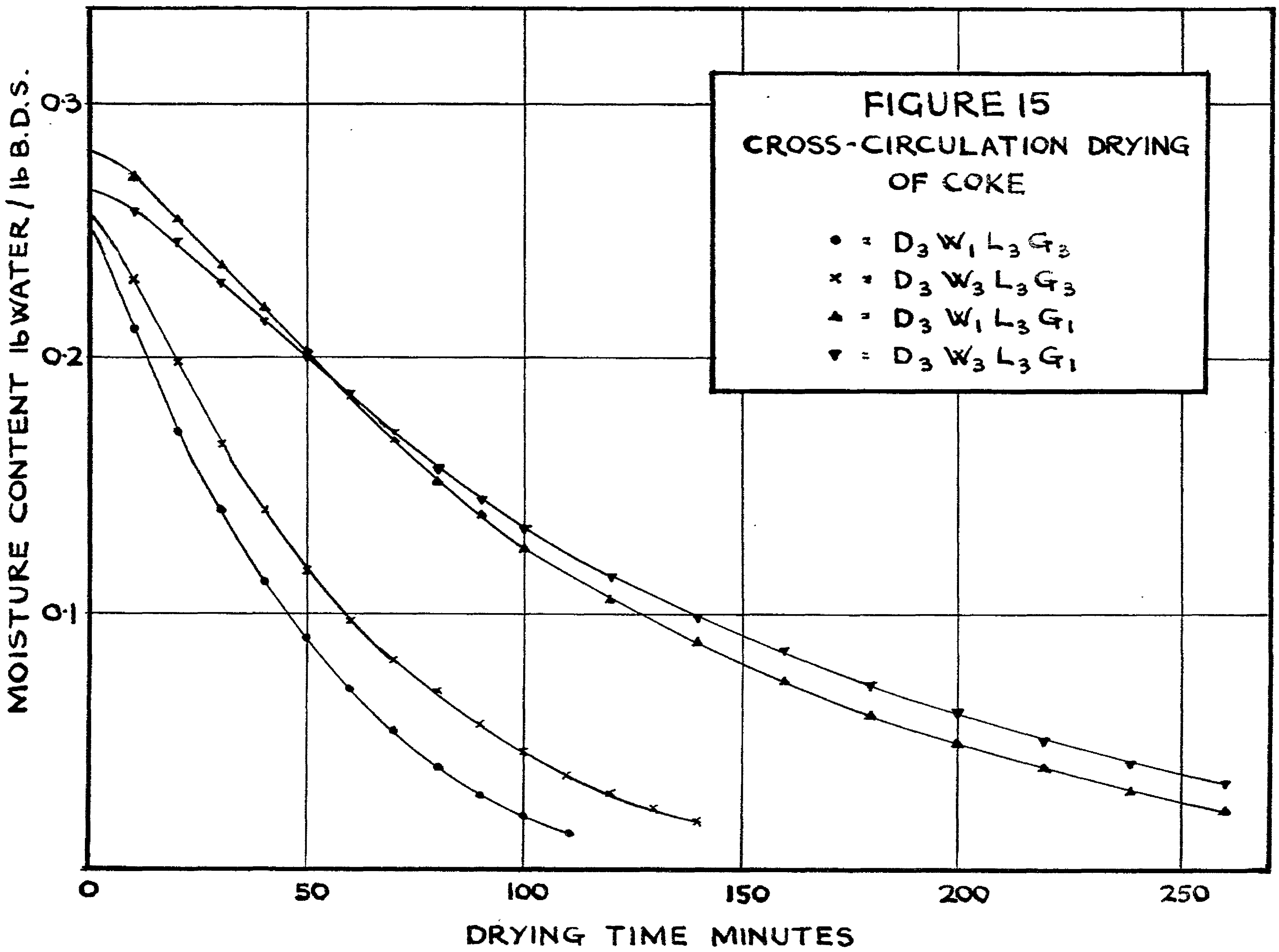
FIGURE 15
CROSS-CIRCULATION DRYING OF COKE
● = $D_3 W_1 L_3 G_3$
× = $D_3 W_3 L_3 G_3$
▲ = $D_3 W_1 L_3 G_1$
▼ = $D_3 W_3 L_3 G_1$
MOISTURE CONTENT lb WATER / lb B.D.S.
0·3
0·2
0·1
0
50
100
150
200
250
DRYING TIME MINUTES

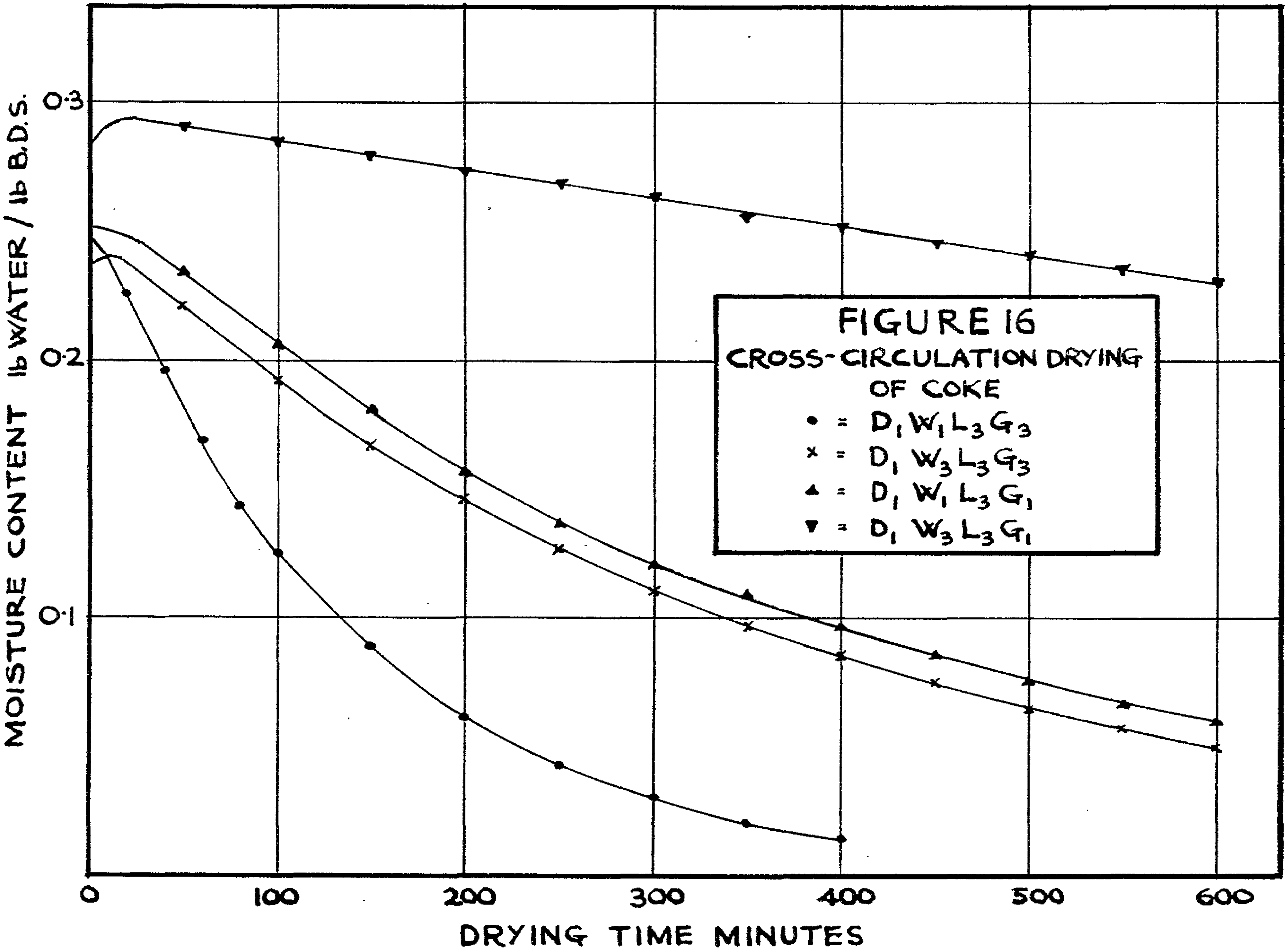
FIGURE 16
CROSS-CIRCULATION DRYING OF COKE
• = D1 W1 L3 G3
× = D1 W3 L3 G3
▲ = D1 W1 L3 G1
▼ = D1 W3 L3 G1
MOISTURE CONTENT lb WATER / lb B.D.S.
0·3
0·2
0·1
0
100
200
300
400
500
600
DRYING TIME MINUTES

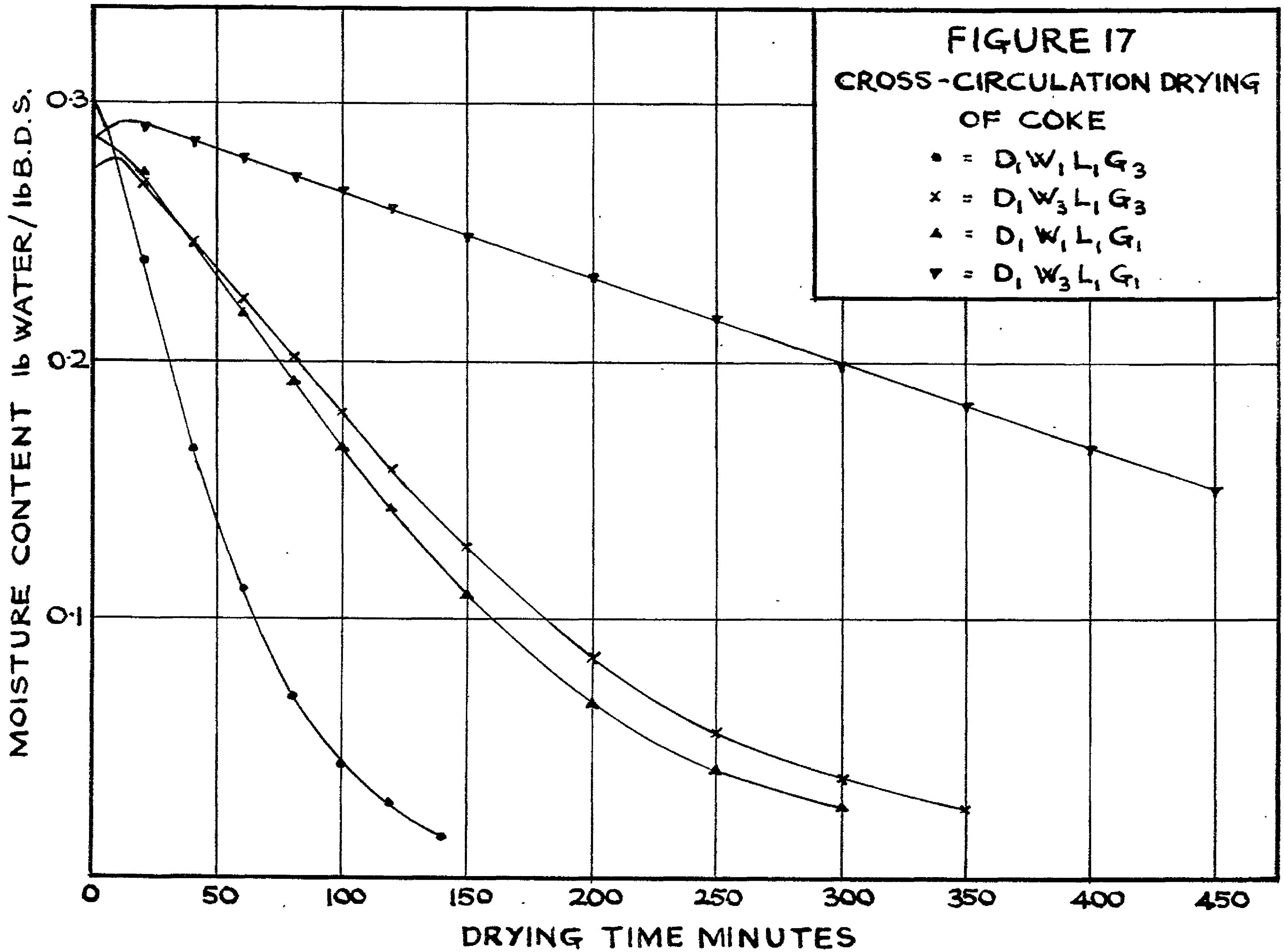
FIGURE 17
CROSS-CIRCULATION DRYING OF COKE
• = $D_1 W_1 L_1 G_3$
× = $D_1 W_3 L_1 G_3$
▲ = $D_1 W_1 L_1 G_1$
▼ = $D_1 W_3 L_1 G_1$
MOISTURE CONTENT lb WATER/lb B.D.S.
0·3
0·2
0·1
0
50
100
150
200
250
300
350
400
450
DRYING TIME MINUTES

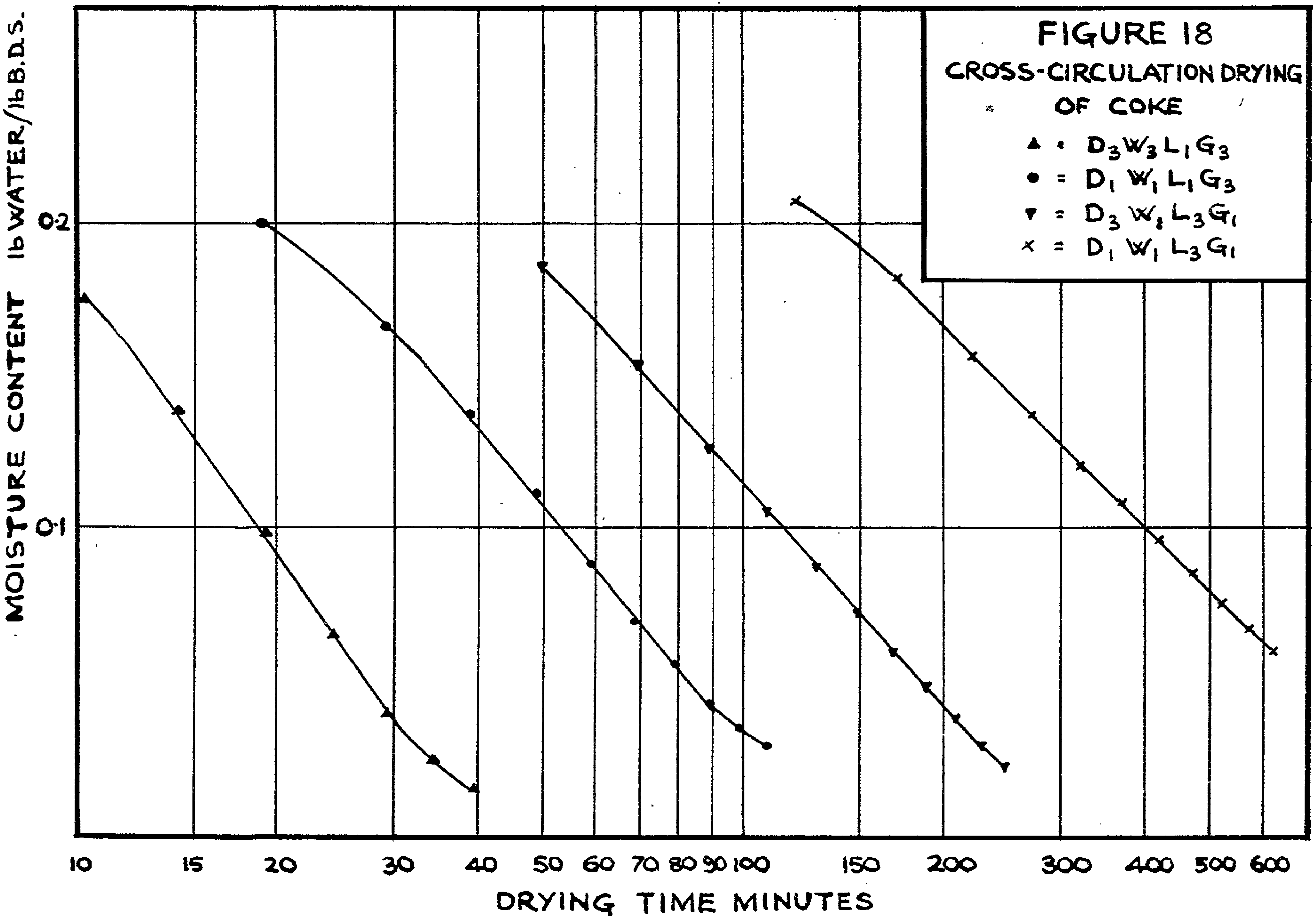

FIGURE 18
CROSS-CIRCULATION DRYING OF COKE
▲ = $D_3 W_3 L_1 G_3$
● = $D_1 W_1 L_1 G_3$
▼ = $D_3 W_1 L_3 G_1$
× = $D_1 W_1 L_3 G_1$
MOISTURE CONTENT lb WATER/lb B.D.S.
0·2
0·1
10
15
20
30
40
50
60
70
80
90
100
150
200
300
400
500
600
DRYING TIME MINUTES

granules. In calculating the values of C for coke, the values of θ' in the curves of W against θ' were measured from a standard W = 0.271.

TABLE 9: Results Of Preliminary Two-Level Factorial Experiment on Coke

Test Conditions	$\frac{dW}{d\theta}$	$\log_{10} \frac{100dW}{d\theta}$	W_{θ}	C
$D_1W_1L_1G_1$	0.072	0.8573	0.152	-0.310
$D_1W_1L_1G_3$	0.220	1.3424	0.155	-0.264
$D_1W_3L_1G_1$	0.019	0.2788	0.140	-0.254
$D_1W_3L_1G_3$	0.067	0.8261	0.150	-0.283
$D_3W_1L_1G_1$	0.282	1.4502	0.141	-0.323
$D_3W_1L_1G_3$	0.660	1.8195	0.152	-0.299
$D_3W_3L_1G_1$	0.216	1.3345	0.145	-0.302
$D_3W_3L_1G_3$	0.560	1.7482	0.142	-0.317
$D_1W_1L_3G_1$	0.031	0.4969	0.182	-0.217
$D_1W_1L_3G_3$	0.088	0.9445	0.172	-0.230
$D_1W_3L_3G_1$	0.007	-0.1549	-	-
$D_1W_3L_3G_3$	0.032	0.5051	0.175	-0.229
$D_3W_1L_3G_1$	0.106	1.0253	0.171	-0.239
$D_3W_1L_3G_3$	0.252	1.4014	0.170	-0.256
$D_3W_3L_3G_1$	0.096	0.9823	0.168	-0.236
$D_3W_3L_3G_3$	0.194	1.2878	0.175	-0.246

No values of W_{θ} and C were obtained for test $D_1W_3L_3G_1$ since the falling-rate period was not reached during this test. Because of these missing values, only the $\frac{dW}{d\theta}$ results were subjected to an Analysis of Variance; the results of the Analysis, which was done on the values of $\log_{10} \frac{100dW}{d\theta}$ as was the Analysis of the porous-ceramic granules results (see Section 6.2), are shown in Table 10. Effects and interactions significant at the 5% level are marked*.

TABLE 10: Analysis Of Variance Of Values Of $\log_{10} \frac{100dW}{d\theta}$ For Coke

Source of Variance	Sum of Squares
D	2.2148881
W	0.3999298
L	0.6275017 *
G	0.8120713
DL	0.0012708
DW	0.2121523 *
DG	0.0285103 *
LW	0.0000722
LG	0.0000429
WG	0.0038564
DLW	0.0000450
DWG	0.0056551
LWG	0.0000774
DLG	0.0019493
Residual	0.0043956
Total	4.3124182

The Analysis indicated that the L main effect and the DW and DG interactions were significant. The constant drying rate $\frac{dW}{d\theta}$ may therefore be defined by the relationship

$$\log \frac{dW}{d\theta} = f(DW) + f(DG) + f(L)$$

which is of the same form as the relationship found for the constant drying rate of the porous-ceramic granules (Section 6.2).

Although no Analyses of Variance were possible for the values of W_e and C because no values for these variables were obtained in test $D_1W_3L_3G_1$, inspection of the values of W_e and C in Table 9 indicates the following points:

(a) the critical moisture content W_c appears to be unaffected by D, W and G, but increaseswith L.

(b) the rate constant C appears to be unaffected by G and W, but decreases (becomes less negative) with increase in L and increases slightly with increase in D.

6.7 Fractional Three-Level Factorial Experiment On Coke

Since the results of the preliminary two-level factorial experiment described in Section 6.6 indicated that D, W, L and G had similar effects on $\frac{dW}{d\theta}$, W_c and C of coke and of porous-ceramic granules, the fractional three-level factorial experiment applied to the porous-ceramic granules (See Section 6.3) was also applied to the coke. The results of this experiment are shown in Tables 11 to 14.

Since the average value of $\log_{10}\frac{dW}{d\theta}$ obtained in the standard $D_2W_2L_2G_2$ test on coke was −0.8570, $\frac{dW}{d\theta}$ for this material may be predicted from the relationship:

$$\log_{10}\frac{dW}{d\theta} = -0.8570 + f(DW) + f(DG) + f(L)$$

The values of the various correction factors were calculated in the same way as were the corresponding quantities in the expression for $\frac{dW}{d\theta}$ of the porous-ceramic granules described in Section 6.3. The values of the various correction factors for the coke were as follows:

Values of f(DW)

D_1W_1 = −0.2029	D_2W_1 = 0.0507	D_3W_1 = 0.3109
D_1W_2 = −0.5086	D_2W_2 = 0.0000	D_3W_2 = 0.2419
D_1W_3 = −0.7494	D_2W_3 = −0.0504	D_3W_3 = 0.2250

These values are shown graphically in Figure 19A.

TABLE 11 : Values of $\frac{dW}{d\theta}$ for coke dried in the cross-circulation drier

	L_1G_1	L_1G_2	L_1G_3	L_2G_1	L_2G_2	L_2G_3	L_3G_1	L_3G_2	L_3G_3
D_1W_1	0.072		0.220				0.031		0.088
D_1W_2		0.077		0.019	0.042	0.065			
D_1W_3	0.019		0.067				0.007		0.032
D_2W_1		0.268		0.076	0.153	0.218			
D_2W_2	0.120	0.259	0.358	0.062	0.139	0.189	0.049	0.094	0.135
D_2W_3		0.218		0.053	0.128	0.178			
D_3W_1	0.282		0.660				0.106		0.252
D_3W_2		0.442		0.131	0.218	0.310			
D_3W_3	0.216		0.560				0.096		0.194

TABLE 12 : Values of $\log_{10} 100\frac{dW}{d\theta}$ for coke dried in the cross-circulation drier

	L_1G_1	L_1G_2	L_1G_3	L_2G_1	L_2G_2	L_2G_3	L_3G_1	L_3G_2	L_3G_3
D_1W_1	0.8573		1.3424				0.4969		0.9445
D_1W_2		0.8865		0.2718	0.6191	0.8136			
D_1W_3	0.2788		0.8261				-0.1549		0.5051
D_2W_1		1.4281		0.8808	1.1847	1.3385			
D_2W_2	1.0792	1.4133	1.5539	0.7924	1.1430	1.2765	0.6893	0.9731	1.1303
D_2W_3		1.3385		0.7275	1.1072	1.2504			
D_3W_1	1.4502		1.8195				1.0253		1.4014
D_3W_2		1.6454		1.1173	1.3385	1.4914			
D_3W_3	1.3345		1.7482				0.9823		1.2878

TABLE 13: Values of Rate Constant C for coke dried in the cross-circulation drier

	L_1G_1	L_1G_2	L_1G_3	L_2G_1	L_2G_2	L_2G_3	L_3G_1	L_3G_2	L_3G_3
D_1W_1	-0.310		-0.264				-0.217		-0.230
D_1W_2		-0.271		—	-0.289	-0.251			
D_1W_3	-0.254		-0.283				—		-0.229
D_2W_1		-0.329		-0.301	-0.293	-0.296			
D_2W_2	-0.302	-0.278	-0.317	-0.286	-0.290	-0.280	-0.218	-0.230	-0.234
D_2W_3		-0.274		-0.278	-0.289	-0.272			
D_3W_1	-0.323		-0.299				-0.239		-0.256
D_3W_2		-0.341		-0.314	-0.294	-0.292			
D_3W_3	-0.302		-0.317				-0.236		-0.246

TABLE 14: Values of W_c for coke dried in the cross-circulation drier

	L_1G_1	L_1G_2	L_1G_3	L_2G_1	L_2G_2	L_2G_3	L_3G_1	L_3G_2	L_3G_3
D_1W_1	0.152		0.155				0.182		0.172
D_1W_2		0.134		—	0.152	0.165			
D_1W_3	0.140		0.150				—		0.175
D_2W_1		0.135		0.135	0.156	0.152			
D_2W_2	0.150	0.142	0.136	0.142	0.153	0.171	0.175	0.165	0.170
D_2W_3		0.162		0.164	0.166	0.155			
D_3W_1	0.141		0.152				0.171		0.170
D_3W_2		0.140		0.140	0.148	0.162			
D_3W_3	0.145		0.142				0.168		0.175

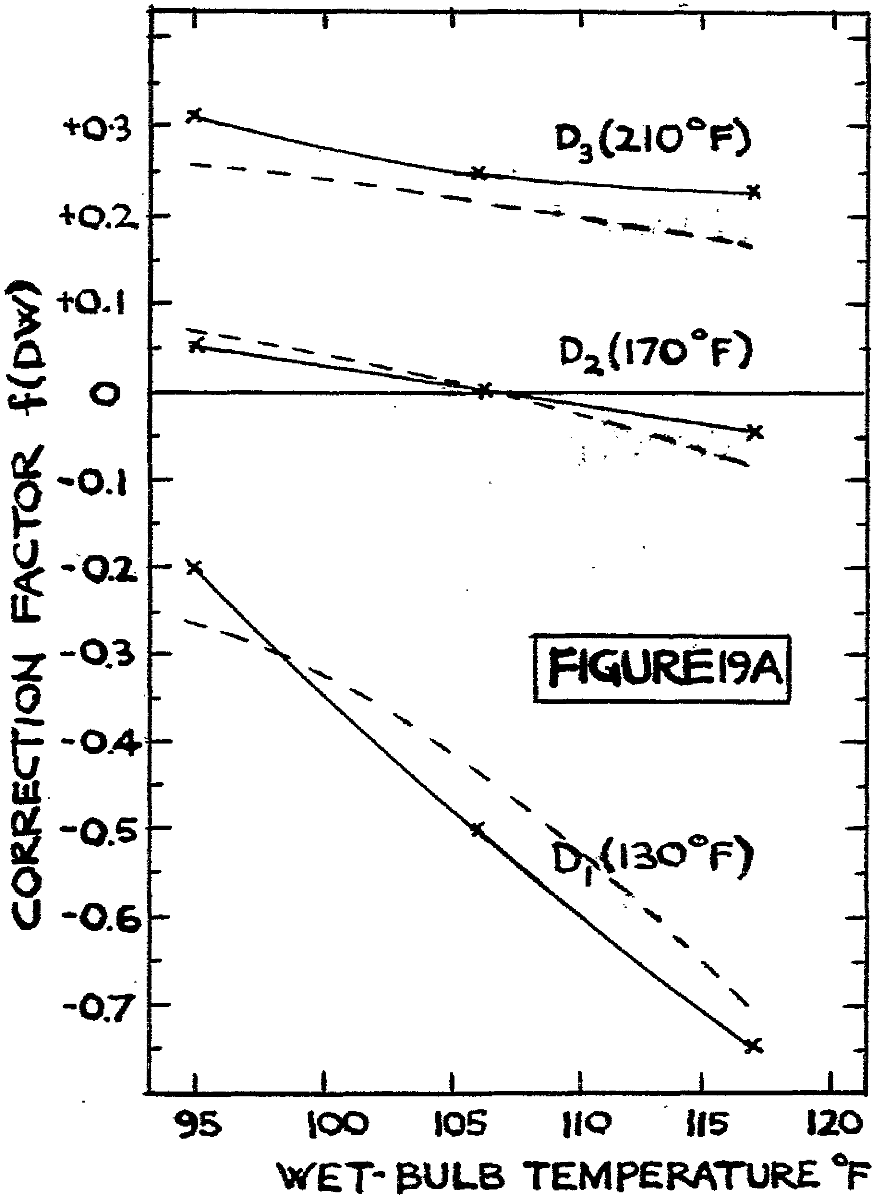

NOTE: THE DOTTED LINES IN THESE FIGURES DENOTE THE DRYING BEHAVIOUR PREDICTED BY DRYING THEORY.

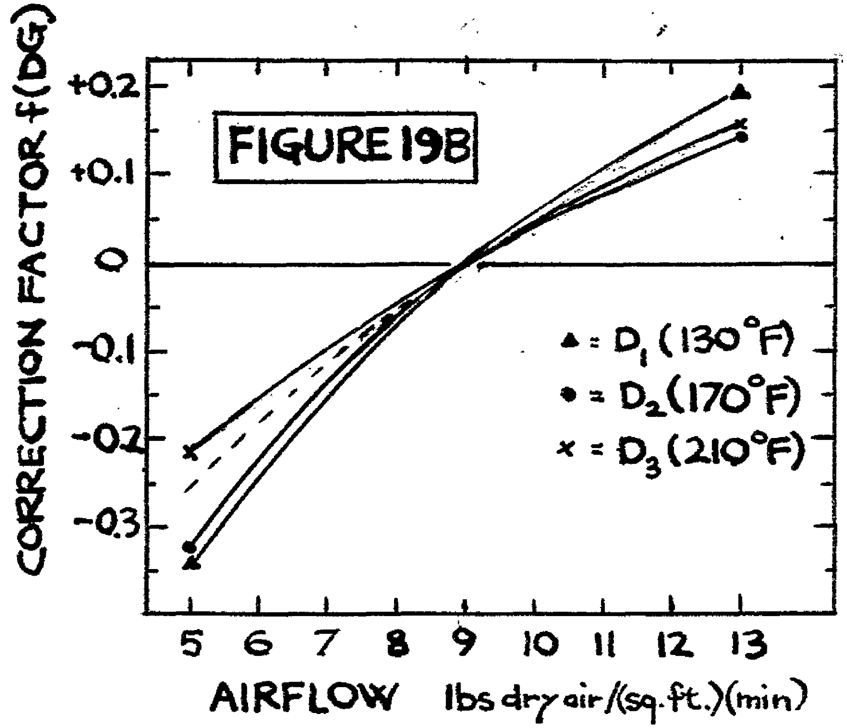

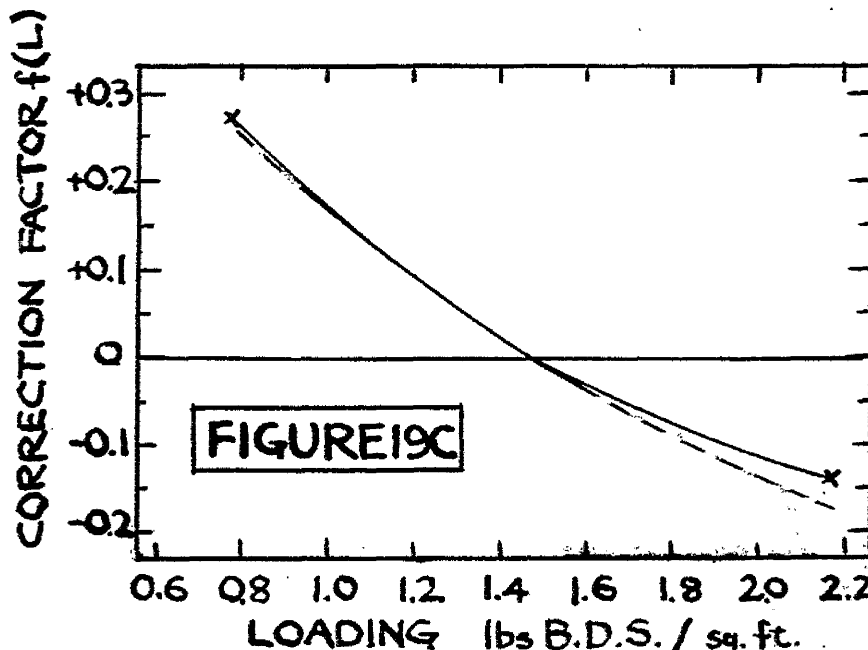

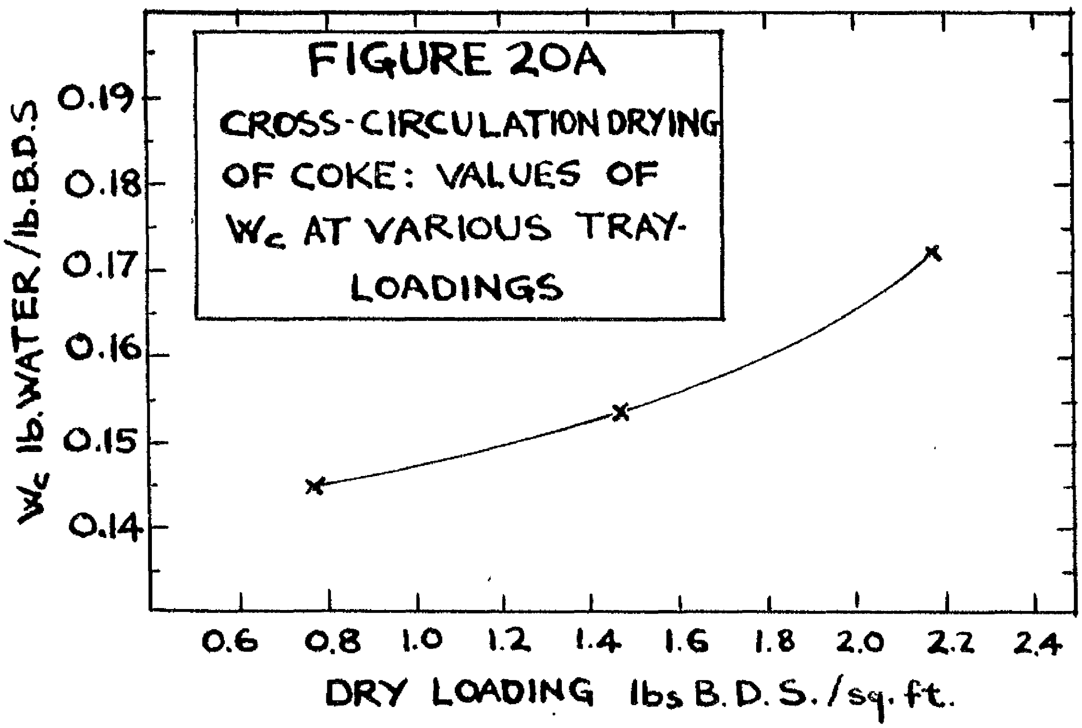

FIGURE 20A
CROSS-CIRCULATION DRYING OF COKE: VALUES OF Wc AT VARIOUS TRAY-LOADINGS
Wc lb. WATER / lb. B.D.S
0.19
0.18
0.17
0.16
0.15
0.14
0.6
0.8
1.0
1.2
1.4
1.6
1.8
2.0
2.2
2.4
DRY LOADING lbs B.D.S./sq.ft.

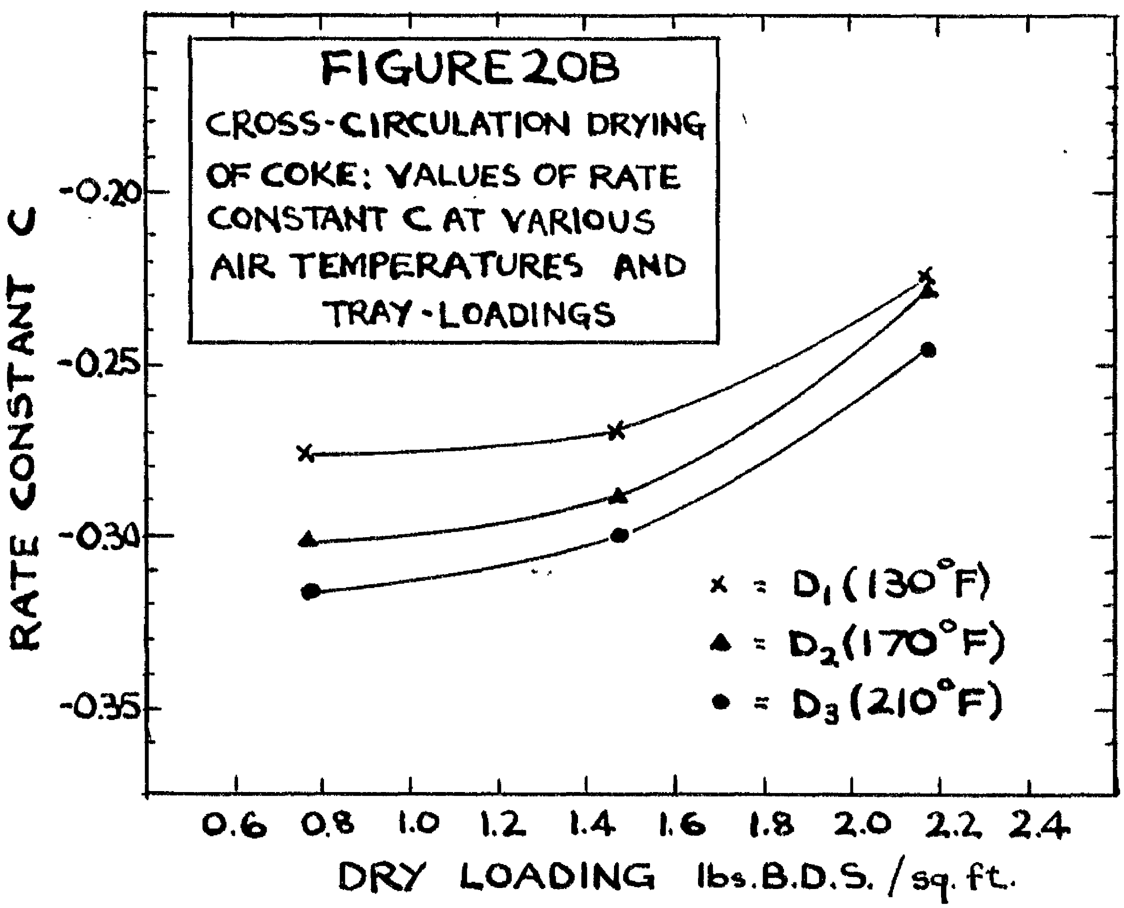

FIGURE 20B
CROSS-CIRCULATION DRYING OF COKE: VALUES OF RATE CONSTANT C AT VARIOUS AIR TEMPERATURES AND TRAY-LOADINGS
RATE CONSTANT C
-0.20
-0.25
-0.30
-0.35
× = D1 (130°F)
▲ = D2 (170°F)
● = D3 (210°F)
0.6
0.8
1.0
1.2
1.4
1.6
1.8
2.0
2.2
2.4
DRY LOADING lbs.B.D.S. / sq. ft.

Values of f(DG)

$D_1G_1 = -0.3425$ $D_2G_1 = -0.3304$ $D_3G_1 = -0.2170$
$D_1G_2 = 0$ $D_2G_2 = 0$ $D_3G_2 = 0$
$D_1G_3 = 0.1939$ $D_2G_3 = 0.1457$ $D_3G_3 = 0.1508$

These values are shown graphically in Figure 19B.

Values of f(L)

$L_1 = 0.2695$ $L_2 = 0$ $L_3 = -0.1397$

These values are shown graphically in Figure 19C.

Inspection of the values of W_c in Table 14 indicated that W_c was unaffected by D, W, and G but increased with increase in L, thus confirming the results of the preliminary two-level experiment. The values of W_c in Table 14, averaged over L_1, L_2 and L_3 were:

$L_1 = 0.145$ $L_2 = 0.154$ $L_3 = 0.172$

These values are shown graphically in Figure 20A.

Examination of the values of C in Table 13 confirmed the results of the preliminary two-level experiment - that the value of C depended on the values of D and L but was independent of the values of G and W. The values of C in Table 13 were therefore averaged over G and W for the various levels of D and L; these values were:

$D_1L_1 = -0.276$ $D_2L_1 = -0.300$ $D_3L_1 = -0.316$
$D_1L_2 = -0.270$ $D_2L_2 = -0.288$ $D_3L_2 = -0.300$
$D_1L_3 = -0.225$ $D_2L_3 = -0.227$ $D_3L_3 = -0.244$

These values are shown graphically in Figure 20B.

6.8 Method Of Predicting The Drying Time Of Coke In The Cross-Circulation Drier

The drying time of coke between various moisture contents and under various drying conditions may be predicted from the experimental results given in Section 6.7 by a method analogous to that described in Section 6.4 for porous-ceramic granules. Thus for coke, the drying time from an initial moisture content W_1 to a final moisture content W_2 is calculated as follows:

(a) $\frac{dW}{d\theta}$ is calculated from the expression:

$$\log_{10} \frac{dW}{d\theta} = -0.8570 + f(DW) + f(DG) + f(L)$$

f(DW), f(DG) and f(L) being found from Figures 19A, 19B and 19C respectively.

(b) W_e is obtained from Figure 20A

(c) θ_c' (measured from a standard moisture content $W_{st} = 0.271$) is found from the expression: $\theta_c' = \dfrac{60(0.271 - W_e)}{\frac{dW}{d\theta}}$

(d) C is found from Figure 20B.

(e) θ_T' is found from the equation:

$$\log_{10} \theta_T' = \log_{10} \theta_c' + (W_2 - W_e)/C$$

(f) θ_1' is found from the relationship:

$$\theta_1' = \frac{60(W_1 - 0.271)}{\frac{dW}{d\theta}}$$

and the drying time between W_1 and W_2 is given by the equation $\theta' = \theta_T' + \theta_1'$

6.9 Drying Of Brewers' Spent-Grain

The fibrous material tested was brewers' spent-grain obtained from R. and J. Tennent Ltd., Wellpark Brewery, Glasgow.

Spent-grain is a by-product of the brewing operation known as "mashing" in which crushed malt and maize are extracted with hot water; it is the part of the crushed malt and maize which remains insoluble during mashing and from which the wort (sugary extract) has been removed by filtration. It has a high protein content and is sold as cattle food; because of its high moisture content (70 to 80%), however, it rapidly goes rotten and it has to be used within a day or two. It may be preserved by drying.

Spent-grain was chosen as representative of a fibrous material mainly because a convenient supply of the material was available, and because, from previous work done in this Department (55), it was known to be suitable for through-circulation drying. The wet grain is in the form of a mash which shrinks on drying and the individual particles of spent-grain separate to form a bed of fairly open structure which has a dry bulk density of approximately 8.5 lb/cub.ft.

Method Of Preparing The Brewers' Spent-Grain For A Drying Test

Since the moisture content of the grain obtained from the Brewery varied considerably, and was frequently very high (greater than 100%), the grain was squeezed by hand to remove most of the free water before the grain was spread on the test-tray. This procedure left the grain with an approximately constant initial moisture content of $W = 2.56$ (a minimum $W = 2.35$ and a maximum

W = 2.83 being obtained).

Drying Conditions Used In The Drying Tests

The drying conditions used in the drying tests on the spent-grain were as follows:

TABLE 15

D_1 = 140	D_2 = 175	D_3 = 210
H_1 = 0.010	H_2 = 0.045	H_3 = 0.080
L_1 = 0.14 (¼ inch layer)	L_2 = 0.27 (½ inch layer)	L_3 = 0.40 (¾ inch layer)
G_1 = 5	G_2 = 9	G_3 = 13

Because of the high moisture content of the grain, each level of D was chosen 10F° higher than those used in the tests on porous-ceramic granules and on coke to give reasonably short drying times in most of the tests. The range of G was the same for all three materials. Since the dry weight L of grain used in a test was not known till the test was completed, the desired value of L for a given test was obtained by measuring the appropriate bed depth of wet grain into the test tray. Note that the effect of H on the drying time of the grain was studied, and not the effect of W, as in the tests on porous-ceramic granules.

6.10 Preliminary Two-Level Factorial Experiment On Brewers' Spent-Grain

Levels 1 and 3 of the four factors D, H, L and G shown in Table 15 were tested in a two-level factorial experiment involving the sixteen drying-tests shown in Table 16. The drying curves obtained in these tests are shown in Figures 21, 22, 23 and 24.

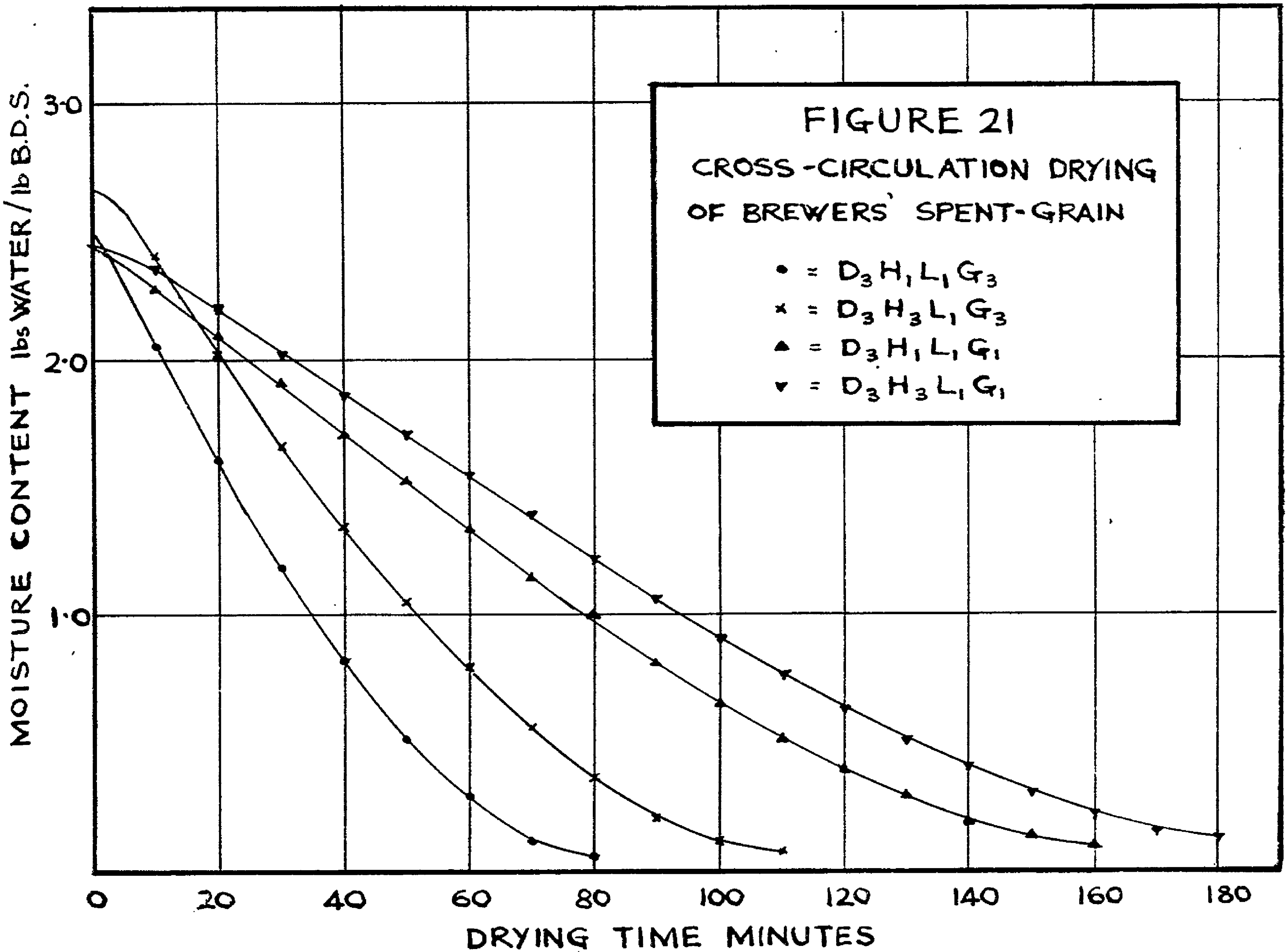
FIGURE 21
CROSS-CIRCULATION DRYING
OF BREWERS' SPENT-GRAIN
• = D3 H1 L1 G3
× = D3 H3 L1 G3
▲ = D3 H1 L1 G1
▼ = D3 H3 L1 G1
MOISTURE CONTENT lbs WATER/lb B.D.S.
3·0
2·0
1·0
0
20
40
60
80
100
120
140
160
180
DRYING TIME MINUTES

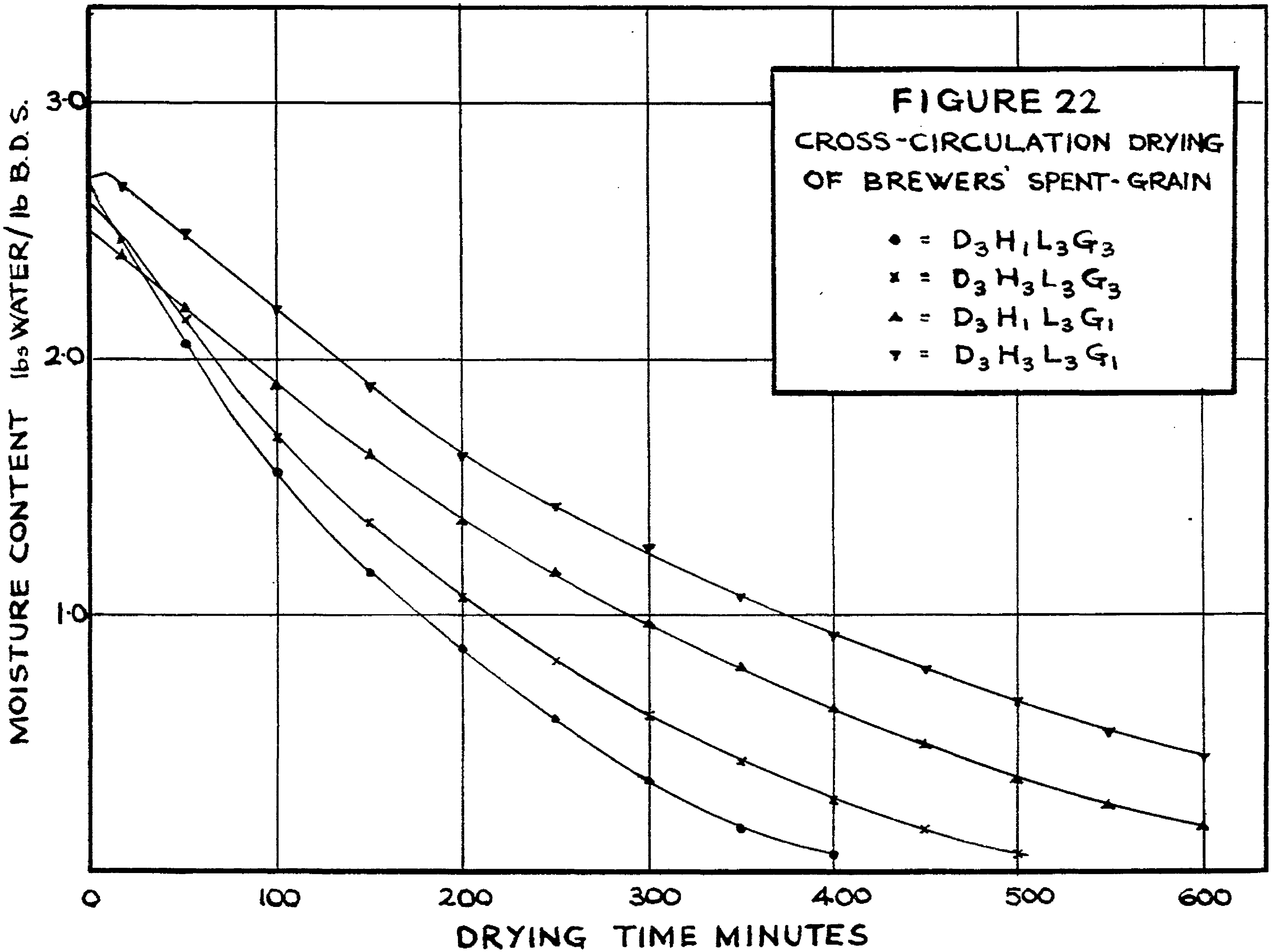

FIGURE 22
CROSS-CIRCULATION DRYING
OF BREWERS' SPENT-GRAIN
● = $D_3 H_1 L_3 G_3$
× = $D_3 H_3 L_3 G_3$
▲ = $D_3 H_1 L_3 G_1$
▼ = $D_3 H_3 L_3 G_1$
MOISTURE CONTENT lbs WATER/lb B.D.S.
3·0
2·0
1·0
0
100
200
300
400
500
600
DRYING TIME MINUTES

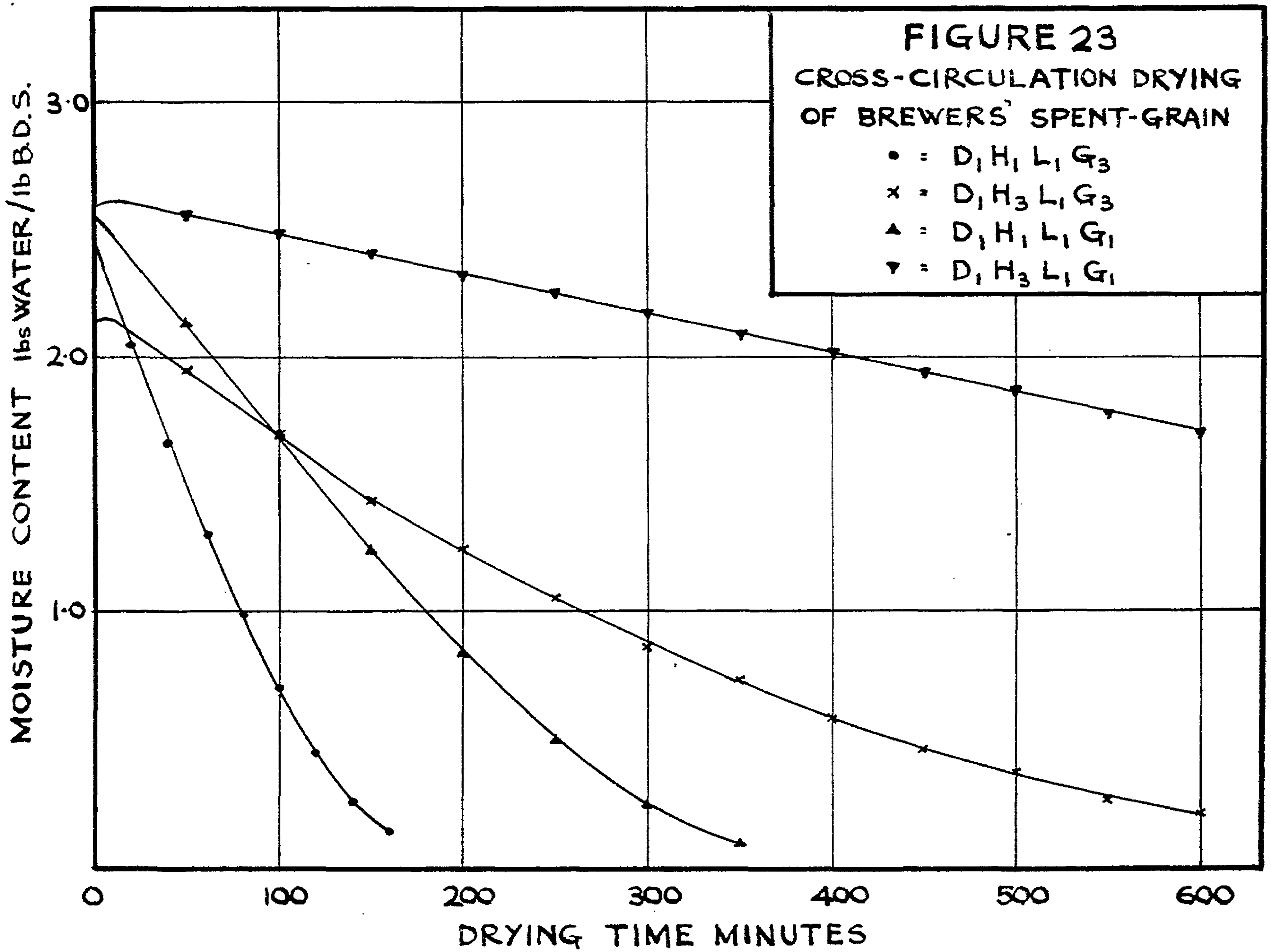
FIGURE 23
CROSS-CIRCULATION DRYING OF BREWERS' SPENT-GRAIN
• = D1 H1 L1 G3
x = D1 H3 L1 G3
▲ = D1 H1 L1 G1
▼ = D1 H3 L1 G1
MOISTURE CONTENT lbs WATER/lb B.D.S.
3.0
2.0
1.0
0
100
200
300
400
500
600
DRYING TIME MINUTES

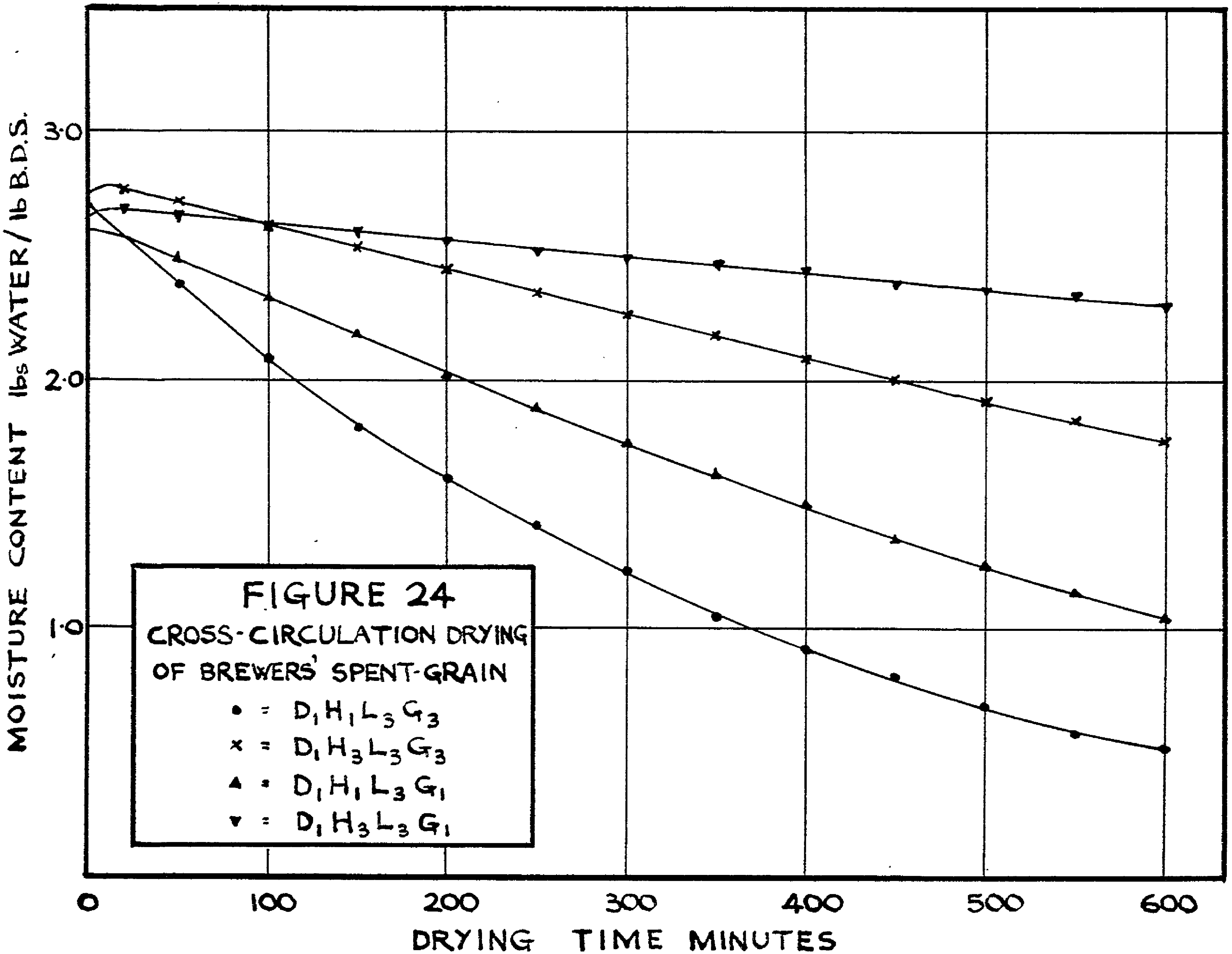
FIGURE 24
CROSS-CIRCULATION DRYING
OF BREWERS' SPENT-GRAIN
• = D1 H1 L3 G3
× = D1 H3 L3 G3
▲ = D1 H1 L3 G1
▼ = D1 H3 L3 G1
MOISTURE CONTENT lbs WATER / lb B.D.S.
3·0
2·0
1·0
0
100
200
300
400
500
600
DRYING TIME MINUTES

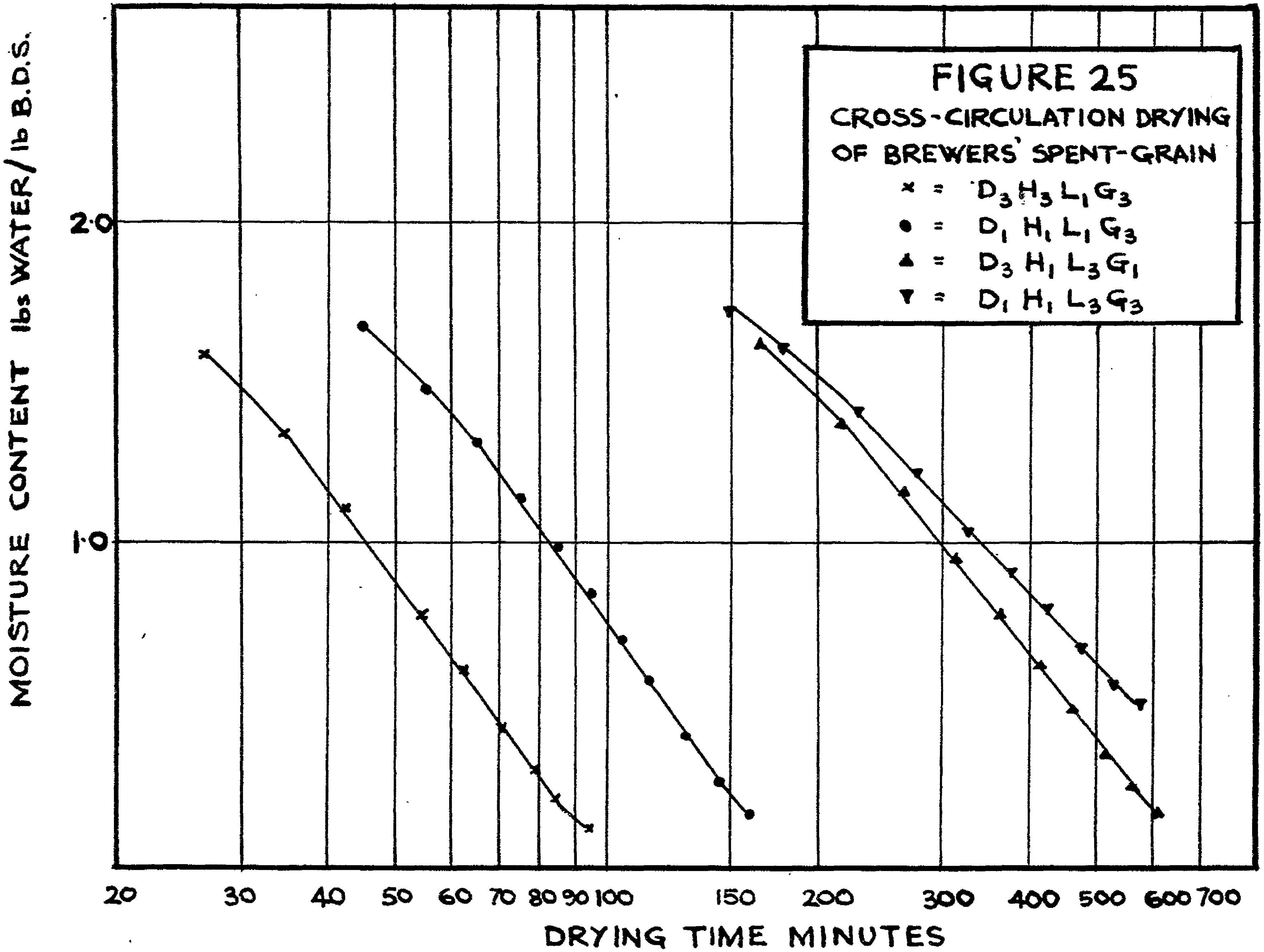

FIGURE 25
CROSS-CIRCULATION DRYING OF BREWERS' SPENT-GRAIN
× = D3 H3 L1 G3
● = D1 H1 L1 G3
▲ = D3 H1 L3 G1
▼ = D1 H1 L3 G3
MOISTURE CONTENT lbs WATER/lb B.D.S.
2·0
1·0
20
30
40
50
60
70
80
90
100
150
200
300
400
500
600
700
DRYING TIME MINUTES

TABLE 16: Results Of Preliminary Two-Level Factorial Experiment On Brewers' Spent-Grain.

Test Conditions	$\frac{dW}{d\Theta}$	$\log_{10} \frac{10dW}{d\Theta}$	W_c	C
$D_1H_1L_1G_1$	0.54	0.7324	1.13	-3.38
$D_1H_3L_1G_1$	0.11	0.0414	-	-
$D_3H_1L_1G_1$	1.12	1.0492	1.15	-3.24
$D_3H_3L_1G_1$	0.96	0.9823	1.15	-3.42
$D_1H_1L_1G_3$	1.20	1.0792	1.40	-3.02
$D_1H_3L_1G_3$	0.30	0.4771	1.45	-2.77
$D_3H_1L_1G_3$	2.71	1.4330	1.50	-3.06
$D_3H_3L_1G_3$	2.22	1.3464	1.48	-2.98
$D_1H_1L_3G_1$	0.18	0.2553	1.80	-2.42
$D_1H_3L_3G_1$	0.04	-0.3979	-	-
$D_3H_1L_3G_1$	0.38	0.5798	1.55	-2.81
$D_3H_3L_3G_1$	0.35	0.5441	1.78	-2.46
$D_1H_1L_3G_3$	0.37	0.5682	1.95	-2.32
$D_1H_3L_3G_3$	0.10	0.0000	1.85	-2.48
$D_3H_1L_3G_3$	0.71	0.8513	1.80	-2.74
$D_3H_3L_3G_3$	0.59	0.7709	1.85	-2.52

The values of $\frac{dW}{d\Theta}$, W_c and C given in Table 16 were obtained in the same way as were the corresponding quantities for the porous-ceramic granules and coke (Sections 6.2 and 6.6). The rate constant C was used to characterize the drying behaviour of the grain in the falling-rate period since the plot of W against log Θ' (See Figure 25) gave the best straight line of the various transformations of W and Θ' tried. The linear relationship between W and log Θ' (Θ' being measured from a standard initial W = 2.56) holds down to W = 0.25. No attempt was made to find a suitable linear transformation of W against Θ' at values of W below 0.25 since samples of grain dried to 0.35/0.30 showed no signs of decomposition after three weeks, and dried on standing to a W_e of 0.11; there is therefore no advantage in drying the grain below W = 0.30.

No values of W_c and C were obtained in the $D_1H_3G_1$ tests since the falling-rate period was not reached during these tests. Because of these missing values, only the $\frac{dW}{d\theta}$ results were subjected to an Analysis of Variance. The results of this Analysis, which was done on values of $\log_{10} \frac{10dW}{d\theta}$, are shown in Table 17; *, as usual, indicates an effect or interaction significant at the 5% probability level.

TABLE 17: Analysis Of Variance Of The Values Of $\log_{10} \frac{10dW}{d\theta}$ Obtained For Brewers' Spent-Grain

Source of Variance	Sum of Squares
D	1.4407801
H	0.4844508
G	0.4690538
L	0.9847089
DL	0.0016061
DG	0.0038162
DH	0.3149736
LG	0.0064521
GH	0.0007494
LH	0.0007440
DLG	0.0019779 *
LGH	0.0000522
DLH	0.0000733
DGH	0.0035490 *
Residual	0.0000281
Total	3.7130155

The Analysis of Variance indicated that the DGH and DLG interactions were significant: the values of $\frac{dW}{d\theta}$ for this material could therefore be expressed by the relationship

$$\log_{10} \frac{dW}{d\theta} = f(DGH) + f(DLG)$$

which is different from that obtained for porous-ceramic granules and coke.

Although no Analyses of Variance were possible for values of W_e and C because no values of these variables were obtained in the $D_1H_3G_1$ tests, inspection of the values of W_e and C in Table 16 indicated the following points:

(a) W_e appears to be independent of D and H but increases with increase in L and increases with increase in G to a degree dependent on the value of L used: i.e. there appears to be an LG interaction.

(b) The rate constant C appears to be independent of D, H and G and decreases (becomes less negative) with increase in L.

6.11 Fractional Three-Level Factorial Experiment On Brewers' Spent-Grain

The fractional three-level factorial experiment used to verify and elucidate the results of the preliminary two-level experiment, involved the 48 tests shown in Table 18. This experiment, which was larger than the experiments on porous-ceramic granules and coke each of which involved 41 tests, provided additional data on the values of f(DHG) and f(DLG) shown by the Analysis of Variance in Table 17 to have significant effects on $\log_{10} \frac{dW}{d\theta}$; it also provided data on the variation of W_e with L and G, and on the variation of

C with L.

Since of the three dependent variables - $\frac{dW}{d\theta}$, W_c and C - $\frac{dW}{d\theta}$ was affected most by the values of D, H, L and G, the enlarged experiment was designed primarily to allow $\frac{dW}{d\theta}$ for any specified drying conditions within the experimental range to be predicted from the value of $\log_{10} \frac{dW}{d\theta}$, (-0.3497), obtained in a standard test $D_2H_2L_2G_2$, and two correction factors to allow for variations in the various factors from their standard values according to the relationship:

$$\log_{10} \frac{dW}{d\theta} = -0.3497 + f(DGH) + f\ (LGD)$$

The values of the correction factor f(LGD) were obtained from the values in Table 19 as the average differences between the values in each LG column at a single level of D and the values in the corresponding DW row in the L_2G_2 column. As an example, the value of f(LGD) for the drying conditions $D_1L_1G_1$ is the average of:

$$0.7324 - 0.6902 = 0.0422$$
$$0.0414 - 0.0414 = 0.0000$$

The various values of f(LGD) obtained in this way are shown in Table 22.

Since the values of f(LGD) in Table 22 for the various levels of LG showed no real trend with change in D, it was concluded that, contrary to the conclusions of the preliminary two-level experiment, the combined effect of L and G on $\log_{10} \frac{dW}{d\theta}$ was independent of the value of D used. The values of f(LGD) in each LG row of Table 22 were therefore averaged over D and the average correction factor denoted by f(LG). The values of f(LG) obtained are shown in

TABLE 18: Values of $\frac{dW}{d\theta}$ for brewers' spent-grain dried in the cross-circulation drier

	L_1G_1	L_1G_2	L_1G_3	L_2G_1	L_2G_2	L_2G_3	L_3G_1	L_3G_2	L_3G_3
D_1H_1	0.54		1.20		0.49		0.18		0.37
D_1H_2		0.42		0.11	0.19	0.34		0.13	
D_1H_3	0.11		0.30		0.11		0.04		0.10
D_2H_1				0.35	0.63	0.74		0.39	0.50
D_2H_2	0.51	0.96	1.20	0.26	0.45	0.61	0.18	0.30	0.38
D_2H_3	0.44	0.84		0.21	0.44	0.54			
D_3H_1	1.12		2.71		0.86		0.38		0.71
D_3H_2		1.47		0.45	0.75	1.05		0.47	
D_3H_3	0.96		2.22		0.66		0.35		0.59

TABLE 19: Values of $\log_{10} \frac{10dW}{d\theta}$ for brewers' spent grain dried in the cross-circulation drier

	L_1G_1	L_1G_2	L_1G_3	L_2G_1	L_2G_2	L_2G_3	L_3G_1	L_3G_2	L_3G_3
D_1H_1	0.7324		1.0792		0.6902		0.2553		0.5682
D_1H_2		0.6232		0.0414	0.2788	0.5315		0.1139	
D_1H_3	0.0414		0.4771		0.0414		-0.3979		0.0000
D_2H_1				0.5441	0.7993	0.8692		0.5911	0.6990
D_2H_2	0.7076	0.9823	1.0792	0.4150	0.6503	0.7853	0.2553	0.4771	0.5798
D_2H_3	0.6435	0.9243		0.3222	0.6435	0.7324			
D_3H_1	1.0492		1.4330		0.9345		0.5798		0.8513
D_3H_2		1.1673		0.6532	0.8751	1.0212		0.6720	
D_3H_3	0.9823		1.3464		0.8195		0.5441		0.7709

TABLE 20: Values of W_c for brewers' spent-grain dried in the cross-circulation drier

	L_1G_1	L_1G_2	L_1G_3	L_2G_1	L_2G_2	L_2G_3	L_3G_1	L_3G_2	L_3G_3
D_1H_1	1.13		1.40		1.90		1.80		1.95
D_1H_2		1.37		—	1.74	2.00		1.78	
D_1H_3	—		1.45		1.80		—		1.85
D_2H_1				1.36	1.75	1.72		1.83	2.03
D_2H_2	1.20	1.45	1.25	1.30	1.74	1.82	1.78	1.90	1.95
D_2H_3	1.58	1.52		1.76	1.60	1.91			
D_3H_1	1.15		1.50		1.92		1.55		1.80
D_3H_2		1.35		1.65	1.91	2.05		1.91	
D_3H_3	1.15		1.48		1.70		1.78		1.85

TABLE 21: Values of Rate Constant C for brewers' spent-grain dried in the cross-circulation drier

	L_1G_1	L_1G_2	L_1G_3	L_2G_1	L_2G_2	L_2G_3	L_3G_1	L_3G_2	L_3G_3
D_1H_1	-3.38		-3.02		-2.93		-2.42		-2.32
D_1H_2		-3.06		—	-2.72	-2.62		-2.51	
D_1H_3	—		-2.77		-2.88		—		-2.48
D_2H_1				-2.88	-2.92	-2.99		-2.73	-2.62
D_2H_2	-3.18	-2.86	-3.08	-3.05	-2.95	-2.95	-2.73	-2.50	-2.65
D_2H_3	-3.08	-3.12		-2.78	-2.94	-2.83			
D_3H_1	-3.24		-3.06		-3.08		-2.81		-2.74
D_3H_2		-3.22		-2.77	-2.90	-2.97		-2.65	
D_3H_3	-3.42		-2.98		-3.03		-2.46		-2.52

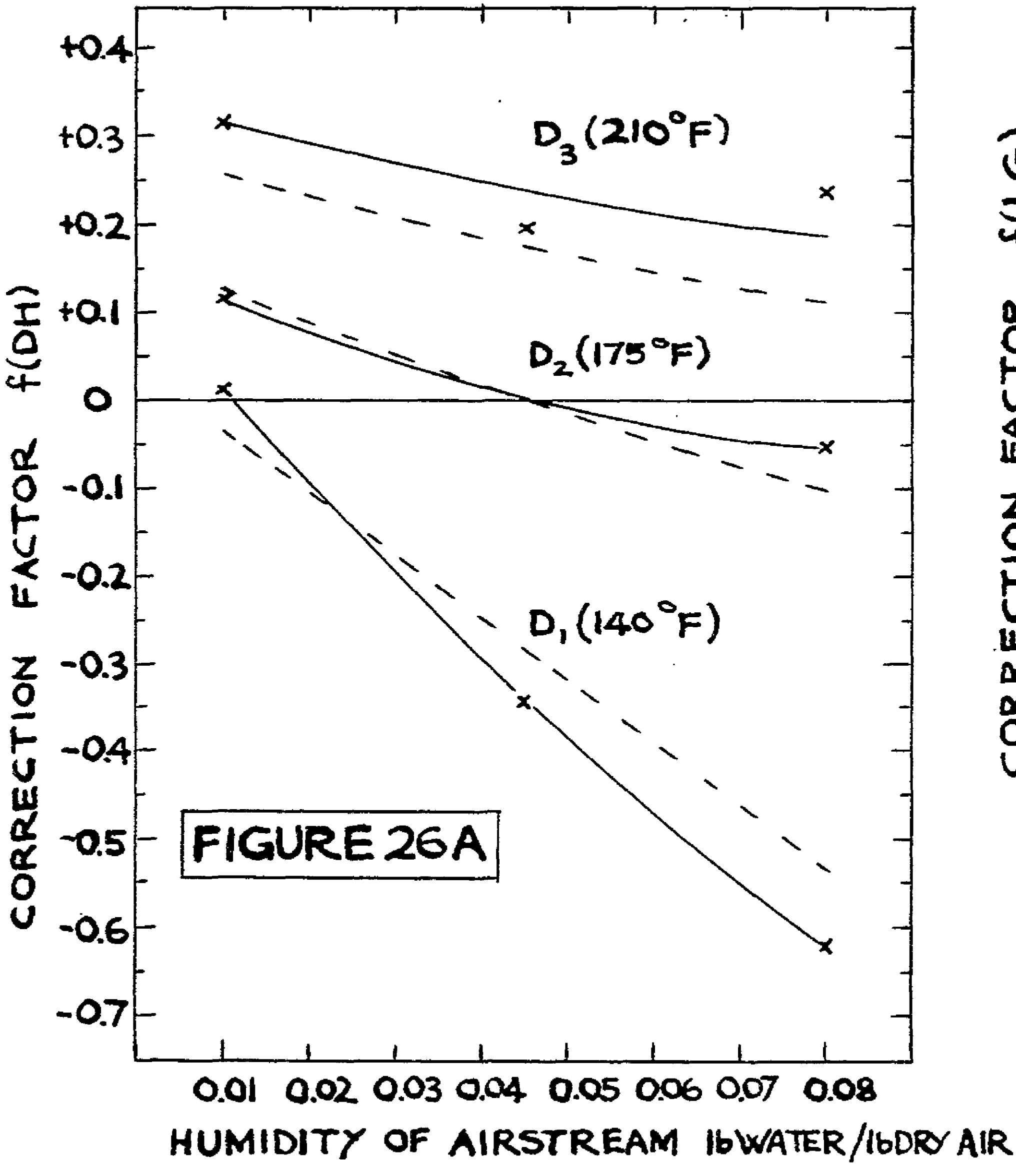

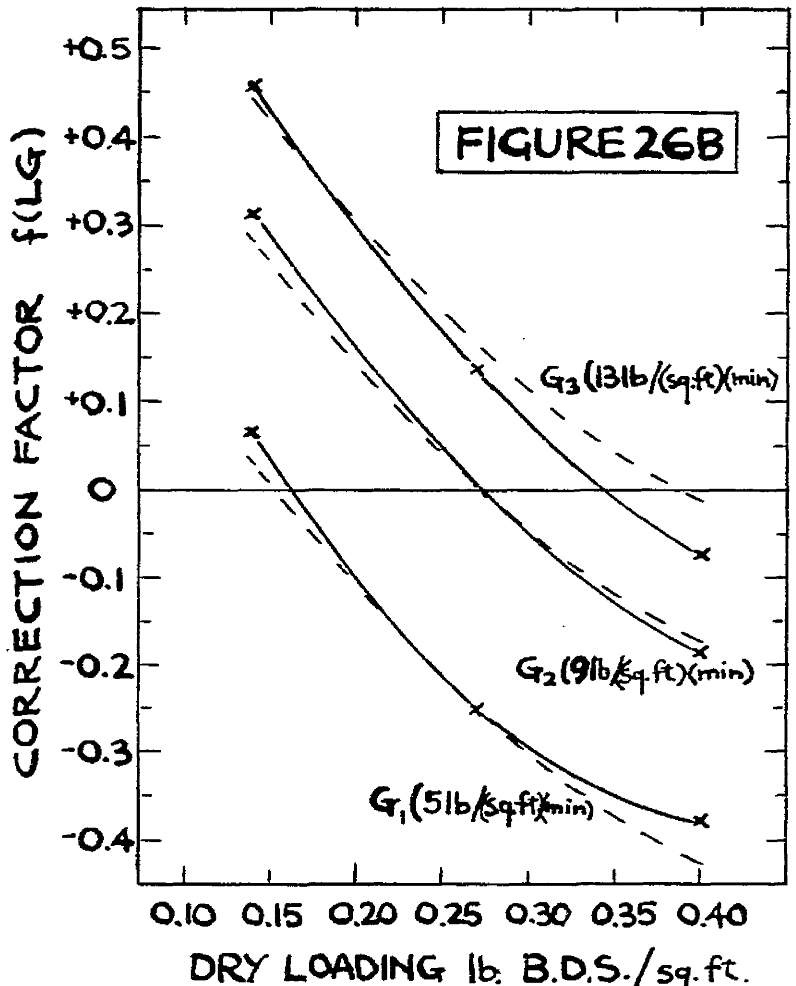

NOTE: THE DOTTED LINES IN FIGURES 26A AND 26B DENOTE THE DRYING BEHAVIOUR PREDICTED BY DRYING THEORY.

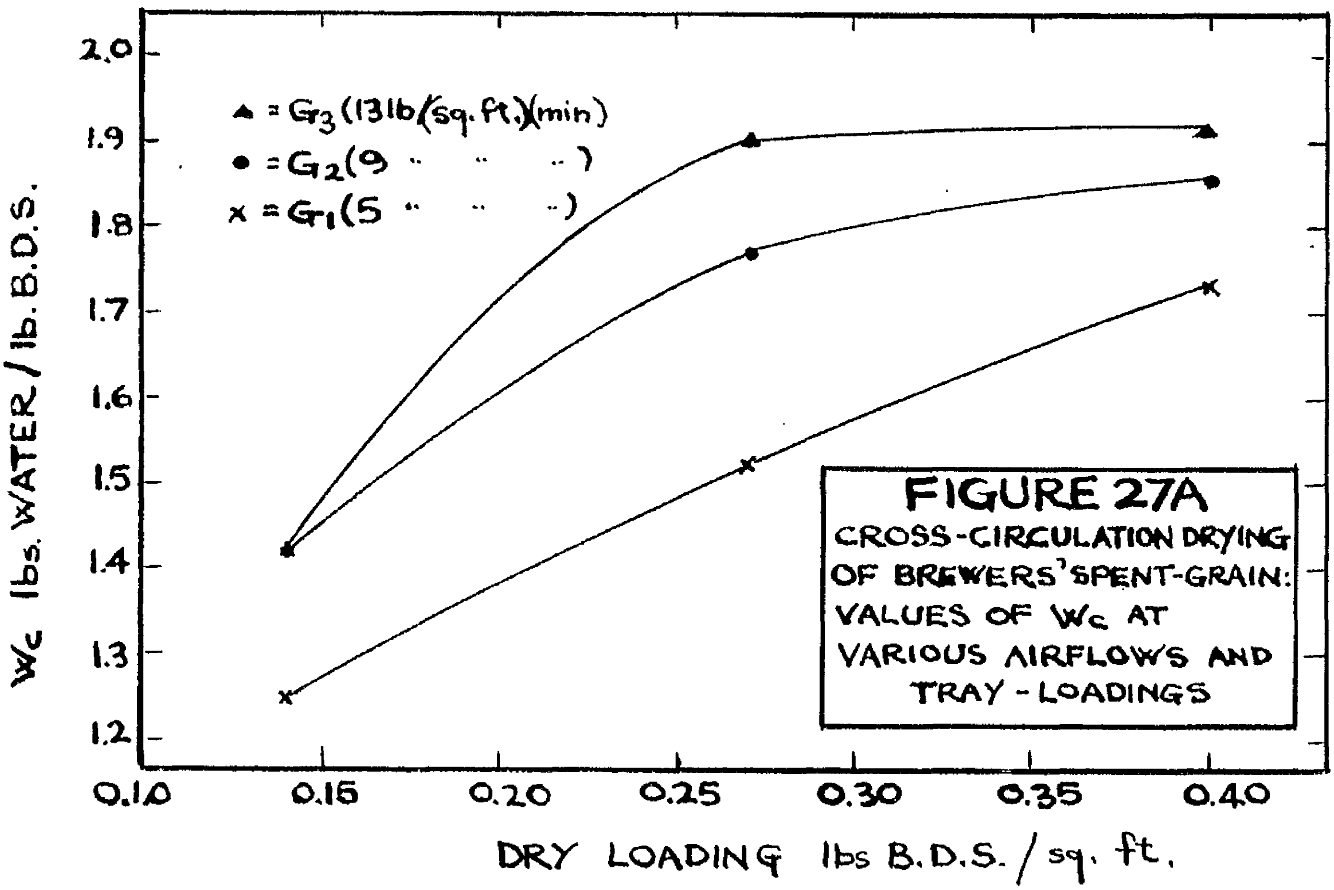

FIGURE 27A
CROSS-CIRCULATION DRYING OF BREWERS' SPENT-GRAIN: VALUES OF Wc AT VARIOUS AIRFLOWS AND TRAY-LOADINGS
▲ = G3 (13 lb/(sq. ft.)(min))
● = G2 (9 " " ")
x = G1 (5 " " ")
Wc lbs. WATER / lb. B.D.S.
2.0
1.9
1.8
1.7
1.6
1.5
1.4
1.3
1.2
0.10
0.15
0.20
0.25
0.30
0.35
0.40
DRY LOADING lbs B.D.S. / sq. ft.

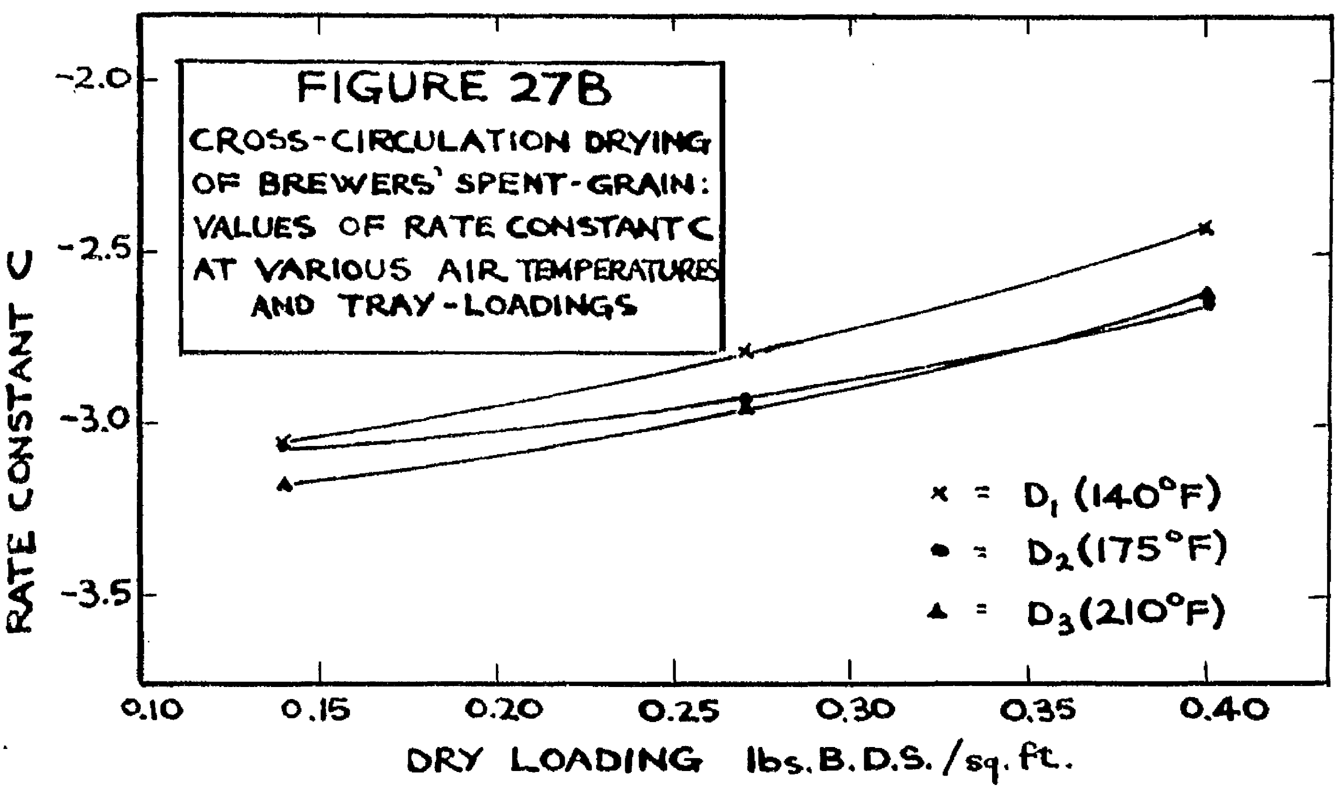

FIGURE 27B
CROSS-CIRCULATION DRYING OF BREWERS' SPENT-GRAIN: VALUES OF RATE CONSTANT C AT VARIOUS AIR TEMPERATURES AND TRAY-LOADINGS
x = D1 (140°F)
● = D2 (175°F)
▲ = D3 (210°F)
RATE CONSTANT C
-2.0
-2.5
-3.0
-3.5
0.10
0.15
0.20
0.25
0.30
0.35
0.40
DRY LOADING lbs. B.D.S. / sq. ft.

column four of Table 22 and are shown graphically in Figure 26B.

TABLE 22: Values of f(LGD) and f(LG) for Brewers' Spent-Grain

	f(LGD)			f(LG)
	D_1	D_2	D_3	Average
L_1G_1	0.0422 0.0000	0.0573 0.0000	0.1147 0.1628	0.0628
L_1G_2	0.3444	0.3320 0.2808	0.2922	0.3123
L_1G_3	0.3890 0.4357	0.4289	0.4985 0.5269	0.4558
L_2G_1	-0.2374	-0.2552 -0.2353 -0.3213	-0.2219	-0.2542
L_2G_2	0	0	0	0
L_2G_3	0.2527	0.0699 0.1350 0.0889	0.1461	0.1385
L_3G_1	-0.4349 -0.4393	-0.3950	-0.3547 -0.2754	-0.3799
L_3G_2	-0.1649	-0.2072 -0.1732	-0.2031	-0.1871
L_3G_3	-0.1220 -0.0414	-0.1003 -0.0705	-0.0832 -0.0486	-0.0777

The values of the correction factor f(DHG) were obtained from the values in Table 19 as the average differences between the values in each DH row at each level of G, and the values in the corresponding LG column in the D_2H_2 row. As an example, the value of f(DHG) for the drying conditions $D_1H_1G_1$ is the average of:

$$0.7324 - 0.7076 = 0.0248$$

$$0.2553 - 0.2553 = 0.0000$$

The values of f(DHG) obtained in this way are shown in Table 23.

TABLE 23: Values of f(DHG) and f(DH) for Brewers' Spent-Grain

	f(DHG)			f(DH)
	G_1	G_2	G_3	Average
D_1H_1	0.0248 0.0000	0.0399	0.0000 -0.0116	0.0106
D_1H_2	-0.3736	-0.3591 -0.3715 -0.3632	-0.2538	-0.3442
D_1H_3	-0.6662 -0.6532	-0.6089	-0.6021 -0.5798	-0.6220
D_2H_1	0.1291	0.1490 0.1140	0.0839 0.1192	0.1190
D_2H_2	0	0	0	0
D_2H_3	-0.0641 -0.0928	-0.0580 -0.0068	-0.0529	-0.0549
D_3H_1	0.3416 0.3245	0.2842	0.3538 0.2715	0.3151
D_3H_2	0.2382	0.1850 0.2130 0.1950	0.2359	0.1934
D_3H_3	0.2747 0.2888	0.1692	0.2672 0.1911	0.2382

Since the values of f(DHG) in Table 23 for the various levels of D and H showed no definite trend with change in D, it was concluded that the effect of DH on $\log_{10} \frac{dW}{d\theta}$ was independent of G; the values of f(DGH) in each DH row of Table 23 were therefore averaged over G. The values of the average correction factor, denoted by f(DH), are tabulated in column four of Table 23, and shown graphically in Figure 26A.

Summing up, the more elaborate experiment showed that $\frac{dW}{d\theta}$ could be predicted for any given drying conditions by the relationship

$$\log_{10} \frac{dW}{d\Theta} = -0.3497 + f(LG) + f(DH)$$

The values of W_c shown in Table 20 confirmed the results of the preliminary two-level experiment - that W_c was unaffected by D and H but depended on L and G. The values in Table 20 were therefore averaged over D and H for the various levels of L and G; these average values were:

L_1G_1	1.25	L_2G_1	1.52	L_3G_1	1.73
L_1G_2	1.42	L_2G_2	1.77	L_3G_2	1.85
L_1G_3	1.42	L_2G_3	1.90	L_3G_3	1.91

These values are shown graphically in Figure 27A.

Examination of the values of C in Table 21 indicated that C was mainly affected by L; was slightly affected by D; and was unaffected by G or H. The values in Table 21 were therefore averaged over G and H for each level of D and L, giving the following values of C at the various levels of D and L:

$D_1L_1 = -3.06$	$D_2L_1 = -3.07$	$D_3L_1 = -3.18$
$D_1L_2 = -2.79$	$D_2L_2 = -2.93$	$D_3L_2 = -2.95$
$D_1L_3 = -2.43$	$D_2L_3 = -2.65$	$D_3L_3 = -2.64$

These values of C are shown graphically in Figure 27B.

6.12 Method Of Predicting The Drying Time Of Brewers' Spent-Grain In The Cross-Circulation Drier

The experimental results given in Section 6.11 may be used as follows to predict the time required to dry the brewers' spent-grain from an initial moisture content W_1, to a final moisture content W_2, under any drying conditions within the experimental ranges of D, H, L and G.

(a) The constant drying rate $\frac{dW}{d\Theta}$ is calculated from the equation:

$$\log_{10} \frac{dW}{d\theta} = -0.3497 + f(DH) + f(LG)$$

The values of the correction factors f(DH) and f(LG) appropriate to the drying conditions used are obtained from Figures 26A and 26B.

(b) The critical moisture content W_c for the appropriate values of L and G is obtained from Figure 27A.

(c) The duration of the constant drying rate period in minutes θ_c' (measured from a standard moisture content $W_{st} = 2.56$) is obtained from the expression:

$$\theta_c' = \frac{60(2.56 - W_c)}{\frac{dW}{d\theta}}$$

(d) The rate constant C for the appropriate values of D and L is obtained from Figure 27B.

(e) θ_F', the time in minutes taken to dry the grain from W_{st} to W_2, is calculated from the expression:

$$\log_{10}\theta_F' = \log_{10}\theta_c' + \frac{W_2 - W_c}{C}$$

(f) θ_1', the drying time of the grain between W_1 and W_{st} is given by the equation:

$$\theta_1' = \frac{60(W_1 - 2.56)}{\frac{dW}{d\theta}}$$

(g) θ', the drying time of the grain between W_1 and W_2 is given by the equation:

$$\theta' = \theta_F' + \theta_1'$$

The method used to predict the drying time of the grain is similar to the methods described previously in Sections 6.4 and 6.8 for predicting the drying times of porous-ceramic granules and coke.

6.13. Discussion Of Cross-Circulation Drying Results

Constant Drying Rate Results The experimental constant drying rates of the porous-ceramic granules, coke and brewers' spent-grain were compared with the constant drying rates predicted by the theoretical equation:

$$\frac{dW}{d\theta} = \frac{K' G^n (D - W)}{L} \quad \ldots \quad \text{Equation A.}$$

which is a general form of Equation 6. To facilitate these comparisons, theoretical values of the empirical correction factors f(DW), f(DH), f(DG), f(L) and f(LG) shown in Figures 12A, 12B, 12C, 19A, 19B, 19C, 26A and 26B were calculated from the logarithmic form of Equation A in the following manner:

f(DW) is the average difference between $\log_{10} \frac{dW}{d\theta}$ for tests done at any values of D and W and $\log_{10} \frac{dW}{d\theta}$ for tests done at the corresponding values of L and G but at the standard values of D and W, namely D_2 and W_2; this may be written mathematically as:

$$f(DW) = \log_{10} \frac{dW}{d\theta} (DWLG) - \log_{10} \frac{dW}{d\theta} (D_2W_2LG) \quad \ldots \quad \text{Equation B.}$$

The logarithmic form of Equation A can be used to give the following equivalent expressions for the terms on the right hand side of Equation B:

$$\log_{10} \frac{dW}{d\theta} (DWLG) = \log_{10} K' + n\log_{10} G + \log_{10} (D - W) - \log_{10} L$$

$$\log_{10} \frac{dW}{d\theta} (D_2W_2LG) = \log_{10} K' + n\log_{10} G + \log_{10} (D_2 - W_2) - \log_{10} L$$

Substituting these values in Equation B we obtain

$$f(DW) = \log_{10} (D - W) - \log_{10} (D_2 - W_2) \quad \ldots \quad \text{Equation C.}$$

Values of f(DW) calculated from Equation C are shown graphically as dotted lines in Figures 12A and 19A.

The theoretical values of f(DH) shown as dotted lines in Figure 26A were calculated for various levels of D and H by converting the H values into values of (D – W)., and applying Equation C.

Since, according to the theoretical Equation A, there is no DG interaction but only a G main effect, the theoretical values of f(DG) shown as dotted lines in Figures 12B and 19B are in fact values of f(G). The following expression for f(G) was derived from the logarithmic form of Equation A:

$$f(G) = \log_{10} \frac{dW}{d\theta}(DWLG) - \log_{10} \frac{dW}{d\theta}(DWLG_2) = n(\log_{10} G - \log_{10} G_2) \quad \ldots \text{ Equation D.}$$

Comparison of the experimental values of f(DG) with values of f(G) calculated from Equation D for various values of n, showed that, in the range of airflows used in the present investigation, n = 1 gave better agreement between the experimental and theoretical values of f(DG) than n = 0.8, found by Shepherd, Hadlock and Brewer (3).

The theoretical values of f(L) shown as dotted lines in Figures 12C and 19C were calculated from the expression:

$$f(L) = \log_{10} \frac{dW}{d\theta}(DWLG) - \log_{10} \frac{dW}{d\theta}(DWL_2G) = \log_{10} L_2 - \log_{10} L \quad \ldots \text{ Equation E.}$$

The theoretical values of f(LG) shown as dotted lines in Figure 26B were obtained by summing the values of f(G) and f(L) calculated from Equations D and E; the totals represent the values of f(LG) which should be obtained if there is no interaction between G and L.

<u>Porous-Ceramic Granules</u> Inspection of Figures 12A, 12B and 12C shows that the experimental values of f(DW), f(DG) and f(L) were very close to the theoretical values. Experimental values of f(DW) at the highest air temperature tested (D_3 = 210°F) were appreciably higher than those predicted by Equation C. The higher drying rate was

probably caused by increased heat conduction and radiation to the wet granules at the higher air temperature (see Section 2.2).

Figure 12B shows that the interaction between D and G was slight, and that the effect of G on the drying rate decreased with increase in D. The theoretical values of f(DG) almost coincided with the experimental values for $D_2 = 170^{\circ}F$.

The experimental and theoretical values of f(L) coincided exactly, thus indicating that for a given set of drying conditions the weight of water removed from a given tray area in unit time was independent of the tray-loading used.

Coke From Figures 19A, 19B and 19C it may be seen that the experimental values of f(DW), f(DG) and f(L) for coke showed slightly greater deviations from the theoretical values than did the experimental values for the porous-ceramic granules. As was found for porous-ceramic granules, the experimental values of f(DW) in Figure 19A for tests done at D_3 were higher than those predicted by Equation C. In addition, the experimental values of f(DW) for tests done at D_1W_2 and D_1W_3 were slightly lower than those predicted by Equation C. The reason for the reduced drying rate is not clear, but it is possible that at the high relative humidities (45 to 65%) used in these tests some condensation could take place on localized cool spots on the coke.

Figure 19B shows that the effect of G on the drying rate decreased with increase in D. This interaction between G and D is similar to, but of greater magnitude than, the GD interaction noted for porous-ceramic granules (Figure 12B). The theoretical values of f(DG) calculated from Equation D coincided with the experimental values for D = 210°F in the airflow range G = 9 to 13.

The theoretical values of f(L) calculated from Equation E agreed closely with the experimental values shown in Figure 19B, but at the heaviest tray loading used, the experimental values were slightly higher than the theoretical. The higher drying rate (weight of water removed from tray per unit time) at the heavy loading was possibly due to better coverage of the test tray with a resultant increase in the wet surface area exposed to the airstream.

Brewers' Spent-Grain. From Figure 26A it can be seen that the experimental values of f(DH) for tests done at D_3 were higher than the theoretical values and the experimental values for tests at D_1H_2 and D_1H_3 were lower than the theoretical values calculated from Equation C. Similar drying behaviour was noted in the drying tests on coke.

Comparison of the theoretical and experimental values of f(LG) shown in Figure 26B indicates that loading had only a minor influence on the effect of airflow on the drying rate - the effect of G on the drying rate decreased slightly with increase in loading.

Comparison Of The Drying Rates Of The Porous-Ceramic Granules, Coke And Brewers' Spent-Grain

To compare the constant drying rates of the porous-ceramic granules, coke and brewers' spent-grain, the average value of the empirical constant K' in Equation A was evaluated for each material by substituting the experimental values of $\frac{dW}{d\theta}$ in the equation, taking $n = 1$. The average values of K' for the various materials were:

Porous-Ceramic Granules = 3.52×10^{-4}

Coke = 3.40×10^{-4}

Brewers' Spent-Grain = 2.23×10^{-4}

It is interesting to note that the value of K' for the brewers' spent-grain, which formed a fairly level bed, agrees closely with the value of $K' = 2.12 \times 10^{-4}$ obtained by Shepherd, Hadlock and Brewer (3) for materials such as sand and clays which form beds with plane surfaces. (Note the value of $K' = 2.12 \times 10^{-4}$ quoted above has been corrected for the fact that the Shepherd, Hadlock and Brewer equation contained $G^{0.8}$ and not G as in the present investigation). The higher drying rates of the coke and porous-ceramic granules are in agreement with the observation (7) that a bed of large particles (greater than about $\frac{1}{8}$ inch mesh), because of the greater wet surface area exposed to the airstream, has a faster constant drying rate than a bed of small particles covering the same tray area.

Critical Moisture Contents

It was found that the critical moisture contents of both porous-granular materials tested were independent of the drying conditions, but increased with increase in tray loading. Calculation of the total amount of moisture removed from the tray of material before W_c was reached (calculated from a standard initial moisture content) showed that the total weight of moisture removed increased as tray loading increased. As an example, the total weights of water removed from a 1 sq.ft. tray of porous-ceramic granules before W_c was reached (measured from a standard initial moisture content $W = 0.296$) were, for various tray-loadings:

$$L_1 = 0.223 \text{ lb.} \qquad L_2 = 0.338 \text{ lb.} \qquad L_3 = 0.434 \text{ lb.}$$

This increase in water removal indicates that as the tray-loading increased, increasing amounts of moisture moved from the interior of the bed to the surface during the constant drying-rate period.

The critical moisture content of the brewers' spent-grain was independent of the air temperature and humidity but increased with increases in tray-loading and airflow. As with the porous-granular materials tested, moisture movement to the surface of the bed during the constant drying rate period was found to increase with tray loading. The increase in W_c with increased airflow was possibly caused by the surface layer of the grain drying out quickly at the high airflows thus destroying the capillary action drawing the water to the surface; at low airflows, however, the surface layer could remain wet for a longer time and the capillary mechanism would not break down until lower average moisture contents were reached.

The Rate Constant C.

Despite the diversity of the physical structures of the porous-ceramic granules, coke and brewers' spent-grain, it was found that the rate constant C could be used to describe the falling-rate drying behaviour of all three materials. Moreover, the values of C for each material were found to be independent of the air humidity and velocity, but increased (became more negative) with increase in air temperature and decreased as tray-loading was increased. From Figures 13A, 20B and 27B it can be seen that L had a much more marked effect on C than had D. The marked increase in the drying time with increase in loading, noted in the present investigation, is a characteristic of cross-circulation drying, arising mainly from the increased distance water has to travel to the surface of the bed of material. The observed increase in drying rate with increase in air temperature was expected, since more heat of vaporization is supplied from the hot airstream to the drying material as the temperature of the airstream increases. The fact that air velocity and air humidity had little effect on C indicates that the drying rate is controlled mainly by the rate of moisture movement to the surface of the material.

Accuracy Of Proposed Method Of Predicting Drying Times

The prediction methods described in Sections 6.4., 6.8 and 6.12 were found to give drying times for the porous-ceramic granules, coke and brewers' spent-grain which were within ± 16% of the experimental values (see Table 23A). This prediction accuracy compares favourably with the experimental error in determining the drying times from an initial moisture content 0.27 to a final moisture content of 0.05 in the standard $D_2W_2L_2G_2$ tests for porous-ceramic granules and coke, and from an initial moisture content 2.56 to a final moisture content 0.5 in the standard $D_2H_2L_2G_2$ test on brewers' spent-grain — ± 13% for porous-ceramic granules, ± 12% for coke, ± 10% for brewers' spent-grain. The examples given in Table 23A were chosen partly from tests included in the factorial experiments used to derive the prediction methods and partly from additional tests done at intermediate values of the various factors used in the factorial experiments. In predicting the drying times for these additional tests the values of W_c, C and all the correction factors for calculating $\frac{dW}{d\theta}$ except f(DW) and f(DH), were obtained from the appropriate Figures by linear interpolation; f(DW) and f(DH) were obtained from the theoretical values by applying a correction estimated by linear interpolation from the difference between the experimental and theoretical values of f(DW) or f(DH) at the various levels of D and W.

It is interesting to compare the information on the drying behaviour of the various materials and the accuracy with which drying times may be predicted from the factorial experiments used in this investigation with the corresponding information on drying behaviour and accuracy of predicting drying times obtainable from classical experiments. Such a comparison may be conveniently made by considering a classical experiment based on the same standard test $D_2W_2L_2G_2$ as used in the factorial experiments and in which the effects of D, W, L and G on the drying behaviour of the various materials are determined by varying each factor in turn, keeping the other factors at their standard values. If each factor is studied at three levels as in the factorial experiments, the effects of the various factors would be estimated from the differences in the drying behaviour observed in the following tests:

Effect of D:	Difference between	$D_1W_2L_2G_2$	and	$D_2W_2L_2G_2$
	" "	$D_3W_2L_2G_2$		
Effect of L:	" "	$D_2W_2L_1G_2$	and	$D_2W_2L_2G_2$
		$D_2W_2L_3G_2$		
Effect of W:	" "	$D_2W_1L_2G_2$	and	$D_2W_2L_2G_2$
		$D_2W_3L_2G_2$		
Effect of G:	" "	$D_2W_2L_2G_1$	and	$D_2W_2L_2G_2$
		$D_2W_2L_2G_3$		

This classical experiment involves nine tests. <u>Note</u> Replacing W by H in these nine tests gives the classical experiment corresponding to the factorial experiment on the brewers' spent-grain. For simplicity, the following remarks refer to the factorial and classical experiments on the porous-ceramic granules and coke - similar remarks, however, may be made about the corresponding experiments on the brewers' spent-grain.

At first sight, it may appear that the classical experiment (9 tests) has the advantage of requiring fewer tests than the factorial experiment (44 tests including three replicates of test $D_2W_2L_2G_2$). This reduction in the number of tests required, however, is gained at the expense of a substantial loss in the information obtained from the experiment; to approach the precision with which the factorial experiment determines the values of f(DW), f(DG), f(L), W_c and C under various drying conditions, each of the nine tests in the basic classical experiment would have to be replicated three times - making 36 tests in all, only eight tests less than the factorial experiment.

Not only is the information obtained from this replicated classical experiment much less than that obtained from the factorial experiment, but also the precision of the data obtained is in general lower than that of the data obtained from the factorial experiment. This may be illustrated by considering the precision (number of independent estimates) with which the classical and factorial experiments determine the quantities f(DW), f(DG), f(L), W_c and C.

The factorial experiment evaluates f(DW) for all nine combinations of the three levels of D and W tested, the value of f(DW) for each level of DW being the average of four independent estimates obtained from four pairs of tests done at various levels of L and G. The fact that the values of f(DW) do not vary with changes in L and G is proof that the effect of D and W on $\frac{dW}{d\theta}$ is exerted independently of the values of L and G used. The classical experiment evaluates f(DW) only for the DW levels

D_1W_2, D_3W_2, D_2W_1, D_2W_2 and D_2W_3, each value being the average of four independent estimates obtained from four pairs of tests all conducted at L_2G_2. In addition to giving fewer values of f(DW) than the factorial experiment, the classical experiment gives no information as to whether f(DW) is affected by the values of L and G used in the tests.

The factorial experiment gives five independent estimates of the effect on $\frac{dW}{d\theta}$ of a change in G from G_1 to G_3 at each level of D, the five pairs of tests involved at each level of D being done at various levels of L and W. The effect of G was found to depend on the value of D but was independent of the values of L and W; the variation in the effect of G with D is allowed for by the f(DG) correction factor. The classical experiment, on the other hand, gives four independent estimates of the effect on $\frac{dW}{d\theta}$ of a change in G from G_1 to G_3 for the D_2 level only, the four pairs of tests involved all being done at L_2W_2. The classical experiment cannot detect a DG interaction.

The factorial experiment gives seven independent estimates of the effect on $\frac{dW}{d\theta}$ of a change in L from L_1 to L_2, and eleven independent estimates of the effect of a change in L from L_1 to L_3, the tests involved being done at various levels of D, W and G. The effect of L on $\frac{dW}{d\theta}$ was found to be independent of the values of D,W and G used in the tests. The classical experiment, however, gives only four independent estimates of the effect on $\frac{dW}{d\theta}$ of a change from L_1 to L_2 and four independent estimates of the effect of a change from L_1 to L_3, all the tests being done at $D_2W_2G_2$. This experiment cannot determine whether the effect of L on $\frac{dW}{d\theta}$ is modified by the values of D, W or G used.

The factorial experiment provides fifteen independent estimates of the value of W_c obtained when a tray loading L_1 is used, eighteen estimates for L_2 and eleven estimates of W_c when a loading L_3 is used. Since the tests at each level of L were done at various values of D,W and G, examination of the W_c values showed that D,W and G had negligible effects on W_c. While the classical experiment gives twenty-eight estimates of W_c from tests done at L_2 and various values of D,W and G, it gives only four estimates of W_c from tests done at $L_1D_2W_2G_2$ and four estimates of W_c from tests done at $L_3D_2W_2G_2$. From the classical experiment it can be concluded that the values of D,W and G have negligible effects on W_c at a loading L_2, but similar conclusions cannot be made for L_1 and L_3.

The factorial experiment provides estimates of the values of C obtained at all nine combinations of the three levels of D and L - three estimates of C are obtained for each of the D_2L_1, D_2L_3, D_3L_2 levels; four estimates for each of the D_3L_1 and D_3L_3 levels; five estimates for each of the D_1L_1, D_1L_2, D_1L_3 levels; and twelve estimates of the value of C for D_2L_2. Since the tests at each level of DL are done at various levels of W and G, it is possible to conclude from the experimental results that the value of C is independent of the values of W and G. The classical experiment, however, provides estimates of the values of C for only five values of DL - the values of C for D_1L_2, D_3L_2, D_2L_1, D_2L_3 each being estimated from four tests and the value for D_2L_2 being estimated from twenty tests. Since only the D_2L_2 tests were done at various values of W and G (the rest being done at W_2G_2), the conclusion that W and G do not affect C is restricted to the D_2L_2 level.

The factorial experiments on the various materials showed that, with the exception of the interaction between the effects of D and W on $\frac{dW}{d\theta}$, the interactions between the effects of the various factors on $\frac{dW}{d\theta}$, W_c and C were small. Since this DW interaction can, however, be estimated from the theoretical Equation A, it should be possible to estimate the drying times of the various materials reasonably accurately from values of $\frac{dW}{d\theta}$ calculated from Equation A and from values of W_c and C obtained in the classical experiment.

An indication of the probable accuracy with which drying times may be estimated by this method is given in Table 23A under the heading "classical experiment". Note: The drying times quoted under this heading were calculated from the prediction methods described in Sections 6.4, 6.8 and 6.12, using values of $\frac{dW}{d\theta}$ calculated from Equation A with n = 1 and the appropriate value of K' obtained in the factorial experiment; values of W_c obtained in the factorial experiment; and values of C obtained in the factorial experiment for the levels of D and L - D_2L_1, D_2L_2, D_2L_3, D_1L_2 and D_3L_2. Values of C for any other values of D and L were estimated by direct extrapolation assuming that the effect of L on C at D_1 and D_3 was similar to that found at D_2.

From Table 23A it would appear that drying times predicted from the results of the classical experiment would only be slightly less accurate than those predicted from the results of the factorial experiment. It should, however, be remembered that in calculating the drying times quoted under "classical experiment" in Table 23A, it was assumed that the W_c and C values obtained in the classical experiment would be the same as those obtained in the factorial experiment; since in practice the classical experiment would estimate these quantities with lower precision than the factorial experiment, the actual accuracy of the estimates of drying times obtainable from the results of the classical experiment would probably be lower than that shown in Table 23A.

TABLE 23A: Comparison Of The Accuracy With Which The Drying Times Of Various Materials Can Be Predicted From The Results Of A Classical And A Factorial Experiment.

Material	Drying Conditions				Moisture Content		Drying Times Mins.			% Error	
	D	W	L	G	W_1	W_2	Fact.	Class.	Expt.	Fact.	Class.
Porous Ceramic Granules	240	100	2.00	11	0.225	0.025	66.5	67.5	64.0	+3.9	+5.5
	210	117	1.40	5	0.280	0.050	113	109	112	+0.9	-2.7
	170	95	2.65	5	0.250	0.050	334	337	308	+8.5	+9.4
	150	145	3.00	6	0.280	0.060	421	413	440	-4.3	-6.1
	130	95	3.85	13	0.265	0.075	373	387	422	-11.6	-8.3
Coke	210	117	0.81	5	0.24	0.06	53	68	61	-13.1	+11.5
	210	95	2.18	5	0.26	0.05	170	229	201	-15.4	+13.9
	190	100	1.92	6.5	0.27	0.08	152	149	159	-4.4	-6.3
	150	112	1.05	11	0.28	0.07	141	123	139	+1.4	-11.5
	130	95	2.18	13	0.23	0.04	240	278	243	-1.3	+14.4
Brewers' Spent Grain	210	114	0.156	9	2.20	0.29	92	117	96	-4.2	+20.8
	190	102	0.380	11	2.30	0.30	280	275	310	-9.7	-11.3
	175	111	0.142	5	2.10	0.40	233	247	233	0	+6.0
	160	101	0.250	7	2.40	0.45	381	341	398	-4.3	-14.3
	140	121	0.144	13	2.60	0.60	291	270	335	-13.2	-19.4

THROUGH-CIRCULATION DRYING

7. INTRODUCTION

The great disadvantage of cross-circulation driers are that they dry a material slowly, and can be used for drying only a shallow bed of material (up to approximately $1\frac{1}{2}$ inches deep). Both disadvantages arise from the fact that only the surface of the bed is in contact with the hot airstream.

Through-circulation driers, however, in which the hot airstream is blown through the bed of material, give greatly increased drying rates, and can successfully dry deeper beds of material (up to approximately 12 inches deep). Rapid drying of deep beds is possible because material at all levels in the bed is contacted by the airstream which passes between the particles at a high velocity.

Granular, fibrous and flaky materials which form beds permeable to an airflow can be dried in this type of drier; so also can certain materials, such as filter-cakes, which, although not naturally in a state suitable for through-circulation drying, can be pre-formed by extrusion or granulation into aggregates of the proper shape and size to form a permeable bed.

Materials forming dense beds which have a high resistance to airflow, and dusty or easily-airborne materials are unsuitable for through-circulation drying.

The outstanding advantage of through-circulation over cross-circulation driers is the much shorter drying times obtained in the former. Another advantage is that drying is easily made a continuous process by passing hot air through the material as it moves through the drier on a wire mesh or perforated-sheet conveyor belt.

For a given output, a through-circulation drier is cheaper to operate than a cross-circulation drier. There are several reasons for this. Firstly, since deeper beds can be used, and because of the shorter drying times required, a smaller drier can give the same output. Secondly, fuel and power costs are lower because more efficient use is made of the airstream (more water is removed per lb dry air). Lastly, labour costs are lower since loading and unloading can be made automatic.

The main operating variables affecting the drying time of a material in a through-circulation drier are similar to those affecting its drying time in a cross-circulation drier - namely, the bed-depth of material, and the temperature, humidity and velocity of the airstream.

Section 8, which follows, describes the present knowledge of the effects of these variables on the drying time of a material by through-circulation drying, and reviews existing methods of predicting the drying time of a material under a given set of operating conditions in this type of drier. Section 10 describes the application of the new empirical method of predicting drying times (described in Section 6) to the through-circulation drying of fibrous and porous-granular materials.

8. PRESENT KNOWLEDGE OF THROUGH-CIRCULATION DRYING

8.1. Theory Of Through-Circulation Drying

Since cross-circulation and through-circulation driers both use a hot airstream as the drying medium, no fundamental difference would be expected in the drying mechanism of a material in the two types of drier. Moreover, a material would be expected to show similar drying characteristics in both types of drier, and the theory of drying described in Section 2 for cross-circulation drying, should also apply to through-circulation drying.

Marshall and Hougen (50) appear to have been the first workers to verify these postulates experimentally. They compared the drying characteristics of a variety of materials under similar constant drying conditions in a through-circulation drier and found that, as in a cross-circulation drier, the materials dried at a constant rate for a time after which the drying rate decreased continuously until drying was complete.

Factors Affecting The Constant Drying Rate

They found, moreover, that the temperature, humidity and velocity of the airstream had similar effects on the constant drying rate of a material in both types of drier; from their experimental results they derived the equation for the constant drying rate of a material in a through-circulation drier:

$$\frac{dW}{d\theta} = K''G^{0.81}(H_s - H_a) \qquad \ldots \text{ Equation 16.}$$

The drying rate also depends, as in cross-circulation drying, on the wet surface area of the material exposed to the airstream.

In through-circulation drying, however, the differences between the drying rates of different materials are much more marked since wet surfaces, not only at the surface of the bed as in cross-circulation drying, but also throughout the bed are in contact with the airstream. The wide range of drying rates of various materials obtainable under similar drying conditions in a through-circulation drier was illustrated by Marshall and Hougen (50) who found that K' in Equation 16 varied from 0.11 to 0.33 for heavy solids such as pigments to 4 to 8 for light fibrous materials such as wool and rayon. They also found that the drying rate of a given material increased with decreasing particle size. This effect of particle size on the drying rate has been noted by several workers (51, 52, 53, 54, 55); it is a result of the increased surface area exposed by the smaller particles.

An outstanding advantage of through-circulation driers over cross-circulation driers is that the drying rate of a material (in lbs water/(unit bed area)(hour)) increases with loading in the former type of drier, whereas in the latter type the drying rate is unaffected by the loading. The increase in drying rate with loading in through-circulation driers is easily understood, since an increase in loading gives a proportional increase in the wet surface area exposed to the airstream. The increase in drying rate is not, however, directly proportional to the increase in loading because the airstream increases in humidity as it passes through a bed with a progressive decrease in its drying capacity as described by the humidity driving force term ($H_s - H_g$) in Equation 16.

Several workers (51, 52, 56) have derived drying rate equations in which the logarithmic mean of the humidity driving force $(H_s - H_a)$ at the inlet and outlet of the bed is used to allow for this decrease in the drying capacity of an airstream in its passage through a bed of material.

Thus Gamson, Thodos and Hougen (51) correlated their experimental results for the constant drying rates of beds of cylindrical and spherical celite catalyst pellets of various porosities, densities and sizes by the equation:

$$\frac{dW}{d\theta} = \frac{0.42\ a' G^{0.59}\ (\Delta H)_m}{\rho_s D_p^{0.41}} \quad \ldots \quad \text{Equation 17.}$$

where a' = drying area sq. ft/cu. ft bed volume.

$(\Delta H)_m$ = log. mean of the humidity driving force $(H_s - H_a)$ at inlet and outlet of the bed lbs water/lb dry air

ρ_s = bulk density of dry granular bed lb/cu. ft.

D_p = average particle diameter ft.

The effects of airflow and particle size on the drying rate given in this equation hold only when the airflow through the bed is turbulent i.e. when the Reynolds Number is greater than 350 (Reynolds Number = $\frac{D_p G}{\mu}$ where μ = air viscosity lb/(hr.)(ft))

Wilke and Hougen (52) derived a modified equation which holds for Reynolds Numbers less than 350 and the airflow through the bed is streamline.

$$\frac{dW}{d\theta} = \frac{0.57\ a' G^{0.49}\ (\Delta H)_m}{\rho_s D_p^{0.51}} \quad \ldots \quad \text{Equation 18.}$$

Glover and Moss (56) found that the effects of loading, air temperature and humidity on the constant drying rate of a filter-cake of a chalk-like organic chemical pre-formed by extrusion into $\frac{1}{4}$ inch diameter cylinders could be expressed by the equation.

$$R_c = K'' L (\Delta H)_m \qquad \ldots \qquad \text{Equation 19.}$$

where R_c = constant drying rate per unit area of bed lbs/(hr) (sq. ft.)

L = loading of dry material lbs/sq. ft.

For the effect of airflow on the constant drying rate they proposed the equation:

$$R_c = b' G^{0.89} (\Delta H)_m \qquad \ldots \qquad \text{Equation 20.}$$

It has been noted that during the constant drying-rate period of very wet materials which present a large surface area per unit volume such as filter-cakes (57) and wool (58), and of deep beds of wheat grain (53), the airstream may leave the bed virtually saturated. When this occurs, the drying rate is independent of the loading and physical properties of the material forming the bed and depends only on the air conditions used; the drying rate can be calculated from the temperature, humidity and velocity of the airstream by the equation:

$$\frac{dw}{d\theta} = A' G (H_s - H_a) \qquad \ldots \qquad \text{Equation 21.}$$

where A' = cross-sectional area of drier sq. ft.

Factors Affecting The Drying Rate In The Falling-Rate Period

In through-circulation drying the main factor controlling the drying rate of a bed of material during the falling-rate period is the rate of moisture movement to the surface of the individual particles of the material forming the bed. As in cross-circulation drying, the physical structure of the material exerts an important influence on the rate of moisture movement, and the diverse nature of the physical structures of different materials produces the diversity of drying behaviour observed for different materials. (See for example the drying rate curves obtained by Marshall and Hougen (50)). At present, there is no theoretical method of predicting the drying behaviour of a material in terms of its physical structure.

The great advantage of a through-circulation drier over a cross-circulation drier is that an increase in the loading of a material causes little difference in the duration of the falling-rate period in the former type of drier; in the cross-circulation drier, on the other hand, an increase in loading causes a great increase in the duration of the falling-rate period. The reason for the different drying behaviour in the two types of drier is that in a through-circulation drier the distance moisture has to travel to contact the airstream is determined only by the particle size of the material; whereas in a cross-circulation drier moisture has to travel to the surface of the particles then to the surface of the bed - a distance depending on the loading used.

Several workers (53, 54, 55) have shown that the drying time of a material in a through-circulation drier can be greatly shortened by decreasing the particle size of the material, because of the reduced distance moisture has to travel to the surface of the smaller particles.

8.2. Limitations Of Drying Theory When Used To Predict Drying Times

To predict the drying time of a material under any specified drying conditions in a through-circulation drier it is necessary to be able to estimate accurately the combined effects of loading, air temperature, humidity and velocity on its drying time.

At present, drying theory is limited to predicting the drying rates in the constant drying rate period of (a) very wet materials and deep beds of materials from which the airstream leaves virtually saturated (Equation 21 may be applied to these materials) and (b) materials of uniform shape and size to which Equation 17 may be applied. Equation 17 cannot be used to predict the drying rates of materials with irregularly shaped particles for which the a' and D_p terms cannot be evaluated; for such materials Equations 16, 19 and 20 may be employed, but for a given material the empirical constants in these equations must be determined by experimental drying tests.

There is insufficient theoretical knowledge on the effects of drying conditions and of the physical structure of a material on its critical moisture content and its drying behaviour in the falling-rate period to allow an accurate prediction of its drying time to be made. The only reliable methods of estimating the drying time of a material in a through-circulation drier are empirical methods based on experimental drying tests on the material in question, conducted as described in Section 4.

8.3. Empirical Methods Of Predicting Drying Times

Prediction Of The Drying Times Of Filter Cakes

Allerton, Brownell and Katz (57) studied the drying mechanism of filter cakes, and found that, at the low airflows and temperatures used in their tests, the air leaving the cake was almost saturated during the constant drying rate period.

They postulated that the airstream picks up moisture from the cake so quickly that drying can be considered as taking place in a narrow zone of vaporization which proceeds through the cake during drying. At any instant the cake above this zone is dry; below, the cake is wet; and in the zone itself there is a moisture gradient. The constant drying rate ends when the vaporization zone reaches the bottom of the cake and the drying rate falls off gradually until the water in the zone is evaporated. (Note In the mechanism postulated above the airstream has been considered as passing down through the filter cake).

They verified this mechanism experimentally by showing that the duration of the constant drying-rate period depended only on the total amount of moisture to be removed per unit area of the cake and on the constant drying rate determined by the air conditions used, as described in Equation 21.

They found that the drying rate in the falling-rate period was affected by the moisture content of the cake and by the size of its component particles. To take these factors into account the drying rates in this period were correlated on the basis of a vaporization efficiency with the constant drying rate, the moisture content of the cake and an empirical drying factor Y thus:

$$\frac{R_F}{R_C} = E = 1 - e^{-Yw'} \qquad \ldots \text{ Equation 22.}$$

where R_F = drying rate in the falling rate period per unit area of bed lbs/(sq. ft) (hr)

E = vaporization efficiency

e = base of natural logarithms

W' = weight of water per unit area of cake lb/sq. ft.

Y = empirical drying factor sq. ft./lb

The drying time of a filter cake under a given set of conditions was estimated by graphical integration of this equation.

Prediction Of The Drying Times Of Beds Of Wheatgrain

Simmonds, Ward and McEwen (53) found that the drying rate of single layers of wheatgrain was proportional to the free moisture content of the grain and expressed their results in the equation.

$$\frac{dW}{d\theta} = 2.303\, m\, (W - W_e) \qquad \ldots \text{ Equation 23.}$$

where m = an empirical constant depending on the properties of the grain and the drying conditions $hr.^{-1}$

They also found that the drying rate was independent of the airflow, was slightly affected by the air humidity, and was greatly affected by the air temperature.

The same workers also studied deeper beds of grain (up to 12 inches deep) and found that beds deeper than 2 inches dried at a constant rate for a period proportional in duration to the bed depth. They found that the constant drying rate depended only on the air conditions used and could be calculated by Equation 21; the drying rate in the subsequent falling-rate period was again found to be proportional to the free moisture content of the grain.

On the basis of the above results, they gave the following approximate method of predicting the drying time of a deep bed of grain from an initial moisture content W_1 to a final moisture content W_2.

The drying time θ_c in the constant drying-rate period was calculated from the equation;

$$\theta_c = \frac{L(W_1 - W_c)}{G(H_s - H_a)} \quad \ldots \text{ Equation 24.}$$

where W_c = critical moisture content of material lbs water/lb dry solid

The drying time θ_f in the falling rate period was calculated from the equation

$$\theta_f = \frac{1}{m'} \log_{10} \frac{(W_c - W_e)}{(W_2 - W_e)} \quad \ldots \text{ Equation 25.}$$

m' was the empirical drying-rate constant in Equation 23, evaluated at the logarithmic mean of the dry-bulb and wet-bulb temperatures of the airstream. The value of W_c was obtained from the relationship:

$$W_c - W_e = \frac{G(H_s - H_a)}{2{\cdot}303m'L} \quad \ldots \text{ Equation 26.}$$

McEwan and O'Callaghan (59) proposed an alternative method of calculating the drying time of a deep bed of grain by considering it as a series of thin layers, the drying rate and water loss from successive layers during a small time increment were found by calculating the humidity (from a moisture balance) and temperature (from a psychrometric chart) of the airstream at the entry to each layer and applying Equation 23. This process was continued for successive time increments until the bed was dried.

Prediction Of The Drying Times Of Beds Of Seaweed

Gardner and Mitchell (54) found that beds of seaweed at average moisture contents between 5 and 0·2 lb water/lb dry solid dried at rates directly proportional to the wet bulb depression of the airstream; they subsequently showed that the empirical method of predicting drying times based on a standard drying curve for a unit wet-bulb depression, used by Ede and Hales (7) and described in Section 4, could be applied to the through-circulation drying of seaweed.

Prediction Of The Drying Times Of Vegetables

Mitchell and his co-workers (55, 60, 61) have applied a modified form of the prediction method for wheatgrain described by Simmonds et. al. (53) to predicting the drying times of various vegetables. Their modified prediction method included an airflow correction factor to be applied to the rate constant m' in Equation 25 and also an empirical correction factor to be applied to the calculated drying time to allow for the fact that all parts of the bed were not contacted by the airflow.

General Method Of Predicting Drying Times

Glover and Moss (56) proposed an approximate method of predicting the drying times of a material which was based on experimental data on the constant drying rate, the critical moisture content, and the shape of the graph of the drying rate against the moisture content of the material in the falling-rate period.

The duration of the constant drying-rate period was calculated from a knowledge of the critical moisture content and the constant drying rate estimated from Equations 19 and 20.

To calculate the duration of the falling-rate period for a material whose drying rate in this period is directly proportional to its moisture content (i.e. the drying-rate curve of drying rate against moisture content is linear) they proposed the equation:

$$\theta_f = \frac{L\,W_c}{R_c} \ln \frac{W_c}{W} \qquad \ldots \text{ Equation 27.}$$

For a material whose drying-rate curve is not a straight line they proposed a modified graphical method of predicting the duration of the falling-rate period; this method involves splitting the rate curve into a number of equivalent straight lines and applying Equation 27 to each section between the appropriate moisture contents.

8.4. Limitations Of Present Empirical Methods Of Predicting Drying Times

Because of the diversity of drying behaviour shown by different materials, none of the empirical methods of predicting drying times described in Section 8.3 is of general application. As a result, the method used to predict the drying times of a given material must be chosen carefully, otherwise greatly inaccurate predictions may be obtained. In the selection of a suitable prediction method for a given material, the following limitations of the available methods should be taken into account.

The method of predicting the constant drying rates of very wet materials and deep beds of material based on Equation 21 (used by Allerton et.al. (57), Simmonds et.al. (53), and Mitchell et.al. (55)) can give accurate predictions only if the airstream leaving the bed of material is saturated. In practice, the airstream leaving the bed is frequently unsaturated, so that the actual drying rate is much less than that predicted by Equation 21; thus, to obtain reasonably accurate predictions of the drying times of deep beds of barley grain (up to approximately six inches) Hughes and Mitchell (60) found it necessary to correct the drying times predicted with the use of Equation 21 by multiplying by an empirical factor of 1·5 to allow for the fact that the airstream leaving the beds was only approximately 75% saturated.

To predict the constant drying rate of shallow beds of material (up to approximately two inches deep) the use of Equation 16, 17, 18 or 20 is preferable to the use of Equation 21, since these equations contain an airflow term G^n (where n is less than unity), which allows for the experimentally observed fact that the airstream leaving a shallow bed of material becomes less saturated as the airflow increases. Since values of n ranging from 0·49 to 0·89 have appeared in the literature (50, 51, 52, 56), the value of n to be used for predicting the constant drying rate of a given material is probably best found experimentally.

The method used by Gardner and Mitchell (54) to predict the drying times of beds of seaweed should be applied only to very wet materials from which the moisture is easily removed and which dry at rates proportional to the wet-bulb depression of the airstream. Generally speaking, this method should not be used to predict the drying times of materials which are to be dried to low moisture contents, since the proportionality between the drying rate of a material and the wet-bulb depression of the airstream usually breaks down at low moisture contents.

The method of predicting the drying times of a material proposed by Glover and Moss (56) is based on the assumptions that the critical moisture content and shape of the drying-rate curve of a material do not change with variations in the drying conditions used. Since, as illustrated even by the experimental results of Glover and Moss, these assumptions usually hold for only a limited range of drying conditions for any given material, predictions obtained by this method are likely to be accurate over a very small range of drying conditions. To use this method successfully the range of drying conditions used in the laboratory drying tests should encompass as closely as possible the drying conditions chosen for the design of the full-scale drier.

All the empirical methods of predicting the drying times of a material in a through-circulation drier described in Section 8·3 have been based on experimental data obtained from programmes of drying tests planned by the classical method of experimentation (described in Section 4.1); by this method the individual effects of loading, air temperature, humidity and velocity on the drying time are determined by varying each factor in turn, keeping the rest constant. The disadvantages of using this method of estimating the various factors are, as mentioned previously in Section 4.1, (a) that interactions between the effects of various factors cannot be detected and (b) that, if there are interactions between the various factors, the predicted drying times will be accurate only for values of the various factors close to the constant values used for each factor in the experimental tests.

An example of interaction between the factors affecting the drying time of a material in a through-circulation drier is that several workers (50, 51, 52, 56), working with shallow beds of material, found the constant drying rate to be proportional to a power function of the airflow G^n (where n varied from 0·49 to 0·89), while other workers (53, 54, 55, 57), working with deeper beds of material, found the constant drying rate to be directly proportional to the airflow G. This is an example of interaction between airflow and loading, since the estimated effect of airflow depends on the value chosen for the loading. For any given material, however, there may be other interactions between the four factors - loading, air temperature, humidity and velocity - affecting its drying time. To detect these interactions a factorial experiment, in which each of the above factors is tested at least at two levels, is required.

8.5. Scope Of The Present Investigation

A two-level factorial experiment is used to detect possible interactions between the effects of loading, air temperature, humidity and velocity on the drying times, in a through-circulation drier, of the fibrous and porous-granular materials tested previously in a cross-circulation drier (see Section 6). From the results of this experiment, a more elaborate fractional three-level factorial experiment is designed to provide the data necessary to give accurate predictions of the drying times of these materials for any operating conditions within the experimentally tested ranges of the above factors. The accuracy of the predictions obtained is compared with the accuracy of predictions based on data obtained in a corresponding classical experiment.

9. EXPERIMENTAL APPARATUS AND PROCEDURE

9.1. Description Of The Experimental Through-Circulation Drier

The drier used is shown in Figures 28 and 29.

A fan produced a steady airstream which was heated and humidified to the desired temperature and humidity, and passed upwards through a bed of the wet material held in a basket with a wire mesh bottom. The progress of drying was followed by removing the basket from the drier at intervals and weighing it.

The airflow through the basket could be varied by altering the fan-speed by means of a ten-position starter (rough control), and a rheostat (fine control) fitted to the D.C. fan-motor. The airflow was measured by a 3 inch diameter orifice plate in the 5 inch diameter inlet pipe, connected to an inclined "U" tube water manometer. Air-flows from 3 to 20 lbs dry air/(sq. ft. basket area)(min) could be maintained through the test basket.

Eighteen 1kW electric bar heaters could heat the airstream to any temperature up to 250°F. Twelve of the heaters were controlled in pairs; six were controlled independently; and one of these was controlled by a "Sunvic" thermostat which could maintain a given temperature within ±0.5F°.

If necessary, the humidity of the airstream could be raised by injecting low pressure steam (at 15 lbs/sq. inch guage.) through five jets in a ½ inch diametercopper tube stretched across the drier duct. A steam separator and steam trap removed condensate from the steam supplied to the jets. A 2 inch high steel weir and a drain were fitted at the foot of the sloping duct to prevent damage to the

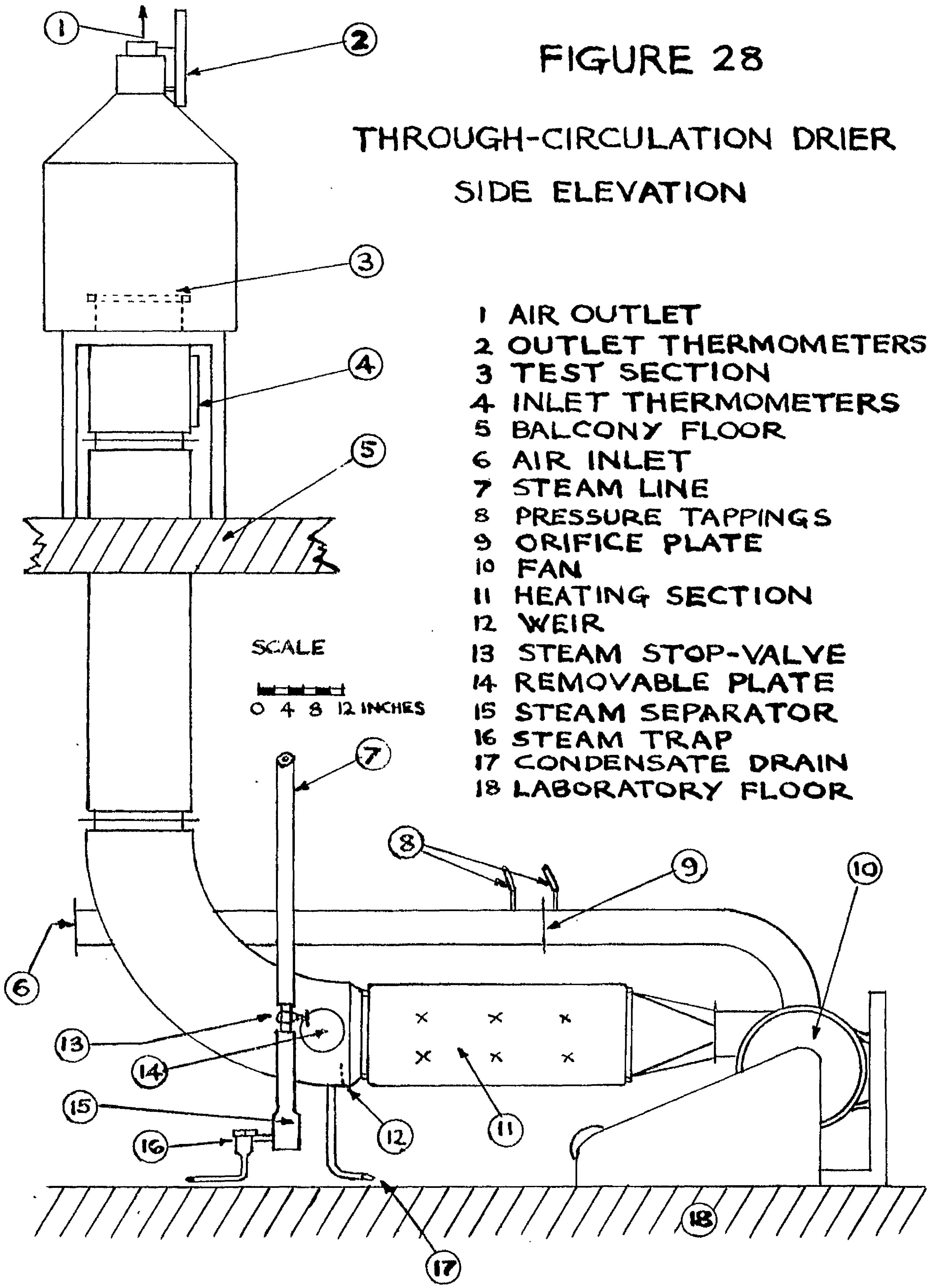

FIGURE 28

THROUGH-CIRCULATION DRIER

SIDE ELEVATION

FIGURE 29

THROUGH-CIRCULATION DRIER

FRONT ELEVATION SHOWING DRIER CONTROLS

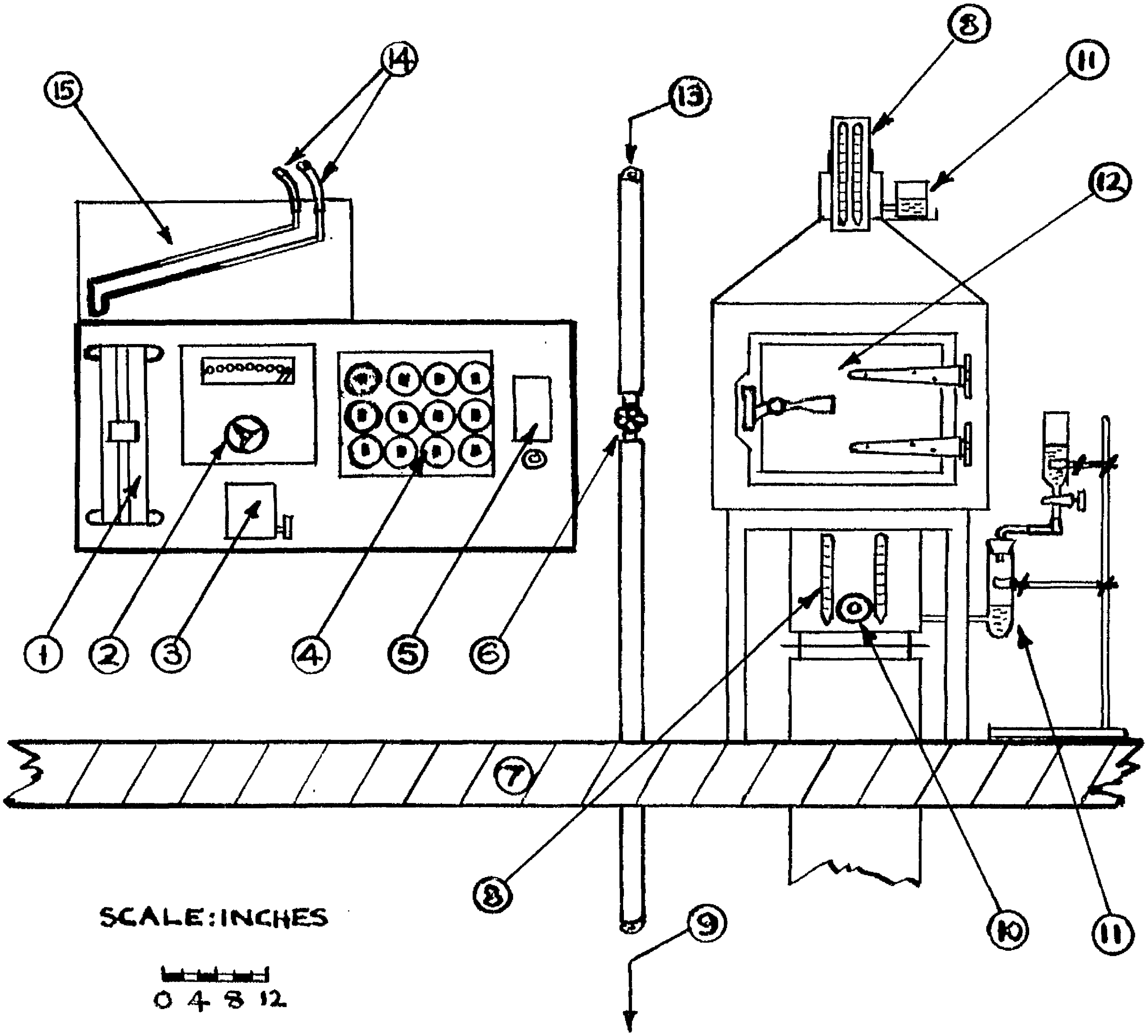

1 RHEOSTAT	7 BALCONY FLOOR	12 DOOR
2 FAN STARTER	8 WET-AND DRY-BULB THERMOMETERS	13 STEAM SUPPLY
3 FAN FUSEBOX	9 STEAM TO INJECTOR	14 CONNECTIONS TO ORIFICE PLATE
4 HEATER SWITCHES	10 THERMOSTAT CONTROL	15 INCLINED WATER MANOMETER
5 THERMOSTAT	11 WET-BULB RESERVOIR	
6 STEAM CONTROL-VALVE		

heaters by condensate running down the duct if the steam trap failed. Manual operation of the steam control-valve kept the airstream humidity constant at the desired value.

The long rising section of the drier was designed to allow disturbances in the airflow, caused by obstructions such as heater bars, the weir, etc., to even out before the airstream reached the test section. The wire mesh base of the test basket also helped to give an even airflow distribution through the test material.

The temperature and humidity of the airstream were measured by dry-bulb and wet-bulb thermometers below and above the test section. The wet-bulb wicks were supplied with distilled water from reservoirs fitted externally on the side of the drier. Since the air pressure in the duct below the test section was slightly above atmospheric pressure when the test basket was in position, the lower reservoir had to be specially designed to give the water sufficient head to allow it to flow to the wet-bulb wick of the inlet thermometer (see Figure 29).

During a drying test the wet material was contained in a 12 inch square aluminium basket with 12 inch sides and a bottom of 1/16 inch mesh copper gauze supported by ½ inch mesh steel net. The basket sat on top of the test section of the drier; the joint between them was made airtight by means of a brass rim on the basket base which fitted into a "U" shaped channel, half-filled with an asbestos-rope gasket, on the top of the test section (see Figure 30). The progress of drying was followed by removing the basket from the drier at intervals and weighing it to an accuracy of ± 0.001 lb. on a "Berkel" automatic balance.

FIGURE 30

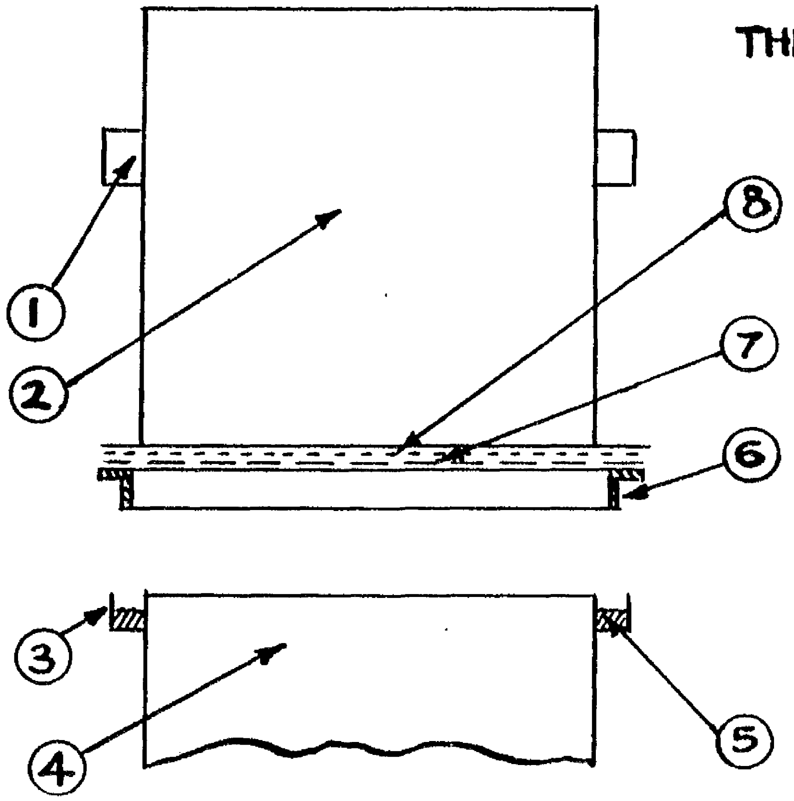

THROUGH-CIRCULATION DRIER

CONSTRUCTION DETAILS OF TEST SECTION AND BASKET

1 BASKET HANDLE
2 BASKET
3 "U" CHANNEL
4 TEST SECTION
5 ASBESTOS GASKET
6 BRASS RIM
7 STEEL NET
8 COPPER GAUZE

FIGURE 31

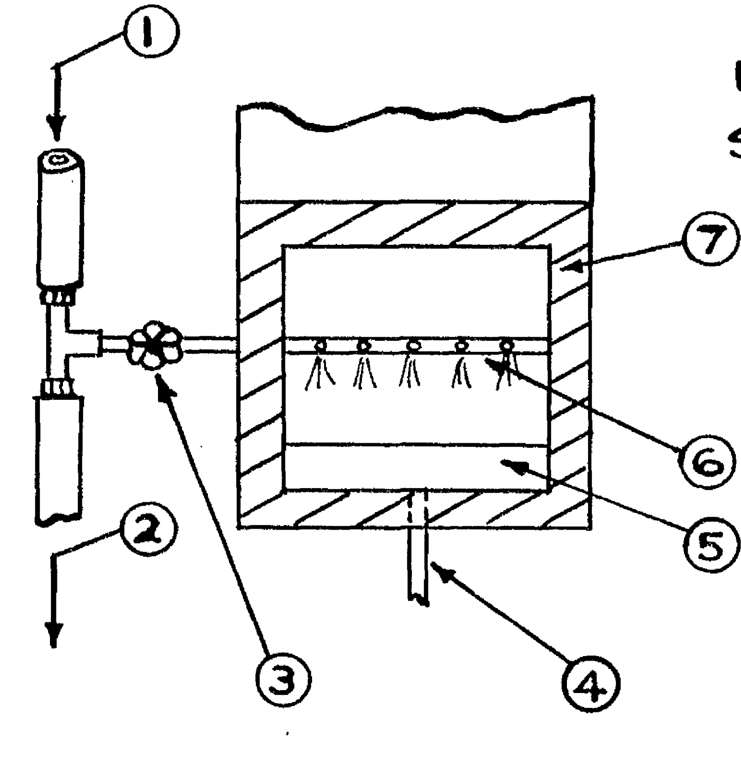

THROUGH-CIRCULATION DRIER

FRONT ELEVATION SHOWING STEAM INJECTION SYSTEM

1 STEAM INLET
2 STEAM TO SEPARATOR
3 STEAM STOP-VALVE
4 CONDENSATE DRAIN
5 WEIR
6 STEAM JETS
7 MAGNESIA LAGGING

The drier ducting was of welded galvanized steel, insulated with a 1 inch layer of magnesia lagging. The heater box was of $\frac{3}{4}$ inch thick "Sindanyo" asbestos-cement insulating board, lagged with asbestos pads. The top board of the heater box could be unscrewed to allow maintenance of the heaters; and access to the steam injector, drain and weir could be obtained by removing a plate in the drier wall.

The fan controls, inclined water manometer, airflow gauge, heater switches and the steam control-valve were mounted on a control panel. The control element of the "Sunvic" thermostat was mounted in the airstream below the test section.

9.2. Calibration Of Control Instruments

The readings of the inclined "U" tube water manometer airflow gauge and of the dry-bulb and wet-bulb thermometers were calibrated by the same methods as described in Section 5.2 for the corresponding instruments on the experimental cross-circulation drier.

9.3. Experimental Procedure

The fan was started and the fan-speed was adjusted to give the desired airflow; this airflow was held steady during the drying test by manual operation of the rheostat.

Sufficient heaters were switched on to heat the airstream to just below the required temperature, and the thermostatically-controlled heater was set to make the final temperature adjustment.

When necessary, the humidity of the airstream was raised by steam injection. Before operating the steam injector, the steam line was cleared of condensate by opening the steam control-valve with the steam stop-valve closed (see Figure 31). When the line was clear, steam was admitted to the drier by opening the steam stop-valve. The humidity of the airstream was raised to the desired value, and maintained at this value during the drying test, by manual operation of the steam control-valve.

While the drier heated up, the test basket was counterpoised on the balance and the required loading of wet material was spread evenly on the floor of the basket. When air conditions in the drier had stabilised at the required temperature, humidity and airflow, the basket was placed on the drier test section, the drier was closed and the timer was started. The progress of drying was followed by removing the basket and weighing it at regular intervals - four minutes for the first hour and ten minutes after that. The timer was stopped during each weighing period (which took approximately twenty seconds) so that only the time the material was inside the drier was recorded. Previous experimenters (51, 54) have shown that the drying and cooling of wet material occurring in such short weighing periods have no appreciable effect on its drying time.

The test was stopped when the weight loss became less than 0.001 lb in ten minutes, and the residual moisture in the material was determined by oven-drying duplicate samples (approximately 9g. for brewers' spent-grain, 50g. for coke and porous-ceramic granules) twenty-four hours at 110°C.

The results of the drying test were calculated in exactly the same way as those for a cross-circulation drying test, described previously in Section 5.4.

10. THROUGH-CIRCULATION DRYING RESULTS

10.1 Drying Of Porous-Ceramic Granules

The porous-ceramic granules were prepared for the through-circulation drying tests by the standard soaking and draining procedure described in Section 6.1. The levels of D, W, L and G studied in these tests were as follows:

TABLE 24

D_1 = 120	D_2 = 160	D_3 = 200
W_1 = 94	W_2 = 102	W_3 = 110
G_1 = 4	G_2 = 8	G_3 = 12
L_1 = 2.06 ($\frac{1}{2}$ inch layer)	L_2 = 5.12 ($1\frac{1}{4}$ inch layer)	L_3 = 8.18 (2 inch layer)

It may be noted that each level of D in Table 24 is 10°F below its counterpart used in the cross-circulation drying tests (see Table 1). Likewise, each level of G in Table 24 is 1 lb/(sq.ft)(min) less than its counterpart in Table 1. It was found necessary to use these lower levels of D and G in the through-circulation drying tests to give drying times in the L_1 tests, long enough (8 to 15 minutes) to be measured reasonably accurately. The range of L studied in the through-circulation drying tests was approximately double the range studied in the cross-circulation drying tests.

10.2 Preliminary Two-Level Factorial Experiment On Porous-Ceramic Granules

Levels 1 and 3 of the four factors D, W, L and G shown in Table 24 were studied in a two-level factorial experiment involving the sixteen drying tests shown in Table 25. The drying curves obtained in these tests are shown in Figures 32 to 35.

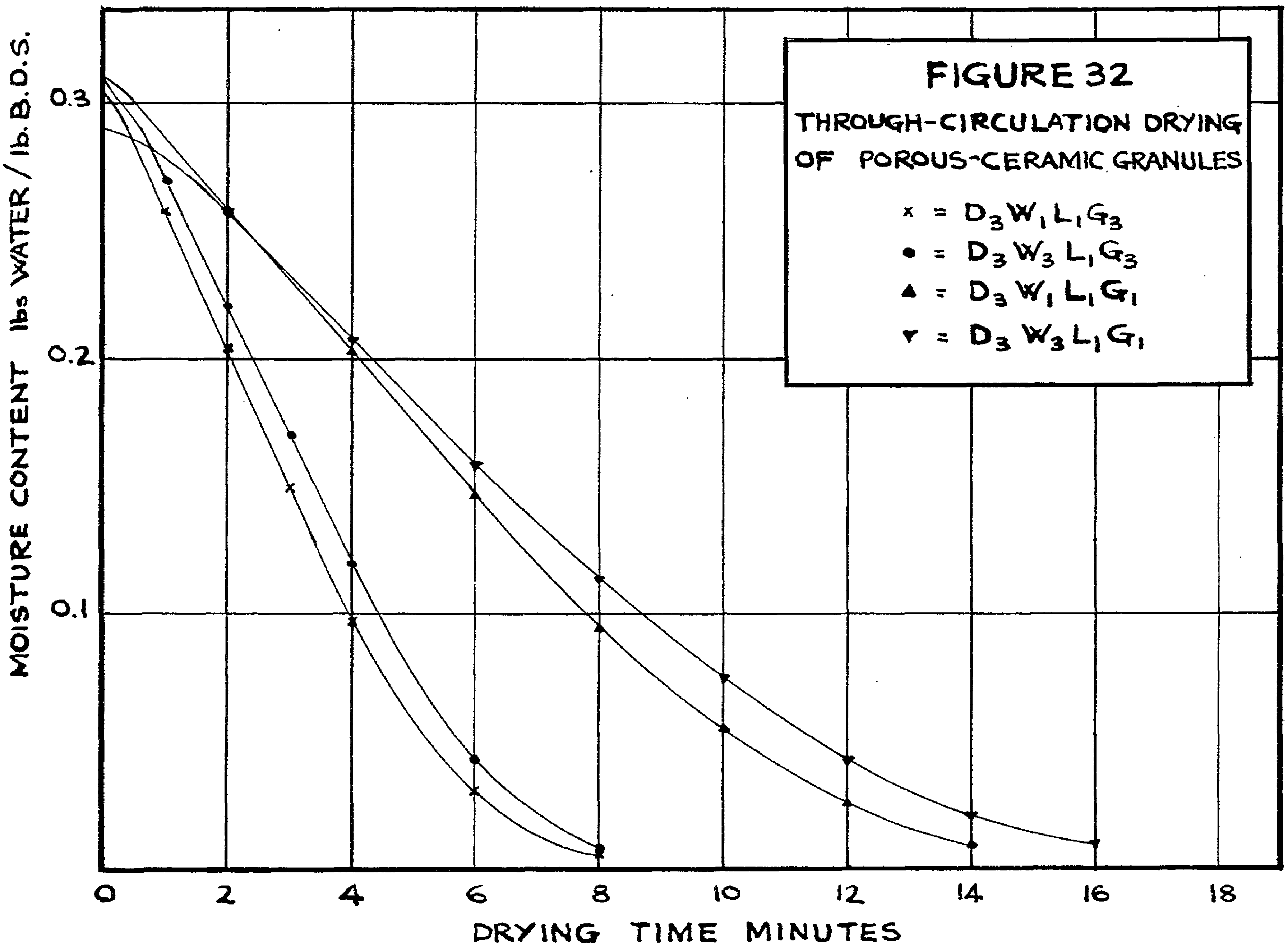
FIGURE 32
THROUGH-CIRCULATION DRYING
OF POROUS-CERAMIC GRANULES
x = $D_3 W_1 L_1 G_3$
● = $D_3 W_3 L_1 G_3$
▲ = $D_3 W_1 L_1 G_1$
▼ = $D_3 W_3 L_1 G_1$
MOISTURE CONTENT lbs WATER / lb. B.D.S.
0.3
0.2
0.1
0
2
4
6
8
10
12
14
16
18
DRYING TIME MINUTES

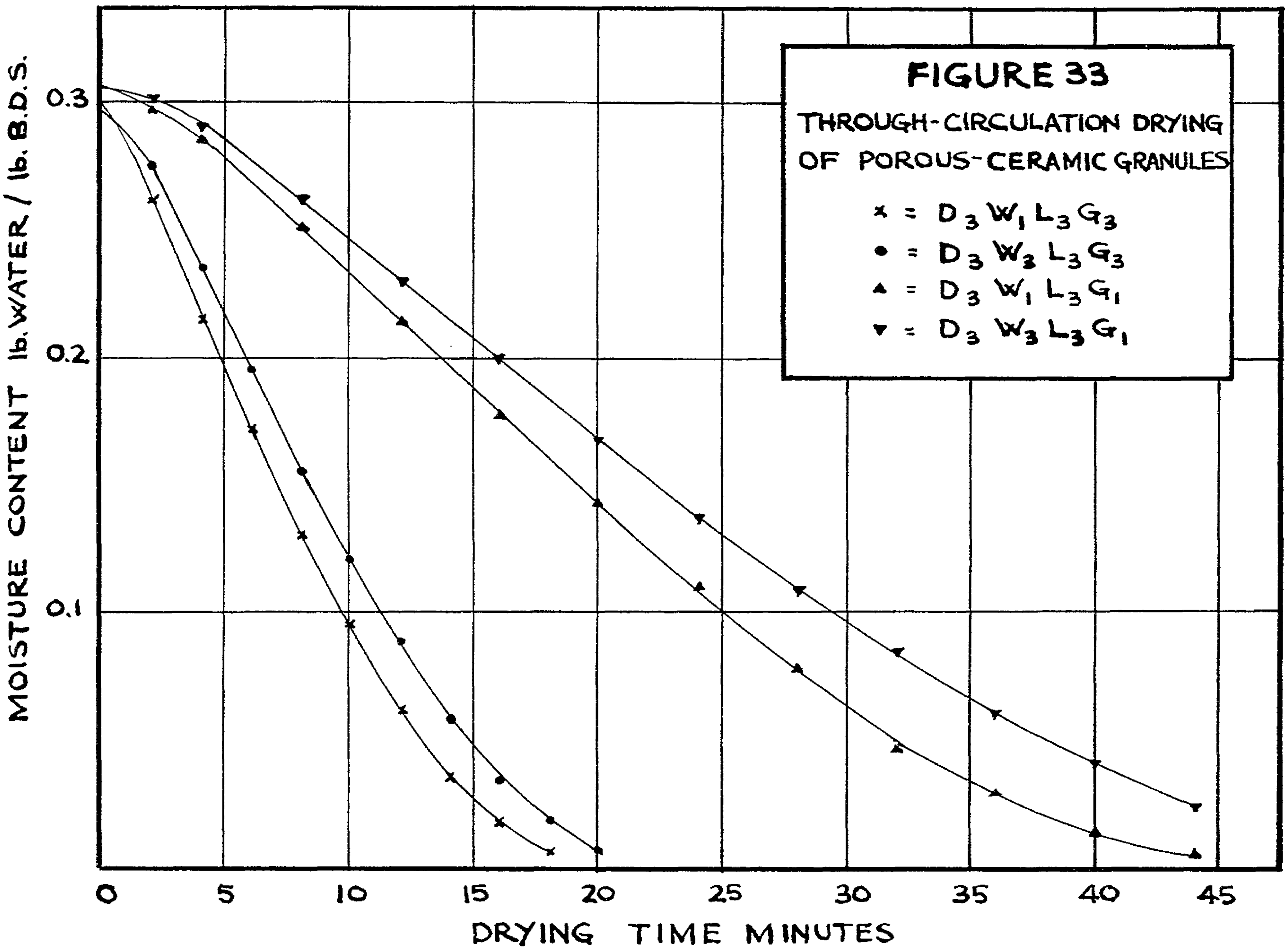

FIGURE 33
THROUGH-CIRCULATION DRYING OF POROUS-CERAMIC GRANULES
× = D3 W1 L3 G3
● = D3 W3 L3 G3
▲ = D3 W1 L3 G1
▼ = D3 W3 L3 G1
MOISTURE CONTENT lb. WATER / lb. B.D.S.
0.3
0.2
0.1
0
5
10
15
20
25
30
35
40
45
DRYING TIME MINUTES

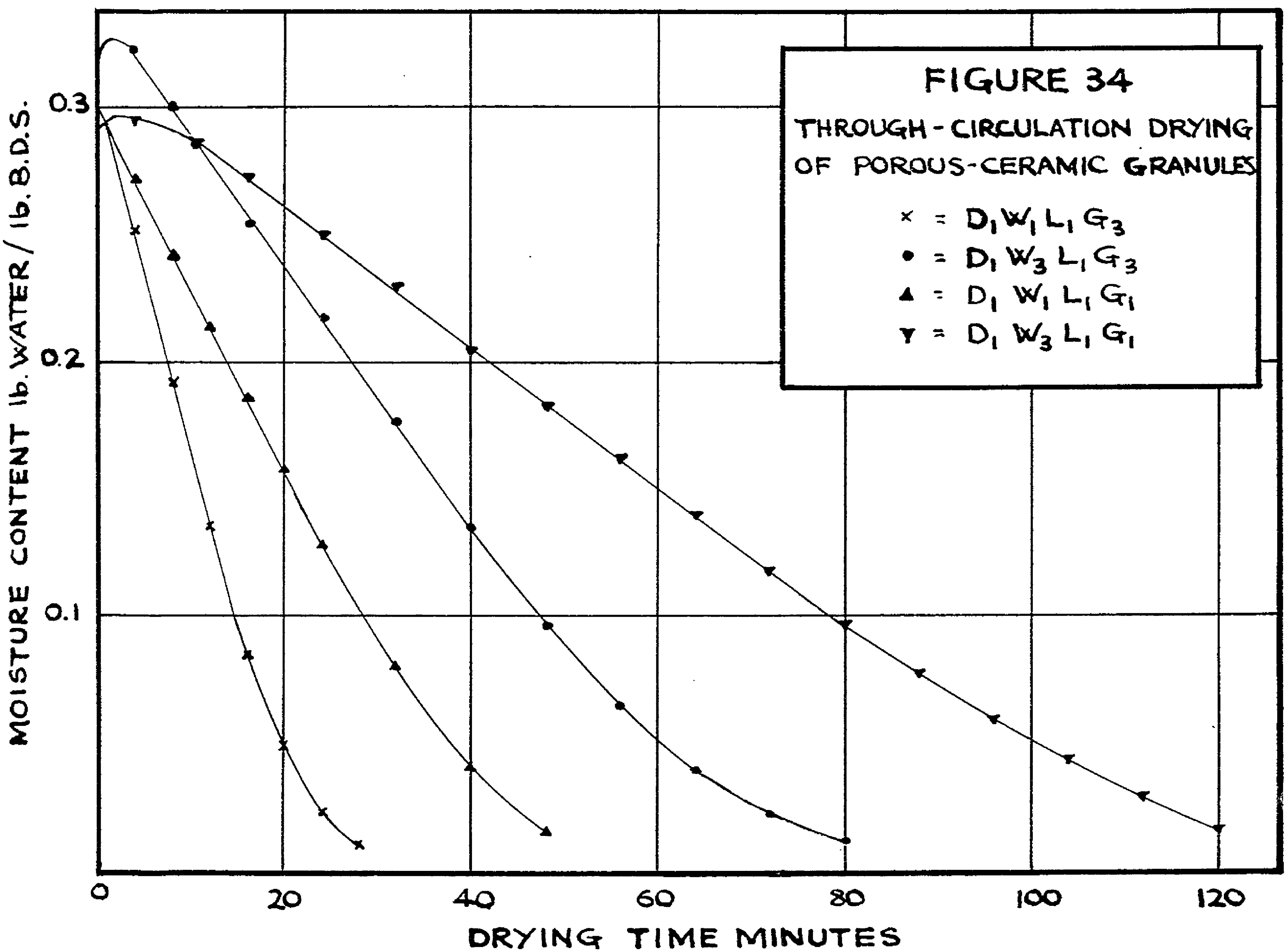
FIGURE 34
THROUGH-CIRCULATION DRYING OF POROUS-CERAMIC GRANULES
× = $D_1 W_1 L_1 G_3$
● = $D_1 W_3 L_1 G_3$
▲ = $D_1 W_1 L_1 G_1$
▼ = $D_1 W_3 L_1 G_1$
MOISTURE CONTENT lb. WATER / lb. B.D.S.
0.3
0.2
0.1
0
20
40
60
80
100
120
DRYING TIME MINUTES

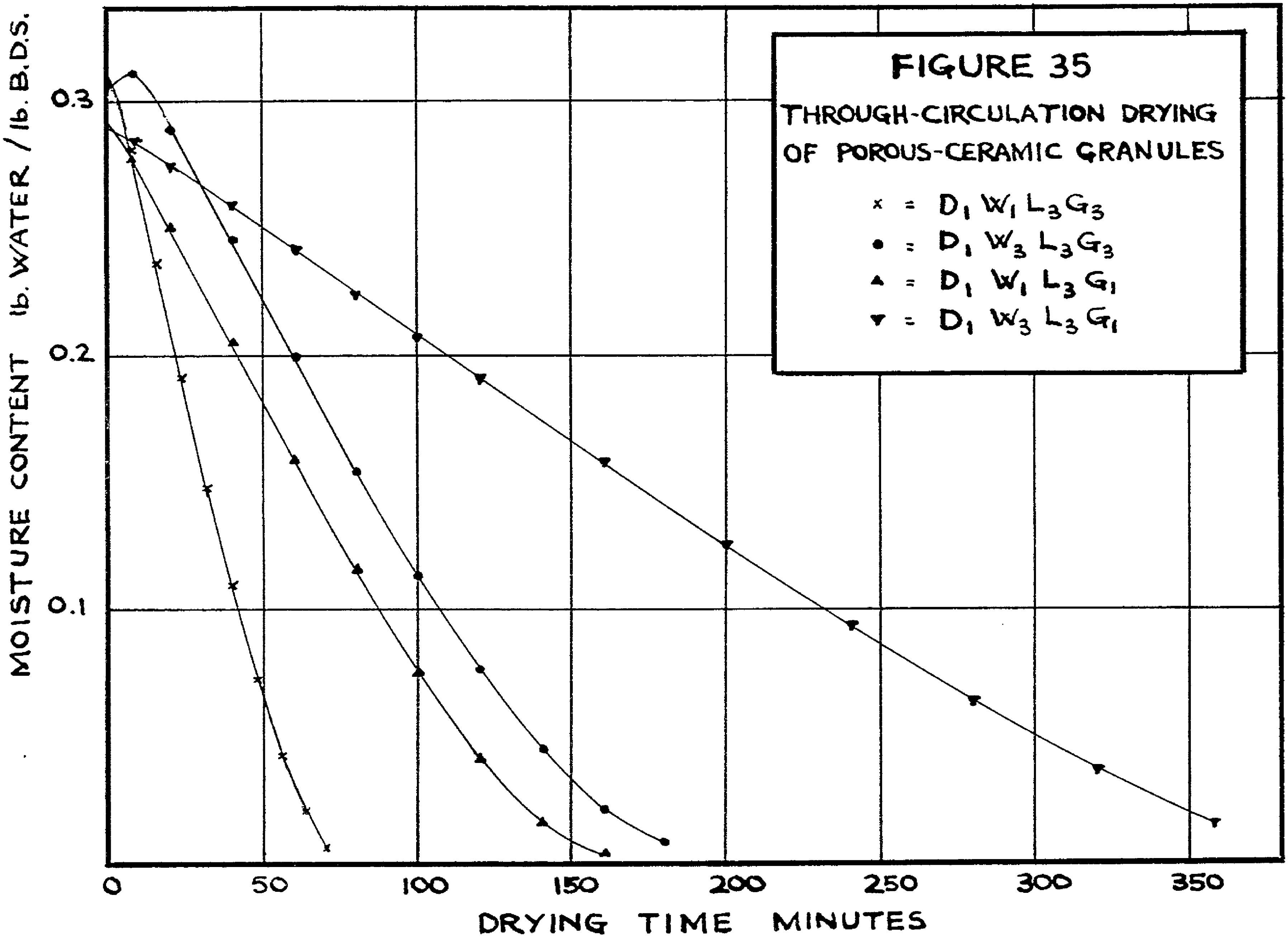
FIGURE 35
THROUGH-CIRCULATION DRYING
OF POROUS-CERAMIC GRANULES
× = $D_1 W_1 L_3 G_3$
● = $D_1 W_3 L_3 G_3$
▲ = $D_1 W_1 L_3 G_1$
▼ = $D_1 W_3 L_3 G_1$
MOISTURE CONTENT lb. WATER / lb. B.D.S.
0.3
0.2
0.1
0
50
100
150
200
250
300
350
DRYING TIME MINUTES

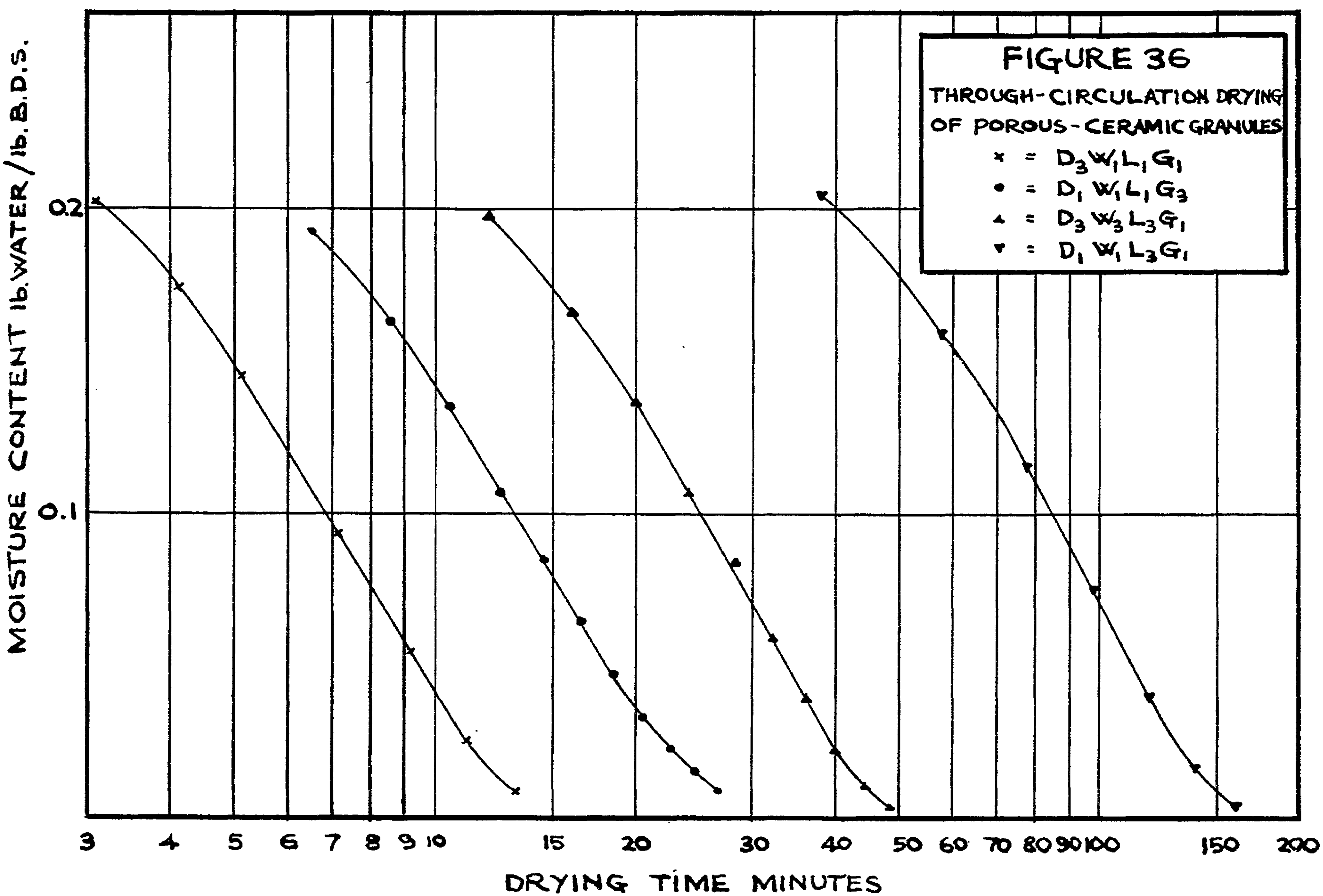

FIGURE 36
THROUGH-CIRCULATION DRYING OF POROUS-CERAMIC GRANULES
× = $D_3 W_1 L_1 G_1$
● = $D_1 W_1 L_1 G_3$
▲ = $D_3 W_3 L_3 G_1$
▼ = $D_1 W_1 L_3 G_1$
MOISTURE CONTENT lb. WATER/lb. B.D.S.
0.2
0.1
DRYING TIME MINUTES
3
4
5
6
7
8
9
10
15
20
30
40
50
60
70
80
90
100
150
200

TABLE 25: Results Of Preliminary Two-Level Factorial Experiment On Porous-Ceramic Granules

Test Conditions	$\frac{dW}{d\theta}$	$\log_{10} \frac{dW}{d\theta}$	W_c	C
$D_1W_1L_1G_1$	0.43	-0.3665	0.140	-0.372
$D_1W_3L_1G_1$	0.16	-0.7959	0.112	-0.377
$D_3W_1L_1G_1$	1.70	0.2304	0.138	-0.360
$D_3W_3L_1G_1$	1.47	0.1673	0.152	-0.375
$D_1W_1L_1G_3$	0.88	-0.0555	0.142	-0.355
$D_1W_3L_1G_3$	0.33	-0.4815	0.126	-0.374
$D_3W_1L_1G_3$	3.67	0.5647	0.132	-0.354
$D_3W_3L_1G_3$	3.10	0.4914	0.119	-0.378
$D_1W_1L_3G_1$	0.13	-0.8861	0.130	-0.397
$D_1W_3L_3G_1$	0.05	-1.3010	0.120	-0.394
$D_3W_1L_3G_1$	0.57	-0.2441	0.142	-0.388
$D_3W_3L_3G_1$	0.47	-0.3279	0.130	-0.381
$D_1W_1L_3G_3$	0.34	-0.4685	0.142	-0.365
$D_1W_3L_3G_3$	0.13	-0.8861	0.140	-0.367
$D_3W_1L_3G_3$	1.35	0.1303	0.150	-0.363
$D_3W_3L_3G_3$	1.18	0.0719	0.139	-0.360

The values of $\frac{dW}{d\theta}$, W_c and C shown in Table 25 were calculated as described in Section 6.2. The rate constant C was used to characterize the drying behaviour of the granules in the falling-rate period, since the plot of W against log θ' (see Figure 36) gave the best straight line of the various transformations of W and θ' tried. The linear relationship between W and log θ' (θ' measured from a standard initial W = 0.296) held down to W = 0.04.

Analyses of Variance were done on the values of $\log_{10} \frac{dW}{d\theta}$, W_c and C given in Table 25. The results of the Analysis of Variance on the $\log_{10} \frac{dW}{d\theta}$ values are shown in Table 26; x indicates effects or interactions significant at the 5% probability level.

TABLE 26: Analysis Of Variance Of Values Of $\log_{10}\frac{dW}{d\theta}$ Obtained For Porous-Ceramic Granules

Source of Variance	Sum of Squares
D	2.50043063
W	0.24169514
L	0.83992642
G	0.52218689
LD	0.00002185
LW	0.00001828
WG	0.00001580
LG	0.00651653 *
DW	0.12413290 *
DG	0.00004000
LDG	0.00043725
LDW	0.00005148
DWG	0.00001314
LWG	0.00005439
Residual	0.00019242
Total	4.23573312

The Analysis of Variance indicated that the LG and DW interactions were significant. $\frac{dW}{d\theta}$ may therefore be derived from an expression of the form:

$$\log_{10} \frac{dW}{d\theta} = f(DW) + f(LG)$$

The Analysis of Variance of the W_c values revealed no significant effects or interactions - the residual sum of squares (experimental error) being greater than the interaction sums of squares and of approximately the same magnitude as the main effect sums of squares.

The Analysis of Variance of the C values indicated a significant LG interaction affecting C.

10.3 Fractional Three-Level Factorial Experiment On Porous-Ceramic Granules

The fractional three-level factorial experiment used to verify the results of the preliminary two-level factorial experiment (see Section 10.2), involved the 45 tests shown in Table 27. This experiment was designed to provide extensive data, obtained under a wide range of drying conditions, on the values of W_c, the values of $f(DW)$ and $f(LG)$ in the relationship $\log_{10} \frac{dW}{d\theta} = f(DW) + f(LG)$, and on the values of C.

Following the method of presenting the experimental data described in Section 6.3, the values of $\frac{dW}{d\theta}$ for any drying conditions within the range of the experiment may be predicted from the average value of $\log_{10} \frac{dW}{d\theta}$ obtained in three replicates of a standard drying test $D_2W_2L_2G_2$ (-0.0448) by applying two correction factors to allow for variations in DW and LG from their standard levels $D_2W_2L_2G_2$ as given by the relationship:

$$\log_{10} \frac{dW}{d\theta} = -0.0448 + f(DW) + f(LG)$$

The values of the correction factor $f(DW)$ were obtained from the values of $\log_{10} \frac{dW}{d\theta}$ in Table 28 as the average difference between the tests in each DW row and the D_2W_2 tests in the corresponding LG column. The experiment was designed to give at least four independent estimates of $f(DW)$ for each level of DW. The average values of $f(DW)$ for the various levels of D and W were:

D_1W_1	-0.3587	D_2W_1	0.0316	D_3W_1	0.2542
D_1W_2	-0.4658	D_2W_2	0	D_3W_2	0.2048
D_1W_3	-0.7816	D_2W_3	-0.0362	D_3W_3	0.1826

These values are shown graphically in Figure 37A.

The values of f(LG) were obtained from the values of $\log_{10} \frac{dW}{d\theta}$ in Table 28 as the average difference between the tests in each LG column and the L_2G_2 tests in the corresponding DW row. The experiment was designed to give at least four independent estimates of f(LG) for each level of LG. As an example the value of f(LG) for drying conditions L_1G_1 is:

$$-0.3979 + 0.3665 = 0.0314$$
$$-0.8239 + 0.7959 = 0.0280$$
$$-0.0448 + 0.0044 = 0.0404$$
$$0.2304 - 0.2095 = 0.0209$$
$$0.1673 - 0.1303 = 0.0370$$
$$\text{Average} = 0.0315$$

The values of f(LG) for the other levels of L and G are

L_1G_1	0.0315	L_2G_1	-0.2310	L_3G_1	-0.4710
L_1G_2	0.2220	L_2G_2	0	L_3G_2	-0.1981
L_1G_3	0.3503	L_2G_3	0.1331	L_3G_3	-0.0678

These values are shown graphically in Figure 37B.

The values of W_e in Table 29 verified that, as indicated by the preliminary two-level factorial experiment, the drying conditions D, W, G and L had little or no effect on W_e. Since the Analysis of Variance of the values of W_e obtained in the preliminary two-level experiment indicated that the LG interaction was significant at the 10% probability level, the values of W_e in Table 29 were averaged over D and W and the average values of W_e at the various levels of L and G were plotted in Figure 38A. As can be seen from this Figure,

TABLE 27: Values of $\frac{dW}{d\theta}$ for porous-ceramic granules dried in the through-circulation drier

	L_1G_1	L_1G_2	L_1G_3	L_2G_1	L_2G_2	L_2G_3	L_3G_1	L_3G_2	L_3G_3
D_1W_1	0.43		0.88		0.40		0.13		0.34
D_1W_2		0.49		0.18	0.31	0.43			
D_1W_3	0.16		0.33		0.15		0.05		0.13
D_2W_1				0.55	0.94	1.35		0.60	
D_2W_2	0.99	1.48	2.02	0.54	0.90	1.19	0.30	0.54	0.77
D_2W_3		1.39			0.81	1.05		0.52	
D_3W_1	1.70		3.67		1.62		0.57		1.35
D_3W_2		2.43		0.82	1.40			0.92	
D_3W_3	1.47		3.10		1.35		0.47		1.18

TABLE 28: Values of $\log_{10}\frac{dW}{d\theta}$ for porous-ceramic granules dried in the through-circulation drier

	L_1G_1	L_1G_2	L_1G_3	L_2G_1	L_2G_2	L_2G_3	L_3G_1	L_3G_2	L_3G_3
D_1W_1	-0.3665		-0.0555		-0.3979		-0.8861		-0.4685
D_1W_2		-0.3098		-0.7447	-0.5086	-0.3665			
D_1W_3	-0.7959		-0.4815		-0.8239		-1.3010		-0.8861
D_2W_1				-0.2596	-0.0269	0.1303		-0.2218	
D_2W_2	-0.0044	0.1703	0.3054	-0.2676	-0.0448	0.0755	-0.5229	-0.2676	-0.1135
D_2W_3		0.1430			-0.0915	0.0212		-0.2840	
D_3W_1	0.2304		0.5647		0.2095		-0.2441		0.1303
D_3W_2		0.3856		-0.0862	0.1461			-0.0362	
D_3W_3	0.1673		0.4914		0.1303		-0.3279		0.0719

TABLE 29: Values of W_c for porous-ceramic granules dried in the through-circulation drier

	L_1G_1	L_1G_2	L_1G_3	L_2G_1	L_2G_2	L_2G_3	L_3G_1	L_3G_2	L_3G_3
D_1W_1	0.140		0.162		0.139		0.130		0.142
D_1W_2		0.125		0.145	0.124	0.132			
D_1W_3	0.112		0.126		0.134		0.120		0.142
D_2W_1				0.130	0.140	0.129		0.135	
D_2W_2	0.142	0.118	0.142	0.153	0.142	0.139	0.137	0.144	0.126
D_2W_3		0.140			0.146	0.130		0.140	
D_3W_1	0.138		0.132		0.149		0.142		0.150
D_3W_2		0.124		0.141	0.132			0.155	
D_3W_3	0.152		0.119		0.144		0.130		0.139

TABLE 30: Values of Rate Constant C for porous-ceramic granules dried in the through-circulation drier

	L_1G_1	L_1G_2	L_1G_3	L_2G_1	L_2G_2	L_2G_3	L_3G_1	L_3G_2	L_3G_3
D_1W_1	-0.372		-0.355		-0.390		-0.397		-0.365
D_1W_2		-0.371		-0.375	-0.407	-0.348			
D_1W_3	-0.377		-0.374		-0.353		-0.394		-0.367
D_2W_1				-0.380	-0.371	-0.404		-0.371	
D_2W_2	-0.372	-0.386	-0.370	-0.365	-0.365	-0.356	-0.389	-0.366	-0.371
D_2W_3		-0.356			-0.361	-0.341		-0.381	
D_3W_1	-0.360		-0.354		-0.372		-0.388		-0.363
D_3W_2		-0.347		-0.354	-0.359			-0.384	
D_3W_3	-0.375		-0.378		-0.370		-0.381		-0.360

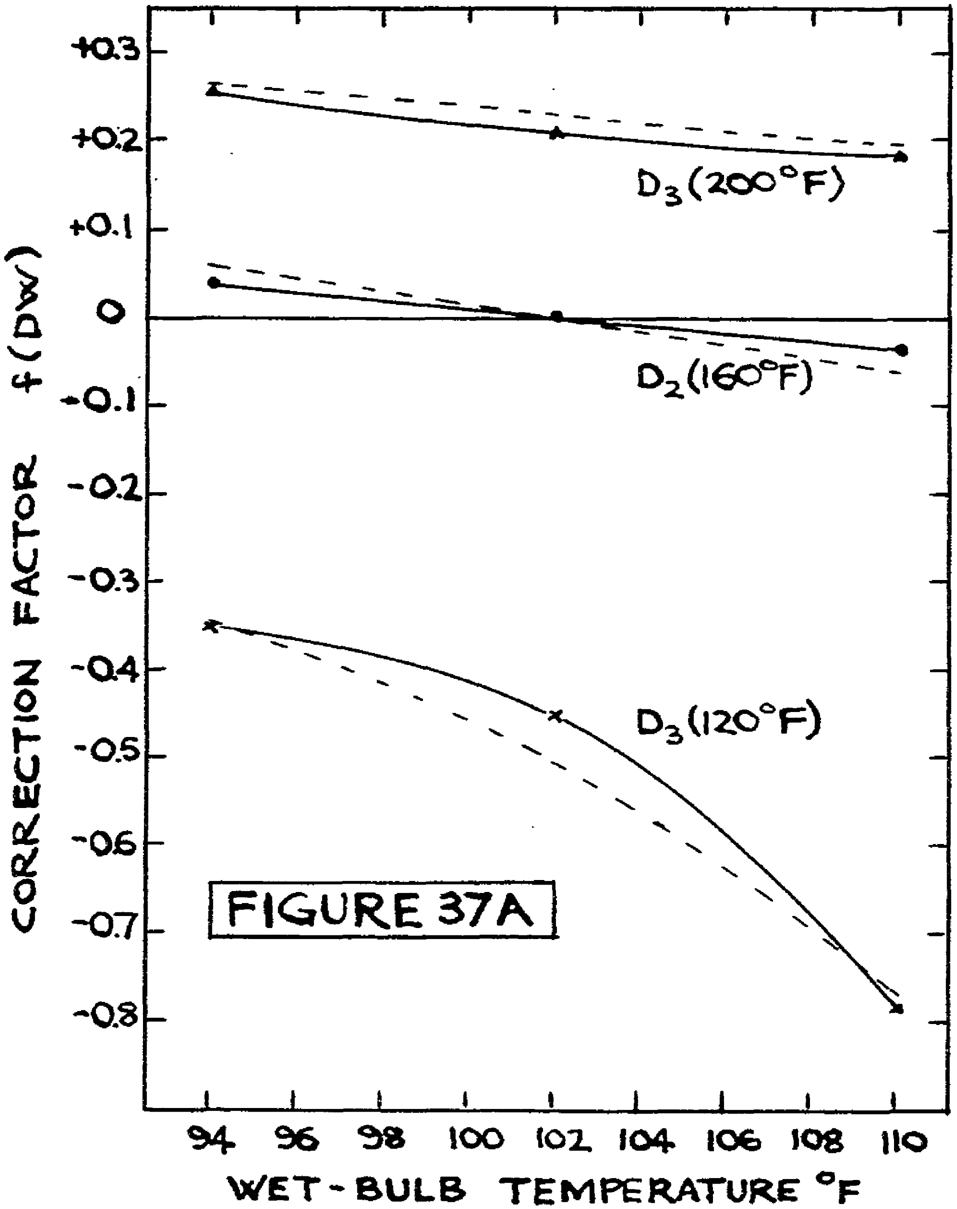

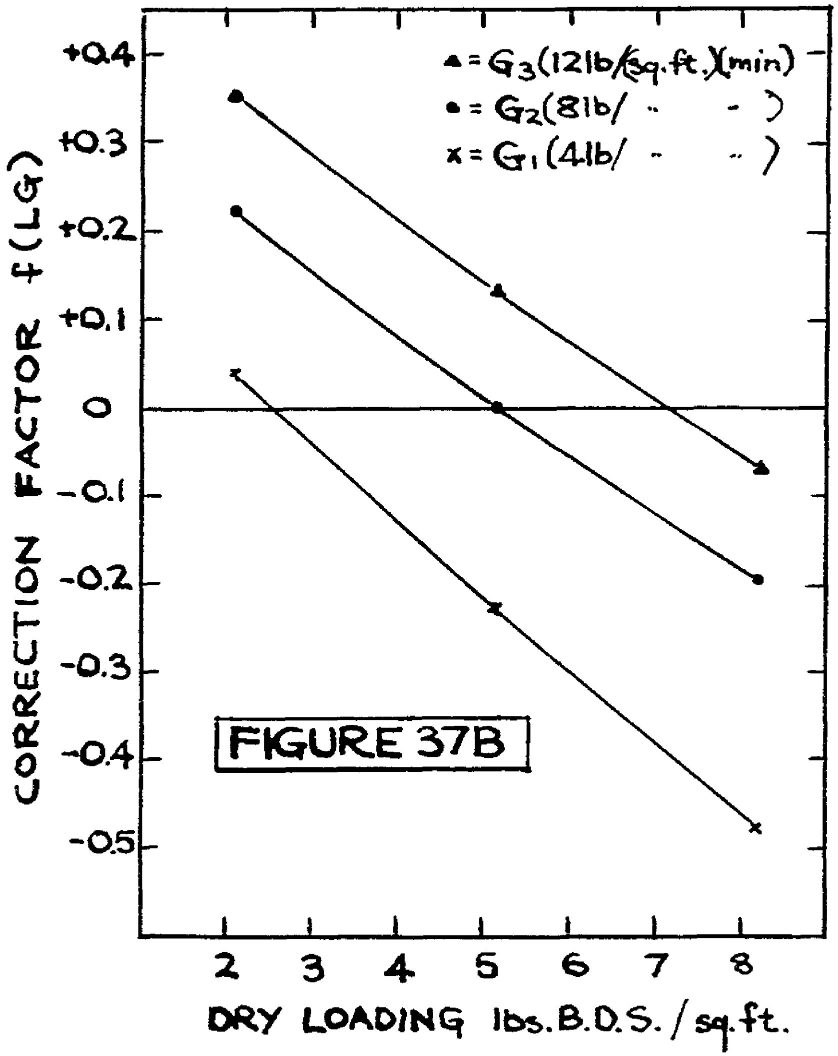

NOTE: THE DOTTED LINES IN FIGURE 37A INDICATE THE VALUES OF f(DW) PREDICTED BY DRYING THEORY.

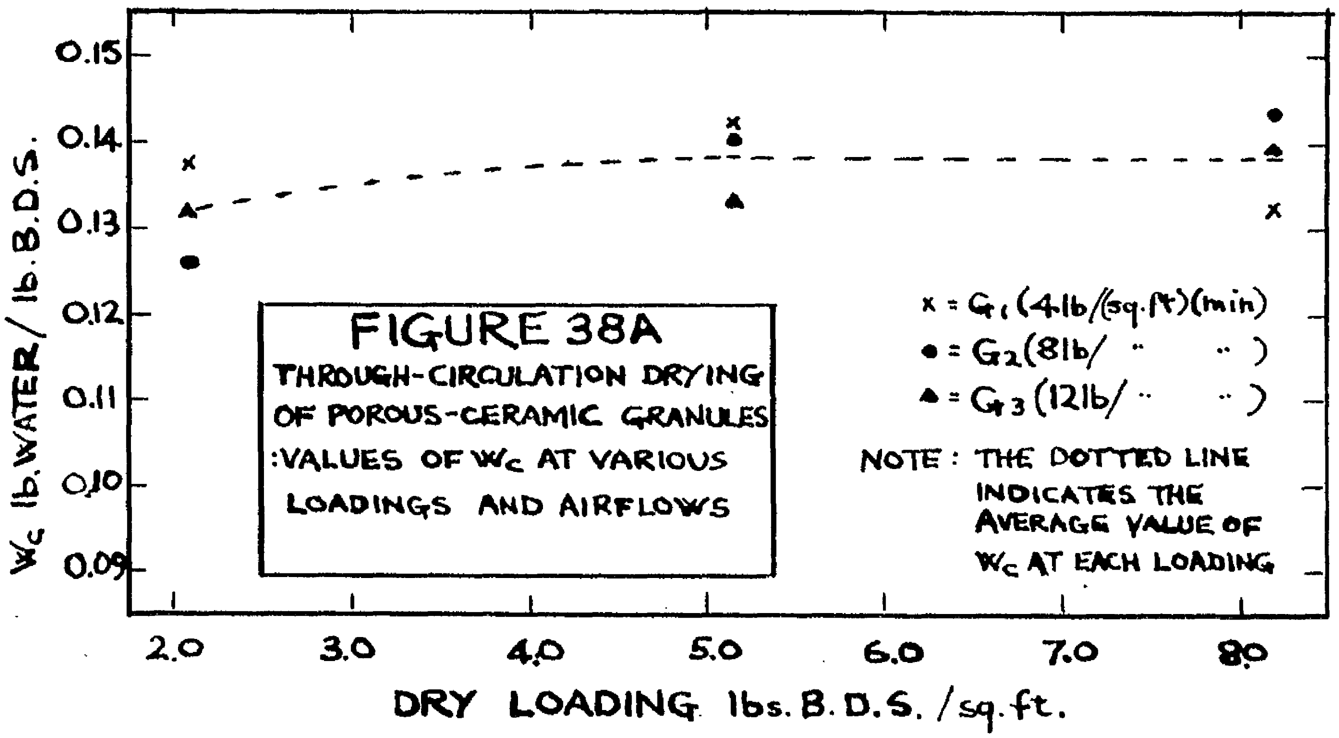
FIGURE 38A
THROUGH-CIRCULATION DRYING OF POROUS-CERAMIC GRANULES :VALUES OF Wc AT VARIOUS LOADINGS AND AIRFLOWS
x = G1 (4 lb/(sq.ft)(min)
• = G2 (8 lb/ " ")
▲ = G3 (12 lb/ " ")
NOTE : THE DOTTED LINE INDICATES THE AVERAGE VALUE OF Wc AT EACH LOADING
Wc lb. WATER / lb. B.D.S.
0.15
0.14
0.13
0.12
0.11
0.10
0.09
2.0
3.0
4.0
5.0
6.0
7.0
8.0
DRY LOADING lbs. B.D.S. /sq. ft.

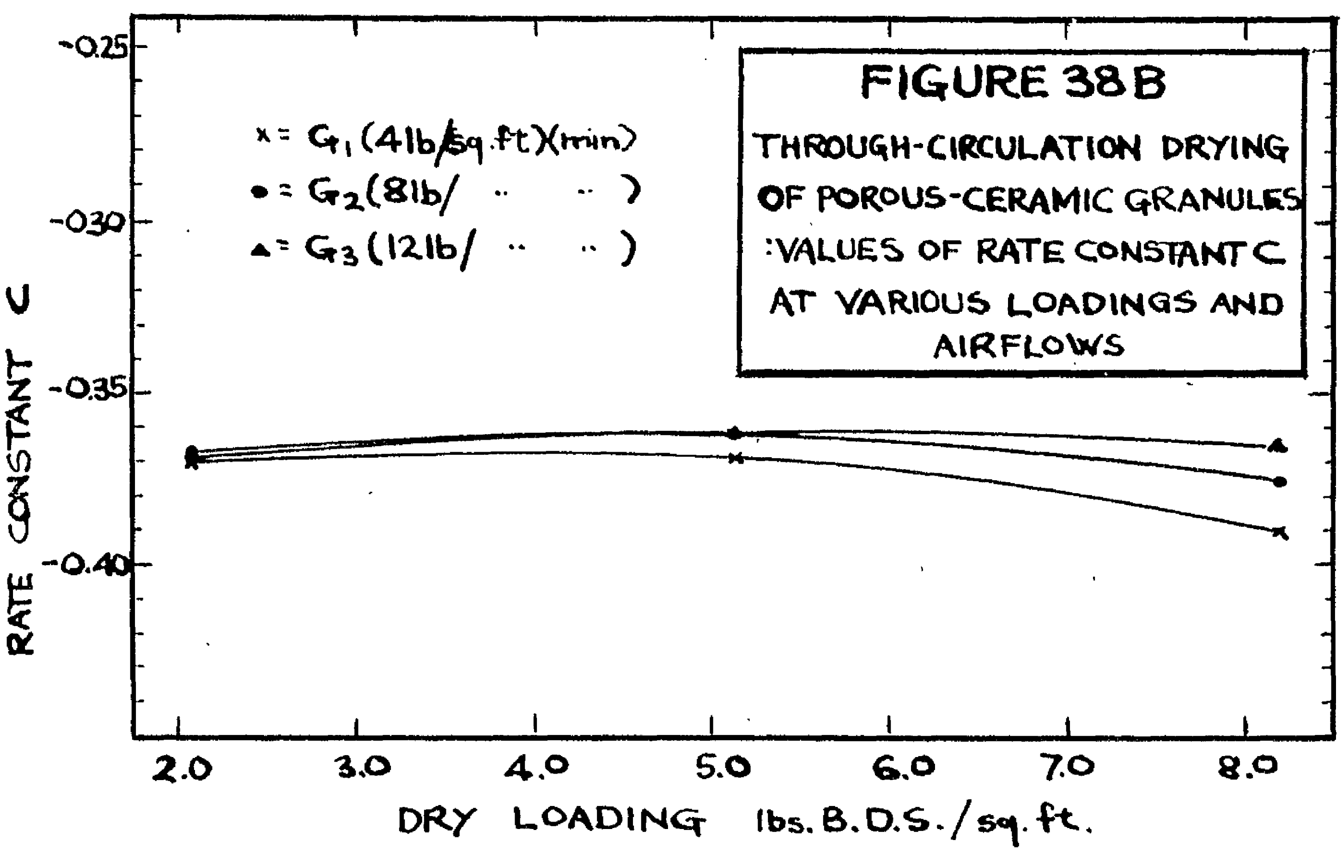
FIGURE 38B
THROUGH-CIRCULATION DRYING OF POROUS-CERAMIC GRANULES :VALUES OF RATE CONSTANT C AT VARIOUS LOADINGS AND AIRFLOWS
x = G1 (4 lb/sq.ft)(min)
• = G2 (8 lb/ " ")
▲ = G3 (12 lb/ " ")
RATE CONSTANT C
-0.25
-0.30
-0.35
-0.40
2.0
3.0
4.0
5.0
6.0
7.0
8.0
DRY LOADING lbs. B.D.S. /sq. ft.

however, the variation of W_c with L at the various levels of G appeared to be irregular and slight. Since W_c appeared to be unaffected by G, the values in Table 29 were averaged over D, W and G for each level of L giving the average values of W_c at L_1 = 0.132, L_2 = 0.138, L_3 = 0.138. These values are shown by the dotted line in Figure 38A.

Examination of the values of C in Table 30 confirmed the presence of a slight LG interaction, indicated by the Analysis of Variance of the values of C obtained in the preliminary two-level factorial experiment. G appeared to have no effect on C at L_1, but increasing effects at L_2 and L_3. The values of C averaged over D and W for each level of L and G were:

L_1G_1	-0.370	L_2G_1	-0.369	L_3G_1	-0.391
L_1G_2	-0.367	L_2G_2	-0.362	L_3G_2	-0.375
L_1G_3	-0.366	L_2G_3	-0.362	L_3G_3	-0.365

These values of C are shown graphically in Figure 38B.

10.4 Method Of Predicting The Drying Time Of Porous-Ceramic Granules In The Through-Circulation Drier

The experimental results presented in Section 10.3 may be used as follows to predict the time required to dry the porous-ceramic granules from an initial moisture content W_1 to a final moisture content W_2 under any drying conditions within the experimental ranges of D, W, L and G.

(a) The constant drying rate $\frac{dW}{d\theta}$ for the appropriate values of D, W, L and G is calculated from the equation:

$$\log_{10} \frac{dW}{d\theta} = -0.0448 + f(DW) + f(LG)$$

The values of the correction factors f(DW) and f(LG) are obtained from Figures 37A and 37B.

(b) The critical moisture content W_c for the appropriate value of L is obtained from Figure 38A.

(c) The duration of the constant drying rate period in minutes θ_c' (measured from a standard moisture content $W_{st} = 0.296$) is obtained from the equation:

$$\theta_c' = \frac{60(0.296 - W_c)}{\frac{dW}{d\theta}}$$

(d) The rate constant C for the appropriate values of L and G is obtained from Figure 38B.

(e) θ_T', the time in minutes required to dry the granules from W_{st} to W_2, is calculated from the equation:

$$\log_{10} \theta_T' = \log_{10}\theta_c' + \frac{W_2 - W_c}{C}$$

(f) θ_1', the drying time of the granules between W_1 and W_{st}, is calculated from the equation:

$$\theta_1' = \frac{60(W_1 - 0.296)}{\frac{dW}{d\theta}}$$

θ', the drying time of the granules from W_1 to W_2, is given by the equation:

$$\theta' = \theta_T' + \theta_1'$$

10.5 Drying Of Coke

The coke was prepared for the through-circulation drying tests by the standard soaking and draining procedure described in Section 6.5. The ranges of D, W, and G studied were the same as those chosen for the tests on the porous-ceramic granules (see Table 24); approximately the same range of L was studied for both materials. The values of D, W, L and G used in the tests on coke were as follows:

TABLE 31

$D_1 = 120$	$D_2 = 160$	$D_3 = 200$
$W_1 = 94$	$W_2 = 102$	$W_3 = 110$
$G_1 = 4$	$G_2 = 8$	$G_3 = 12$
$L_1 = 1.26$	$L_2 = 4.71$	$L_3 = 7.97$
($\frac{5}{8}$ inch layer)	($2\frac{1}{2}$ inch layer)	(4 inch layer)

10.6 Preliminary Two-Level Factorial Experiment On Coke

A preliminary two-level factorial experiment testing levels 1 and 3 of the four factors D, W, G and L shown in Table 31 was done. This experiment involved the sixteen tests shown in Table 32. The drying curves obtained in the tests are shown in Figures 39, 40, 41 and 42, and the shapes of the curves are described in Table 32 as values of $\frac{dW}{d\theta}$, W_c and C. These quantities were derived from the various drying curves as described in Section 6.2.

The rate constant C was used to describe the drying behaviour of the coke in the falling-rate period since the plots of W against log θ' (see Figure 43) were linear from W_c down to $W = 0.06$. In calculating C, θ' was measured from a standard $W_{st} = 0.271$.

Analyses of Variance were done on the values of $\log_{10} \frac{dW}{d\theta}$, W_c and C shown in Table 32.

The Analysis of Variance of the $\log_{10} \frac{dW}{d\theta}$ values, shown in Table 33, indicated that the LG and DW interactions were significant. It is interesting to note that the same interactions were shown to have significant effects on the values of $\log_{10} \frac{dW}{d\theta}$ for porous-ceramic granules

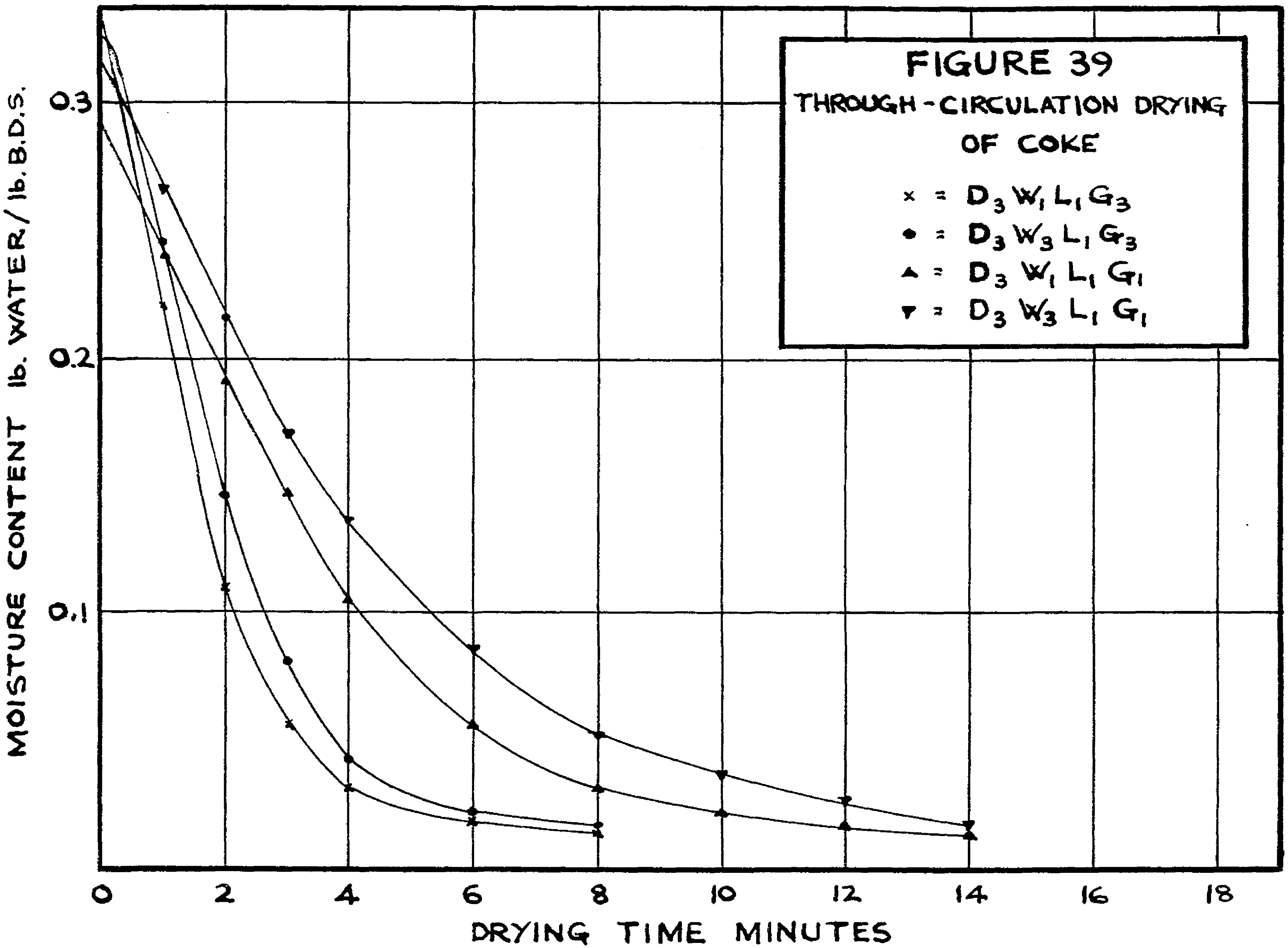
FIGURE 39
THROUGH-CIRCULATION DRYING OF COKE
× = $D_3 W_1 L_1 G_3$
● = $D_3 W_3 L_1 G_3$
▲ = $D_3 W_1 L_1 G_1$
▼ = $D_3 W_3 L_1 G_1$
MOISTURE CONTENT lb. WATER/lb. B.D.S.
0.3
0.2
0.1
0
2
4
6
8
10
12
14
16
18
DRYING TIME MINUTES

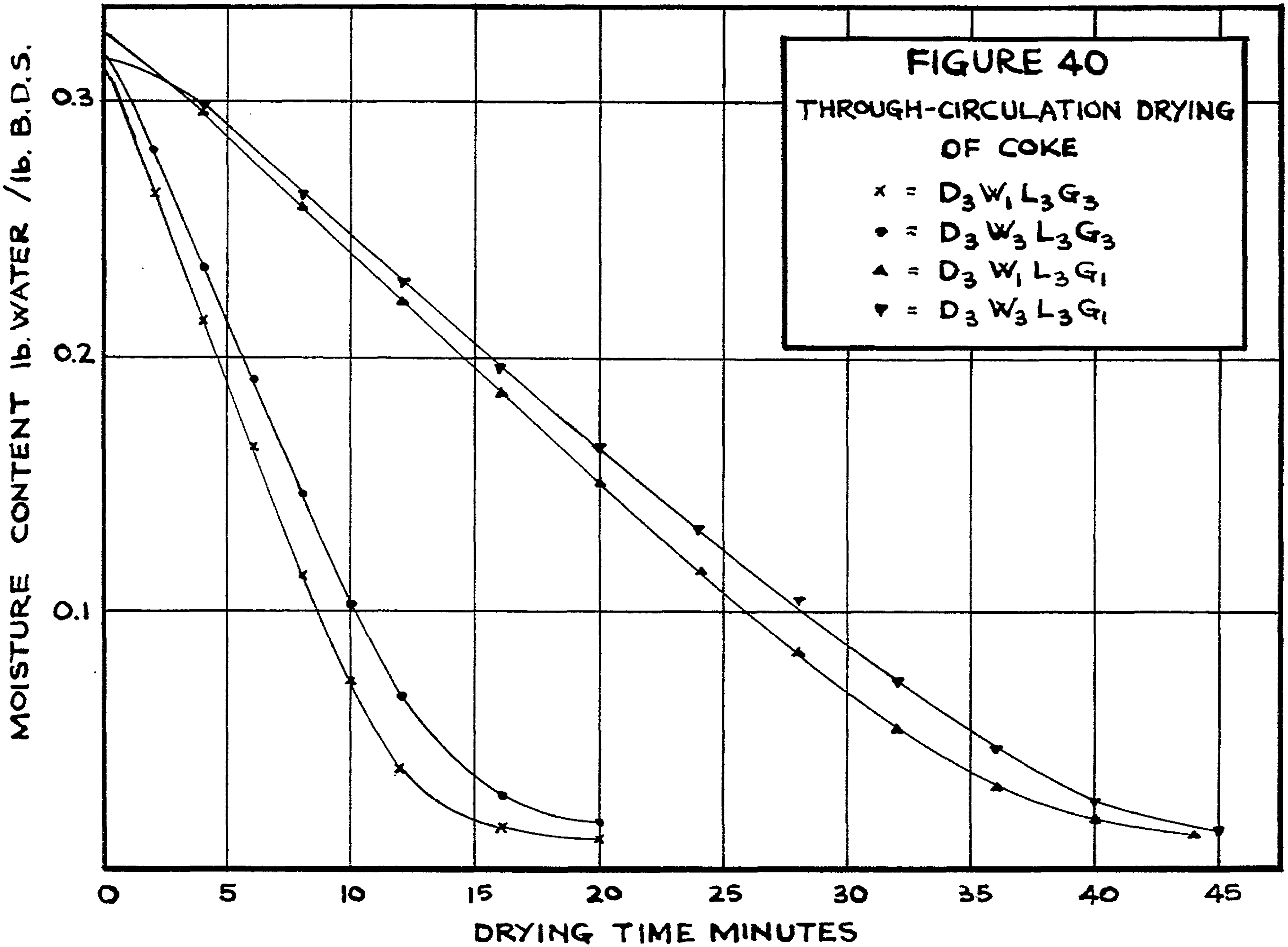
FIGURE 40
THROUGH-CIRCULATION DRYING OF COKE
× = D3 W1 L3 G3
● = D3 W3 L3 G3
▲ = D3 W1 L3 G1
▼ = D3 W3 L3 G1
MOISTURE CONTENT lb. WATER /lb. B.D.S.
0.3
0.2
0.1
0
5
10
15
20
25
30
35
40
45
DRYING TIME MINUTES

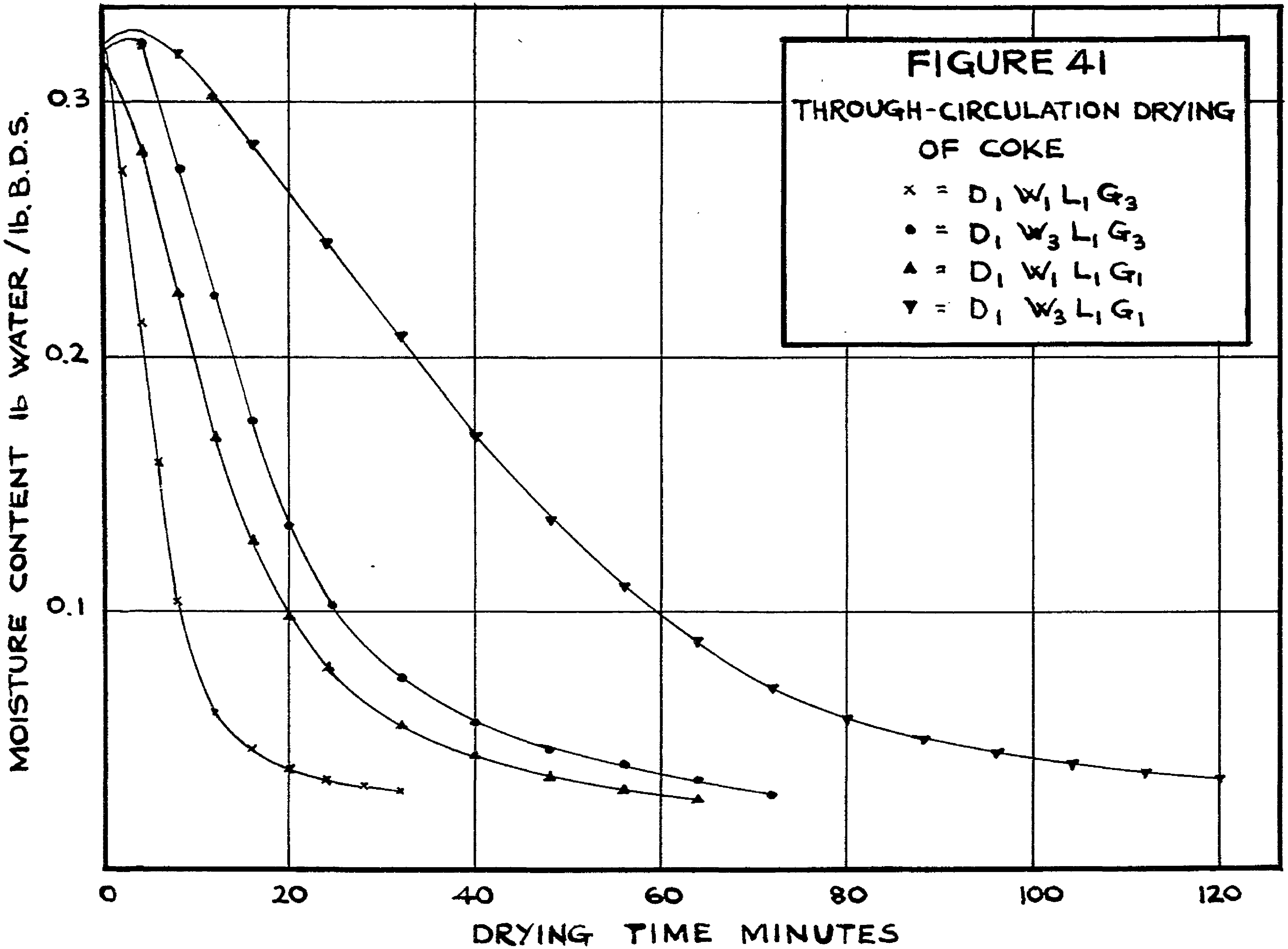
FIGURE 41
THROUGH-CIRCULATION DRYING OF COKE
× = D1 W1 L1 G3
● = D1 W3 L1 G3
▲ = D1 W1 L1 G1
▼ = D1 W3 L1 G1
MOISTURE CONTENT lb WATER / lb. B.D.S.
0.3
0.2
0.1
0
20
40
60
80
100
120
DRYING TIME MINUTES

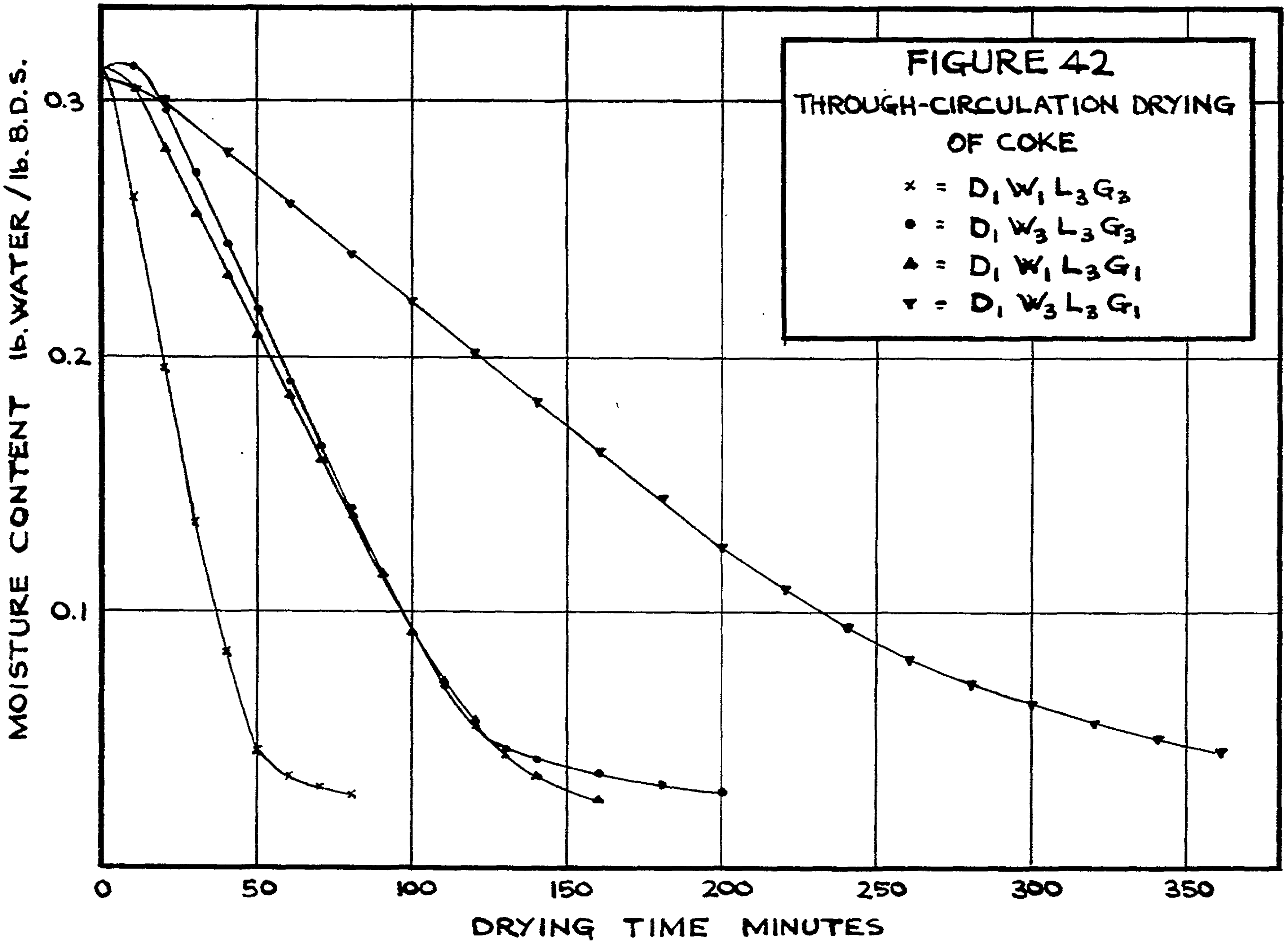

FIGURE 42
THROUGH-CIRCULATION DRYING OF COKE
× = $D_1 W_1 L_3 G_3$
● = $D_1 W_3 L_3 G_3$
▲ = $D_1 W_1 L_3 G_1$
▼ = $D_1 W_3 L_3 G_1$
MOISTURE CONTENT lb. WATER / lb. B.D.S.
0.3
0.2
0.1
0
50
100
150
200
250
300
350
DRYING TIME MINUTES

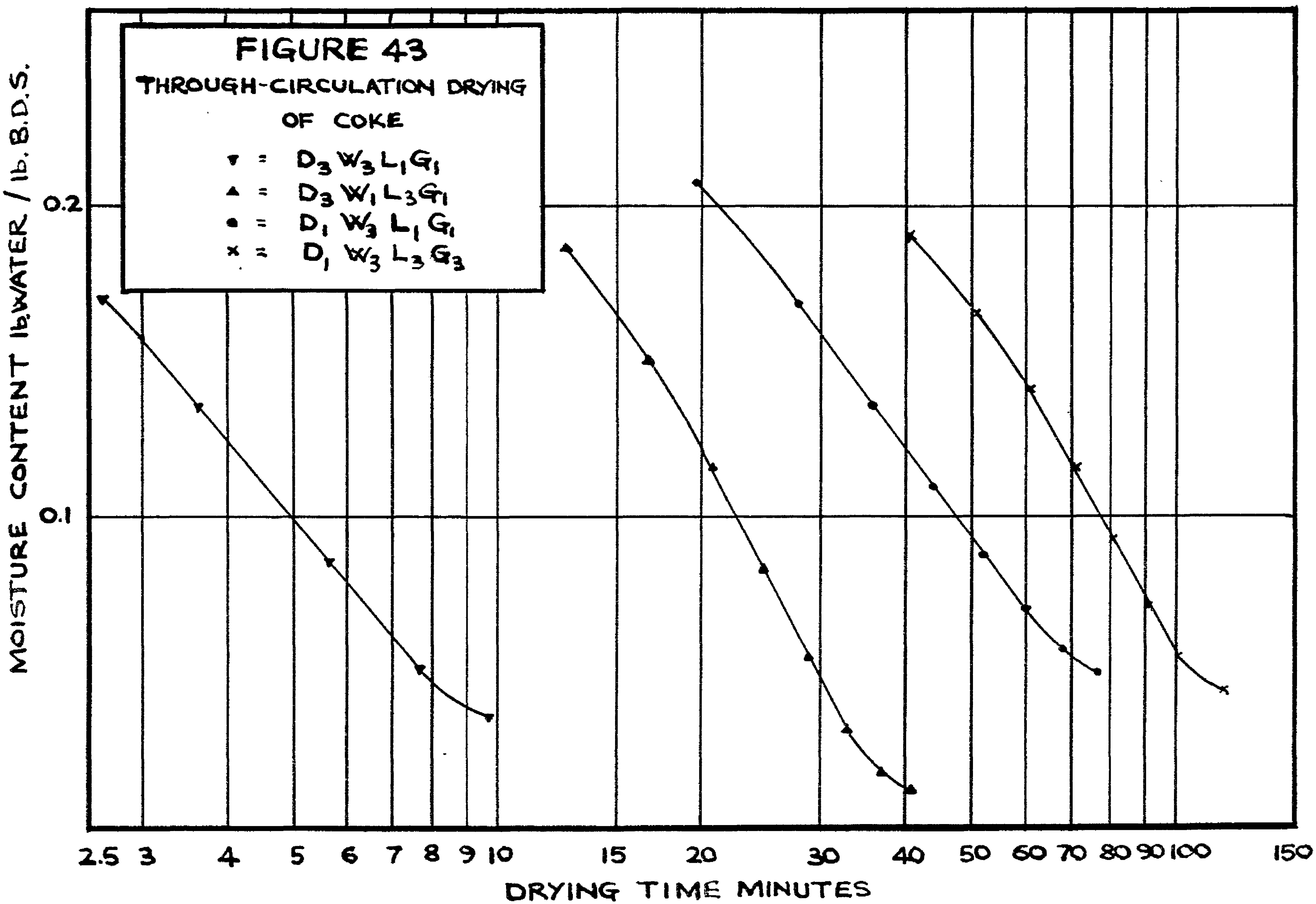
FIGURE 43
THROUGH-CIRCULATION DRYING
OF COKE
▼ = D3 W3 L1 G1
▲ = D3 W1 L3 G1
● = D1 W3 L1 G1
× = D1 W3 L3 G3
MOISTURE CONTENT lb.WATER / lb. B.D.S.
0.2
0.1
2.5 3 4 5 6 7 8 9 10 15 20 30 40 50 60 70 80 90 100 150
DRYING TIME MINUTES

(see Section 10.2). $\frac{dW}{d\theta}$ for coke may therefore be calculated from an expression of the form:

$$\log_{10} \frac{dW}{d\theta} = f(DW) + f(LG)$$

TABLE 32: Results Of The Two-Level Factorial Experiment On Coke

Test Conditions	$\frac{dW}{d\theta}$	$\log_{10} \frac{dW}{d\theta}$	W_e	C
$D_1W_1L_1G_1$	0.85	-0.0706	0.163	-0.251
$D_1W_3L_1G_1$	0.30	-0.5229	0.165	-0.283
$D_3W_1L_1G_1$	3.13	0.4955	0.160	-0.305
$D_3W_3L_1G_1$	3.02	0.4800	0.170	-0.280
$D_1W_1L_1G_3$	1.67	0.2227	0.130	-0.270
$D_1W_3L_1G_3$	0.66	-0.1805	0.150	-0.269
$D_3W_1L_1G_3$	6.79	0.8319	0.144	-0.334
$D_3W_3L_1G_3$	5.66	0.7528	0.145	-0.313
$D_1W_1L_3G_1$	0.15	-0.8239	0.120	-0.410
$D_1W_3L_3G_1$	0.06	-1.2218	0.125	-0.375
$D_3W_1L_3G_1$	0.55	-0.2596	0.134	-0.410
$D_3W_3L_3G_1$	0.49	-0.3098	0.142	-0.422
$D_1W_1L_3G_3$	0.38	-0.4202	0.112	-0.379
$D_1W_3L_3G_3$	0.15	-0.8239	0.123	-0.396
$D_3W_1L_3G_3$	1.48	0.1703	0.086	-0.404
$D_3W_3L_3G_3$	1.36	0.1335	0.116	-0.395

TABLE 33: Analysis Of Variance Of Values Of $\log_{10} \frac{dW}{d\theta}$ Obtained For Coke

Source of Variance	Sum of Squares
D	2.35292590
W	0.21130110
L	1.93508966
G	0.53279051
DW	0.13606877 x
LW	0.00023639
LG	0.01155086 x
LD	0.00047633
DG	0.00012712
WG	0.00000297
LDG	0.00060149
LDW	0.00013398
DWG	0.00054640
LWG	0.00003054
Residual	0.00108734
Total	5.18296936

x Denotes interactions significant at the 5% probability level.

The Analysis of Variance of the W_c values indicated that the LG interaction was significant.

The Analysis of Variance of the values of C indicated that the LD interaction was significant.

10.7 Fractional Three-Level Factorial Experiment On Coke

The fractional three-level factorial experiment, used to verify the results of the preliminary two-level experiment described in Section 10.6, involved the same 45 tests as did the corresponding

TABLE 34: Values of $\frac{dW}{d\theta}$ for coke dried in the through-circulation drier

	L_1G_1	L_1G_2	L_1G_3	L_2G_1	L_2G_2	L_2G_3	L_3G_1	L_3G_2	L_3G_3
D_1W_1	0.85		1.67		0.47		0.15		0.38
D_1W_2		0.91		0.20	0.35	0.50			
D_1W_3	0.30		0.66		0.17		0.06		0.15
D_2W_1				0.69	1.13	1.71		0.62	
D_2W_2	1.97	2.71	3.87	0.62	1.05	1.49	0.34	0.54	0.89
D_2W_3		2.46			0.92	1.37		0.48	
D_3W_1	3.13		6.79		1.77		0.55		1.48
D_3W_2		4.12		0.94	1.62			1.20	
D_3W_3	3.02		5.66		1.58		0.49		1.36

TABLE 35: Values of $\log_{10}\frac{dW}{d\theta}$ for coke dried in the through-circulation drier

	L_1G_1	L_1G_2	L_1G_3	L_2G_1	L_2G_2	L_2G_3	L_3G_1	L_3G_2	L_3G_3
D_1W_1	-0.0706		0.2227		-0.3279		-0.8239		-0.4202
D_1W_2		-0.0410		-0.6990	-0.4559	-0.3010			
D_1W_3	-0.5229		-0.1805		-0.7696		-1.2218		-0.8239
D_2W_1				-0.1612	0.0531	0.2330		-0.2076	
D_2W_2	0.2945	0.4330	0.5877	-0.2076	0.0212	0.1732	-0.4685	-0.2676	-0.0506
D_2W_3		0.3909			-0.0362	0.1367		-0.3188	
D_3W_1	0.4955		0.8319		0.0480		-0.2596		0.1703
D_3W_2		0.6149		-0.0269	0.2095			0.0809	
D_3W_3	0.4800		0.7528		0.1987		-0.3098		0.1335

TABLE 36: Values of W_e for coke dried in the through-circulation drier

	L_1G_1	L_1G_2	L_1G_3	L_2G_1	L_2G_2	L_2G_3	L_3G_1	L_3G_2	L_3G_3
D_1W_1	0.163		0.130		0.137		0.120		0.112
D_1W_2		0.135		0.156	0.162	0.140			
D_1W_3	0.165		0.150		0.132		0.125		0.123
D_2W_1				0.150	0.110	0.140		0.099	
D_2W_2	0.130	0.163	0.112	0.130	0.133	0.108	0.115	0.101	0.145
D_2W_3		0.139			0.139	0.137		0.125	
D_3W_1	0.160		0.144		0.122		0.134		0.086
D_3W_2		0.134		0.132	0.143			0.124	
D_3W_3	0.170		0.145		0.125		0.142		0.116

TABLE 37: Values of Rate Constant C for coke dried in the through-circulation drier

	L_1G_1	L_1G_2	L_1G_3	L_2G_1	L_2G_2	L_2G_3	L_3G_1	L_3G_2	L_3G_3
D_1W_1	-0.251		-0.270		-0.364		-0.407		-0.379
D_1W_2		-0.307		-0.405	-0.371	-0.350			
D_1W_3	-0.283		-0.269		-0.385		-0.375		-0.396
D_2W_1				-0.403	-0.397	-0.361		-0.437	
D_2W_2	-0.330	-0.315	-0.295	-0.410	-0.389	-0.405	-0.402	-0.417	-0.393
D_2W_3		-0.322			-0.383	-0.376		-0.400	
D_3W_1	-0.305		-0.334		-0.397		-0.410		-0.404
D_3W_2		-0.327		-0.367	-0.392			-0.403	
D_3W_3	-0.280		-0.313		-0.404		-0.422		-0.395

experiment (see Section 10.3) used to investigate the through-circulation drying behaviour of the porous-ceramic granules. This enlarged experiment provided additional data on the values of f(DW) and f(LG) in the relationship $\log_{10} \frac{dW}{d\theta} = f(DW) + f(LG)$; it also provided extra information on the effect of L and G on W_e, and on the effect of L and D on the rate constant C.

To facilitate the application of the $\frac{dW}{d\theta}$ results shown in Table 34 to the prediction of the value of $\frac{dW}{d\theta}$ under any specified drying conditions within the experimental ranges of D, W, L and G, the values in Table 34 were converted to values of $\log_{10} \frac{dW}{d\theta}$; these values are shown in Table 35. $\frac{dW}{d\theta}$ could then be predicted from the average value of $\log_{10} \frac{dW}{d\theta}$, (0.0212), obtained in the three replicates of the standard drying test $D_2W_2L_2G_2$ by applying two correction factors to allow for variations in DW and LG from their standard levels. The method of predicting $\frac{dW}{d\theta}$ may be represented by the equation:

$$\log_{10} \frac{dW}{d\theta} = 0.0212 + f(DW) + f(LG)$$

The values of f(DW) and f(LG) for the various levels of D, W, L and G were obtained from the values in Table 35 in the same way as were the corresponding correction factors in the expression for $\frac{dW}{d\theta}$ for the porous-ceramic granules (see Section 10.3) the values of f(DW) obtained were:

D_1W_1	-0.3608	D_2W_1	0.0495	D_3W_1	0.2204
D_1W_2	-0.4792	D_2W_2	0	D_3W_2	0.1844
D_1W_3	-0.7806	D_2W_3	-0.0468	D_3W_3	0.1742

These values are shown graphically in Figure 44A.

The values of f(LG) obtained were:

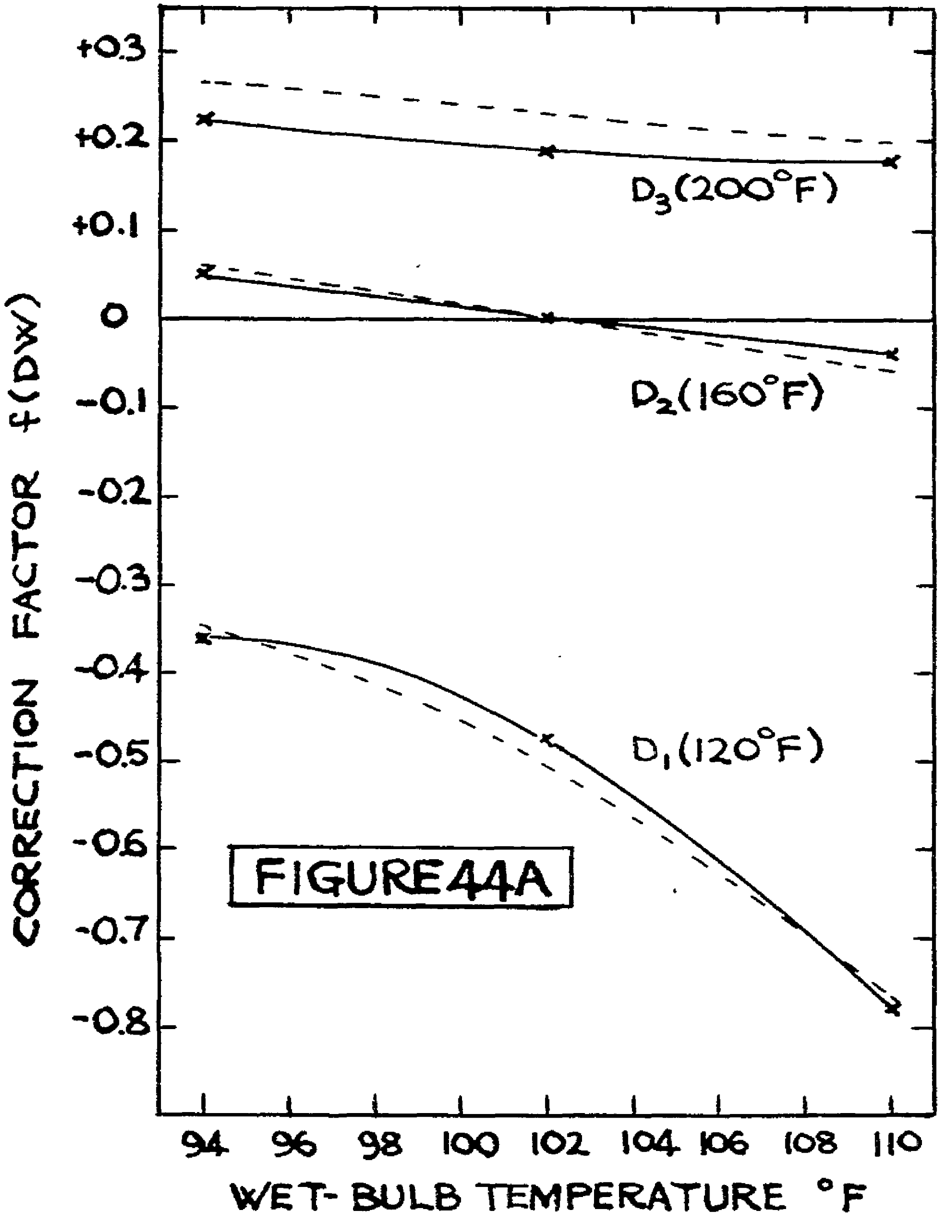

FIGURE 44A

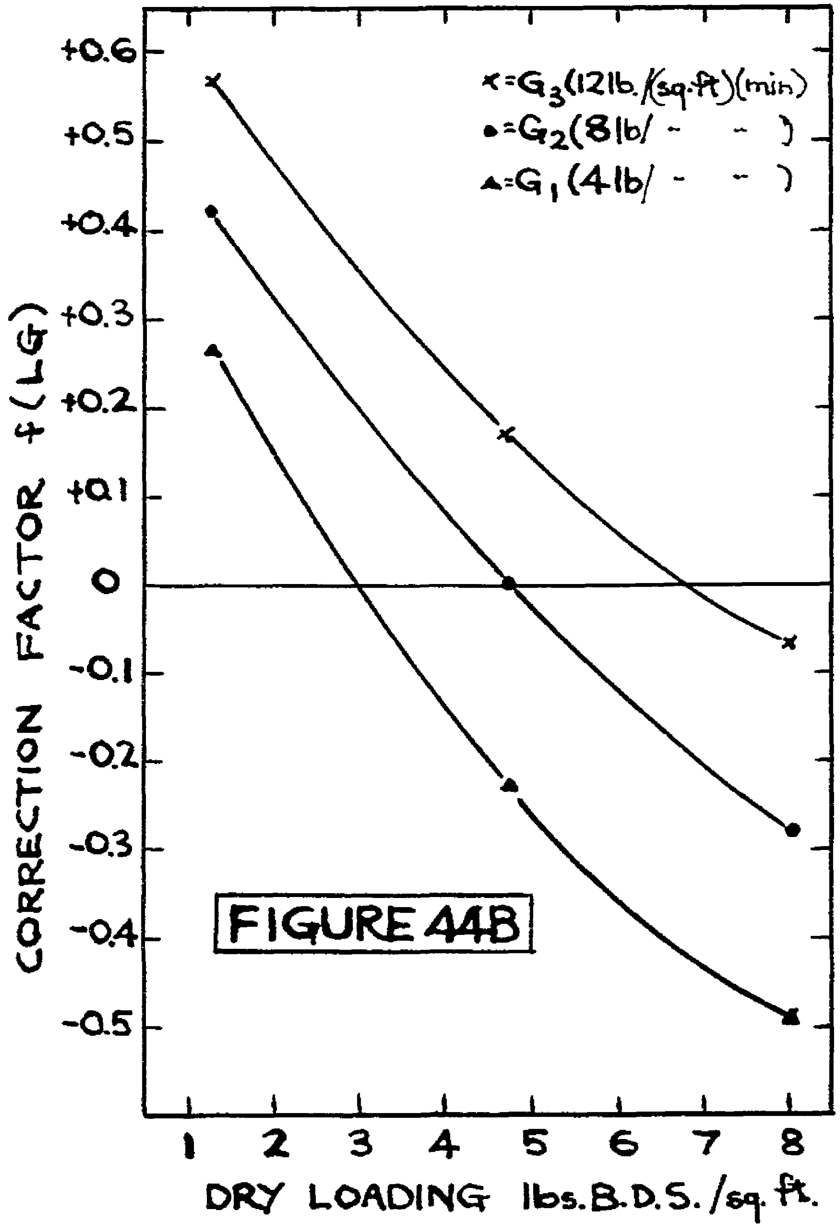

FIGURE 44B

NOTE: THE DOTTED LINES IN FIGURE 44A INDICATE THE VALUES OF f(DW) PREDICTED BY DRYING THEORY.

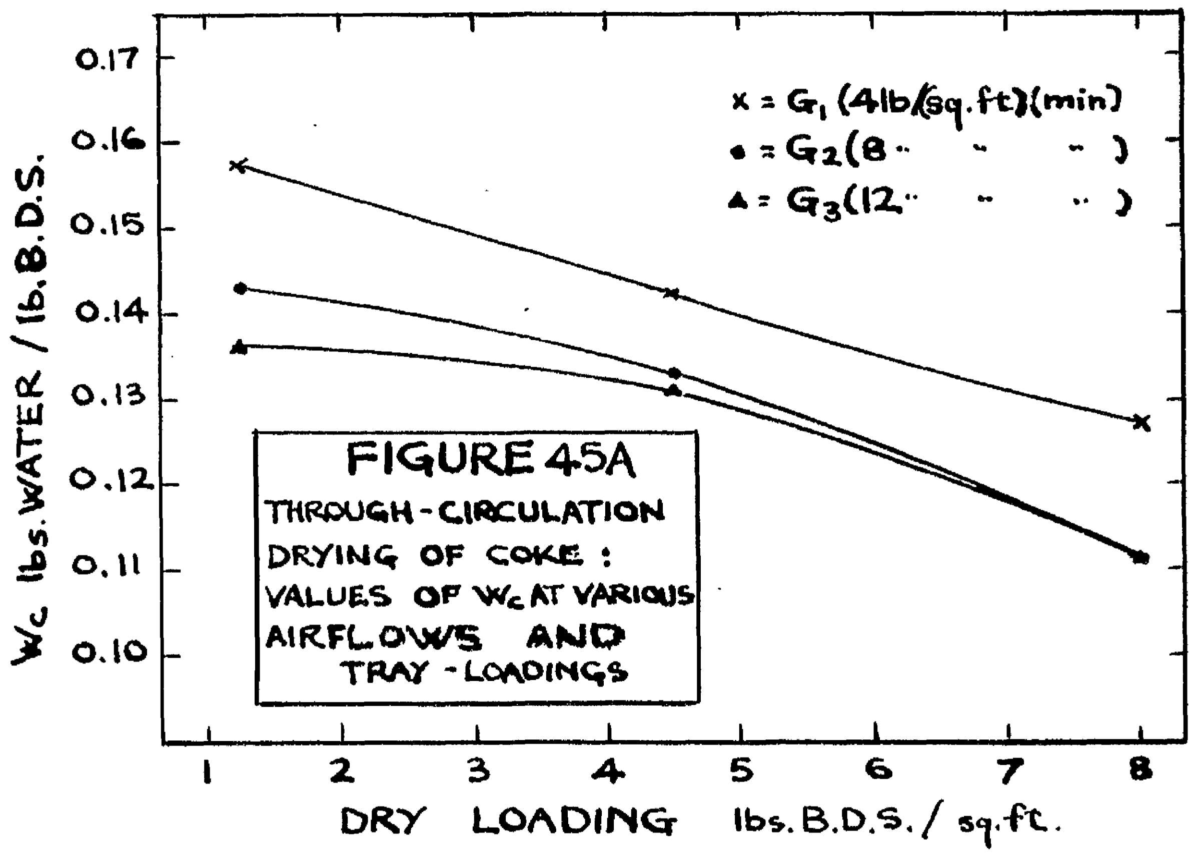

FIGURE 45A
THROUGH - CIRCULATION DRYING OF COKE : VALUES OF W_c AT VARIOUS AIRFLOWS AND TRAY - LOADINGS

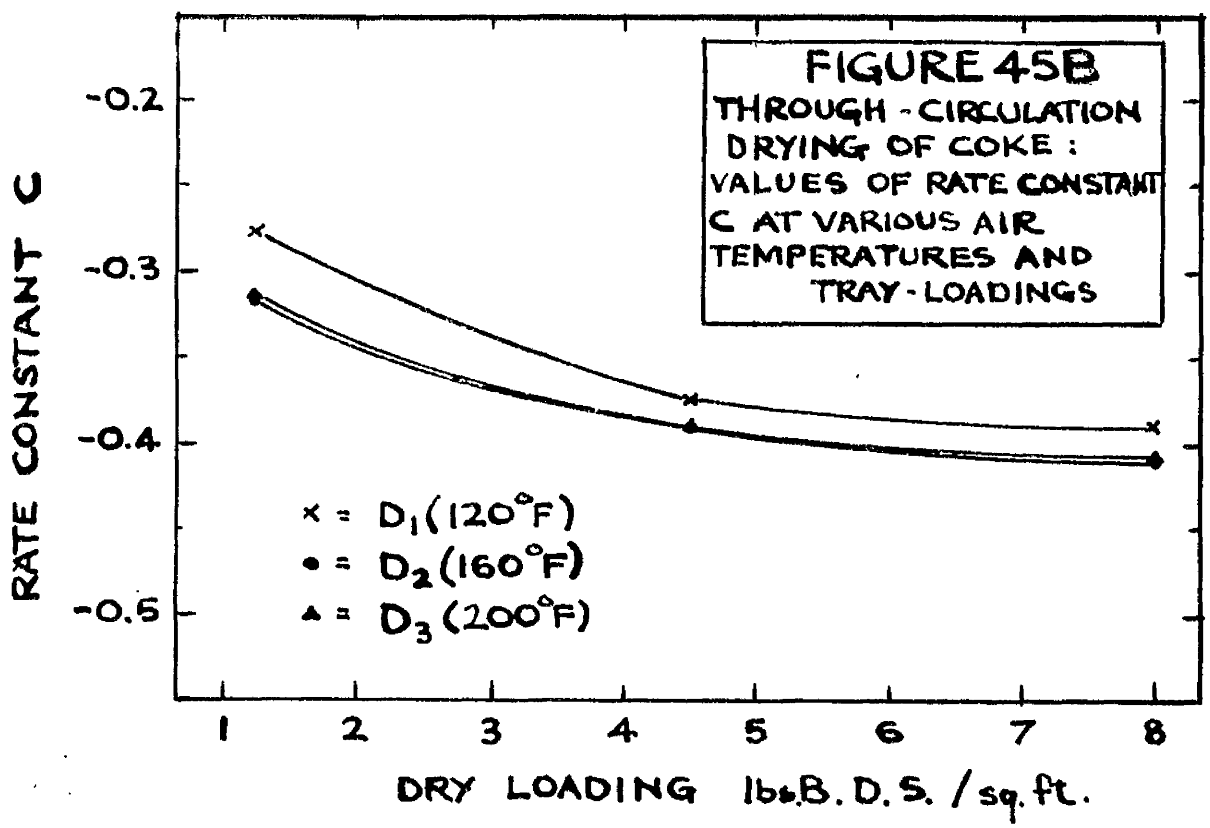

FIGURE 45B
THROUGH - CIRCULATION DRYING OF COKE : VALUES OF RATE CONSTANT C AT VARIOUS AIR TEMPERATURES AND TRAY - LOADINGS

L_1G_1	0.2612	L_2G_1	0.2357	L_3G_1	-0.4908
L_1G_2	0.4148	L_2G_2	0	L_3G_2	-0.2806
L_1G_3	0.5688	L_2G_3	0.1649	L_3G_3	-0.0723

These values are shown graphically in Figure 44B.

Examination of the values of W_e shown in Table 36 indicated that W_e was unaffected by D or W, but decreased with increase in L and decreased slightly with G, thus confirming the results of the preliminary two-level experiment which indicated a significant LG interaction. The values of W_e in Table 36 were therefore averaged over D and W for each level of L and G, giving the following average values of W_e at each level of L and G:

L_1G_1	0.158	L_2G_1	0.142	L_3G_1	0.127
L_1G_2	0.145	L_2G_2	0.133	L_3G_2	0.112
L_1G_3	0.136	L_2G_3	0.131	L_3G_3	0.111

These values are shown graphically in Figure 45A.

Examination of the values of C shown in Table37 indicated that C increased (became more negative) with increase in L, increased with increase in D, and was unaffected by G and W. These results were in agreement with the results of the preliminary two-level factorial experiment. The values of C in Table 37 were subsequently averaged over G and W, giving the following average values of C for the various levels of L and D:

D_1L_1	-0.276	D_2L_1	-0.316	D_3L_1	-0.312
D_1L_2	-0.375	D_2L_2	-0.390	D_3L_2	-0.390
D_1L_3	-0.389	D_2L_3	-0.410	D_3L_3	-0.407

These values are shown graphically in Figure 45B.

10.8 Method Of Predicting The Drying Time Of Coke In The Through-Circulation Drier

The time required to dry the coke from an initial moisture content W_1

to a final moisture content W_2 under any drying conditions within the experimental ranges of D, W, L and G may be predicted from the experimental results given in Section 10.7 in the following manner:

(a) The constant drying rate $\frac{dW}{d\theta}$ is calculated from the equation:

$$\log_{10} \frac{dW}{d\theta} = 0.0212 + f(DW) + f(LG)$$

The values of the correction factors f(DW) and f(LG) are obtained from Figures 44A and 44B.

(b) The critical moisture content W_c for the appropriate values of L and G is obtained from Figure 45A.

(c) The duration of the constant drying rate period in minutes θ_c' (measured from a standard moisture content $W_{st} = 0.271$) is obtained from the equation:

$$\theta_c' = \frac{60\ (0.271 - W_c)}{\frac{dW}{d\theta}}$$

(d) The rate constant C for the appropriate values of L and D is obtained from Figure 45B.

(e) θ_T', the time in minutes required to dry the coke from W_{st} to W_2, is calculated from the equation:

$$\log_{10} \theta_T' = \log_{10} \theta_c' + \frac{W_2 - W_c}{C}$$

(f) θ_1', the drying time of the coke between W_1 and W_{st}, is calculated from the equation:

$$\theta_1' = \frac{60\ (W_1 - 0.271)}{\frac{dW}{d\theta}}$$

θ', the time required to dry the granules from W_1 to W_2, is given by the equation: $\theta' = \theta_T' + \theta_1'$

10.9 Through-Circulation Drying Of Brewers' Spent-Grain

The brewers' spent-grain was prepared for the through-circulation drying tests as described previously in Section 6.9. The levels of D, H, L and G studied in the tests were as follows:

TABLE 38

$D_1 = 130$	$D_2 = 165$	$D_3 = 200$
$H_1 = 0.010$	$H_2 = 0.045$	$H_3 = 0.080$
$G_1 = 4$	$G_2 = 8$	$G_3 = 12$
$L_1 = 0.56$ (1 inch layer)	$L_2 = 1.32$ ($2\frac{1}{2}$ inch layer)	$L_3 = 2.06$ (4 inch layer)

The levels of G studied were the same as those used in the through-circulation drying tests on porous-ceramic granules and coke. The levels of H studied were the same as those used in the cross-circulation drying tests on brewers' spent-grain. Because of the high moisture content of the grain, it was found necessary to use a value of D_1 10°F higher than that used in the through-circulation drying tests on porous-ceramic granules and coke to give reasonably short drying times in the $D_1L_1G_1H_3$ and $D_1L_3G_3H_3$ tests. The range of bed depth studied was approximately the same as that used in the through-circulation drying tests on coke. Since the spent-grain shrank on drying, a minimum bed depth of 1 inch was used in the tests - this being the minimum bed depth of grain which, when dried, could cover the bottom of the test basket evenly. Thinner layers of spent-grain developed holes on drying which resulted in uneven and slower drying due to a proportion of the hot airstream passing through the holes, thus by-passing the main bulk of the material.

10.10 Preliminary Two-Level Factorial Experiment On Brewers' Spent-Grain

Levels 1 and 3 of the four factors D, H, L and G shown in Table 38 were tested in a two-level factorial experiment. Since small day-to-day variations in the drying behaviour of the spent-grain had been noted during the cross-circulation drying tests, each of the sixteen tests in the present experiment was replicated to obtain a better estimate of the experimental error variance than was possible in the simple non-replicated experiments used in the previous Sections. (More precise conclusions may be drawn from an Analysis of Variance based on an improved estimate of the experimental error).

The results of the thirty-two tests involved in this experiment are tabulated in Table 39; the drying curves for the first tests shown in Table 39 in each pair of tests at each value of DHLG are shown in Figures 46, 47, 48 and 49 (the drying curves for the replicate tests are not shown to avoid confusing the Figures). The values of $\frac{dW}{d\theta}$, W_c and C quoted in Table 39 were obtained from the drying curves as described in Section 6.2, the rate constant C again being used to characterize the drying behaviour of the spent-grain in the falling-rate period since the plots of W against log θ' (see Figure 50) were linear from W_c down to W = 0.30. The drying behaviour below this moisture content was somewhat erratic due possibly to uneven drying caused by shrinkage, by channelling, and by movement of the bed of grain caused by vibration during the removal of the test basket from the drier for weighing.

Since no values of W_c and C were obtained in the $D_1H_3L_3G_1$ tests, an Analysis of Variance was possible only on the values of $\log_{10} \frac{dW}{d\theta}$ in Table 39.

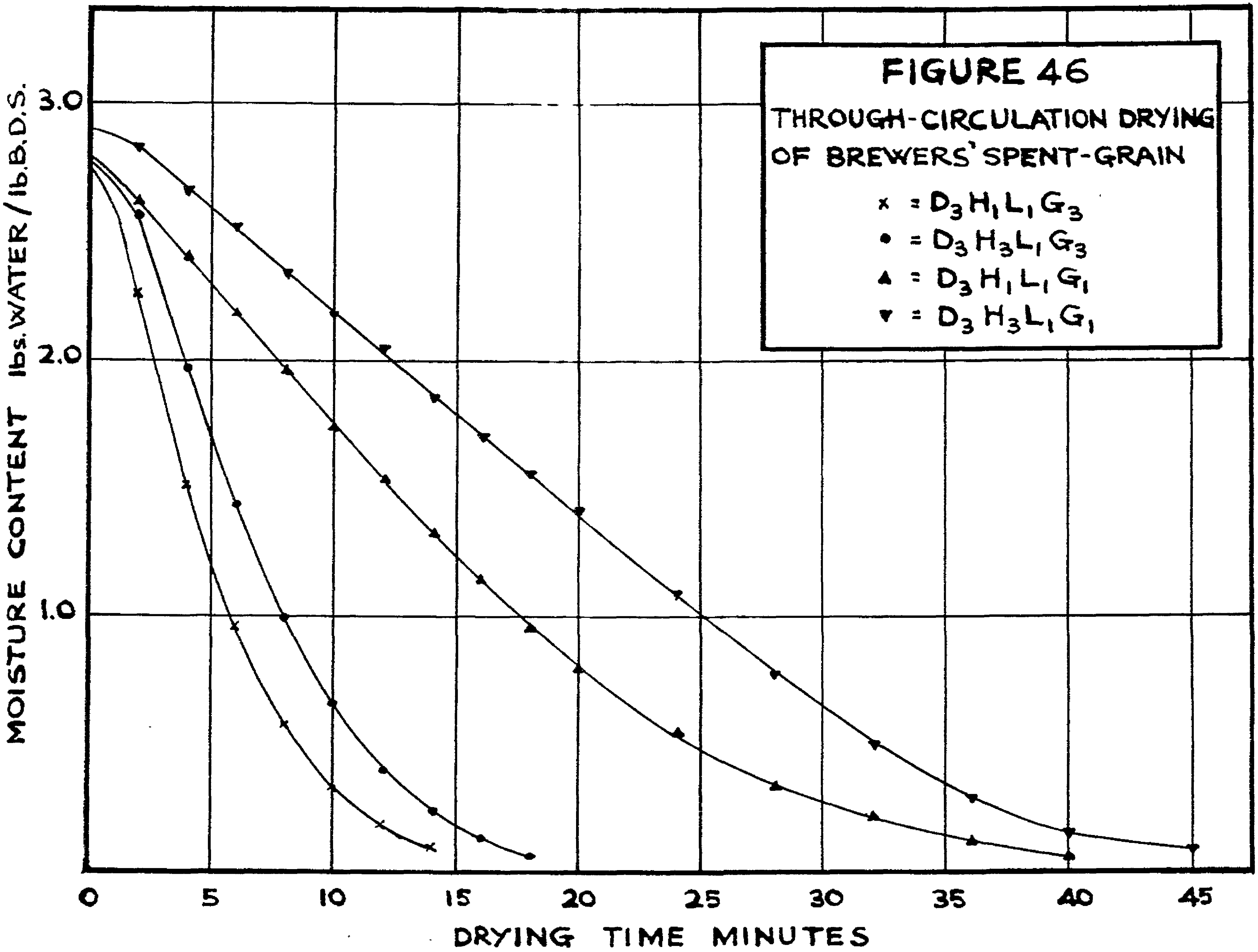
FIGURE 46
THROUGH-CIRCULATION DRYING OF BREWERS' SPENT-GRAIN
× = D3 H1 L1 G3
• = D3 H3 L1 G3
▲ = D3 H1 L1 G1
▼ = D3 H3 L1 G1
MOISTURE CONTENT lbs. WATER / lb. B.D.S.
3.0
2.0
1.0
0
5
10
15
20
25
30
35
40
45
DRYING TIME MINUTES

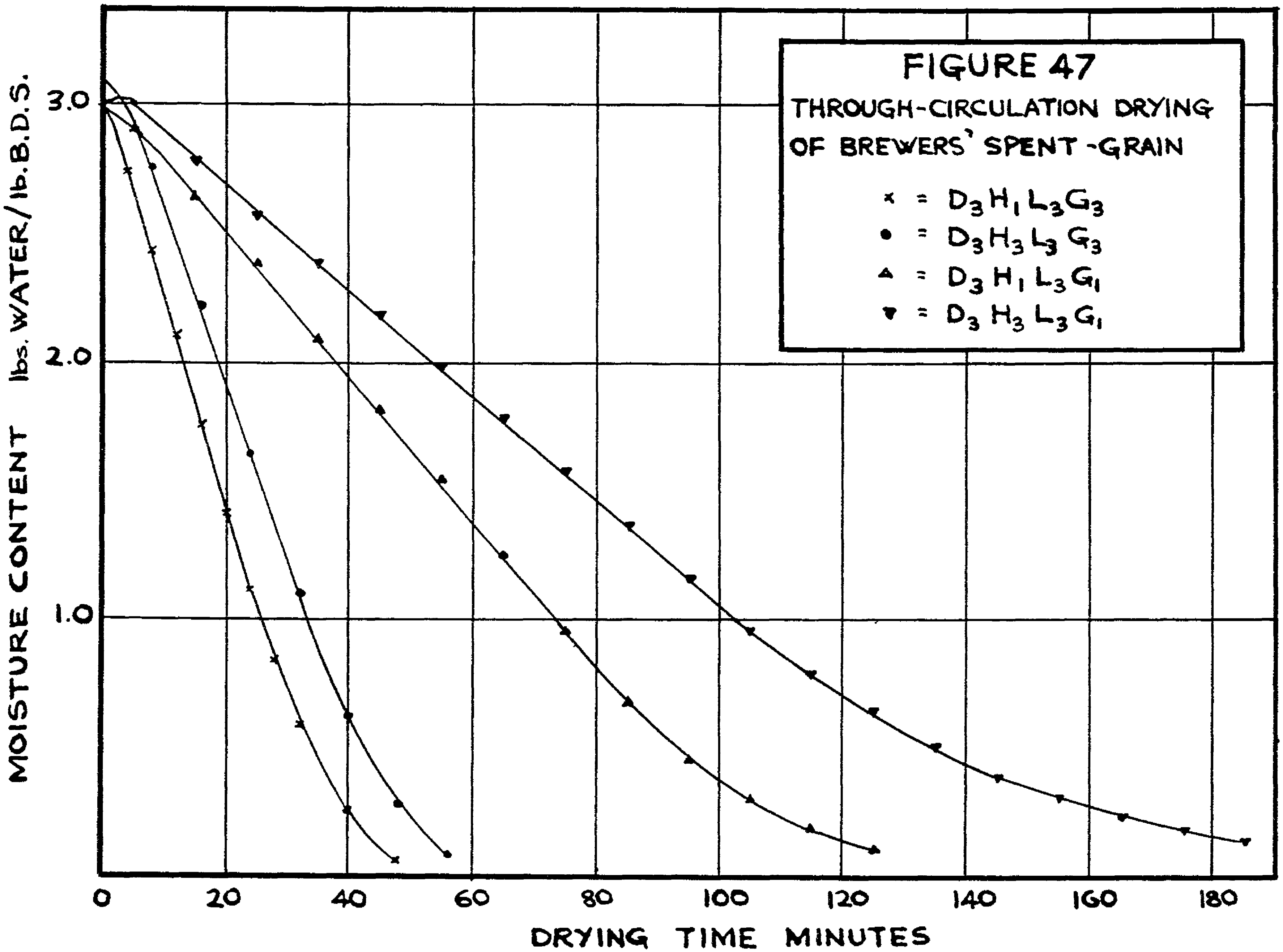
FIGURE 47
THROUGH-CIRCULATION DRYING OF BREWERS' SPENT-GRAIN
× = $D_3 H_1 L_3 G_3$
● = $D_3 H_3 L_3 G_3$
▲ = $D_3 H_1 L_3 G_1$
▼ = $D_3 H_3 L_3 G_1$
MOISTURE CONTENT lbs. WATER/lb. B.D.S.
3.0
2.0
1.0
0
20
40
60
80
100
120
140
160
180
DRYING TIME MINUTES

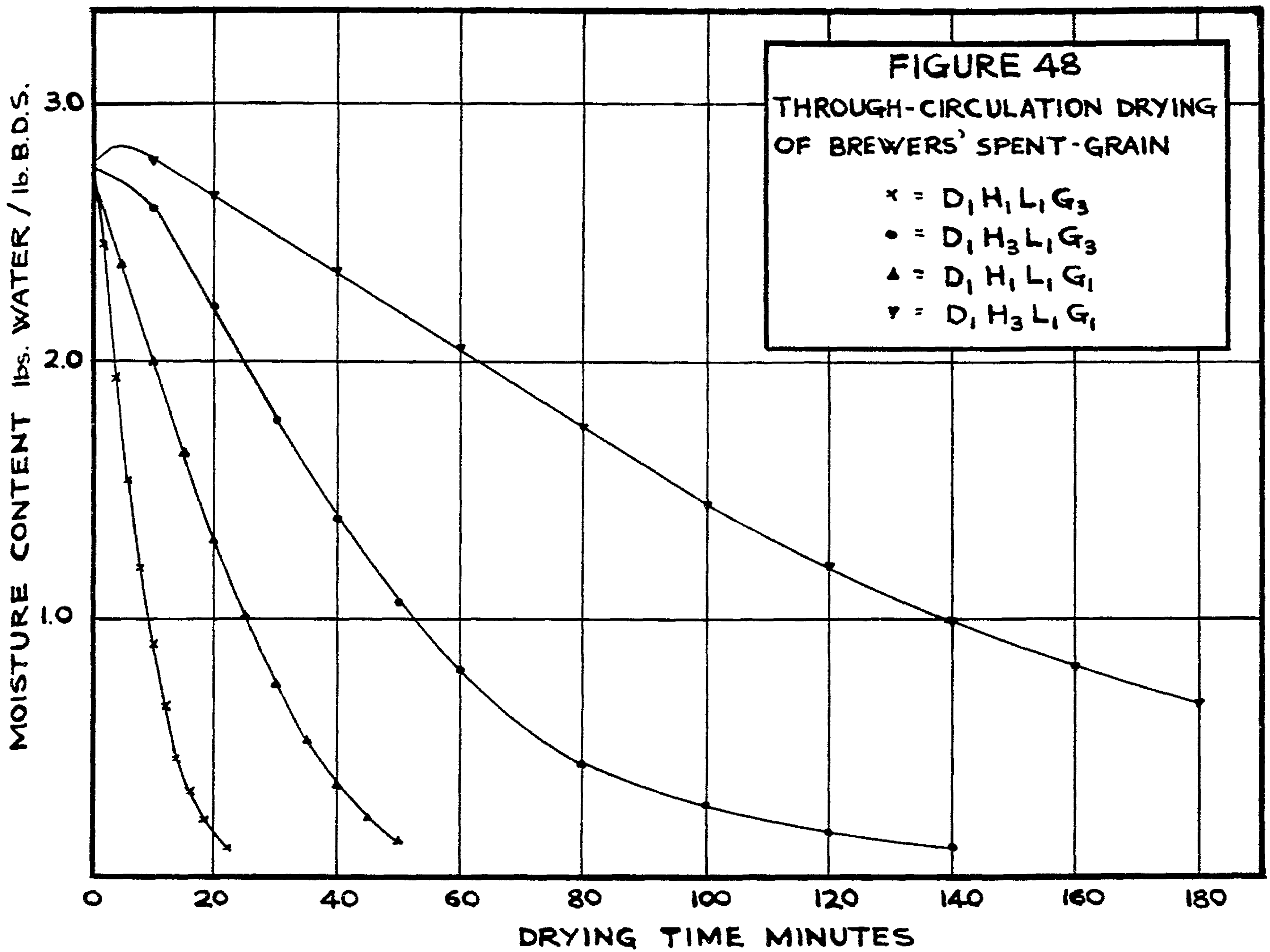
FIGURE 48
THROUGH-CIRCULATION DRYING OF BREWERS' SPENT-GRAIN
x = $D_1 H_1 L_1 G_3$
• = $D_1 H_3 L_1 G_3$
▲ = $D_1 H_1 L_1 G_1$
▼ = $D_1 H_3 L_1 G_1$
MOISTURE CONTENT lbs. WATER / lb. B.D.S.
3.0
2.0
1.0
0
20
40
60
80
100
120
140
160
180
DRYING TIME MINUTES

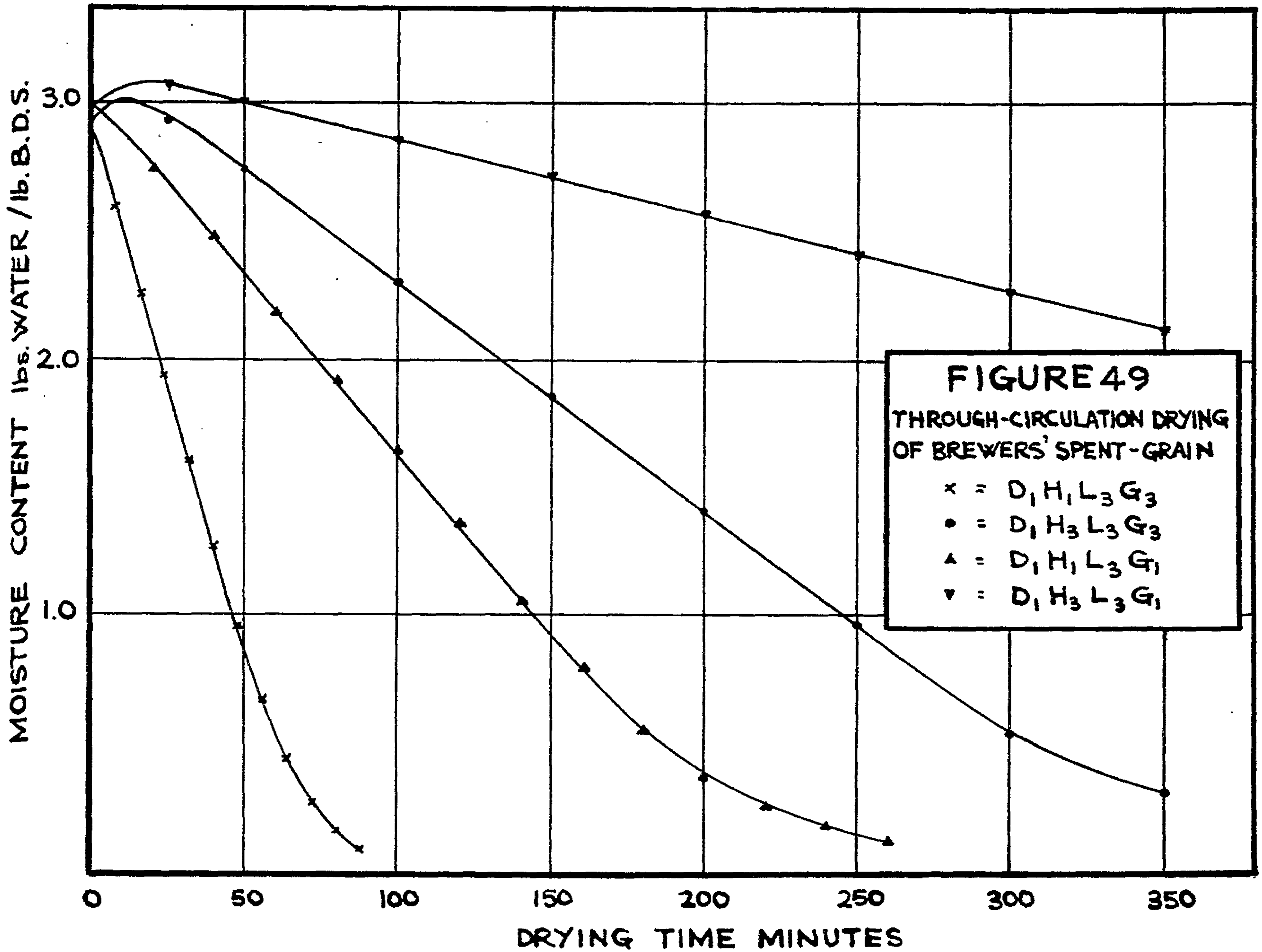
FIGURE 49
THROUGH-CIRCULATION DRYING OF BREWERS' SPENT-GRAIN
× = $D_1 H_1 L_3 G_3$
● = $D_1 H_3 L_3 G_3$
▲ = $D_1 H_1 L_3 G_1$
▼ = $D_1 H_3 L_3 G_1$
MOISTURE CONTENT lbs. WATER / lb. B.D.S.
3.0
2.0
1.0
0
50
100
150
200
250
300
350
DRYING TIME MINUTES

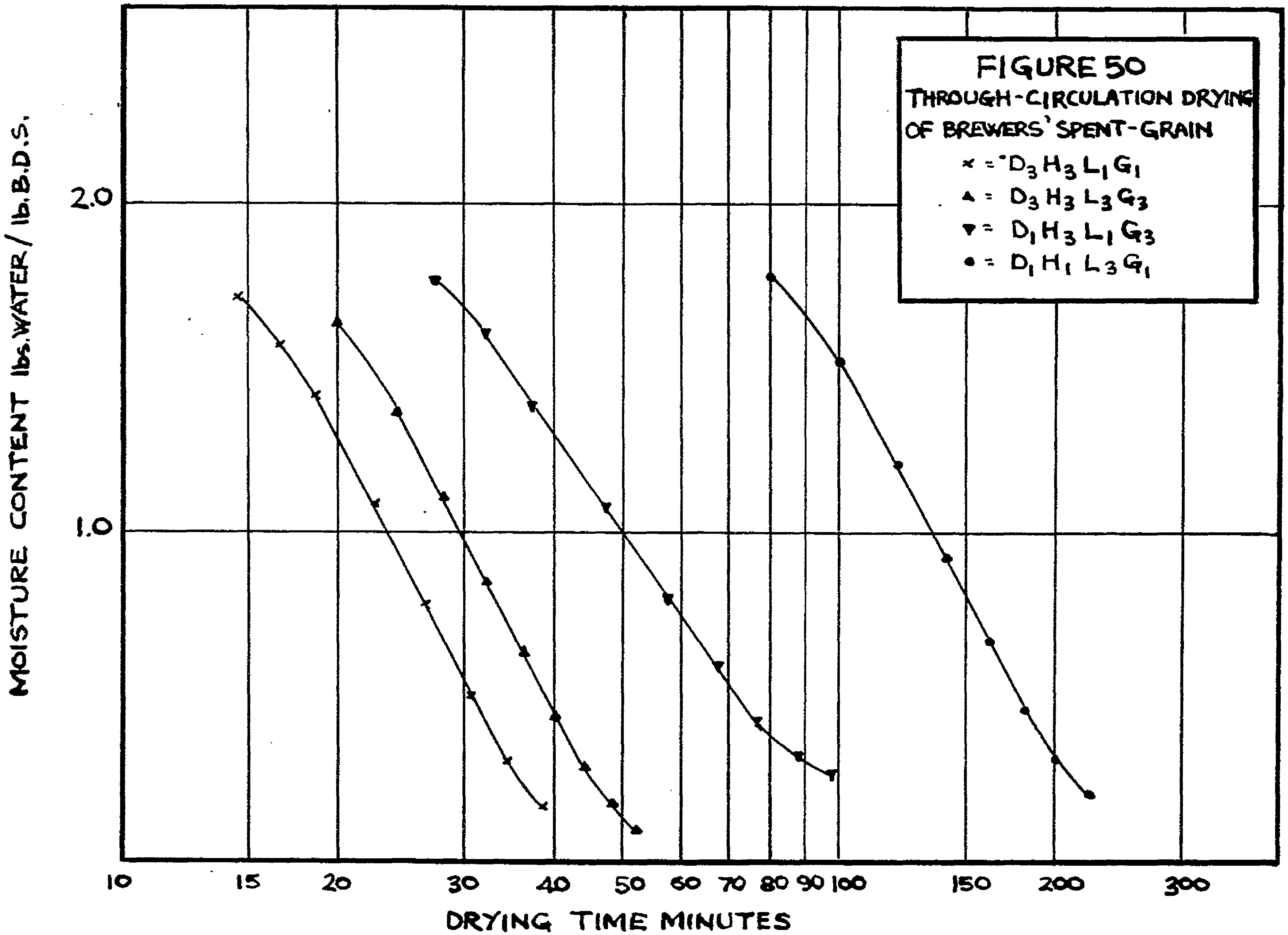
FIGURE 50
THROUGH-CIRCULATION DRYING OF BREWERS' SPENT-GRAIN
× = D3 H3 L1 G1
▲ = D3 H3 L3 G3
▼ = D1 H3 L1 G3
● = D1 H1 L3 G1
MOISTURE CONTENT lbs. WATER / lb. B.D.S.
2.0
1.0
10
15
20
30
40
50
60
70
80
90
100
150
200
300
DRYING TIME MINUTES

TABLE 39: Results Of Preliminary Replicated Two-Level Factorial Experiment On Brewers' Spent-Grain

Test Conditions	$\frac{dW}{d\theta}$	$\log_{10} \frac{dW}{d\theta}$	W_c	C
$D_1H_1L_1G_1$	4.26	0.6294	1.42	-3.37
	3.88	0.5888	1.51	-3.30
$D_1H_3L_1G_1$	0.88	-0.0555	1.75	-3.10
	0.89	-0.0506	1.58	-2.95
$D_1H_1L_1G_3$	11.75	1.0701	1.55	-3.35
	11.73	1.0694	1.50	-3.15
$D_1H_3L_1G_3$	2.45	0.3892	1.60	-3.15
	2.38	0.3766	1.50	-3.04
$D_3H_1L_1G_1$	6.00	0.7782	1.61	-2.80
	6.56	0.8169	1.49	-3.64
$D_3H_3L_1G_1$	6.54	0.8156	1.70	-3.29
	4.80	0.6812	1.55	-3.51
$D_3H_1L_1G_3$	22.00	1.3424	1.50	-3.86
	22.10	1.3444	1.46	-2.91
$D_3H_3L_1G_3$	18.55	1.2684	1.36	-3.68
	17.25	1.2368	1.54	-3.05
$D_1H_1L_3G_1$	0.82	-0.0862	0.85	-4.23
	0.77	-0.1135	1.01	-4.15
$D_1H_3L_3G_1$	0.16	-0.7959	-	-
	0.18	-0.7447	-	-
$D_1H_1L_3G_3$	2.54	0.4048	1.32	-3.88
	2.52	0.4014	1.13	-4.26
$D_1H_3L_3G_3$	0.53	-0.2757	1.15	-3.48
	0.58	-0.2366	0.85	-4.30
$D_3H_1L_3G_1$	1.48	0.1703	0.88	-4.31
	1.75	0.2430	0.95	-4.61
$D_3H_3L_3G_1$	1.14	0.0569	0.90	-3.87
	1.22	0.0864	0.89	-4.00
$D_3H_1L_3G_3$	4.94	0.6937	1.04	-3.51
	4.93	0.6928	1.29	-3.66
$D_3H_3L_3G_3$	4.15	0.6180	1.04	-4.29
	3.81	0.5809	0.75	-4.39

This Analysis was conducted by a procedure similar to that described in Appendix 2; because of the replication of tests in the present experiment, the Sum of Squares corresponding to the LDGH interaction could be calculated and the Residual Sum of Squares had 16 degrees of freedom. (Note: The values of F used to test the significance of the various main effects and interactions, were the quotient of the Mean Squares corresponding to the various main effects or interactions divided by the Residual Mean Squares). The results of the Analysis of Variance are shown in Table 40, main effects and interactions significant at the 5% probability level being marked *

TABLE 40: Analysis of Variance Of Values Of $\log_{10} \frac{dW}{d\theta}$ Obtained In The Two-Level Factorial Experiment On Brewers' Spent-Grain

Source of Variance	Degrees of Freedom	Sum of Squares	Mean Squares
L	1	3.5150273	3.5150273 *
D	1	2.4502892	2.4502892
G	1	1.9782097	1.9782097 *
H	1	1.1608690	1.1608690
LD	1	0.0032381	0.0032381
GH	1	0.0000242	0.0000242
LH	1	0.0006045	0.0006045
DH	1	0.6669835	0.6669835 *
DG	1	0.0028407	0.0028407
LG	1	0.0008999	0.0008999
GDH	1	0.0000209	0.0000209
LDG	1	0.0030478	0.0030478
GLH	1	0.0017629	0.0027629
LDH	1	0.0014622	0.0014622
LGHD	1	0.0002759	0.0002759
Residual	16	0.0174176	0.0010886
Total	31	9.8029734	-

The Analysis of Variance showed that the G and L main effects and the DH interaction were significant; $\frac{dW}{d\theta}$ may therefore be expressed by a relationship of the form:

$$\log_{10} \frac{dW}{d\theta} = f(DH) + f(G) + f(L).$$

Although no Analyses of Variance were possible for the W_e and C results, examination of the values of these variables in Table 39 indicated the following points

(a) W_e appears to be independent of D, H and G but decreases with increase in L.

(b) C appears to be independent of G and H but increases (becomes more negative) with increase in L and increases slightly with increase in D.

10.11 Fractional Three-Level Factorial Experiment On Brewers' Spent-Grain

The fractional three-level factorial experiment, used to verify the results of the preliminary two-level factorial experiment, involved the forty-five tests shown in Table 41. Of these forty-five tests, the twenty-nine tests in excess of the sixteen replicated tests studied in the two-level experiment were not replicated, except the standard test $D_2H_2L_2G_2$ which was replicated three times. The enlarged experiment was designed to provide detailed data on the values of f(DH), f(G) and f(L) in the relationship $\log_{10} \frac{dW}{d\theta} = f(DH) + f(G) + f(L)$, and to examine more fully the effect of L on W_e, and the effects of D and L on the rate constant C.

To facilitate the prediction of the constant drying rate $\frac{dW}{d\theta}$ under any conditions within the experimental ranges of D, H, L and G,

TABLE 41: Values of $\frac{dW}{d\theta}$ for brewers' spent-grain dried in the through-circulation drier

	L_1G_1	L_1G_2	L_1G_3	L_2G_1	L_2G_2	L_2G_3	L_3G_1	L_3G_2	L_3G_3
D_1M_1	4.07		11.74		2.88		0.80		2.53
D_1M_2		4.12			1.56	2.60		0.77	
D_1M_3	0.89		2.42		0.61		0.17		0.56
D_2M_1				1.63	4.00	6.44		2.16	
D_2M_2	4.20	9.24	13.56	1.37	3.12	5.26	0.78	1.65	2.79
D_2M_3		7.39		1.05	2.50	3.95			
D_3M_1	6.28		22.05		5.34		1.62		4.94
D_3M_2		15.97		1.87	5.04			2.88	
D_3M_3	5.67		17.90		4.44		1.18		3.98

TABLE 42: Values of $\log_{10}\frac{dW}{d\theta}$ for brewers' spent-grain dried in the through-circulation drier

	L_1G_1	L_1G_2	L_1G_3	L_2G_1	L_2G_2	L_2G_3	L_3G_1	L_3G_2	L_3G_3
D_1M_1	0.6091		1.0698		0.4594		-0.0999		0.4031
D_1M_2		0.6149			0.1931	0.4150		-0.1135	
D_1M_3	-0.0531		0.3829		-0.2147		-0.7703		-0.2562
D_2M_1				0.2122	0.6021	0.8089		0.3345	
D_2M_2	0.6232	0.9657	1.1323	0.1367	0.4944	0.7210	-0.1079	0.2175	0.4456
D_2M_3		0.8686		0.0212	0.3978	0.5977			
D_3M_1	0.7976		1.3434		0.7275		0.2067		0.6933
D_3M_2		1.2033		0.2718	0.7024			0.4594	
D_3M_3	0.7484		1.2526		0.6474		0.0717		0.5995

TABLE 43. Values of W_e for brewers' spent-grain dried in the through-circulation drier

	L_1G_1	L_1G_2	L_1G_3	L_2G_1	L_2G_2	L_2G_3	L_3G_1	L_3G_2	L_3G_3
D_1H_1	1.47		1.53		1.16		0.93		1.23
D_1H_2		1.42			0.92	1.04		0.85	
D_1H_3	1.58		1.55		0.90		——		1.00
D_2H_1				1.19	0.92	1.00		0.73	
D_2H_2	1.30	1.39	1.65	0.81	0.95	0.85	0.90	0.84	1.04
D_2H_3		1.50		1.25	0.88	1.05			
D_3H_1	1.38		1.48		1.32		0.92		1.17
D_3H_2		1.56		1.15	0.88			1.00	
D_3H_3	1.63		1.45		1.06		0.90		0.89

TABLE 44: Values of Rate Constant C for brewers' spent-grain dried in the through-circulation drier

	L_1G_1	L_1G_2	L_1G_3	L_2G_1	L_2G_2	L_2G_3	L_3G_1	L_3G_2	L_3G_3
D_1H_1	-3.34		-3.25		-3.47		-4.19		-4.07
D_1H_2		-3.37			-3.75	-3.62		-3.60	
D_1H_3	-3.08		-3.10		-4.20		——		-3.89
D_2H_1				-4.30	-4.15	-4.15		-4.37	
D_2H_2	-3.40	-3.45	-3.46	-4.18	-4.24	-4.40	-4.15	-4.41	-3.83
D_2H_3		-3.35		-3.90	-3.69	-4.30			
D_3H_1	-3.22		-3.38		-4.12		-4.46		-3.59
D_3H_2		-3.15		-3.54	-3.75			-4.15	
D_3H_3	-3.40		-3.37		-3.78		-3.94		-4.34

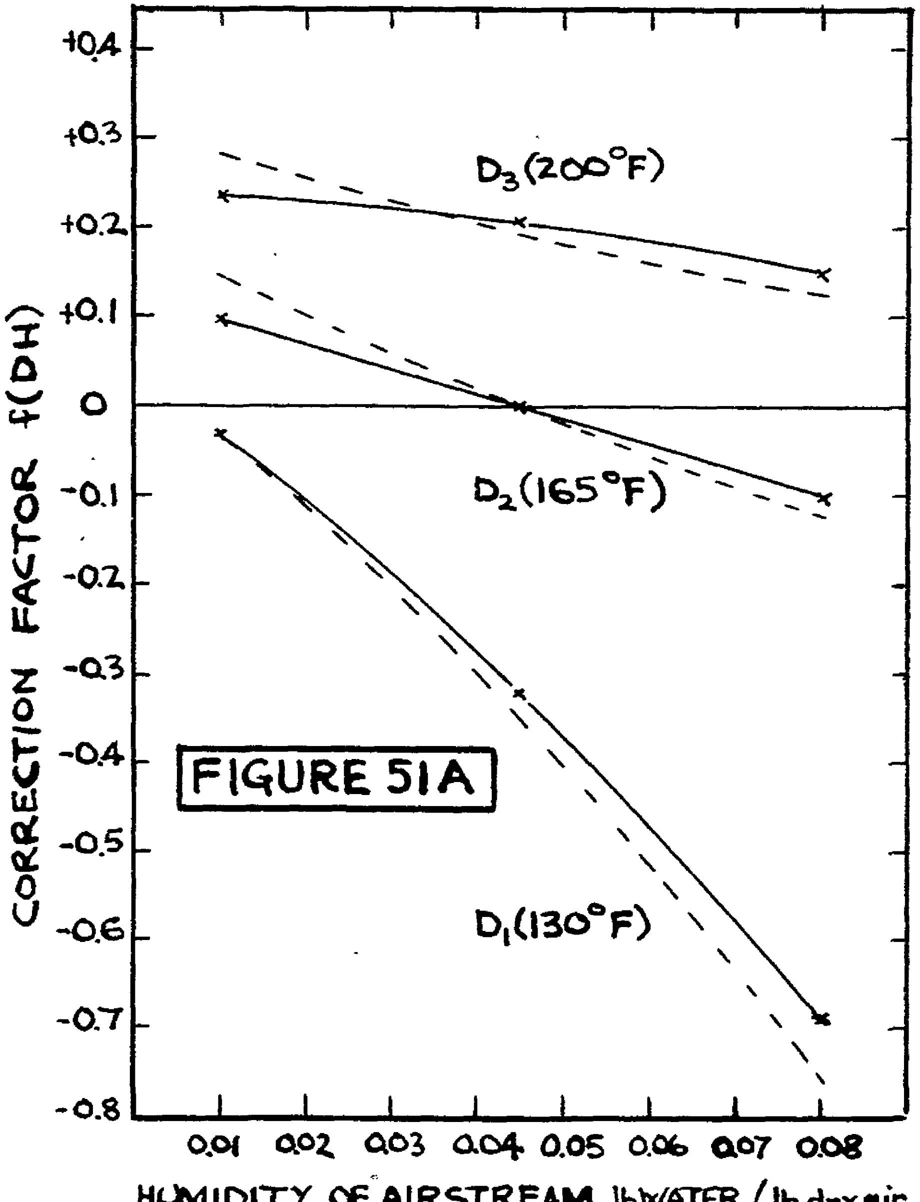

FIGURE 51A

NOTE: THE DOTTED LINES IN FIGURES 51A, B AND C INDICATE THE DRYING BEHAVIOUR PREDICTED FROM DRYING THEORY.

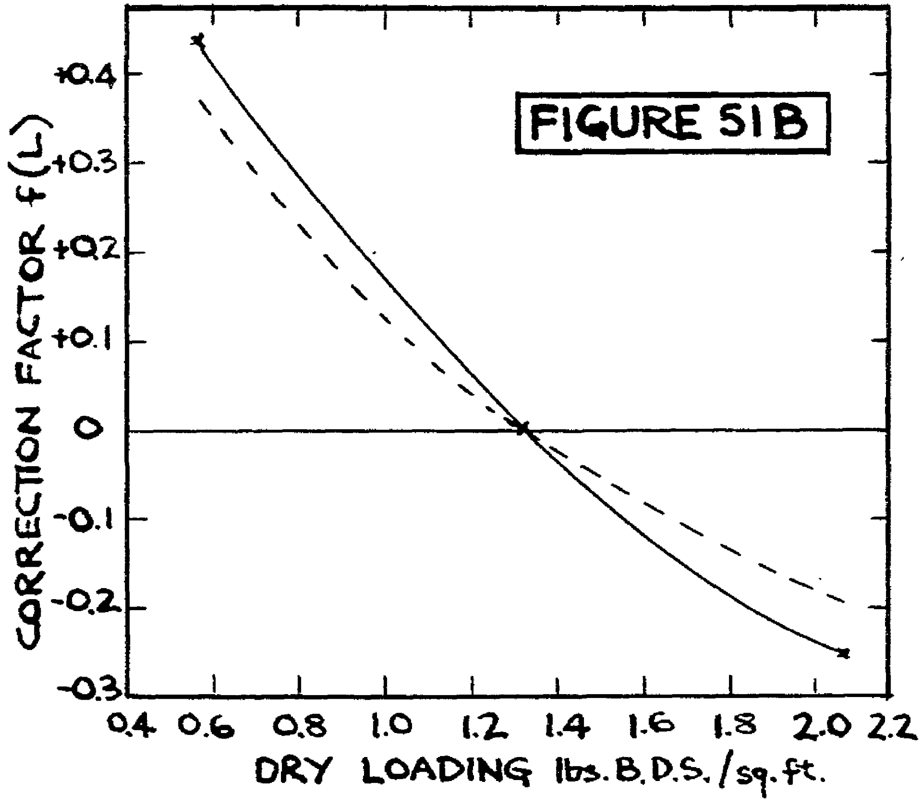

FIGURE 51B

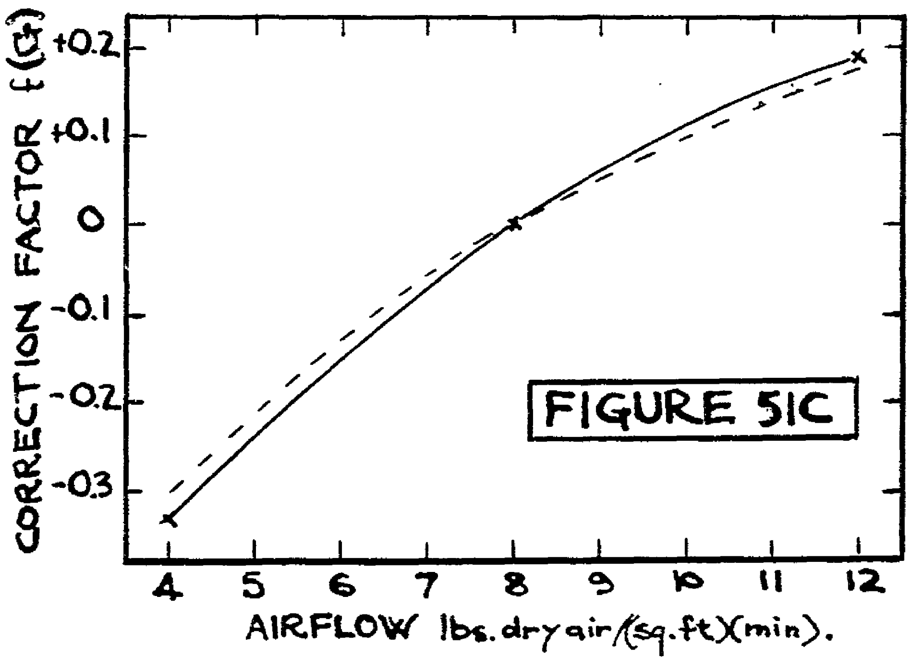

FIGURE 51C

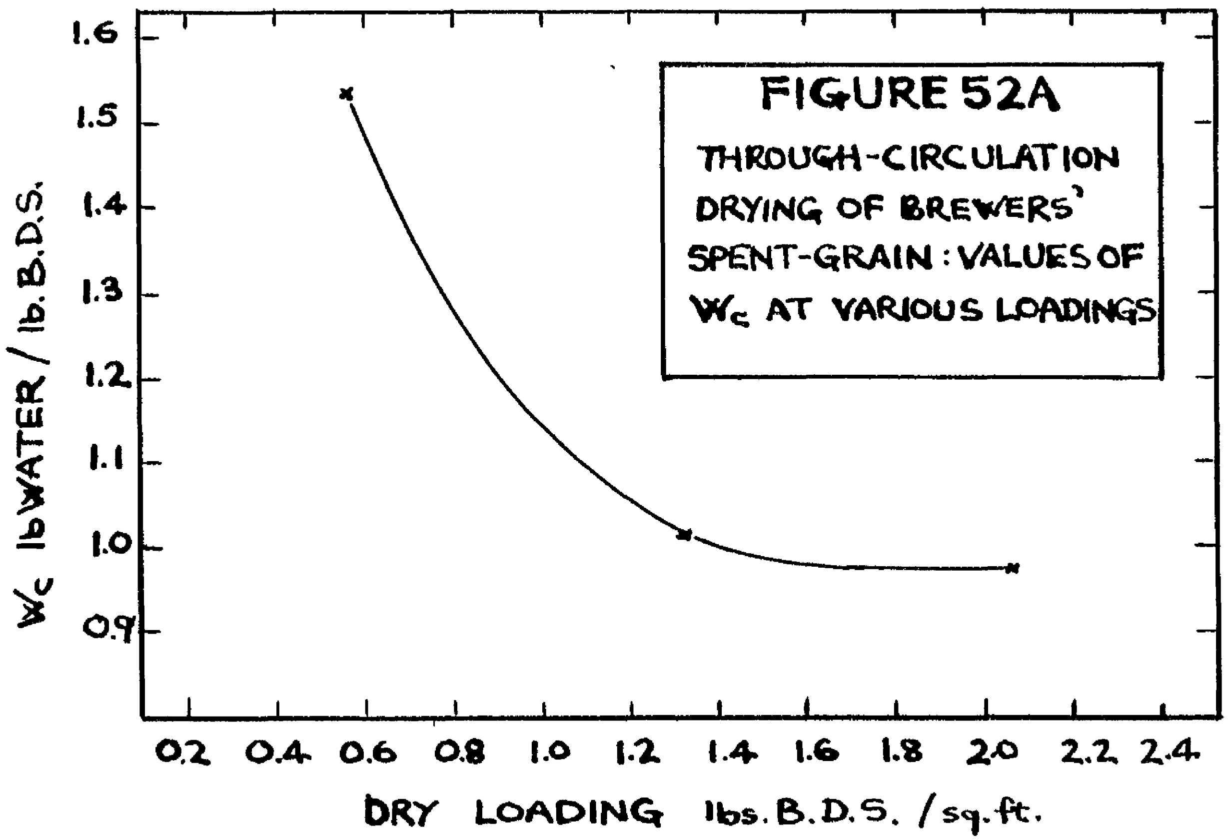

FIGURE 52A
THROUGH-CIRCULATION DRYING OF BREWERS' SPENT-GRAIN : VALUES OF W_c AT VARIOUS LOADINGS

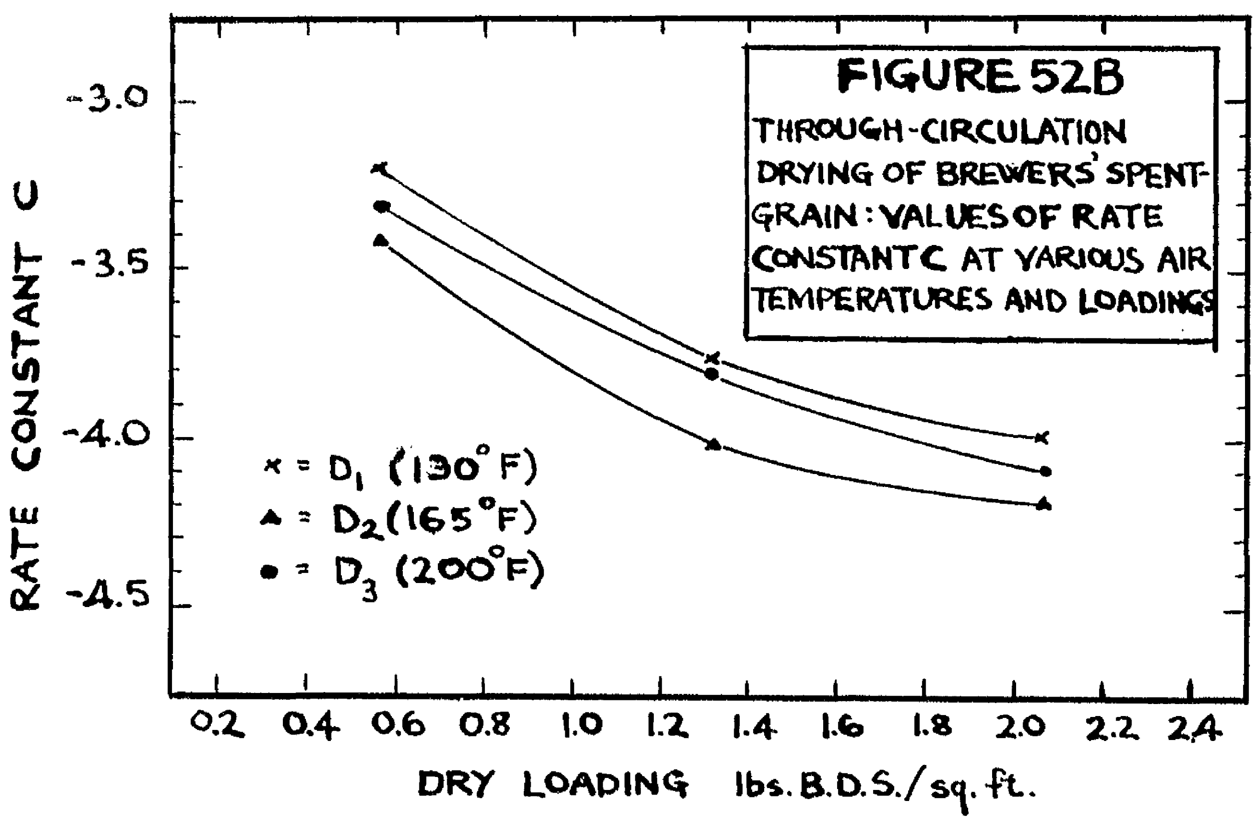

FIGURE 52B
THROUGH-CIRCULATION DRYING OF BREWERS' SPENT-GRAIN : VALUES OF RATE CONSTANT C AT VARIOUS AIR TEMPERATURES AND LOADINGS

the experimental values of $\frac{dW}{d\Theta}$ shown in Table 41 were converted to $\log_{10} \frac{dW}{d\Theta}$ (see Table 42) and the value of $\log_{10} \frac{dW}{d\Theta}$ obtained for each test was compared with the average value of $\log_{10} \frac{dW}{d\Theta}$ obtained in the standard test $D_2H_2L_2G_2$ (0.4944). $\frac{dW}{d\Theta}$ could then be derived from the expression:

$$\log_{10} \frac{dW}{d\Theta} = 0.4944 + f(DH) + f(G) + f(L)$$

The value of the correction factor f(DH) for each level of D and H was obtained from the values in Table 42 as the average difference between tests in each DH row and the D_2H_2 tests in the corresponding LG columns. The average values of f(DH) obtained were:

D_1H_1	-0.0324	D_2H_1	0.0970	D_3H_1	0.2356
D_1H_2	-0.3223	D_2H_2	0	D_3H_2	0.2057
D_1H_3	-0.6998	D_2H_3	-0.1081	D_3H_3	0.1464

These values are shown graphically in Figure 51A.

The values of the correction factor f(L) were obtained from the values of $\log_{10} \frac{dW}{d\Theta}$ in Table 42 by dividing the average difference between values in the L_1 and L_3 columns at corresponding levels of DH and G in the proportions: average difference between values in the L_1 and L_2 columns at corresponding levels of D, H and G to the average difference between values in the L_2 and L_3 columns at corresponding values of D, H and G. The values of f(L) obtained in this way were:

$$L_1 = 0.4343, \ L_2 = 0, \ L_3 = -0.2535$$

These values are shown graphically in Figure 51B.

Note: f(L) was evaluated more accurately by proportioning the average L_1 to L_3 difference as described above than by using the average L_1 to

L_2 and L_2 to L_3 differences directly, since the L_1 to L_3 difference was estimated from 13 pairs of tests while the L_1 to L_2 and L_2 to L_3 differences were each estimated from only 4 pairs of tests.

The values of f(G) were obtained from the values of $\log_{10} \frac{dW}{d\theta}$ in the Table 42 in a similar manner, by proportioning the average difference between values in the G_1 and G_3 columns at corresponding values of L, D and H in the ratio: average difference between values in the G_1 and G_2 columns, to the average difference between values in the G_2 and G_3 columns - all differences being measured between tests done at similar levels of D, H and L. The values of f(G) obtained in this way were:

$$G_1 = -0.3348 \qquad G_2 = 0 \qquad G_3 = 0.1882$$

These values are shown graphically in Figure 51C.

Examination of the values of W_e in Table 43 indicated that W_e was unaffected by D, H or G but decreased with increase in L, thus confirming the results of the preliminary two-level experiment. The values of W_e in Table 43 were therefore averaged over D, H and G, giving the following values of W_e for each level of L:

$$L_1 \;\; 1.53 \qquad L_2 \;\; 1.01 \qquad L_3 \;\; 0.97$$

These values are shown graphically in Figure 52A.

From an inspection of the values of C in Table 44 it was apparent that G and H had no effect on C; an increase in D from D_1 to D_2 caused a slight increase in C (C became more negative), but an increase in D from D_2 to D_3 caused no appreciable further change in C; an increase in L caused an increase in C. The values of C in Table 44 were averaged over G and H, giving the following average values of C at various levels of L and D:

D_1L_1	-3.20	D_1L_2	-3.76	D_1L_3	-3.99
D_2L_1	-3.42	D_2L_2	-4.02	D_2L_3	-4.19
D_3L_1	-3.32	D_3L_2	-3.80	D_3L_3	-4.09

These values are shown graphically in Figure 52B.

10.12 Method Of Predicting The Drying Time Of Brewers' Spent-Grain In The Through-Circulation Drier

The time required to dry the brewers' spent-grain from an initial moisture content W_1 to a final moisture content W_2 under any drying conditions within the experimental ranges of D, H, G and L may be predicted in the following manner from the experimental results presented in Section 10.11.

(a) The constant drying rate $\frac{dW}{d\theta}$ for the appropriate values of D, H, L and G is calculated from the equation:

$$\log_{10} \frac{dW}{d\theta} = 0.4944 + f(DH) + f(L) + f(G)$$

The values of the correction factors f(DH), f(L) and f(G) are obtained frome Figures 51A, 51B and 51C.

(b) The critical moisture content W_c for the appropriate value of L is obtained from Figure 52A.

(c) The duration of the constant drying rate period in minutes θ_c' (measured from a standard initial moisture content $W_{st} = 2.56$) is obtained from the equation:

$$\theta_c' = \frac{60(2.56 - W_c)}{\frac{dW}{d\theta}}$$

(d) The rate constant C for the appropriate values of L and D is obtained from Figure 52B.

(e) Θ_T', the time in minutes required to dry the spent-grain from W_{st} to W_2, is calculated from the equation:

$$\log_{10} \Theta_T' = \log_{10} \Theta_c' + \frac{W_2 - W_c}{C}$$

(f) Θ_1', the drying time of the spent-grain between W_1 and W_{st}, is calculated from the equation:

$$\Theta_1' = \frac{60(W_1 - 2.56)}{\frac{dW}{d\Theta}}$$

Θ', the drying time of the spent-grain from W_1 to W_2, is given by the equation:

$$\Theta' = \Theta_T' + \Theta_1'$$

10.13 Discussion Of Through-Circulation Drying Results

Constant Drying Rate Results

The values of the various correction factors shown in Figures 37A, 37B, 44A, 44B, 51A, 51B and 51C, which summarized the experimentally observed constant drying rates for the porous-ceramic granules, coke and brewers' spent-grain, were compared with theoretical values of the correction factors derived as in Section 6.13.

Porous-Ceramic Granules and Coke

From Figures 37A and 44A it can be seen that the experimental values of f(DW) for the porous-ceramic granules and coke agreed closely with the theoretical values of f(DW) - shown as dotted lines on the Figures. This indicates that the effect of air temperature and humidity on $\frac{dW}{d\theta}$ can be predicted satisfactorily from the approach air temperature and humidity, and that it is unnecessarily complicated to use for this purpose, equations, such as Equations 17 and 20, containing a logarithmic mean humidity driving force term $(\Delta H)_m$. Indeed, without a knowledge of $\frac{dW}{d\theta}$ under the desired drying conditions, the humidity of the airstream leaving the material, which must be known before $(\Delta H)_m$ can be evaluated, cannot readily be calculated. It is simpler and probably more accurate to use empirical functions of L and G, such as f(LG), f(L) and f(G) used in the present investigation, to estimate the effect on $\frac{dW}{d\theta}$ of the increase in humidity of the airstream as it passes through a bed of material.

As a result of this increase in humidity of the airstream as it passes through the material, there were fairly wide discrepancies between the experimental values of f(LG) shown in Figures 37B and 44B and the theoretical values of f(LG) (shown in Figures 37B and 44B as dotted lines) ; moreover, the gradual divergence with increase in L of the f(LG) lines for the various levels of G indicated that the effect of airflow on the drying rate increased with increase in tray-loading. If there had been no interaction between the effects of G and L on the drying rate these lines would all have had a similar curvature.

Brewers' Spent-Grain

From Figure 51A it can be seen that the experimental values of f(DH) were close to the theoretical values. This indicated that, as was found for the porous-ceramic granules and the coke, it was unnecessary to use a $(\Delta H)_m$ term to predict the effect of air temperature and humidity on the constant drying rate of the brewers' spent-grain.

Comparison of the experimental values of the empirical functions f(G) and f(L) in Figures 51B and 51C with theoretical values calculated from Equations D and E indicated that the experimental values of f(G) agreed closely with the theoretical values, and the experimental values of f(L) were higher at L_1 and lower at L_3 than the theoretical values of f(L). The experimental values of f(L), which allowed for the decrease in the drying power of the airstream as it picked up moisture in passing through the grain, were found to agree with values of f(L) given by the empirical equation $f(L) = 1.25\ (\log_{10} L_2 - \log_{10} L)$.

It was found that the constant drying rate of the spent-grain could be estimated within ± 25% of the experimental values by using the empirical equation:

$$\frac{dW}{d\theta} = \frac{0.0103G\ (D - W)}{L^{1.25}} \qquad \ldots \quad \text{Equation F.}$$

Critical Moisture Contents

From Figure 38A it can be seen that the W_c values for the porous-ceramic granules were virtually independent of the drying conditions used.

Figure 45A shows that the W_c values for the coke were independent of the air temperature and humidity but decreased with increase in tray-loading and decreased with increase in airflow. The decrease in W_c with increase in loading is in agreement with the postulate (57) of a zone of vaporization passing through the bed of coke, since at higher loadings greater amounts of dry coke would be below the vaporization zone when it reached the top of the bed. While the fact that the total amount of moisture left in the bed at W_c increased with increase in L would appear to imply that the vaporization zone was broader in the deeper beds, it is possible that the greater amounts of moisture left in the deeper beds were a result of a greater degree of uneven drying. The higher values of W_c obtained at airflows of G = 4 were possibly also due to greater unevenness of drying caused by poor air contact at this low airflow.

Figure 52A shows that W_c values for the brewers' spent-grain were independent of the airflow, air temperature and humidity, but decreased with increase in loading.

The fact that the values of W_c for the various materials dried by a through-circulation airstream remained constant or decreased with increase in tray-loading, illustrates the advantage of this method for drying deep beds of material over the cross-circulation method, for which the values of W_c increased markedly with increase in loading (see Figures 13B, 20A and 27A).

Rate Constant C

It was found that the rate constant C could be used to describe the falling-rate drying curves of all three materials tested in the through-circulation drier.

Figure 38B shows that the values of C for the porous-ceramic granules were independent of air temperature and humidity; but the values of C increased slightly (became more negative) with increase in loading and increased slightly with decrease in airflow - the effect of airflow increased as loading increased. Figure 45B shows that the values of C for coke were independent of airflow and air humidity but increased with increase in loading and increased slightly with increase in air temperature. Similar variations in C with changes in the operating conditions were found for the brewers' spent-grain (see Figure 52B).

The greatest difference between the effects of the operating conditions on the values of C obtained in the through-circulation drying tests and on the values of C obtained in the cross-circulation drying tests (see Figures 13A, 20B and 27B) was the increase in C with loading in the through-circulation drying tests as opposed to the decrease in C with increase in loading in the cross-circulation drying tests. These results illustrate the advantage of using a through-circulation drier for drying deep beds of material since in this type of drier the falling-rate period does not increase greatly with increase in loading as in the cross-circulation drier.

Accuracy Of Proposed Method Of Predicting Drying Times

Examples are given in Table 44A of the application of the prediction methods described in Sections 10.4, 10.8 and 10.12 to the prediction of the drying times of the porous-ceramic granules, coke and brewers' spent-grain in the through-circulation drier. The prediction accuracy of ± 10% obtained is almost the same as the experimental error in determining the drying times of the porous-ceramic granules and the coke from an initial moisture content of 0.27 to a final moisture content 0.05 in the standard $D_2W_2L_2G_2$ tests, and in determining the drying time of the brewers' spent-grain from a moisture content 2.56 to a moisture content 0.50 in the $D_2H_2L_2G_2$ test – ± 4% for the porous-ceramic granules, ± 7% for the coke, ± 11% for the brewers' spent-grain.

An indication of the probable accuracy with which drying times may be estimated from the results of the classical experiment described in Section 6.13 is given in Table 44A. The predicted drying times quoted for the classical experiment were calculated from the prediction methods described in Sections 10.4, 10.8 and 10.12 using values of f(DW) calculated from the theoretical Equation B, and values of f(LG), W_c and C obtained in the factorial experiment (extrapolated when necessary as described in Section 6.13). It is probable that the ± 16% prediction accuracy obtainable by the above method is higher than would be obtained in practice from the results of the classical experiment, since in this experiment the values of f(LG), W_c and C would be determined with a lower precision than in the factorial experiment.

TABLE 44A: Comparison Of The Accuracy With Which The Drying Times Of Various Materials In The Through-Circulation Drier Can Be Predicted From The Results Of A Classical And A Factorial Experiment.

Material	Drying Conditions				Moisture Content		Drying Time Mins.			% Error	
	D	W	L	G	W_1	W_2	Fact.	Class.	Expt.	Fact.	Class
Porous-	200	110	8.18	4	0.27	0.07	27.0	25.5	27.0	0	-12.9
Ceramic	160	95	5.12	6	0.28	0.06	27.4	24.7	28.6	-4.2	-13.6
Granules	150	100	6.17	10	0.27	0.04	21.3	20.6	20.2	+5.3	+2.0
	120	110	2.06	4	0.29	0.05	98	102	91	+7.7	+12.1
	120	110	8.14	12	0.29	0.05	118	113	117	+0.8	-3.4
Coke	200	94	7.97	4	0.26	0.06	22.3	20.0	23.4	-4.7	-14.5
	180	105	7.31	6	0.28	0.07	19.8	19.2	21.5	-7.9	-10.7
	160	110	1.64	5	0.26	0.05	7.9	9.4	8.1	-2.5	+16.0
	140	103	6.45	10	0.25	0.06	33.4	34.1	31	+10.0	+7.8
	120	110	7.85	12	0.27	0.05	100	106.5	95	-5.3	+10.8
Brewers'	200	112	2.10	8	2.40	0.50	40.6	37.0	42.0	-3.3	-11.9
Spent-	180	95	1.84	9	2.35	0.55	48.0	40.1	36.5	+3.3	-13.7
Grain	150	114	0.82	6	2.50	0.60	39.7	44.5	38.0	+4.5	+13.2
	150	120	0.59	4	2.65	0.67	171	158	160	+8.2	-1.3
	130	120	2.04	12	2.70	0.40	265	267	270	-1.8	-1.1

Conclusions

The high degree of accuracy with which the drying times of the porous-ceramic granules, coke and brewers' spent-grain can be predicted from the data obtained in the fractional three-level factorial experiments used in the present investigation illustrates the effectiveness with which these experiments determine the effects of airflow, air temperature, humidity and loading of material on the drying times of the various materials. While it is possible that the same fractional three-level experiments and methods of presenting drying data could be used to give accurate estimates of the effects of the above four factors on the drying times of a variety of materials, a preferable approach to the problem is to adapt the fractional three-level factorial experiment and the method of presenting the drying data to suit the drying characteristics of the material in question.

A two-level four-factor experiment involving sixteen drying tests provides a convenient method of conducting a preliminary survey of the drying characteristics of a material over a wide range of drying conditions. The drying data obtained in each test can be concisely presented as values of the constant drying rate $\frac{dW}{d\Theta}$, the critical moisture content W_c, and of the falling-rate constant C. With some materials, a plot of log W against Θ', log W against log Θ' or other transformation of W against Θ' may show a better linear relationship in the falling-rate period than the plot of W against log Θ' used in the present investigation; the falling-rate drying behaviour of these materials may be characterised by the slope of the plot of the transformation of W against Θ' which shows the best linear relationship.

The data obtained in the two-level factorial experiment should be analysed to find which factors have significant effects on $\frac{dW}{d\theta}$, W_c and on whichever rate constant is used to describe the falling-rate period, and to find if the effects of the various factors vary with the levels of the other factors. In making such an analysis, a statistical Analysis of Variance of the data is generally useful, especially when the experimental error is large.

A fractional three-level factorial experiment including tests done at the median values of each factor range can be designed to obtain confirmatory data on the effects and interactions of the various factors shown to be significant by the preliminary two-level factorial experiment. The tests included in this experiment should be chosen carefully to give the maximum amount of information on the significant effects and interactions; tests which give information on only insignificant effects and interactions should be excluded.

In addition to describing the drying behaviour of a material over a wide range of drying conditions, the data obtained in the fractional three-level factorial experiment can be used to trace the relationships between the levels of the various factors and the values of $\frac{dW}{d\theta}$, W_c and the falling rate-constant. These relationships can be conveniently shown graphically, and can be used by means similar to those described in this thesis to predict the drying times of a material between any moisture contents and under any drying conditions within the range of the experiment.

While it is probable that a fractional three-level factorial experiment of approximately the same size as those used in the present investigation could be used to give accurate predictions of the drying times of any material, the forty or more tests required may be prohibitively time-consuming for an industrial experimenter to undertake.

Assuming the drying behaviour of other porous granular and fibrous materials to be similar to that noted for the porous-ceramic granules, coke and brewers' spent-grain tested in the present investigation, it is possible that reasonably accurate (± 30% approximately) drying time predictions could be obtained from smaller fractional three-level factorial experiments involving 22 tests.

A suitable small fractional three-level factorial experiment to determine the drying characteristics of porous-granular and fibrous materials in a cross-circulation drier can be designed bearing in mind the following points from the present work on porous-ceramic granules, coke and brewers' spent-grain:

(a) The effects of loading of material L, air temperature D, humidity W or H, and airflow G on the constant drying rate $\frac{dW}{d\Theta}$ can be accurately described by the equation

$$\frac{dW}{d\Theta} = \frac{K' \, G \, (D - W)}{L} \quad \ldots \quad \text{Equation A.}$$

The value of K' must be determined experimentally at several air temperatures since the values of K' tend to increase slightly as air temperature increases, due possibly to increased heat radiation and conduction to the material on the drying tray.

(b) Only loading has a significant effect on the critical moisture content W_c of the porous-granular materials, while loading and airflow have significant effects on W_c of the fibrous materials; since air temperature and humidity have no appreciable effects on W_c, the tests to determine the effects of L, or L and G on W_c for both types of material may be conducted at any values of D and W.

(c) The values of the falling-rate constant C obtained for the porous-granular and fibrous materials depend only on the values of loading and air temperature used; the tests to determine the effects of these factors on C may be conducted at any values of G and W.

Summing up, it would appear to be unnecessary to conduct tests at various air humidities since air humidity only affects the value of $\frac{dW}{d\theta}$ and its effect can be readily calculated from Equation A. A fractional three-level, three-factor factorial experiment on D, L and G could supply the required information on the effects of these factors on $\frac{dW}{d\theta}$, W_c and C (see paragraphs (a), (b) and (c) above). An experiment capable of giving this information is shown in Table 45. This experiment involves eleven tests, but to obtain reasonable accuracy in predicting drying times it is advisable that each test be replicated, making a total of twenty-two tests. Air at atmospheric humidity may be used for all the tests.

TABLE 45: Suggested Fractional Three-Level Factorial Experiment To Determine The Drying Behaviour Of Porous-Granular And Fibrous Materials

	L_1			L_2			L_3		
	G_1	G_2	G_3	G_1	G_2	G_3	G_1	G_2	G_3
D_1			x		x				x
D_2		x		x	x	x		x	
D_3	x				x		x		

In designing a small fractional three-level factorial experiment to determine the drying characteristics of porous-granular and fibrous materials in a through-circulation drier the following points from the work on porous-ceramic granules, coke and brewers' spent-grain should be noted:

(d) There is no theoretical equation comparable to Equation A for cross-circulation drying which can give accurate estimates of the effects of D, W, L and G on $\frac{dW}{d\Theta}$. It is, however, possible to estimate the effect of changes in the approach air temperature and humidity on $\frac{dW}{d\Theta}$ by applying the correction factor f(DW) calculated from Equation B (Section 6.13) to the value of $\log_{10} \frac{dW}{d\Theta}$ determined in a standard test $D_2W_2L_2G_2$ (using air of atmospheric humidity). Since the effects of G and L on $\frac{dW}{d\Theta}$ interact to a degree depending on the material, it is necessary to determine the effect of G at various levels of L - the experimental results may be conveniently described in the empirical correction factor f(LG) (see Section 10.3) which is applied to the value of $\log_{10} \frac{dW}{d\Theta}$ obtained in the standard $D_2W_2L_2G_2$ test.

(e) Only L had a significant effect on the W_e values of the porous-ceramic granules and brewers' spent-grain; L and G had effects on the W_e values of coke. Since air temperature and humidity do not appear to affect W_e, tests to determine the effects of L and G on W_e of a material may be conducted at any values of D and W.

(f) The values of the falling-rate constant C for the porous-ceramic granules were affected by L and G and the values of C for coke and the brewers' spent-grain by L and D.

Since airstream humidity does not affect the values of C, tests to determine the effects of L and G, or L and D on C may be performed with an airstream of atmospheric humidity.

The information required on the effects of D, W, L and G on $\frac{dW}{d\theta}$, W_e and C (see paragraphs (d),(e),(f) above) can be obtained from the fractional three-level factorial experiment shown in Table 45. The eleven tests involved in this experiment may be conveniently conducted using an airstream of atmospheric humidity.

It was possible to predict the drying times of the porous-ceramic granules, coke and brewers' spent-grain under the drying conditions shown in Tables 23A and 44A from data obtained in the eleven tests shown in Table 45 since these tests comprised part of the fractional three-level four-factor experiments used in the present investigation. The drying time predictions obtained in this way were within ± 30% of the experimental values in the cross-circulation drying tests and within ± 20% of the experimental values in the through-circulation drying tests. Since this prediction accuracy was obtained from experiments in which only five ($D_1L_1G_3$; $D_1L_3G_3$, $D_2L_2G_2$; $D_3L_1G_1$; $D_3L_3G_1$) of the eleven drying tests shown in Table 45 were replicated, the prediction accuracy obtainable from the fully replicated experiment will probably be slightly higher.

NOMENCLATURE

a	= slab thickness	ft.
a'	= drying area	sq.ft/cu.ft bed volume
A	= area of drying surface	sq.ft.
A'	= cross-sectional area of drier	"
b	= factor depending on packing of spherical particles	
b'	= empirical coefficient	
D	= diffusivity of water	$ft^2/hr.$
D_p	= average particle diameter	ft.
e	= base of natural logarithms	
E	= vaporization efficiency	
F	= variance ratio used in test of significance	
g	= acceleration due to gravity	cm/sec^2
G	= airflow	lb dry air/(sq.ft drier cross-section)(hr)
h	= distance below meniscus in capillary	cm.
h'	= distance below surface of bed	"
h_f	= frictional resistance to flow through bed	cm. water
h_s	= height of capillary rise	" "
h_c	= convection coefficient of heat transfer	B.T.U./(hr)(sq.ft)(°F)
h_t	= overall " " " "	B.T.U./(hr)(sq.ft)(°F)
H_a	= humidity of airstream	lb water/lb dry air
H_s	= saturation humidity corresponding to wet-bulb temperature of airstream	" " " " "

$(\Delta H)_m$	=	logarithmic mean of humidity driving force $(H_s - H_a)$ at inlet and outlet of bed	lb water/lb dry air
K	=	coefficient of mass transfer	lb/(hr)(sq.ft)(atm. partial pressure difference)
K', K'', K'''	=	empirical coefficients	
L	=	loading of dry material	lb/sq.ft.
m, m'	=	empirical coefficients	
n	=	empirical exponent	
p_a	=	partial pressure of water vapour in the airstream	atm.
p_s	=	vapour pressure of water at drying surface	"
p_w	=	vapour pressure of water at the wet-bulb temperature	"
P	=	entry suction potential of a pore	cm. water
P_1	=	" " " " a surface pore	" "
P_2	=	" " " " a pore h' cm below surface	" "
P_s	=	suction potential just below meniscus in capillary	" "
P_h	=	suction potential h cm below meniscus in capillary	" "
q	=	rate of heat transfer	B.T.U./hr.
r	=	radius of spherical particle	cm.
r'	=	radius of capillary	"
R_c	=	constant drying rate per unit area of bed	lb/(hr)(sq.ft)
R_f	=	drying rate in falling rate period per unit area of bed	" " " "
t_a	=	airstream dry-bulb temperature (D.B.T.)	°F

t_s	=	temperature of wet surface	°F
t_w	=	wet-bulb temperature (W.B.T.) of airstream	"
w'	=	weight of water per unit area of filter cake	lb/sq.ft.
W	=	moisture content of material	lb water/lb dry solid.
W_1	=	initial moisture content of material	" " " " "
W_2	=	final moisture content of material	" " " " "
W_c	=	critical moisture content of material	" " " " "
W_e	=	equilibrium moisture content of material	" " " " "
$\frac{dw}{d\theta}$	=	drying rate	lb water/hr.
$\frac{dW}{d\theta}$	=	drying rate	lb water/(lb dry solid)(hr).
$\frac{\partial W}{\partial \theta}$	=	rate of moisture movement through a material by diffusion	" " " " " "
x	=	distance from midplane of material in direction of diffusion	ft.
Y	=	empirical drying factor	sq.ft/lb.
λ	=	latent heat of water at the W.B.T.	B.T.U./lb.
σ	=	surface tension of water	g/sec^2
μ	=	air viscosity	lb/(hr)(ft).
ρ	=	density of water	g/cm^3
ρ_s	=	bulk density of dry solid	lb/cu.ft.
θ	=	drying time	hours.

θ'	=	drying time	minutes.

In addition to the foregoing symbols, the following symbols have been used in describing the experimental results in this thesis.

B.D.S.	=	bone dry solid	
C	=	rate constant defined by equation	$W = C \log_{10}\theta' +$ a constant
D_1, D_2, D_3	=	dry-bulb temperature of airstream	°F
W_1, W_2, W_3	=	wet-bulb temperature of airstream	°F
H_1, H_2, H_3	=	humidity of airstream	lb water/lb dry air
L_1, L_2, L_3	=	dry loading	lb B.D.S./sq.ft.
G_1, G_2, G_3	=	airflow	lb dry air/(sq.ft)(min.)

Subscript 1 refers to the minimum value; 2 to the medium value; and 3 to the maximum value of the respective factors.

A subscript c used with a drying rate or drying time denotes a value in the constant-rate period; and a subscript f, a value in the falling-rate period.

REFERENCES

1. Walker, Lewis, McAdams and Gilliland, "Principles of Chemical Engineering," McGraw-Hill, New York, 3rd. Edition, 1937, p619.
2. Coagloke, N.H. and Hougen, O.A., Ind. Eng. Chem., 1937, 29, 805.
3. Shepherd, C.B., Hadlock, C. and Brewer, R.C., Ind. Eng. Chem., 1938, 30, 388.
4. Molstad, M.C., Farevaag, P. and Farrell, J.A., Ind. Eng. Chem., 1938, 30, 1131.
5. Powell, R.W. and Griffiths, E., Trans. Inst. Chem. Eng., 1935, 13, 175.
6. Powell, R.W., Trans. Inst. Chem. Eng., 1940, 18, 36.
7. Ede, A.J. and Hales, K.C., "D.S.I.R. Food Investigation Special Report No53" H.M.S.O. 1948.
8. Sherwood, T.K. and Comings, E.W., Ind. Eng. Chem., 1933, 25, 311.
9. Corben, R.W. and Newitt, D.M., Trans. Inst. Chem. Eng., 1955, 33, 52.
10. Maisel, D.S. and Sherwood, T.K., Chem. Eng. Prog., 1950, 46, 131.
11. Pratt, H.R.C., Trans. Inst. Chem. Eng., 1950, 28, 177.
12. Carrier, W.H., Ind. Eng. Chem., 1921, 13, 432.
13. Perry, J.H. (Editor) "Chemical Engineers Handbook" McGraw-Hill, New York, 3rd. Edition, 1950.
14. Hinchley, J.W. and Himus, G.W., Trans. Inst. Chem. Eng., 1924, 2, 57.
15. Thiesenhusen, H., Gesundh.-Ing., 1930, 53, 113.
16. Lurie, M. and Michailoff, N., Ind. Eng. Chem., 1936, 28, 345.
17. Kamei, S., Mizuno, S. and Shiomi, S., J. Soc. Chem. Ind. (Japan), 1935, 38, 460.

18. Sherwood, T.K., Ind. Eng. Chem., 1929, 21, 12, 976.

19. Gilliland, E.R. and Sherwood, T.K., Ind. Eng. Chem., 1933, 25, 1134.

20. Newman, A.B., Trans. Amer. Inst. Chem. Eng., 1931, 27, 203, 310.

21. Comings, E.W. and Sherwood, T.K., Ind. Eng. Chem., 1934, 26, 1096.

22. Pearse, J.F., Oliver, T.R. and Newitt, D.M., Trans. Inst. Chem. Eng., 1949, 27, 1.

23. Macey, H.H., Trans. Brit. Ceramic Soc., 1922, 41, 73.

24. Lewis, W.K., Ind. Eng. Chem., 1921, 13, 427.

25. Kamei, S. and Shiomi, S., J. Soc. Chem. Ind. (Japan) 1937, 40, 325, 366.

26. Hougen, O.A., McCauley, H.J. and Marshall, W.R.Jr. Trans. Amer. Inst. Chem. Eng., 1940, 36, 183.

27. Peck, R.E., Griffith, R.T. and Rao, K.N., Ind. Eng. Chem. 1952, 44, 664.

28. Van Arsdel, W.B., Chem. Eng. Prog., 1947, 43, 13.

29. Sherwood, T.K., Trans. Amer. Inst. Chem. Eng., 1936, 32, 150.

30. Haines, W.B., J. Agric. Sci. 1927, 17, 264 and 1930, 20, 97.

31. Oliver, T.R. and Newitt, D.M., Trans. Inst. Chem. Eng., 1949, 27, 9.

32. Newitt, D.M. and Coleman, M., Trans. Inst. Chem. Eng., 1952, 30, 28.

33. Simons, H.P., Koffolt, J.H. and Withrow, J.R., Trans. Amer. Inst. Chem. Eng., 1943, 39, 133.

34. Perry, R.L., Trans. Amer. Soc. Mech. Eng., 1944, 66, 447.

35. Van Krevelen, D.W. and Hoftigzer, P.J., J. Soc. Chem. Ind., 1949, 68, 58.

36. Wheat, J.A. and MacLeod, D.A., Canad. J. Chem. Eng., 1959, 37, 47.

37. Nissan, A.H., George, H.H. and Bellos, T.V., A. I. Chem. E. Journal, 1960, 6, 406.

38. Brown, A.H. and Kilpatrick, P.W., Trans. Amer. Soc. Mech. Eng., 1943, 65, 837.

39. Van Arsdel, W.B., U.S. Dept. Agric. Publication AIC-300, 1951.

40. Brownlee, K.A., "Industrial Experimentation" H.M.S.O. London, 4th. Edition, 1949.

41. Fisher, R.A., "The Design of Experiments" Oliver and Boyd, 4th. Edition, 1947.

42. Yates, F., "Design and Analysis of Factorial Experiments," Imperial Bureau of Soil Science, Harpenden, 1937.

43. Davies, O.L. (Editor) "Statistical Methods in Research and Production," Oliver and Boyd, 1947.

44. Davies, O.L. (Editor) "The Design and Analysis of Industrial Experiments," Oliver and Boyd, 1954.

45. Cox, D.R., "Planning of Experiments" Chapman and Hall, 1958.

46. Bennett, C.A. and Franklin, N.L. "Statistical Analysis in Chemistry and in the Chemical Industry," Wiley and Sons, New York, 1954.

47. Lindley, D.V. and Miller, J.C.P. "Cambridge Elementary Statistical Tables" Cambridge Univ. Press, 1958.

48. Finney, D.J., Ann. Eugen., 1945, 12, 291.

49. Carr, J.M.Jr. and McCracken, E.A., Ind. Eng. Chem., 1960,56,56.

50. Marshall, W.R.Jr. and Hougen, O.A., Trans. Amer. Inst. Chem. Eng., 1942, 38, 91.

51. Gamson, B.W., Thodos, G. and Hougen, O.A., Trans. Amer. Inst. Chem. Eng., 1943, 39, 1.

52. Wilke, C.R. and Hougen, O.A., Trans Amer. Inst. Chem. Eng. 1945,41,445.

53. Simmonds, W.H.C., Ward, G.T. and McEwan, E., Trans. Inst. Chem. Eng., 1953, 31, 265, 279.

54. Gardner, R.G. and Mitchell, T.J., J. Sci Food Agric., 1953, 4, 113, 237, 364.

55. Mitchell, T.J. and Potts, C.S., J. Sci. Food Agric., 1958, 9, 20, 29, 93, 99.

56. Glover, H.C. and Moss, A.A.H., Trans. Inst. Chem. Eng., 1957, 35, 208.

57. Allerton, J., Brownell, L.E. and Katz, D.L., Chem. Eng. Prog., 1949, 45, 619.

58. Downes, J.G. and McMahon, G.B., Textile Research Journal, 1959, 29, 1006.

59. McEwan, E. and O'Callaghan, J.R., The Engineer, 1954, 198, 817.

60. Hughes, J.M. and Mitchell, T.J., J. Sci. Food Agric., 1959, 10, 39, 45.

61. Davidson, C.M., Hughes, J.M. and Mitchell, T.J., J. Sci. Food Agric., 1959, 10, 180.

APPENDIX 1.

Specimen Results Of A Drying Test

MATERIAL : Porous-Ceramic Granules TEST No. 17. DATE : 25/3/60.

DRIER : Through-Circulation Drier.

DRYING CONDITIONS : D.B.T. 160°F.

W.B.T. 102°F.

Airflow 4lb. dry air/(sq. ft. drier cross Section)(min.)

Time Minutes	Weight of bed lbs.	Weight of water in bed lbs.	Moisture Content of Material lb./lb. B.D.S.
0	6.600	1.510	0.296
4	6.510	1.420	0.279
8	6.324	1.234	0.242
12	6.130	1.040	0.204
16	5.955	0.860	0.169
20	5.782	0.692	0.136
24	5.616	0.526	0.103
28	5.477	0.387	0.076
32	5.360	0.270	0.053
36	5.265	0.175	0.034
40	5.195	0.105	0.021
44	5.150	0.060	0.012
48	5.123	0.033	0.007
52	5.110	0.020	0.004
56	5.105	0.015	0.003
60	5.104	0.014	0.003

Moisture Content of granules at end of test period = 0.27%

∴ Weight of B.D.S. in test bed $= 5.104 - \frac{0.27 \times 5.104}{100}$

$= 5.090$ lbs.

APPENDIX 2
Four-Factor Experiment
Arithmetical Procedure Of The Analysis Of Variance Of A Two-Level Four-Factor Experiment

While a full description of the theory of the Analysis of Variance and its application to various problems can be found in the textbooks by Davies et. al. (43, 44) the following outline of the theory may help to elucidate the various steps in the arithmetical procedure described in this Appendix.

The total variance V of a number of observations is defined as:

$$V = \frac{\sum (x - \bar{x})^2}{N - 1}$$

where x = individual observation

$\bar{x}$ = arithmetic mean of all the observations

N = total number of observations

The numerator in this equation is known as the "Sum of Squares" of deviations of the observations from their mean. The denominator is known as the degrees of freedom of the estimate of variance: i.e. the number of independent values of $(x - \bar{x})$ used in obtaining the estimate.

The various combinations of factor levels used in the tests required by a factorial experiment generally produce a range of values in the dependent variable, the total variance of which can be estimated by the above equation. In addition, by considering the test results in groups corresponding to a change in the level of one or more factors, smaller variances can be attributed to the effects of various factors and to interactions between factors. Since variance is an additive property, the variance in the test results due to experimental error can be estimated as the difference (residual) between the total variance and the sum of the variances attributed to the various effects and interactions.

To estimate the variance due to the effect of a factor A from the results of a two-level factorial experiment, the test results are considered in two groups, with the results of tests conducted with factor A at A_1 in one group, and the results of tests conducted with factor A at A_2 in the other group. The variance due to the effect of factor A is then estimated as the Sum of Squares of the deviations of the two group means $\bar{x}_i$ from the mean of all the test results $\bar{x}$: i.e. $\sum n_i (\bar{x}_i - \bar{x})^2$ where n_i = number of test results in each group. (Sums of Squares can be used directly as estimates of the variance due to the various main effects, interactions and the residual in the Analysis of Variance of a two-level factorial experiment since these estimates of variance each have 1 degree of freedom - in more elaborate experiments it would, however, be necessary to divide the Sums of Squares by the appropriate degrees of freedom).

Several methods of calculating the Sums of Squares due to interactions between factors are available - the method described in this Appendix is that used by Brownlee (40). The theory of the "F test" used to test the significance of the variances due to the various effects and interactions, has been outlined previously on pages 38 and 39.

The arithmetical procedure of the Analysis of Variance for a two-level four-factor factorial experiment is illustrated by the analysis of the constant drying rate results obtained in the cross-circulation drying tests on porous-ceramic granules. The analysis is conducted on the values of $\log_{10} 100 \frac{dW}{d\theta}$ given in column two of Table 2 page 51.

These values may be tabulated as follows:

L_1							
G_1				G_3			
D_1		D_3		D_1		D_3	
W_1	W_3	W_1	W_3	W_1	W_3	W_1	W_3
0.6749	0.2122	1.2041	1.1370	1.0569	0.6665	1.5635	1.4893

L_3							
G_1				G_3			
D_1		D_3		D_1		D_3	
W_1	W_3	W_1	W_3	W_1	W_3	W_1	W_3
0.1614	-0.2757	0.7679	0.6435	0.6444	0.1875	1.1206	1.0374

Four Tables are then formed by summing over each of the four variables L, G, D and W.

Summing over L

G_1				G_3			
D_1		D_3		D_1		D_3	
W_1	W_3	W_1	W_3	W_1	W_3	W_1	W_3
0.8363	-0.0635	1.9720	1.7805	1.7013	0.8540	2.6841	2.5267

Summing over G

L_1				L_3			
D_1		D_3		D_1		D_3	
W_1	W_3	W_1	W_3	W_1	W_3	W_1	W_3
1.7318	0.8787	2.7676	2.6263	0.8058	-0.0882	1.8885	1.6809

Summing over D

L_1				L_3			
G_1		G_3		G_1		G_3	
W_1	W_3	W_1	W_3	W_1	W_3	W_1	W_3
1.8790	1.3492	2.6204	2.2558	0.9293	0.3678	1.7650	1.2249

Summing over W

L_1				L_3			
G_1		G_3		G_1		G_3	
D_1	D_3	D_1	D_3	D_1	D_3	D_1	D_3
0.8871	2.3411	1.7254	3.0528	-0.1143	1.4114	0.8319	2.1580

A further six Tables are formed by summing over the four variables L, G, D and W, two at a time.

Summing over L and D

	W_1	W_3	Totals
G_1	2.8083	1.7170	4.5253
G_3	4.3854	3.3807	7.7661
Totals	7.1937	5.0977	12.2914

Summing over L and W

	G_1	G_3	Totals
D_1	0.7728	2.5553	3.3281
D_3	3.7525	5.2108	8.9633
Totals	4.5253	7.7661	12.2914

Summing over G and D

	L_1	L_3	Totals
W_1	4.4994	2.6943	7.1937
W_3	3.5050	1.5927	5.0977
Totals	8.0044	4.2870	12.2914

Summing over D and W

	G_1	G_3	Totals
L_1	3.2282	4.7762	8.0044
L_3	1.2971	2.9899	4.2870
Totals	4.5253	7.7661	12.2914

Summing over L and G

	W_1	W_3	Totals
D_1	2.5376	0.7905	3.3281
D_3	4.6561	4.3072	8.9633
Totals	7.1937	5.0977	12.2914

Summing over G and W

	L_1	L_3	Totals
D_1	2.6105	0.7176	3.3281
D_3	5.3939	3.5694	8.9633
Totals	8.0044	4.2870	12.2914

The computation of the various Sums of Squares may be facilitated by the use of the following equivalent expressions:

$$\sum (x - \bar{x})^2 = \sum x^2 - \frac{S^2}{N}$$

$$\sum n_i(\bar{x}_i - \bar{x})^2 = \sum\left(\frac{S_i^2}{n_i}\right) - \frac{S^2}{N}$$

where S = sum of the individual observations

S_i = sum of a group of observations

The first term of the expressions on the right hand side of these equations is known as the "Crude Sum of Squares" and the second term as the "Correction due to the Mean" (denoted hereafter by C.M.)

Since in the present experiment S = 12.2914 and N = 16 the C.M. is $(12.2914)^2/16 = 9.4424071$

To calculate the Sum of Squares for the main effect of factor G, the G_1 and G_2 totals (S_i) are squared, the squares are summed and divided by 8 (= n_i), and the C.M. is subtracted from this.

i.e. $(4.5253^2 + 7.7661^2)/8 - 9.4424071 = 0.6564241$

The Sum of Squares for the other main effects are obtained similarly. Thus –

For L: $(8.0044^2 + 4.2870^2)/8 - 9.4424071 = 0.8636914$

For D: $(3.3281^2 + 8.9633^2)/8 - 9.4424071 = 1.9847174$

For W: $(7.1937^2 + 5.0977^2)/8 - 9.4424071 = 0.2745760$

The Sum of Squares corresponding to the first-order interaction between factors G and W (which measures the extent to which the effect of the one factor depends on the value of the other) is calculated as the difference between the Sum of Squares corresponding to the individual values in the two-way Table for G and W and the sum of the G and W Sum of Squares i.e.

$(2.8083^2 + 1.7170^2 + 4.3854^2 + 3.3807^2)/4$

$- 9.4424071 - 0.6564241 - 0.2745760 = 0.0004687$

(Note: n_i = 4 for the individual values in each two-way Table)
The Sums of Squares corresponding to the other five first-order interactions are derived similarly.

The Sum of Squares corresponding to the second-order interaction between factors G, W and D (which measures the extent the interaction between any two of these factors depends on the value of the third factor) is calculated as the difference between the Sum of Squares corresponding to the individual values in the three-way Table for G, W and D, and the sum of the Sums of Squares corresponding to the main effects and interactions involving these factors: i.e. the D, W and G main effects and the DW, DG and WG interactions. i.e.

$(0.8363^2 + (-0.0635)^2 + \ldots + 2.6841^2 + 2.5267)^2/2 - 9.4424071$

$- 1.9847174 - 0.2745760 - 0.6564241 - 0.1221853 - 0.0065691$

$- 0.0004687 = 0.0000211$

(Note: n_i = 2 for the individual values in each three-way Table)
The Sums of Squares corresponding to the other three second-order interactions are obtained similarly.

The Total Sum of Squares is calculated by squaring the original test values, summing the squares, and subtracting the C.M. from this. i.e.

$(0.6749^2 + 0.2122^2 + \ldots + 1.1206^2 + 1.0374^2)$

$- 9.4424071 = 3.9127180$

The Sum of Squares corresponding to the Residual (which is used as an estimate of the experimental error) is calculated as the difference between the Total Sum of Squares and the sum of the Sums of Squares corresponding to the four main effects, the six first-order interactions, and the four second-order interactions.

The complete Analysis of Variance Table is as follows:

Source of Variance	Sums of Squares
G	0.6564241
L	0.8636914
D	1.9847174
W	0.2745760
GW	0.0004687
DW	0.1221853
DG	0.0065691
DL	0.0002925
GL	0.0013104
LW	0.0007183
GWD	0.0000211
DLG	0.0003515
DLW	0.0000401
LWG	0.0001199
Residual	0.0012322
Total	3.9127180

In testing the significance of the various main effects and interactions in the Analysis of Variance Table by the F Test, the Residual Sum of Squares is compared with the Sums of Squares corresponding to (a) the second-order interactions, (b) the first-order interactions, and (c) the main effects, in that order; the smallest Sum of Squares in each group being tested first.

Proceeding with the analysis, it can be seen that all the Sums of Squares corresponding to the various second-order interactions are smaller than the Residual Sum of Squares. Therefore, since these interactions probably do not exist, their Sums of Squares may be considered as independent estimates of the experimental error and may be pooled with the original Residual Sum of Squares to give a new Residual Mean Sum of Squares which gives a more accurate estimate of the experimental error (i.e. an estimate with a greater number of degrees of freedom). The new Residual Mean Sum of Squares is:

$$(0.0012322 + 0.0000211 + 0.0001199 + 0.000401 + 0.0003515)/5$$

$$= (0.0017648)/5 = 0.0003530 \text{ with 5 degrees of freedom.}$$

Testing the first-order interaction Sums of Squares, it can be seen that the DL Sum of Squares is smaller than the Residual Mean Sum of Squares; this interaction Sum of Squares is therefore pooled as before to give a new Residual Mean Sum of Squares of 0.0003429 with 6 degrees of freedom.

Testing the smallest of the remaining first-order interaction Sums of Squares (i.e. that corresponding to the GW interaction) against this new Residual Mean Sum of Squares, the variance ratio F = $\frac{0.0004687}{0.0003429} = 1.36$ is obtained. In this ratio the numerator has $v_1 = 1$, and the denominator $v_2 = 6$ degrees of freedom. Since the value of F at the 5% probability level for these degrees of freedom is 5.99 (Reference 47), the GW interaction is not significant, and the Sum of Squares corresponding to this interaction may be pooled as before to give another new Residual Mean Sum of Squares with 7 degrees of freedom.

This procedure is repeated for the other first-order interactions until a value of F greater than that given for the 5% probability level for the appropriate degrees of freedom is obtained, when the interaction is considered significant. In this way, the DG and DW interactions are found to be significant.

When an interaction is found to be significant it is pointless to test the significance of the main effects involved in the interaction, since the effect of each factor then depends on the value of the other factor. Thus a result of an F test indicating that the main effect of one factor is insignificant merely means that the average effect of that factor is approximately zero over the two levels of the other factor used in the original experiment. Since the DG and DW interactions are significant, only the L main effect need be tested by the F Test. This main effect is found to be significant.

The Analysis of Variance has therefore indicated the existence of an L main effect, and DW and DG interactions.